UNIVERSIDADE DE SÃO PAULO
INSTITUTO DE QUÍMICA

Programa de Pós-Graduação em Química

ANDRÉS CAMILO GUERRERO-PERILLA

CHEMICAL DIVERSITY AND ONTOGENY OF *PIPER* SPECIES

Versão corrigida da Tese conforme Resolução CoPGr 5890

O original se encontra disponível na Secretaria de Pós-Graduação do IQ-USP

São Paulo

Data do Depósito na SPG:

23/11/2021

ANDRÉS CAMILO GUERRERO-PERILLA

DIVERSIDADE QUÍMICA E ONTOGENIA DE ESPÉCIES DE *PIPER*

Tese apresentada ao Instituto de Química da Universidade de São Paulo para obtenção do Título de Doutor em Química.

Orientador: Prof. Dr. Massuo Jorge Kato

São Paulo

2021

To my parents, to whom I owe everything...

Acknowledgments

To the University of São Paulo and the Institute of Chemistry for this great opportunity.

To the Fundação de Amparo à Pesquisa do Estado de São Paulo (FAPESP- processo Nº2016/00778-0) for the financial support during these five years.

To Prof. Dr. Massuo J. Kato for his friendship, instruction, kindness, and patience during all this process.

To Dra. Lydia Yamaguchi for her friendship, advice, and help.

To my friends and colleagues from the LQPN-USP: Abdelaaty, Aline, André Jun, Bruna, Daniel, Dimitre, Giancarlo, Iza, Larissa, Leonardo, Marcilio, Mariana, Thiago, Valdirene, Vare, Vivian and Welber, for their support and friendship.

To my family for their endless support.

To Dr. Ericsson Coy for believing in me and helping me to get this opportunity.

To my friends from the LQBO-UMNG: Freddy Bernal, Lorena Orduz, Paola Borrego and Ronald Marentes, for their support and friendship, even from so far away.

To the Central Analítica -USP, especially to Cristiane, Giovanna, Janaina and Vânia.

To Prof. Dra. Eny I. S. Floh and Amanda Macedo for their help with the HPLC-FLD analyses.

To Prof. Dr. Alcindo dos Santos and his staff.

To Prof. Dr. Marcelo Pena and the staff from the Laboratório de Fitoquímica (IB/USP), especially to Lucas and Victor (and Nina), for all the learning and good moments.

To Dr. Lee Dyer and Beto for providing the plant material.

To my Brazilian friends Marcus T. Scotti, Luana Morais, Luciana Scotti, Felipe Wouters and Juliana Araujo.

To Mrs. Chi Ting and her family.

To my brothers in arms: Ricardo Cano, Fabián Cuadrado, Elkin Franco and Sebastián Yoria.

To my friends: Carolina Torres, Juan S. Arias, Andrea Rodríguez, Sandra Crespo, Natalia Reyes, Ricardo Monsalve, Alonso Pardo, Chonny Herrera, Alejandra Ocampo, Juan C. Ito, Sandra Molina, Tatiana Morales, Karen Mejía, Jairo Quintana, Cristina Becerra and Yasmín Valero.

To my friends from São Paulo: Lina, Mario, Miguel, and Tania. For giving me the strength to carry on, for being my home.

To Tatiana Ríos, for all the love, motivation, and good times.

To Inés Súarez, for taking care of me when I needed it most.

To my schoolteachers: Carlos Barreto, Laksmi Latorre and Sara Castelblanco.

And to all those who made this possible...

" The *scientist does not study nature because it is useful to do so.*

He studies it because he takes pleasure in it and takes

pleasure in it because it is beautiful. If nature were not beautiful,

it would not be worth knowing, and life would not be worth living."

Henri Poincaré.

Resumo

Guerrero-Perilla, A.C. **Diversidade química e ontogenia de espécies de *Piper***. 2021. 164 p. Tese-Programa de Pós-Graduação em Química. Instituto de Química. Universidade de São Paulo.

Piper (Piperaceae) é um gênero de grande importância econômica e medicinal, com mais de 1000 espécies, tendo a maior diversidade entre as angiospermas basais. No entanto, apesar dos inúmeros usos tradicionais, um número considerável de espécies não foi ainda estudado sob o ponto de vista químico. No caso de *P. auritum*, uma análise fitoquímica completa foi conduzida para adultos e plântulas. Folhas, frutos e raízes foram extraídos e os principais metabólitos identificados por métodos espectrométricos e espectroscópicos. Flavonoides *C*-glicosilados, fenilbutenolidos, amidas e fenilpropanoides foram as principais famílias de compostos caracterizados. Análises de HPLC possibilitaram uma comparação entre adultos (folhas, raiz e frutos) e plântulas (folhas) onde evidenciou-se o aumento dos flavonoides *C*-glicosilados ao longo da ontogenia, além da presença da amida pelitorina durante o estágio inicial, bem como a ausência de fenilbutenolidos e de outras amidas, sugerindo que a química dos estágios iniciais corresponde a uma composição híbrida entre folhas jovens e raízes. As espécies *P. lindbergii* e *P. chimonantifolium* também foram estudadas; vários metabólitos como as dihidrochalconas mirigalona H, dihidroflavokawaina C e asebogenina, assim como a chalcona stercurensina, foram identificadas por HPLC-ESI-HRMS e NMR (1D e 2D). Vários outros metabólitos análogos foram anotados para ambas as espécies, projetando-os como fontes promissoras de metabólitos do tipo chalcona. Além disso, sete espécies de *Piper* foram cultivadas. Mudas de seis meses foram extraídas e seus perfis de HPLC e RMN de ^{1}H foram comparados com os adultos por análise multivariada objetivando caracterizar diferenças em suas composições. Duas metodologias foram utilizadas: uma para indivíduos de *P. umbellatum, P. glabratum* e *P. diospyrifolium*; e outra para indivíduos de *P. caldense, P. regnellii, P. crassinervium* (IQ e Colômbia) *e P. chimonantifolium*. O PCA mostrou diferenças entre as espécies e o estágio fenológico. As análises por HPLC também foram mais informativas do que por NMR, mostrando o forte efeito dos

interferentes e do procedimento de extração. *P. glabratum* foi comparada usando ambas as metodologias, com o PCA discriminando o indivíduo, os agrupados e os adultos de uma maneira melhor através dos dados de HPLC. As anotações feitas por HPLC-ESI-HRMS mostraram que flavonoides *C*-glicosilados são recorrentes em todas as espécies, adultas e plântulas, enquanto os adultos tornam-se mais variados, produzindo lignoides, chalconas, dihidrocalconas, ácidos benzoicos prenilados e quinonas. Finalmente, devido à ocorrência persistente de aristolactamas nas espécies estudadas, uma metodologia de HPLC-FLD foi desenvolvida e validada para se quantificar a esses compostos em extratos de EtOAc de raízes de dezessete espécies de *Piper*. Durante o isolamento do padrão de cefaranona B, foram identificados os compostos piperolactamas A-C e aristolactama DIII. *P. aduncum*, *P. aleyreanum, P. hispidum, P. cubataonum* e *P. krukoffi* exibiram o maior conteúdo desses compostos. O método foi altamente seletivo e sensível para este estudo e demonstrou alta robustez. De uma forma geral, os dados obtidos demonstraram a presença de compostos como flavonoides glicosilados e de aristolactamas como onipresentes em espécies de *Piper* e que estudos das plantas ao longo da ontogenia podem contribuir para a descoberta de novos metabólitos secundários.

Palavras Chave

Piper, fitoquímica, ontogenía, metabólitos secundários, aristolactamas.

Abstract

Guerrero-Perilla, A.C. **Chemical diversity and ontogeny of *Piper* species**. 2021. 164 p. PhD Thesis-Graduate Program in Chemistry. Instituto de Química. Universidade de São Paulo.

Piper (Piperaceae) is a genus of economic and medicinal importance, with over 1000 species, having the highest species diversity among the basal angiosperms. However, a considerable number of species have not been studied despite their widespread and traditional uses. In the case of *P. auritum*, a comprehensive phytochemical analysis was conducted for adults and plants at early stages. Leaves, fruits and roots were extracted, and the major metabolites were identified by spectrometric and spectroscopic methods. C-glycosylflavonoids, phenylbutenolides, amides and phenylpropanoids were the main sets of compounds in the species. After chromatographic profiling using HPLC-UV-HRESI, a comparison between adults (leaves, root and fruit) and seedlings (leaves) showed the rise of C-glycosylflavonoids and amide pellitorine during the early stage of ontogeny as well as the lack of phenylbutenolides and other amides, suggesting that the chemistry of the early stages corresponds to a hybrid between young leaves and roots. The species *P. lindbergii* and *P. chimonantifolium* were also studied; several metabolites like dihydrochalcones myrigalone H, dihydroflavokawain C and asebogenin, as well as chalcone stercurensin, were identified by HPLC-ESI-HRMS and NMR (1D and 2D). Several other chalcone-type metabolites were annotated for both species, suggesting them as promising sources of chalcone-type metabolites. Additionally, seven species of *Piper* (*P. umbellatum, P. glabratum, P. diospyrifolium, P. caldense, P. regnellii, P. crassinervium* (IQ and Colombia) and *P. chimonantifolium* were planted. Six-month-old seedlings were collected, extracted, and their HPLC and ^{1}H NMR profiles were compared with the adults by multivariate analysis and through the differences in their composition. Two methodologies were used: individuals of *P. umbellatum, P. glabratum* and *P. diospyrifolium;* and pooled *P. caldense, P. regnellii, P. crassinervium* (IQ and Colombia) and *P. chimonantifolium.* Multivariate analysis displayed visible differences between species and phenological stage, especially for the pooled species with better clustering while individuals showed a

high dispersion. HPLC results were also superior to NMR, showing the strong effect of interferents and extraction procedure in the latter. *P. glabratum* was compared using both methodologies, with the PCA discriminating the individual, pooled and adult samples in a better way for HPLC data. HPLC-ESI-HRMS annotations showed that C-glycosylflavonoids are conspicuous in all species, adult and seedlings, while the adults become more variated, producing lignoids, chalcones, dihydrochalcones, prenylated benzoic acids and quinones. Finally, due to the ubiquitous occurrence of aristolactams in the studied species, an HPLC-FLD methodology was developed and validated to quantify the total amount of these compounds in EtOAc extracts from roots of eighteen species of *Piper*. During the standard cepharanone B isolation, piperolactams A-C and aristolactam DIII were identified. *P. aduncum, P. aleyreanum, P. hispidum, P. cubataonum* and *P. krukoffi* displayed the highest content of these compounds. The method was highly selective and sensitive for this study and also demonstrated high ruggedness. In general, the data obtained demonstrated the presence of compounds such as glycosylated flavonoids and aristolactams as ubiquitous in *Piper* species and that plant studies along ontogeny could contribute to the discovery of new secondary metabolites.

Keywords

Piper, phytochemistry, ontogeny, secondary metabolites, aristolactams.

List of Abbreviations

AA	Aristolochic acid
Ac	Acetyl group
ACN	Acetonitrile
AL	Aristolactams
Ap	Apiose
BPC	Base Peak Chromatogram
COSY	Correlation Spectroscopy
DAD	Diode Array Detector
DCM	Dichloromethane
EI	Electron ionization
ESI	Electrospray Ionization
EtOAc	Ethyl acetate
FLD	Fluorescence Detector
GC	Gas Chromatography
Glu	Glucose
Hex	Hexane
HMBC	Heteronuclear Multiple-Bond Correlation
HPLC	High-Performance Liquid Chromatography
HPLC-MS	High-Performance Liquid Chromatography-Mass Spectrometry
HSQC	Heteronuclear Single Quantum Coherence
HRMS	High-Resolution Mass Spectrometry
IHD	Index of Hydrogen Deficiency
J	Coupling Constant
LOD	Limit of Detection
LOQ	Limit of Quantification
m/z	Mass to Charge Ratio
MeOH	Methanol
MeOD	Deuterated methanol
MS	Mass Spectrometry
MRM	Multiple Reaction Monitoring

PC	Principal Component
PCA	Principal Component Analysis
ppm	Parts per million
ppb	Parts per billion
Rha	Rhamnose
rt	Retention time
RPCC	Reverse Phase Column Chromatography
TLC	Thin layer chromatography
TMS	Tetramethylsilane
VLC	Vacuum Liquid Chromatography
^{1}H-NMR	Proton Nuclear Magnetic Resonance
^{13}C-NMR	Carbon 13 Nuclear Magnetic Resonance
δ	Chemical Shift
s	Singlet
d	Doublet
dd	Doublet of doublets
t	Triplet
q	Quartet
qd	Quartet of doublets
m	Multiplet

List of Figures

List of Tables

Summary

Chapter 1. The phytochemistry of *Piper auritum* Kunth.

1.1. Introduction

1.1.1 Plant Secondary Metabolites

The chemical compounds present in living organisms can be divided into two main groups: primary and secondary metabolites (despite, in practice, there is an important overlapping between these two terms). The primary metabolites are produced and involved in vital growth, development, and reproduction processes, while secondary metabolites are derived with more diverse functions. Primary metabolites can be gathered into a few families; these families are the building blocks of life, possess universal functions and are common in all living beings (Martin Luckner, 2013; Seigler, 1998).

Secondary metabolites are numerous and widespread, especially in plants. Their purpose is related to the ecological process, mediating its interaction with the environment, in theory, disposable for growth and development but, in practice, indispensable for the survival of populations as well unique, diverse and adaptative roles (Figure 1). The most remarkable feature of secondary metabolism is its high structural diversity, restricted occurrence, and intraspecific variability, with more than 100.000 chemical structures isolated and identified (Hartmann, 1996; Lehninger et al., 2004). Plant secondary metabolites can be classified into four major groups: Terpenes, phenolics, sulfur-containing, and nitrogen-containing compounds, with all groups including a wide range of subcategories (Mazid et al., 2011).

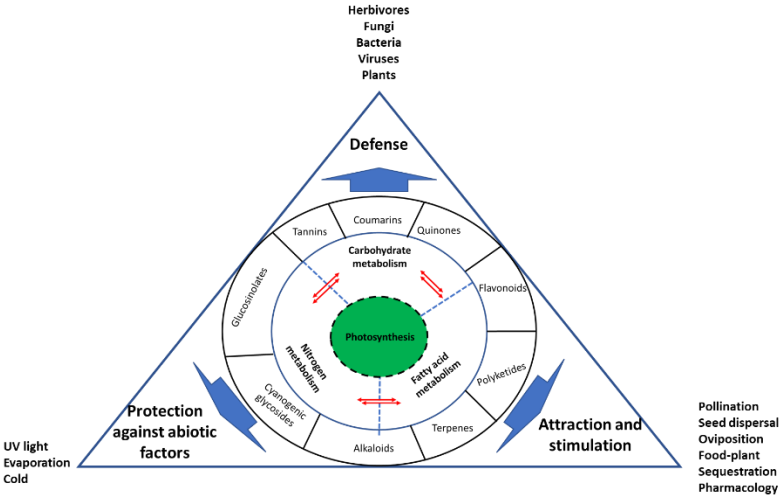

Figure 1. The general scheme of secondary metabolites originated from common precursors of primary metabolism and their functions in plants. Based on Hartmann´s work (Hartmann, 1996).

Secondary metabolites are not necessarily expressed under all conditions; in many cases, their function in a specific organism is unknown. They can be classified according to their "building block" type; these building blocks are derived from primary metabolism pathways like Kreb's cycle, photosynthesis, or glycolysis, and contrary to the high number of metabolites involved, the number of building blocks is surprisingly low. They can be grouped according to their biological pathway as derivates from acetate, mevalonate, shikimate, and methylerythritol phosphate. For example, Acetyl-CoA is derived from the oxidative decarboxylation of pyruvic acid (an intermediate in the glycolytic pathway) or the β-oxidation of fatty acids; this building block could lead to more complex metabolites like phenols, prostaglandins, or macrolides. More elaborate metabolites could be achieved by mixing two or more of these synthetic pathways, always as an enzyme-mediated sequence of reactions involving processes of alkylation (nucleophilic substitutions and electrophilic additions), rearrangement, condensation (aldol and Claisen), imine-mediated, Mannich, transamination, oxidations, reduction and glycosylation reactions, among others (Dewick, 2009).

1.1.2. Piperaceae family

The order of Piperales is one of the most species-rich clades among basal angiosperms; it comprises approximately 4300 species (Wanke et al., 2007), with the Piperaceae family as one of the major ones. Piperaceae has a pantropical distribution and is highly diverse, with approximately 3700 species composed of five genera: *Zippelia*, *Manekia*, *Verhuellia, Peperomia,* and *Piper* (Figure 2) (Chase et al., 2016). For *Zippelia* and *Manekia*, only seven species have been reported as well as only two species for *Verhuellia*, while *Peperomia* and *Piper* are the most representative, with more than 2000 species (Isnard et al., 2012).

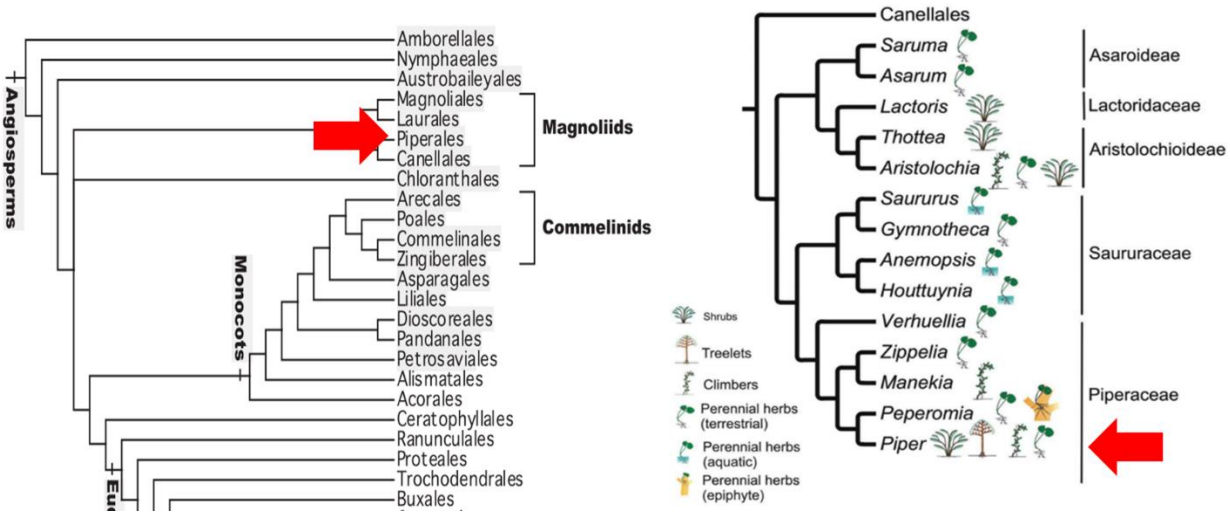

Figure 2. APG IV (left) with orders and some families (Chase et al., 2016) and phylogeny of Piperales order (right) (Isnard et al., 2012).

1.1.3. Genus *Piper*

The genus *Piper* has over 1000 species distributed pantropically (Figure 3); this genus is one of the most diverse lineages among basal angiosperms (Jaramillo and Manos, 2001), going from herbs to shrubs and also small trees (Dyer and Palmer, 2004). The genus has a great economic and medicinal importance, and peppers are a vital product in the worldwide spice markets. *Piper nigrum* is the most important member of the genus; however, there are several other *Piper* species of importance, for instance, *Piper betle L.* is used in some south Asian countries for chewing, especially in combination

with areca nut, lime, or tobacco (Ravindran, 2000). *Piper longum L*. is a crucial ingredient in the Indian systems of medicine, a decoction of roots and fruits are used in chronic bronchitis, cough, and cold treatment (Ravindran, 2000). *Piper chaba* Hunter is used all over India similarly to *P. longum L*. *Piper cubeba L* possesses a substantial amount of essential oil that is widely used due to its antibacterial and antifungal activity as well as a flavoring agent for liqueurs, cigarettes, sauces, and perfumery. *P. hispidinervium Trel*. is widely cultivated in Brazil due to its high safrole content, a valuable natural chemical for various industrial uses (Lima, 2015; Ravindran, 2000). The roots of *P. methysticum* G. Frost are used as the basis of a narcotic beverage produced in the South Pacific Islands known as "kava-kava" it is a cerebral depressant that does not show some of the drawbacks of alcohol (Ravindran, 2000), despite several other adverse effects that have been demonstrated (Whitton et al., 2003). Besides its notable medicinal and industrial uses, species like *P. auritum HBK*, *P. borneense N.E.Br.Her, P. decurrens DC, P. magnificum Trel, P. metallicum Hallier f, P. ornatum N.E.Br, P. porphyropbyllum* (Lindl.) *N.E.Br, P. rubronodosum Nichols* and *P. rubrovenosum* hort. ex Rodigas are also used as ornamental (Ravindran, 2000).

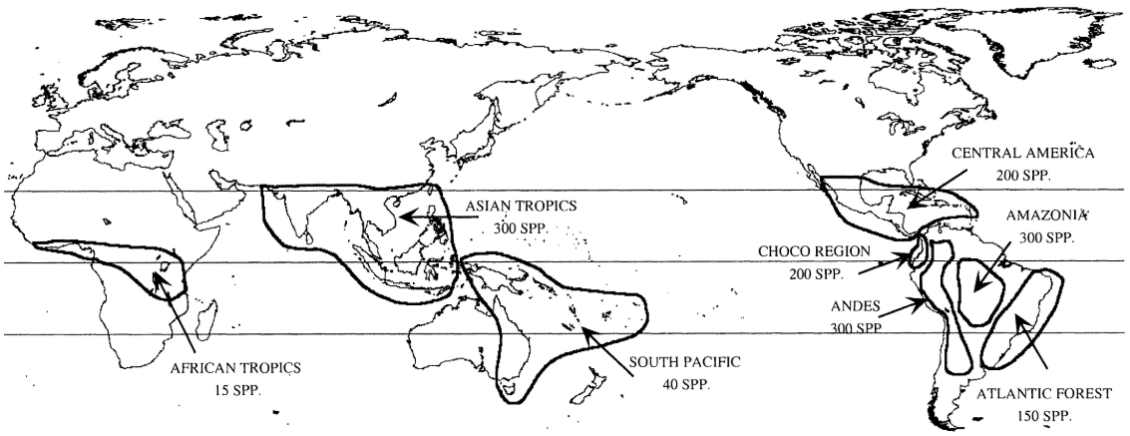

Figure 3. Geographical distribution of the genus *Piper* and estimated species by region (Jaramillo and Manos, 2001).

The phytochemistry of the genus *Piper* is rich in metabolites, with approximately 667 chemical compounds identified from about 112 species. These compounds can be classified in a vast number of families as alkaloids/amides, lignans, neolignans, terpenes, propenylphenols, steroids, kavapyrones,

chalcones, dihydrochalcones, flavones, flavanones, piperolides (butenolides), among several others (Dyer and Palmer, 2004; Parmar et al., 1997). Several species are known for their high content of essential oils, which displayed a remarkable activity against strains of *Aedes aegypti,* among other biological properties (Pereira Filho et al., 2021).

1.1.4. *Piper auritum* Kunth.

Piper auritum is a shrub native to the Central America tropics, also known as; Hoja Santa, Acoyo, Hoja de la Estrella, or Momo in Mexico and Central America, and Mexican pepperleaf or root beer plant in the United States. Possess large ear-shaped leaves that can grow over 30 cm long, as well as a characteristic aroma, similar to sassafras but also with hints of anise and pepper. Thus, it is widely used in culinary (McBurnett et al., 2006) and also as bait for fish feeders (Joly, 1981).

Most studies from this species were focused on its essential oil, highlighting the dominance of phenylpropanoids like safrole (Monzote et al., 2010; Salehi et al., 2019), myristicin (Castañeda et al., 2007; Garcia Rios et al., 2007; McBurnett et al., 2006), elemicin and eugenol, as well as a wide range of terpenes (Parmar et al., 1997). Several non-volatile compounds have been reported, as piperochromenoic acid, piperochromanoic acid, piperoic acid, and 4-hydroxy-5-(*E*,*E*-farnesyl)benzoic acid, dictyochromenol (prenylated benzoic acids and derivates); (-)-γ-muurolene and *trans*-phytol (terpenoids); olean-12-ene-28-methyl ester-3-*O*-α-L-arabinofuranosyl-(1→2)-β-D-glucopyranoside, 3β-hydroxy-21-*O*-angeloyl-olean-12-en-28-oic acid (saponins) (Salleh, 2021); and cepharadiones A and B (alkaloids) (Parmar et al., 1997).

The species *P. auritum* has shown a prominent activity with different traditional uses to treat fever, sore throat, gout, angina, erysipelas, colic, headache, dysmenorrhea, snakebites, as well as a diuretic, appetite stimulant, local anesthetic, and wound poultice (Salehi et al., 2019). Methanolic extracts from leaves displayed reasonable radical scavenging, insecticidal, anti-diabetic, anti-leishmanial, and cytotoxic activities (Salleh, 2021).

1.2. Objectives

1.2.1. Main Goal

To conduct a comprehensive phytochemical analysis of *P. auritum* and characterize the chemical differences between organs and during ontogeny.

1.2.2. Specific Goals

To conduct a metabolic fingerprinting of different organs of *P. auritum* by HPLC.

To purify and identify the most abundant secondary metabolites from the different organs/ages by chromatographic, spectrometric, and spectroscopic methods.

To establish differences in its metabolic profile during ontogeny.

1.3. Results and Analysis

1.3.1. Phytochemistry

1.3.1.1. Chromatographic fingerprinting and method optimization

The methanolic extracts of leaves, fruits, stems, and roots of *P. auritum* were analyzed by HPLC-DAD at 270 nm, and the chromatograms of each organ (Figure 4) displayed notorious differences among profiles excepting the stem, in which no significant peaks were detected. The chromatographic profiles and its PCA (Figure 5) suggested considerable differences in secondary metabolite content composition in each organ. The roots possess most of their significant peaks at the end of the chromatogram analysis suggesting the presence of hydrophobic compounds, while leaves and fruits contained more polar compounds eluting with shorter retention times.

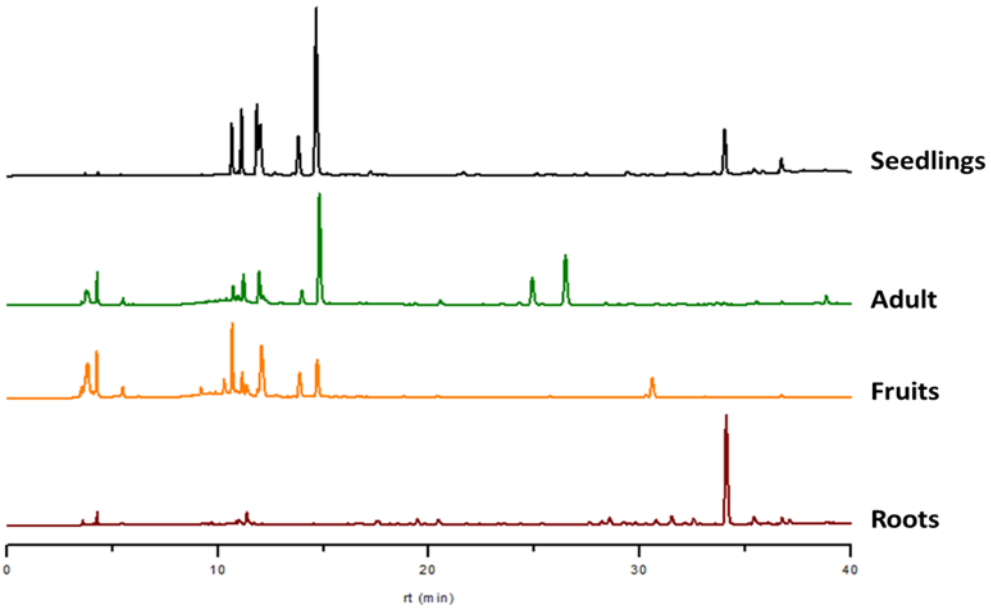

Figure 4. HPLC-DAD (270 nm) profiles of leaves (seedling and adult), fruits, and roots of *P. auritum*

(Normalized and autoscaled)

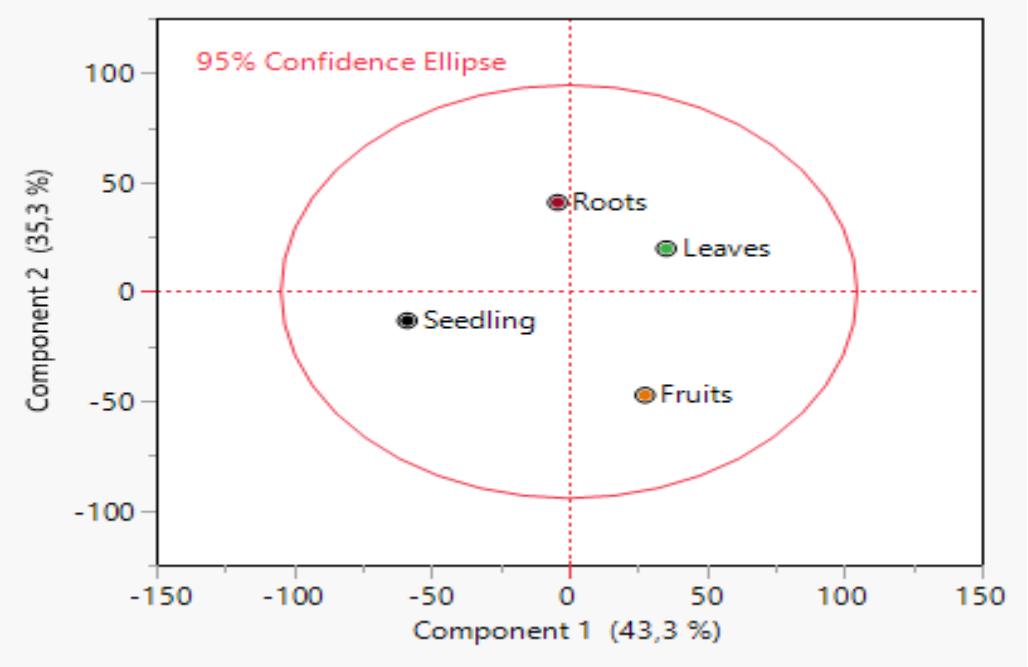

Figure 5. Score plot based on HPLC-DAD from crude extracts of adult and seedling leaves, roots, and fruits of *P. auritum.*

1.4.1.2. Roots

The dried and ground roots (102.03 g) were extracted in MeOH, yielding 11.06 g of extract, then submitted to a partition with DCM leading to 1.73 g of a fraction. Next, this fraction was submitted to a flash column chromatography (7 cm x 8.5 cm column; 100 g of silica gel, Sigma-Aldrich, 70 – 230 Mesh), eluted with hexane-ethyl acetate (Hex-EtOAc), yielding 36 fractions of 150 mL. Then, two volumes of EtOAc and MeOH were used to wash the column and recover the most polar compounds. All fractions were analyzed by TLC (Hex / EtOAc 7 -3) under UV light (Figure 6). From fractions 1-2, eight compounds were identified by GCMS as octadecan-1-ol (**1**), 14-methylpentadecanoic acid methyl ester (**2**), 1-heneicosyl formate (**3**), docosane (**4**), nonadecane (**5**), nonacosane (**6**), 1-pentacosanol (**7**), and dotriacontane (**8**), according to the Wiley 19 library.

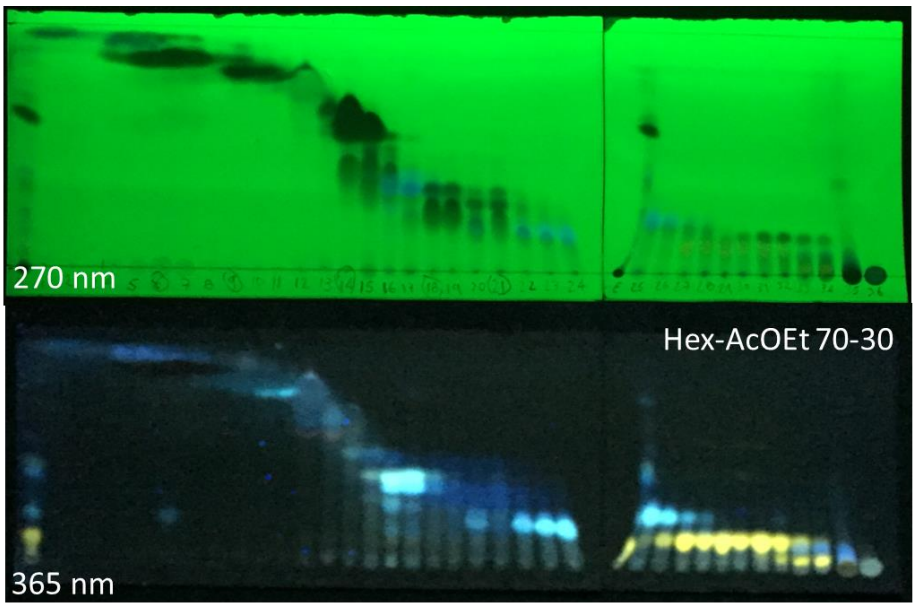

Figure 6. TLC of the column fractions from methanolic extract of roots of *P. auritum* at 254 nm (up) and 365 nm (bottom).

Fraction 5 (48 mg) displayed a major peak in 32.1 minutes with a $[M+H]^+$ of 223.0980 Da (calculated for $C_{12}H_{15}O_4$). Its ^1H NMR spectrum displayed signals at δ 6.30 (1H s, Ar), 5.94 (3H m, olefinic H and -O-CH_2-O), 5.04 (2H m, terminal olefinic moiety), 3.87 (OCH_3, s), 3.85 (OCH_3, s) and 3.30 (2H, bd, 13.7Hz).

These data matched with the structure of the phenylpropanoid dillapiole (**9**), a typical compound in the essential oil of *P. aduncum* (De Almeida et al., 2009), *P. solmsianum*, *P. regnellii,* and *P. gaudichaudianum*.

Fraction 14 (200 mg) corresponds to the major compound in the extract; its HPLC-MS chromatogram showed a single peak with $[M+H]^+$ at 224.2049 Da corresponding to the formula $C_{14}H_{25}NO$. 1D-NMR spectrum was complex, and therefore ^{13}C, ^{1}H-2D experiments HMBC and HSQC were carried out (Table *1*), and the amide pellitorine (**21**) was identified (Dembitsky, 2007; Malhotra et al., 1990).

Table 1. HSQC correlations of pellitorine (**21**).

Position	^{1}H δ *J* (Hz)	^{13}C δ
1	-	166.6
2	5.79 (1H d, 15.0)	121.8
3	7.19 (1H dd, 15.0, 10.4)	141.3
4	6.07 (2H m)	128.2
5	6.11(2H m)	143.3
6	2.14 (2H dd,14.2, 7.1)	32.9
7	1.36 -1.28 (4H m)	31.9
8	1.36 -1.28 (4H m)	28.5
9	1.46 – 1.38 (2H m)	22.4
10	0.89 (3H t, 7.0)	14.0
1´	3.16 (2H t, 6.5)	47.4
2´	1.80 (1H m)	28.6
3´	0.92 (6H d, 6.7)	20.1
NH	5.83 (1H bs)	-

Pellitorine (Figure 7), identified as the major compound in the fraction, was reported previously from *Piper nigrum* (Miyakado et al., 1979).

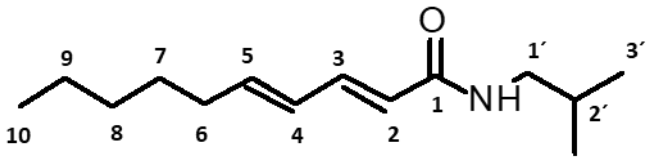

Figure 7. Structure of pellitorine (**21**).

Three compounds (Figure 8) were identified in fractions 26-32 (36 mg). HPLC-MS displayed the $[M+H]^+$ peaks in 306.0748 Da, 322.1088 Da, and 202.1228 Da, corresponding to cepharadione A (**11**), cepharadione B (**12**), and *N*-cinnamoylpyrrolidine (**13**), respectively. These compounds were reported for several *Piper* species (De Oliveira Chaves et al., 2003) (Parmar et al., 1997). The minor compounds were annotated directly from the methanolic extract based on HPLC-ESI data obtained in the positive mode (Figure 8). *N*-cinnamoylpyrrolidine was the major compound; the ^{1}H NMR spectrum of the mixture displayed a characteristic pattern for a cinnamoyl moiety: δ7.70 (1H d, 15.5 Hz), 7.54 (2H d, 6.47 Hz), 7.37 (3H m) and 6.73 (1H d, 15.5 Hz) and the BPC showed a diagnostic fragment in 131 m/z. Compounds 11 and 12 were minor, and only small multiplets around 9.5 ppm were observed.

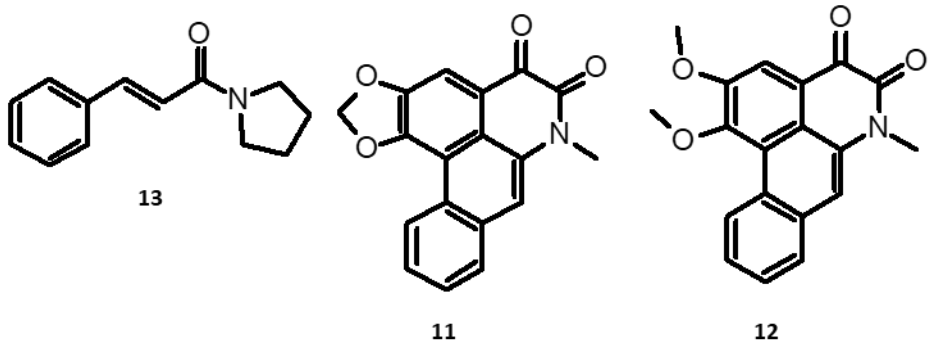

Figure 8. Structures of **13** *N*-cinnamoylpyrrolidine, **11** cepharadione A and **12** cepharadione B.

Table 2. Annotations of secondary compounds in the roots of *P. auritum* by LC-MS^2.

					LC-MS²		
No	**rt (min)**	**$[M+H]^+$ (Da)**	**Fragmentary Ions (*m/z*)**	**Formula**	**Error (ppm)**	**ID**	**Ref.**
10	9.6	342.1712	237.0911 (16), 265.0857(74), 282.0983 (16),297.1127 (95), 342.1712(85)	$C_{21}H_{27}NO_3$	< 100	Unknown	
13	22.8	202.1229	103.0447 (98), 131.0475 (31)	$C_{13}H_{16}NO$	1.48	1-cinnamoylpyrrolidine	(Achenbach and Witzke, 1979; De Oliveira Chaves et al., 2003)
	23.4	308.0933	209.0852 (33), 265.0768 (55), 293.0829 (79, 308.0973 (39)	$C_{18}H_{13}NO_4$	5.2	Unknown	Unknown
11	26.3	306.0766	220.0766 (14), 248.0673 (15), 278.0844 (53), 306.0787 (89)	$C_{18}H_{11}NO_4$	1.96	cepharadione A	(Chen et al., 2004; Dyer and Palmer, 2004; Lin et al., 2013; R Mata et al., 2004; Parmar et al., 1997)
15	28.0	274.1459	115.0517 (20), 135.0420 (82), 143.0471 (16), 171.0436 (14), 201.0548 (56)	$C_{16}H_{19}NO_3$	3.28	piperlonguminine isomer	(Kyung et al., 2004; Parmar et al., 1998)
16	28.6	274.1466	115.0511 (62), 135.0421 (83), 143.0471 (24), 171.0434 (24), 201.0545 (63)	$C_{16}H_{19}NO_3$	4.38	piperlonguminine isomer	(Kyung et al., 2004; Parmar et al., 1998)
12	28.9	322.1091	261.0790 (10), 278.0828 (17), 306.0748 (63), 322.1285 (64)	$C_{19}H_{15}NO_4$	2.48	cepharadione B	(Michinori et al., 1974)(R Mata et al., 2004)

17	29.7	274.1455	115.0518 (29), 135.0419 (81), 143.0475 (32), 171.0442 (18), 201.0552 (82)	$C_{16}H_{19}NO_3$	2.92	piperlonguminine isomer	(Kyung et al., 2004; Parmar et al., 1998)
18	31.0	302.1786	135.0422 (84)	$C_{18}H_{23}NO_3$	5.29	1-[7-(3,4-methylenedioxyphenyl)-2,6-heptadienoyl]pyrrolidine isomer	(Likhitwitayawuid et al., 1987)
19	31.8	304.1937	107.0450 (6)123.0409 (19), 135.0422 (82), 173.0951 (9), 304.1941 (19)	$C_{18}H_{25}NO_3$	3.28	pipercallosidine	(Pring, 1982)
20	33.6	330.2072	135.0415 (80), 257.1009 (24)	$C_{20}H_{27}NO_3$	2.72	pipercallosine	(Pring, 1982)
21	33.7	224.2039	151.1106 (74), 168.1380 (77)	$C_{14}H_{25}NO$	4.46	pellitorine	(Loder et al., 1969) (Parmar et al., 1997)(Tuntiwachwuttikul et al., 2006)(Vasques et al., 2002)
22	35.0	238.2195	98.0548 (72), 109.0940 (70), 123.1126 (45), 168.1408 (34)	$C_{15}H_{27}NO$	8.4	2,4-Decadienoic acid 2-methylbutylamide	(Stohr et al., 1999)

1.4.1.3. Fruits

From the previous chromatographic data, it was known that the fruits contained a set of compounds of high and low polarities. To simplify the purification steps, a sequential extraction was considered starting with 68 g of dried and ground fruits, extracted exhaustively with DCM and then with MeOH, yielding 4.03 g and 8.88 g, respectively. The new profiles (Figure 9) showed an adequate separation between both types of metabolites, the DCM extract (DF) was an oleoresin, analyzed by HPLC-MS, GCMS and ^{1}H NMR, while the methanolic extract (MF), too polar for normal phase chromatography, was analyzed by HPLC-MS and ^{1}H NMR.

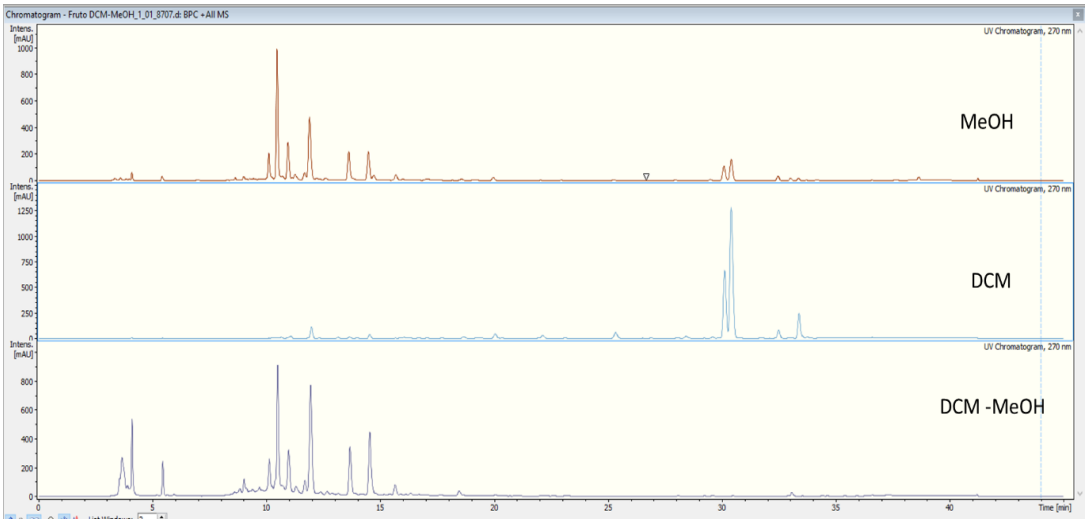

Figure 9. HPLC-DAD chromatogram detected at 270 nm, comparison between methanolic extract, DF, and MF.

The HPLC-DAD of DF contained two major peaks in 30.1 and 30.4 min. However, since the ionization under HPLC-ESI was not efficient, the samples were submitted to GCMS analysis which showed three predominant peaks. While the MS data of the largest one matched with the phenylpropanoid asarone (**10**), the other compounds were identified as myristicin (Santos et al., 1998) **(23)** and methyleugenol (**24**) (Rachel Mata et al., 2004). The analysis of ^{1}H NMR spectra showed signals of a phenylpropene moiety and confirmed the structure of elemicin (**25**), a common phenylpropanoid in *Piper* (Usia et al., 2005), as the main component. Elemicin and

methyleugenol were reported for *P. auritum* for the first time, while myristicin was described for several *Piper* species (Parmar et al., 1997).

Since MF contained high polarity compounds, not suitable for normal phase chromatography, separations by RP C-18 CC and Sephadex LH-20 in MeOH were attempted without successful purification. Thus, a semipreparative HPLC approach improved the previously developed method and escalated it to semipreparative conditions (Figure 10). Using this procedure, seventeen fractions were collected, yielding eight compounds (Figure 11) and subsequently analyzed by HPLC-MS (Table 3) and NMR (Table 4).

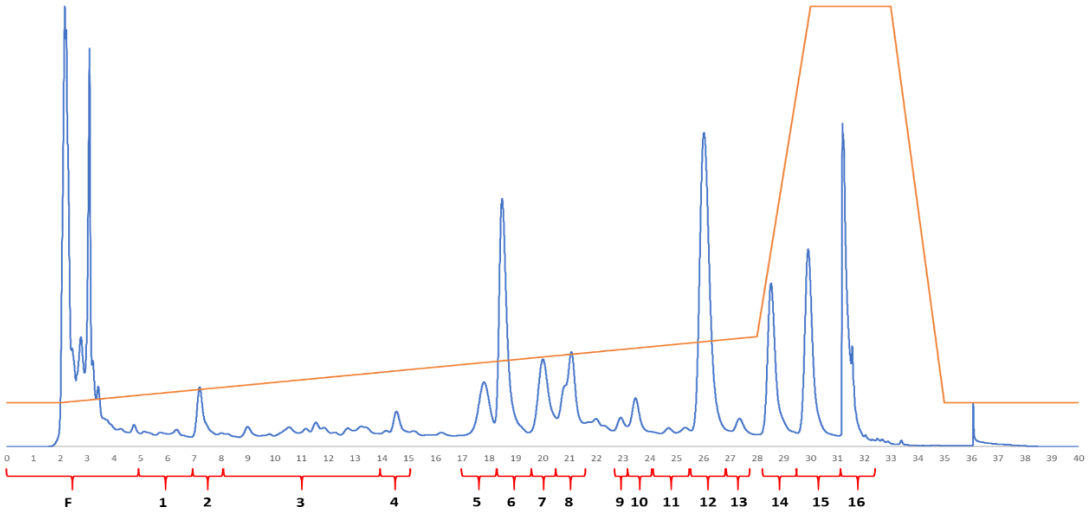

Figure 10. HPLC-DAD chromatogram detected at 270 nm of MF at semipreparative conditions.

Only the peaks between 16 and 26 min (in the analytic method) were considered for further analysis; the molecular formulas were calculated using the $[M+H]^+$ and $[M+Na]^+$ peaks. Due to the poor fragmentation and the similarity among most of the mass spectra, the collision energy was increased up to 40 eV to obtain a higher fragmentation and additional structural information. Eight glycosyl flavones derived from apigenin and luteolin were annotated (Table 3). The fraction F8 was shown to contain two coeluted compounds.

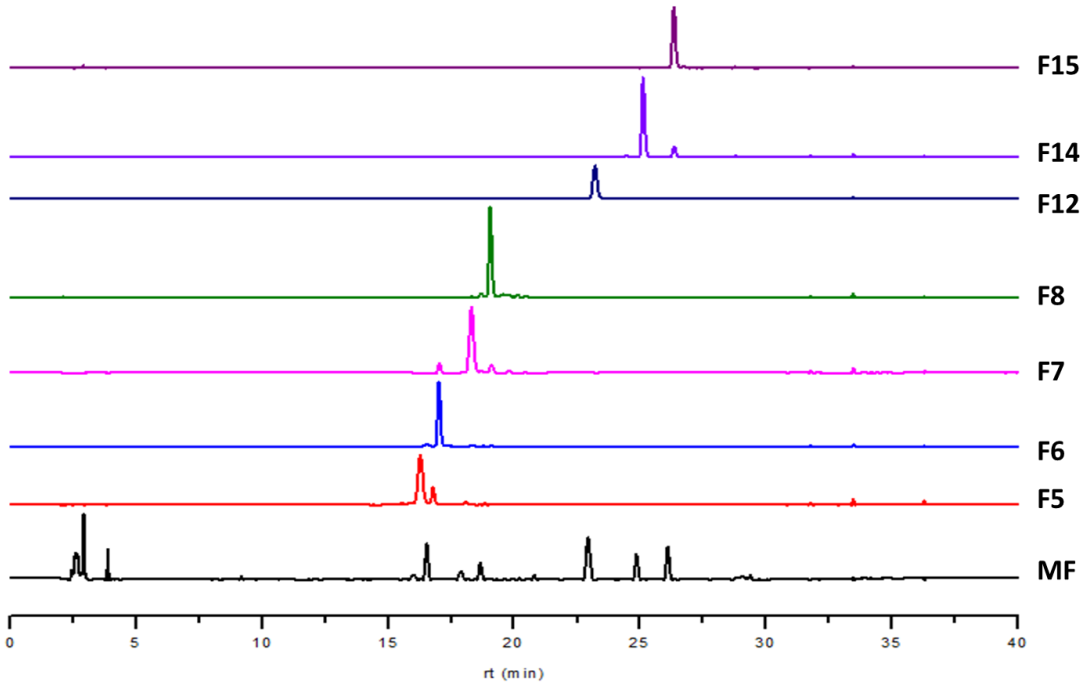

Figure 11. HPLC-DAD chromatogram detected at 270 nm of MF and relevant fractions.

Then, NMR (^{1}H, HSQC, HMBC, and NOESY) analyses of the isolated flavonoids were conducted, and the identities of the compounds were confirmed (Table 4).

Table 3. Annotated compounds from MF .

Code	rt (min)	Quantity (mg)	$[M+H]^+$ (Da)	$[M-H]^-$ (Da)	MW (Da)	Formula	Ref MW (Da)	Error (ppm)	UV/Vis λ_{max} (nm)	ID
F5	16.1	2.2	595.1670	593.1501	594.1591	$C_{27}H_{30}O_{15}$	594.1585	-4.0	230, 256, 267, 348.	**vitexin -*O*-glucoside**
F6	16.6	5.3	449.1109	447.0867	448.1030	$C_{21}H_{20}O_{11}$	448.1006	1.8	209, 255, 266, 347.	**orientin**
F7	17.8	4.3	579.1730	577.1561	578.1651	$C_{27}H_{30}O_{14}$	578.1635	-1.6	194, 228, 268, 336.	**vitexin -*O*-rhamnnoside**
F8a	18.7	0.6	433.1135	431.0908	432.1056	$C_{21}H_{20}O_{10}$	432.1056	2.5	215, 267, 342.	**vitexin**
F8b			463.1265	461.1018	462.1186	$C_{22}H_{22}O_{11}$	462.1162	0.2		**scoparin**
F9	20.2	0.2	463.1256	461.1086	462.1177	$C_{22}H_{22}O_{11}$	462.1162	0.7	243, 269, 333.	**swertiajaponin Isomer**
F12	22.9	1.8	593.1889	591.1721	592.1810	$C_{28}H_{32}O_{14}$	592.1792	-4.0	197, 215, 269, 332.	**margaritene**
F14	24.8	1.0	447.1319	445.1086	446.1240	$C_{22}H_{22}O_{10}$	446.1213	0.4	196, 223, 268, 330.	**trematin**
F15	26.0	1.0	461.1483	459.1239	460.1404	$C_{23}H_{24}O_{10}$	460.1370	-0.5	197, 223, 268, 330.	**isoembigenin**

Table 4. Annotated C-glycosylflavonoids isolated by semipreparative HPLC from MF.

No		tr (min)	Compound	R	R_1	R_2	R_3	R_4
26	**F5**	16.1	vitexin-6''-O-glucoside	H	H	H	Glu-Glu-	H
27	**F6**	16.6	orientin	H	H	H	Glu-	OH
28	**F7**	17.8	vitexin-2''-O-rhamnoside	H	H	H	Rha-Glu-	H
29	**F8-a**	18.7	vitexin	H	H	H	Glu-	H
30	**F8-b**		scoparin	H	H	H	Glu-	OMe
31	**F12**	22.9	margaritene	Me	H	H	Rha-Glu-	H
32	**F14**	24.8	trematin	Me	H	H	Glu-	H
33	**F15**	26.0	isoembigenin	Me	Me	H	Glu-	H

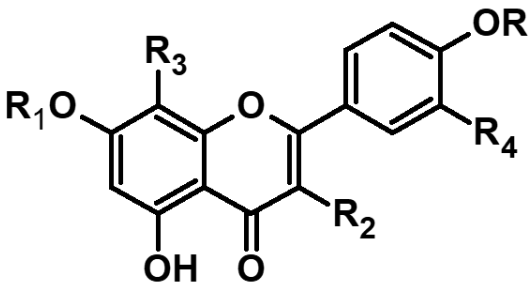

1.4.1.4. Leaves

An amount of 525 g of dry and ground leaves of *P. auritum* was extracted exhaustively with distilled methanol (IQ-USP). The solution was concentrated under reduced pressure (Buchi R-215) and dried at room temperature yielding 87.7 g of crude extract. Chlorophyll was removed by flocculation with a MeOH-H_2O (8-2) mixture and vacuum filtration in Celite® 545 (Sigma-Aldrich); the remaining solution was extracted twice, first with hexane and then with dichloromethane (3 times with 140 mL for each solvent) according to the described protocol (Fernandes et al., 1997). Both fractions were analyzed by TLC under UV light (254 and 340 nm), 5.0 g of the DCM fraction and 3.24 g of the hexane fraction were obtained.

The DCM fraction obtained from *P. auritum* leaves (5.0 g) was submitted to a flash silica gel (Sigma-Aldrich, 200-400 Mesh, 200 g), a column (30 cm x 5 cm) using a mixture of Hex-EtOAc (9-1) and with increasing the amount of EtOAc and then with EtOAc-MeOH until pure MeOH yielding a total of 36 fractions, all fractions were analyzed by TLC (Hex / EtOAc 6-4) under UV light (Figure 12).

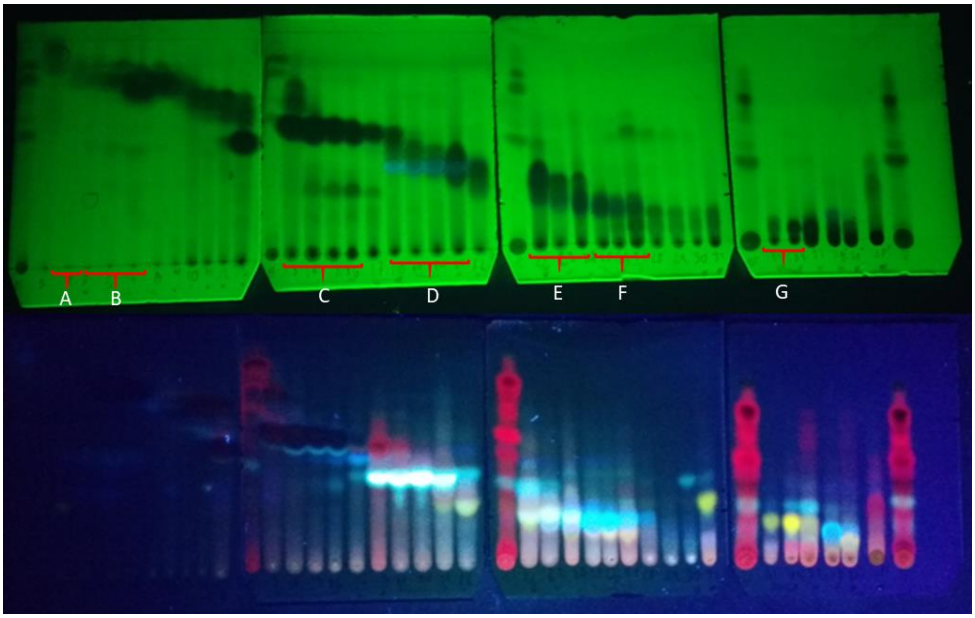

Figure 12. TLC of the column fractions from methanolic extract of leaves *P. auritum* at 254 nm (up) and 365 nm (bottom).

The fractions were pooled according to their similarity, and after several purification steps, compounds **34** and **35** were isolated from subfraction C as white needle crystals; HPLC-MS and NMR analysis were conducted. Two main peaks with different retention times (24.4 and 25.9 min, respectively) but the same $[M+H]^+$ (233.0736 Da) and similar ^1H NMR spectra (Table *5*) were obtained; after 2D-NMR analyses, structures (Figure 13) were identified as 4,6-dimethoxy-5-*Z*-phenylbutenolide (**34**) and 4,6-dimethoxy-5-*E*-phenylbutenolide (**35**) found in leaves of *P. malacophylum* (Lago et al., 2005).

Table 5. Phenylbutenolides and dimer from leaves of *P. auritum*.

Position	**35** (*E*)		**34** (*Z*)		**36**			
	^1H (mult, *J*)	**^{13}C (mult, *J*)**	**^1H (mult, *J*)**	**^{13}C (mult, *J*)**	**^1H (mult, *J*)**	**HSQC**	**HMBC**	**NOESY**
2		167.9 (C=O)		168.1 (C=O)		170.53 (C=O)		
3	5.13 (s)	87.5 (CH)	5.29 (s)	88.9 (CH)	5.18 (s)	91.47(CH)	C-2, C-4	6-OCH_3, 4-OCH_3, H-8/12
4		170.8 (C)		171.7 (C)		180.90 (C)		
5		128.9 (C)		134.9 (C)		89.5 (C)		
6		144.0 (C)		144.6 (C)		89.28 (C)		
7		130.7 (C)		131.0 (C)		135.29 (C)		
8	7.37-7.47 (m)	130.2 (CH)	7.72-7.74 (m)	128.9 (CH)	7.46 - 7.52 (m)	128.67 (CH)	C-5, C-6, C-9	6-OCH_3, 4-OCH_3, 3-H
9	7.37-7.47 (m)	127.9 (CH)	7.37-7.47 (m)	128.5 (CH)	7.31-7.36 (m)	128.60 (CH)	C-7, C-8	6-OCH_3, 4-OCH_3
10	7.37-7.47 (m)	130.0 (CH)	7.37-7.47 (m)	130.0 (CH)	7.31-7.36 (m)	128.60 (CH)	C-7, C-9/11	6-OCH_3, 4-OCH_3
11	7.37-7,47 (m)	127.9 (CH)	7.37-7.47 (m)	128.5 (CH)	7.31-7.36 (m)	128.60 (CH)	C-7, C-8	6-OCH_3, 4-OCH_3
12	7.37-7,47 (m)	130.1 (CH)	7.72-774 (m)	128.9 (CH)	7.46 - 7.52 (m)	128.67 (CH)	C-6, C-5, C9	6-OCH_3, 4-$OCH_3$5, H-3, H-8/12.

4-OCH_3	3.60 (s)	58.9 (CH_3)	4.05 (s)	59.6 (CH_3)	3.45	59.92 (CH3)	C-4	6-OCH_3, H-3, H-8, H-9.
6-OCH_3	3.75 (s)	58.8 (CH_3)	3.66 (s)	60.3 (CH_3)	2.97	54.05 (CH3)	C-6	4-OCH_3, H-3, H-8, H-9.

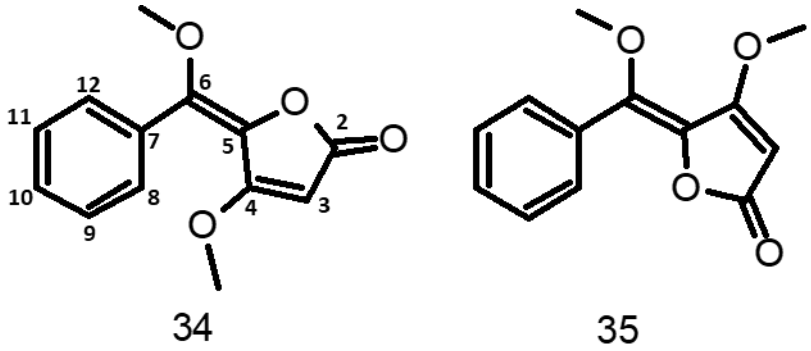

Figure 13. Structures of phenylbutenolides **34** and **35**.

During the process, compound **36** with almost identical spectroscopic and spectrometric features was found in fraction F. However, differences in the retention time (27.5 min) and the chemical shift of one signal suggested differences in its structure. The BPC also showed substantial similarity to the butenolides, displaying the base peak at 233.078 Da and the $[2M+H]^+$ peak at 465.157 Da. The occurrence of dimers is frequent and has been observed in a large number of samples, in this case, the $[2M+H]^+$ peak was observed while it was not present in the extract or the pure compounds; thus, an MRM analysis (Figure 14) was conducted using lower collision energy (2.0 eV) and obtaining the same peaks again. Then, it was concluded that the peak at 465.1574 Da is, in fact, the *quasimolecular* ion $[M+H]^+$ of a dimer (Figure 15) of the phenylbutenolides.

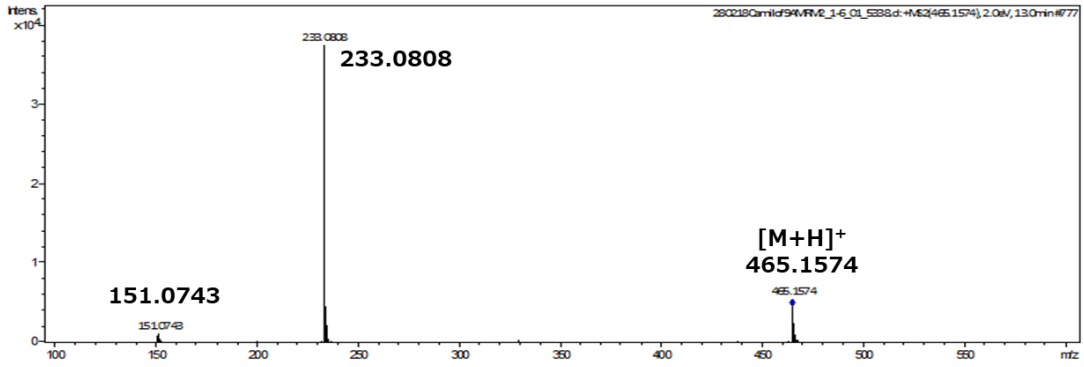

Figure 14. BPC of a dimer from the phenylbutenolides.

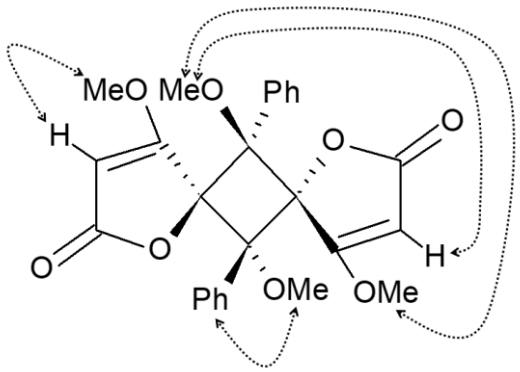

Figure 15. Structure of phenylbutenolide cyclobutane-type dimer (**36**) with its NOESY correlations.

Dimerization induction test will be conducted using methanolic solutions of compounds **34** and **35** to confirm the formation of this dimer.

From subfraction D, successive chromatographic steps yielded a solid (yellow needles), HPLC-MS analysis showed a $[M+H]^+$ at 280.1106 Da and $[M-H]^-$ of 278.0643 Da, corresponding to a molecular formula of $C_{17}H_{13}NO_3$. The ^1H NMR (500 MHz, $CDCl_3$) data at δ 9.27 2H m (H-6), 7.94 1H bs (NH), 7.85- 7.83 2H m (H-3, H-10), 7.61 2H m (H-7, H-8), 7.11 1H s (H-9), 4.16 3H s (5-OMe), 4.16 3H s (4-OMe) corresponded to the aristolactam cepharanone B (**37**) (Desai et al., 1988).

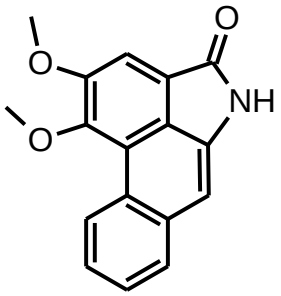

Figure 16. Structure of cepharanone B (**37**).

Subfraction F was submitted to several chromatographic purification steps. First, a fluorescent compound was partially purified, despite the low quality of the ^{1}H NMR spectra; it presented some similarities to the ^{1}H NMR spectrum of cepharanone B, a similar fluorescence and odd molecular mass, suggesting the presence of a nitrogen atom. Second, HPLC-MS analysis showed a $[M+H]^{+}$ of 266.0872 Da, and the calculated formula $C_{16}H_{16}NO_3$ corresponding to piperolactam A (**38**).

Finally, fraction A was analyzed by GCMS due to its low polarity and its similarity to the essential oil of the plant. The chromatogram displayed two major peaks with retention times of 15.9 min and 19.9 min and an M^{+} of 208 and 232 Da, respectively. The ^{1}H NMR spectrum presented a profile intense peaks of aromatic and olefinic hydrogens, as well as the of three methoxy groups: ^{1}H NMR (500 MHz, $CDCl_3$) δ 7.02 (d, *J* = 8.6 Hz, 1H), 6.73 (d, *J* = 8.6 Hz, 1H), 6.70 (s, 1H), 6.53 (s, 1H), 5.96 (ddt, *J* = 16.8, 10.2, 6.5 Hz, 1H), 5.42 (s, 1H), 5.06 – 5.00 (m, 2H), 3.87 (s, 3H), 3.82 (s, 3H), 3.79 (s, 3H), 3.32 (d, *J* = 6.5 Hz, 2H), 2.60 – 2.56 (m, 1H), 2.27 – 2.22 (m, 1H), 1.99 – 1.93 (m, 1H), 1.36 – 1.21 (m, 4H), 0.88 (t, *J* = 7.0 Hz, 2H). Signals A, B, E, G, H, I, J, and K (see supplementary material) corresponded to isoasarone (66.5%) while the remaining signals corresponded to gibbilimbol B (33.5%), both of them reported in *Piper marginatum* and *P. gibbilimbum,* respectively (Orjala et al., 1998; Santos et al., 1998).

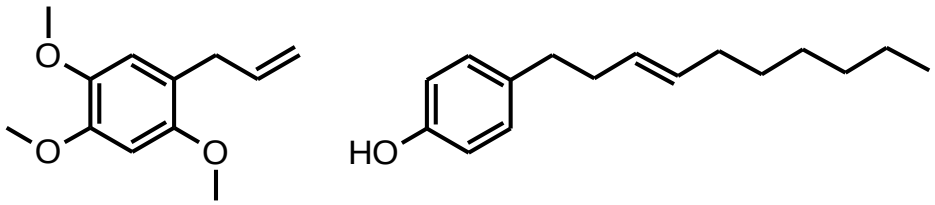

Figure 17. Structures of isoasarone (**39**) (left) and gibbilimbol B (**40**) (right).

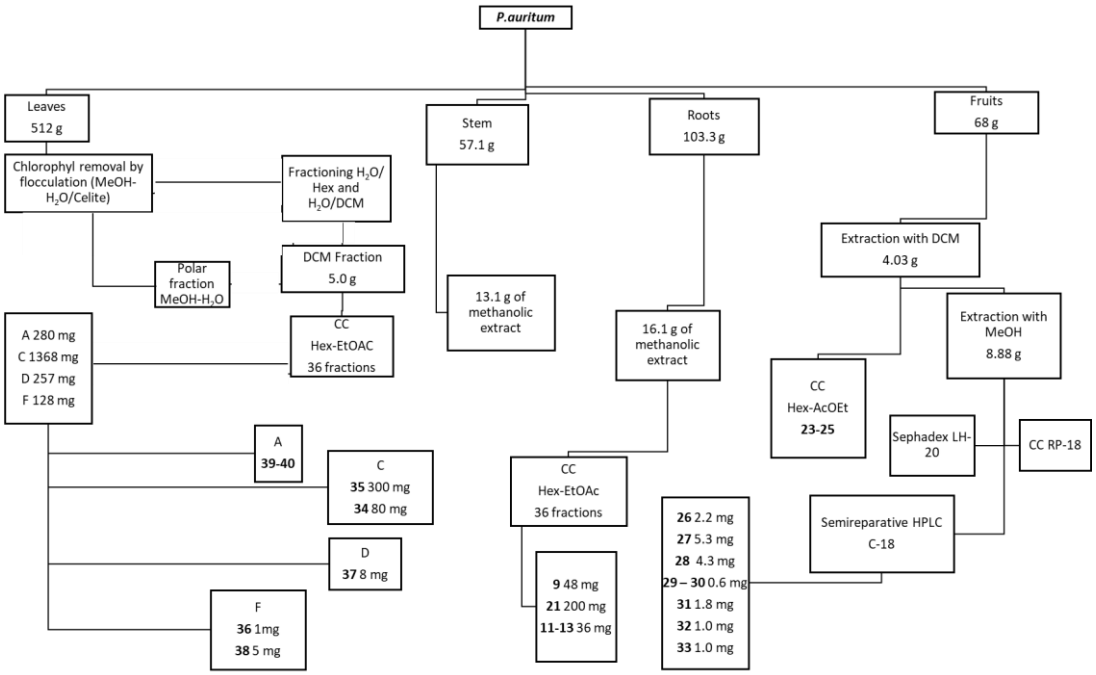

Figure 18. Summary of the purification steps for *P. auritum.*

1.3.2. Ontogeny

The analysis during the ontogeny of *P. auritum* plants was investigated by analyzing the composition of seedlings at different ages (Figure 19). Although no evident changes during the first months of development were noticeable, the PCA (Figure 20) showed at least two different clusters of seedlings. This fact could be explained using a single individual for the analysis; intraspecific variations and slight differences in the plant's environment could express the different amounts of metabolites. Nevertheless, the ratio among them indicated a reduction in the production of flavonoids at the adult stage except for isoembigenin (**33**) (Table 4).

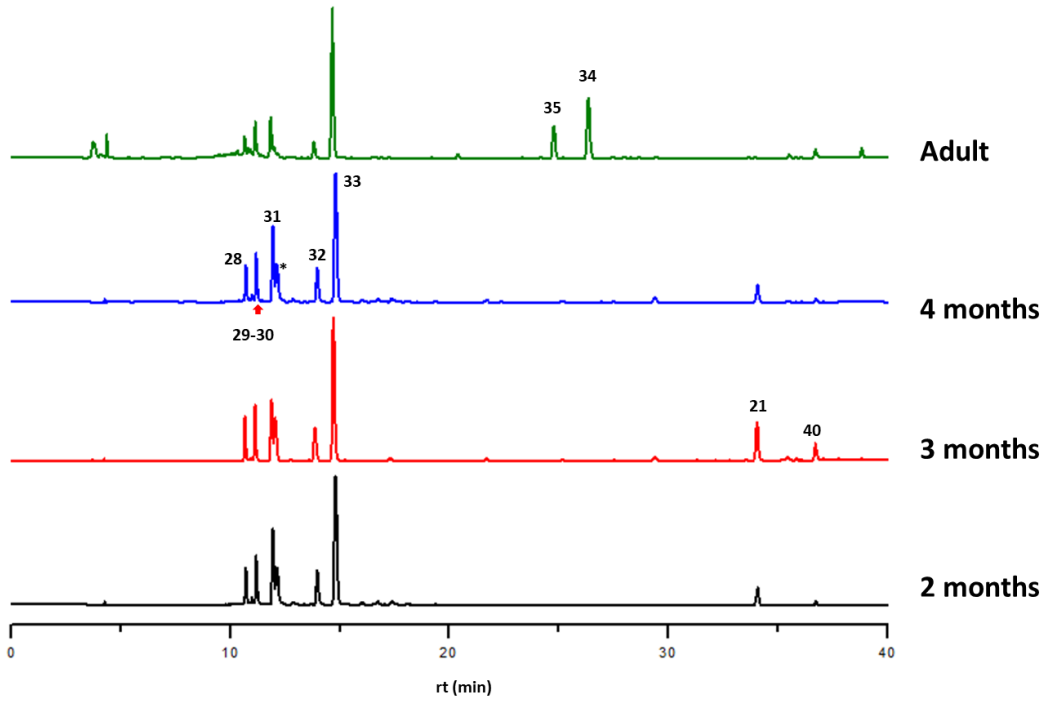

Figure 19. HPLC profiles of *P. auritum* leaves of 2-4 months old and adult leaves (270 nm).

These compounds are well known for their remarkable antioxidant and radical scavenging activities (Rauter et al., 2007); they could protect the plant against oxidative stress during the early developmental stages of the plants. On the other hand, the phenylbutenolides (**34-35**) were found exclusively in the adult stage. Finally, the amide pellitorine (**21**), the major compound in roots, was also expressed during the first stages in leaves (Figure 19), while it was not expressed in the adult stage in a similar fashion to *P. permucronatum* and *P. richardiaefolium* (Gaia et al., 2021), suggesting that chemistry during the early stages becomes a hybrid between leaves and roots and highlighting a viable defensive role of pellitorine and C-glycosylflavonoid during the early stages of development in the species.

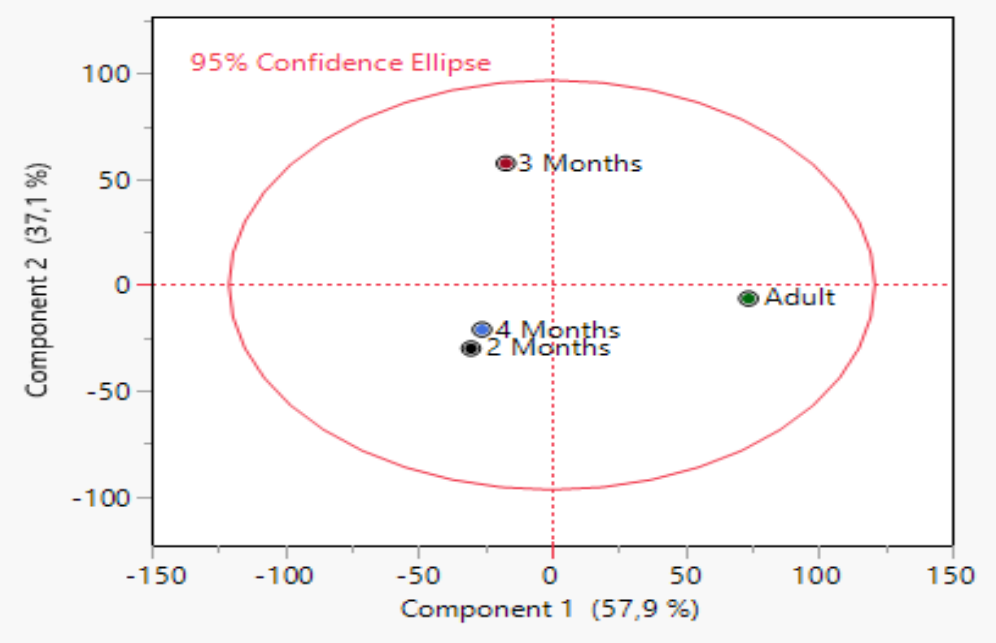

Figure 20. Score plot based on HPLC-DAD from crude extracts of seedling and adults of *P. auritum.*

Since most of the glycosyl flavonoid region peaks were not well resolved, the samples were analyzed with the HPLC method used to analyze MF, which allowed a better comparison with the identified compounds (Figure 21). In both development stages, isoembigenin (**33**) was the major compound, while vitexin (**29**), scoparin (**30**), and trematin (**32**) were also present in lower amounts. Additionally, another peak in 20.2 min with formula $C_{22}H_{22}O_{11}$ was observed, and it was annotated as a swertiajaponin isomer. The absence of vitexin-2''-O-rhamnoside (**28**) and the presence of margaritene (**31**) in trace amounts in the adult stage were the most significant differences during the plant's development.

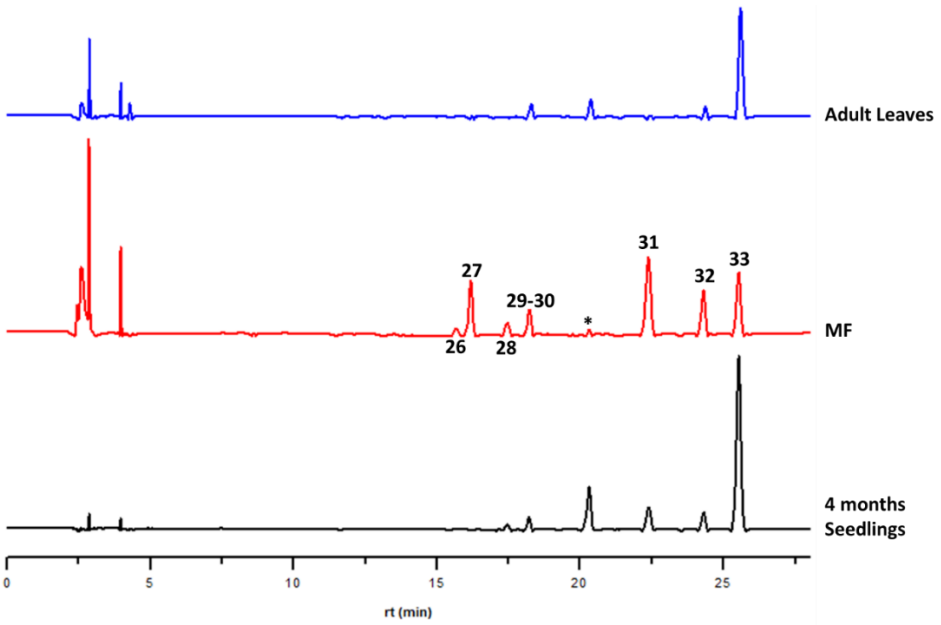

Figure 21. Comparison of the glycosyl-flavones region of adults, seedlings and MF by the new HPLC methodology (270 nm).

1.4. Conclusions

A high diversity of secondary metabolites was found in *P. auritum*, and the multivariate analysis showed remarkable differences among the organs, adults, and seedlings. The identified and annotated secondary metabolites could be grouped into four main sets of compounds: C-glycosylflavonoids, phenylbutenolides, amides and phenylpropanoids. While the roots were primarily composed of amides such as pellitorine as the major one, leaves and fruits were rich in *C*-glycosylflavonoids and phenylpropanoids. Furthermore, notable changes during the development were observed in leaves; pellitorine appeared as a significant compound in seedlings, presumably as a remnant or a translocation product from roots, while the phenylbutenolides are exclusive of adults (Figure 22).

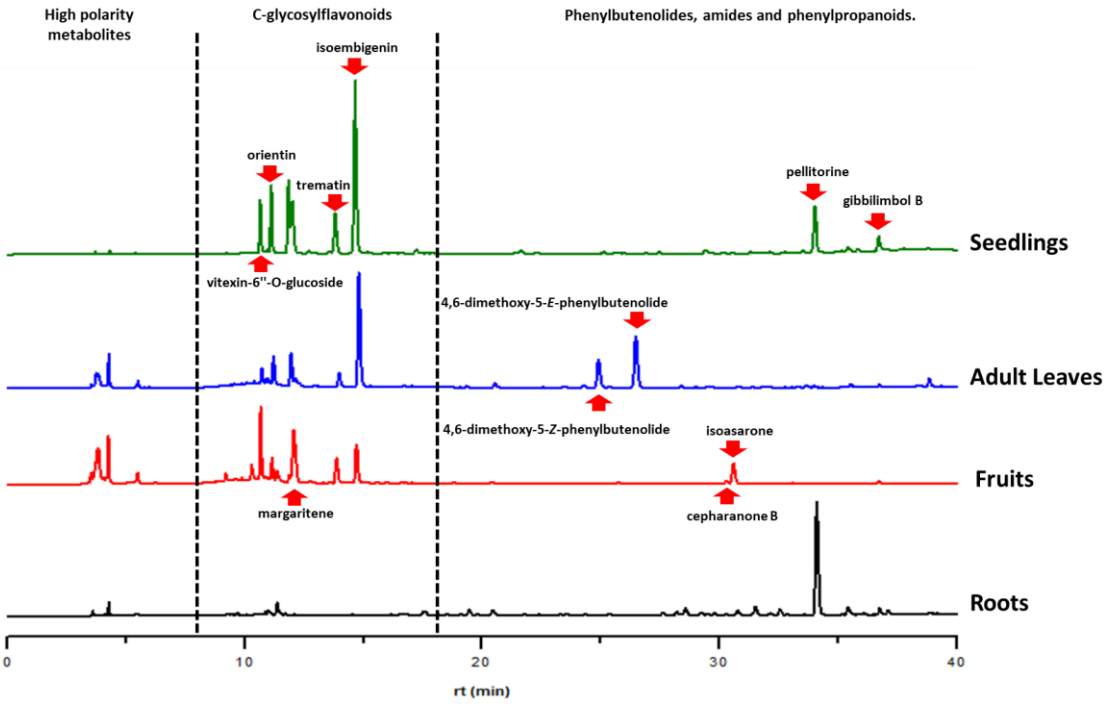

Figure 22. HPLC-DAD (270nm) profiles of the different organs of *P. auritum.*

Leaves were the most chemically diverse organ of the species with the most relevant metabolites, C-glycosyl flavonoids, conspicuous in young and adult plants. All the identified C-glycosyl flavonoids were reported for the first time in the Piperaceae family, while some analogs were found in *Peperomia* (Velozo et al., 2009), displaying a modest antifungal activity. The phenyl butenolides have been described from *P. fadyenii* (Nair et al., 1986; Pelter et al., 1981) and *P. malacophyllum,* displaying a potent activity against the phytopathogenic fungi *Cladosporium cladosporioides* and *C. sphaerospermum* (Lago et al., 2005). As detected in its essential oil, leaves also possessed a significant amount of phenylpropanoids, mainly composed of phenylpropanoids like safrole and elemicin (Garcia Rios et al., 2007) (Castañeda et al., 2007). These phenylpropanoids and some derivatives displayed a strong larvicidal activity against *Spodoptera litura* (Bhardwaj et al., 2010) as well as carcinogenic, insecticide (Pereira Filho et al., 2021), and antifeedant activities (Seigler, 1998). The alkylphenol gibbilimbol B belongs to the family of phenolic lipids, like resorcinols, which have demonstrated key antifungal, cytotoxic and antibacterial activities (Marentes-Culma et al.,

2019; Orjala et al., 1998). The roots were composed almost exclusively of amides, with pellitorine as the most abundant, and phenylpropanoids like dillapiole. Additionally, a large number of minor compounds (mostly amides) were annotated. Pellitorine is well known for its antifungal activity (Navickiene et al., 2000), like several amides from *Piper* (Gbewonyo et al., 1993). Therefore, the presence of analog compounds in *Piper* organs could be involved in the defense strategy of the plant. The synergic defensive effect of amides of *P. cenocladum* and *P. imperiale* against specialist (*Eois nympha*, Geometridae) and generalist (*Spodoptera frugiperda*, Noctuidae) has been demonstrated against pest insects; these amides disturbed the insect's fitness, had a negative effect on its survival, pupal mass or parasitoid resistance (Richards et al., 2010, 2003), reported from *P. gibbilimbum*, displayed a relevant cytotoxic and antimicrobial activity against *Staphylococcus epidermis* and *Bacillus cereus* (Orjala et al., 1998). Thus, it is well known that some of these compounds are expressed by plants as a response to different sources of stress produced by pathogens, wounding, and UV-irradiation (Solecka, 1997), supporting the idea of their function as a defensive role against biotic and abiotic factors.

Finally, fruits possessed compounds of opposite polarity, and they could be grouped in two sets: phenylpropanoids and *C*-glycosyl flavonoids. The latter was the most abundant in the whole plant, and that remained nearly constant during its development; these metabolites also showed different biological activities like antifeedant in combination with other compounds (Talhi and Silva, 2012).

Chapter 2. The phytochemistry of *Piper lindbergii C. DC.* and *Piper chimonantifolium* Kunth.

2.1. Introduction.

Piper lindbergii C.DC. (also known as *P. amplum* Kunth) and *Piper chimonantifolium* Kunth are two species not well chemically investigated. The only reports dealt with studies focused on their essential oils or crude extracts. This chapter is addressed to describe the main secondary compounds from samples collected in the Southern region of Brazil. The species *P. lindbergii* C.DC. has a high occurrence in Paraná state, and different biological properties have been described, including analgesics, cytotoxic, fungistatic, antitrypanosomal, insecticide and molluscicide. Its essential oil from leaves is composed mainly of monoterpenes like α-pinene, caryophyllene, caryophyllene oxide, and valencene (Bergo, 2010; Calderari, 2002; Costa et al., 1989; Pereira Filho et al., 2021).

The species *P. chimonantifolium* is a shrub native from the southeast region of Brazil (Monteiro and Guimarães, 2009); its essential oil was described as a source of mono- and sesquiterpenes, as well as phenylpropanoids (Riani et al., 2017). The only report of non-volatiles highlighted the chromene gaudichaudianic acid, flavonoids; dihydrooroxylin and pinocembrin, steroids; sitosterol, sitosteryl palmitate and stigmasterol (Lago et al., 2012).

2.2. Objectives

2.2.1. Main Goal

To describe the phytochemical composition of *P. lindbergii* C.DC. and *P. chimonantifolium* to contribute to the studies of plant-herbivore interactions.

2.2.2. Specific Goals

To identify the most abundant secondary metabolites from leaves of *P. chimonantifolium* by chromatographic, spectrometric, and spectroscopic methods.

To identify the most abundant secondary metabolites from leaves and roots of *P. lindbergii* C.DC. by chromatographic, spectrometric, and spectroscopic methods.

2.3. Results and Analysis

2.3.1. P. lindbergii C.DC.

First, 83.3 g of dry leaves were ground, extracted exhaustively with MeOH and analyzed by HPLC-DAD at 270 nm; the chromatogram (Figure 23) displayed two regions. A mild-polarity one with several peaks around 20-35 minutes and a lipophilic one around 45- 50 minutes showed the most intense peaks. For the purification of the main metabolites, 11.01 g of the extract were fractionated by flash chromatography (14 cm x 15 cm column; 500 g of silica gel, Sigma-Aldrich, 35-75μm / 22-440 Mesh) eluted with hexane-ethyl acetate (Hex-EtOAc), yielding 18 fractions of 500 mL, followed by two washes with methanol, acidic methanol, and water.

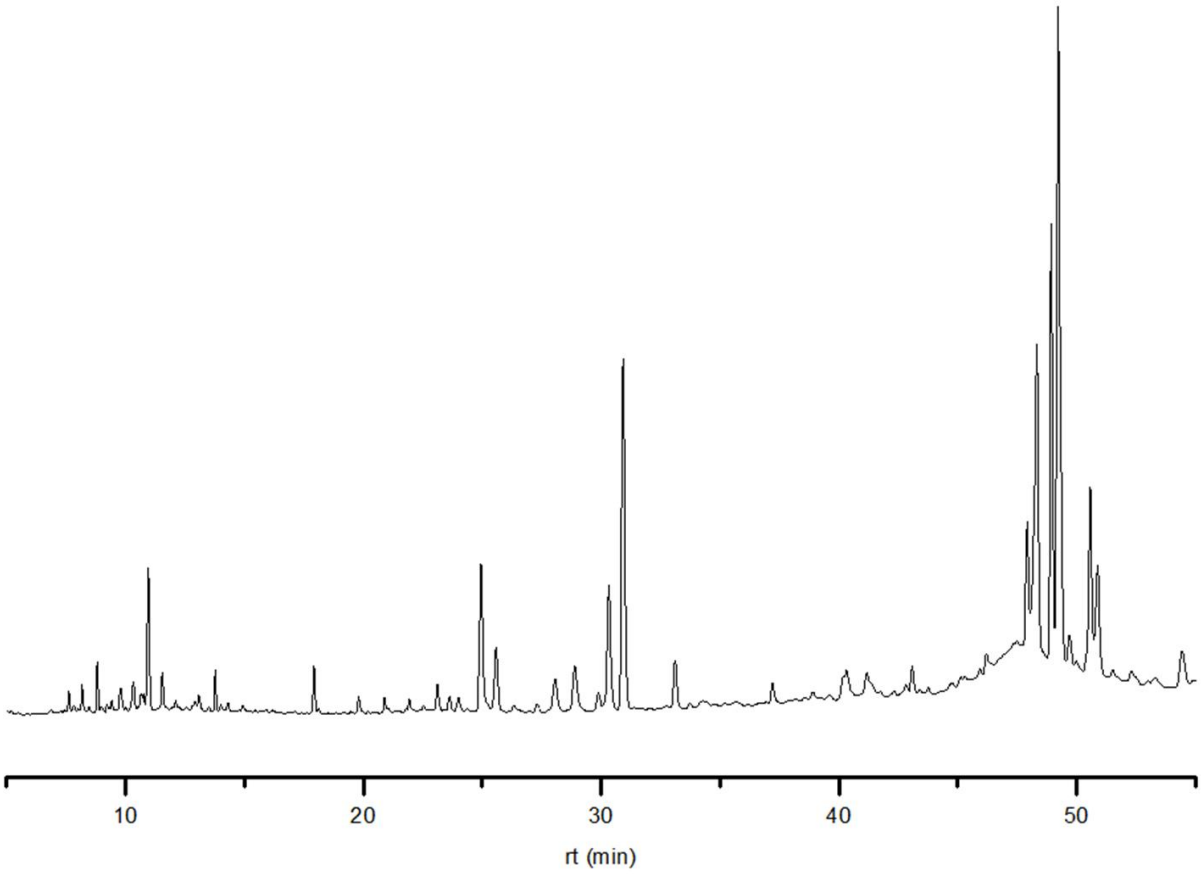

Figure 23. HPLC-DAD chromatogram of leaves from *P. lindbergii. C. DC*. (270 nm).

From fraction 12, a white solid was identified, and further chromatographic purifications steps yielded 10.0 mg of white crystals. The HPLC-DAD analysis showed that it corresponded to the peak in 30.93 min. The HRMS in positive and negative modes displayed a $[M+H]^+$ ion of 287.1287 Da and a $[M-H]^-$ of 285,1286 Da, corresponding to the molecular formula $C_{17}H_{18}O_4$. The ^1H NMR spectra (Figure 24) showed the following data:(500 MHz, $CDCl_3$)δ 14.27 (s, 1H), 7.30 (t, J = 7.4 Hz, 2H), 7.25 – 7.18 (m, 3H), 5.92 (s, 1H), 3.82 (s, 3H), 3.32 (d, J = 7.8 Hz, 2H), 3.00 (d, J = 7.8 Hz, 2H), 2.05 (s, 3H).suggested the presence of a chelated proton, a monosubstituted aromatic ring, a methoxy group and a methyl linked to an sp^2 carbon as well as two vicinal methylenes.

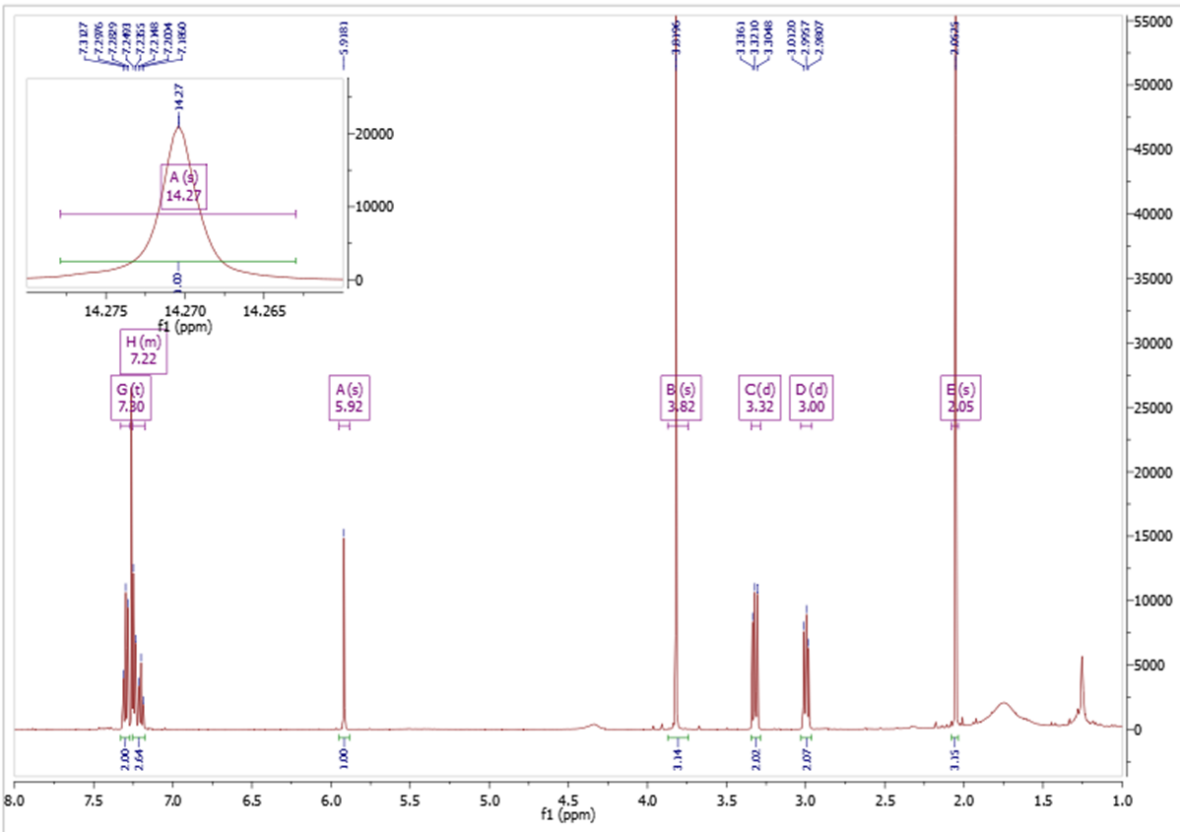

Figure 24. ^1H NMR spectra of myrigalone H (**41**).

HSQC, HMBC and MS^2 experiments confirmed the previous observations and revealed that the singlet in 5.92 ppm corresponded to an aromatic proton. The analysis concluded that the compound was the dihydrochalcone myrigalone H (**41**), reported for *Syzygium jambos*

(Jayasinghe et al., 2007), *Syzygium samarangense* (Kuo et al., 2004) (Myrtaceae) and *Myrica serrata* (Gafner et al., 1996)(Myricaceae).

Table 6. NMR spectral data of myrigalone H (**41**).

Position	^{1}H δ *J*(Hz)	^{13}C δ	HMBC
1	-	105.45	
2	-	164.94	
3	-	103.15	
4	-	160.43	
5	5.92 (s)	89.91	C-3, C-1, C-4, C-7
6	-	160.25	
7	-	204.60	
8	3.33 (t, 7.82)	45.67	C-9, C-10, C-7
9	3.01 (t, 7.82)	30.88	C-8, C-12, C-13, C-7
10	-	141.74	
11	7.25 (m)	128.29	C-9, C-12, C-13
12	7.30 (m)	128.30	C-11, C-10
13	7.21 (m)	125.79	C-12
14-Me	2.05 (s)	6.92	C-3, C-6, C-2
15-OMe	3.82 (s)	55.35	C-5, C-4
2-OH	14.27 (s)	-	C-3, C-1, C-6, C2, C-7

Fraction 13 yielded a considerable amount of yellow needle crystals; after several chromatographic steps, 8 mg were obtained. The HPLC-DAD analysis showed that it corresponded to the peak in 30.30 min. The HRMS in positive and negative modes displayed a $[M+H]^+$ ion of 285,1113 Da and a $[M-H]^-$ of 283.1040 Da, corresponding to the molecular formula $C_{17}H_{16}O_4$. The ^{1}H NMR spectrum (*Figure 25*) (500 MHz, $CDCl_3$) δ 14.46 (s, 1H), 7.90 (d, J = 15.6 Hz, 1H), 7.78 (d, J = 15.6 Hz, 1H), 7.61 (dd, J = 7.6, 1.7 Hz, 2H), 7.40 (m, 3H), 5.97 (s, 1H), 3.91 (s, 3H), 2.08 (s, 3H). This spectrum resembled myrigalone H but lacked the vicinal methylenes and displayed a different aromatic pattern with two additional protons (two doublets, 1H, J = 15.6 Hz). This fact suggested a trans double bond of a chalcone (Zaki et al., 2016) instead of the vicinal

methylenes, and the differences in the molecular formulas showed an additional IHD, supporting this observation.

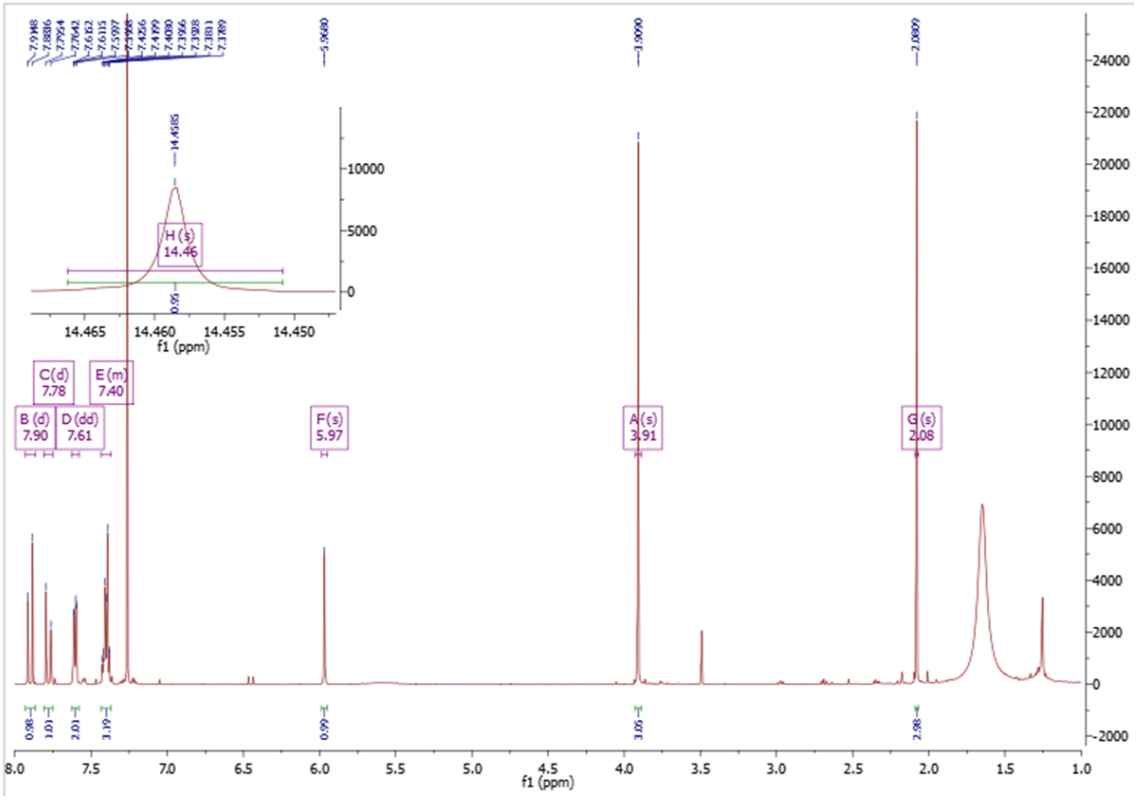

Figure 25. ^{1}H NMR spectra of stercurensin (**42**).

HSQC, HMBC (Table 7), NOESY and MS^{2} concluded that the compound was the chalcone stercurensin (**42**), reported *for Sterculia urens*, *Comptonia peregrina* (Harborne and Mabry, 1982; Wollenweber et al., 1985) and *Syzygium samarangense* (Kuo et al., 2004).

Table 7. NMR spectral data of stercurensin (42).

Position	^{1}H δ *J*(Hz)	^{13}C δ	HMBC
1	-	106.20	
2	-	165.5	
3	-	103.10	
4	-	160.10	
5	5.97(s)	90.60	C-3, C-1, C-4, C-7
6	-	160.80	
7	-	192.70	

8	7.90 (d, 15.6)	127.70	C-10, C-9, C-7
9	7.78 (d, 15.6)	142.0	C-11, C-7, C-8
10	-	135.0	
11	7.61 (dd, 7.6, 1.7)	128.2	C-12, C-9
12	7.40 (m)	128.8	C-11, C-10
13	7.40 (m)	128.8	C-12, C-10
14-Me	2.08 (s)	6.90	C-3, C-4, C-2
15-OMe	3.91 (s)	55.70	C-6
2-OH	14.46 (s)	-	C-3, C-1, C-2

NOESY only correlation was between 15-OMe and H-5.

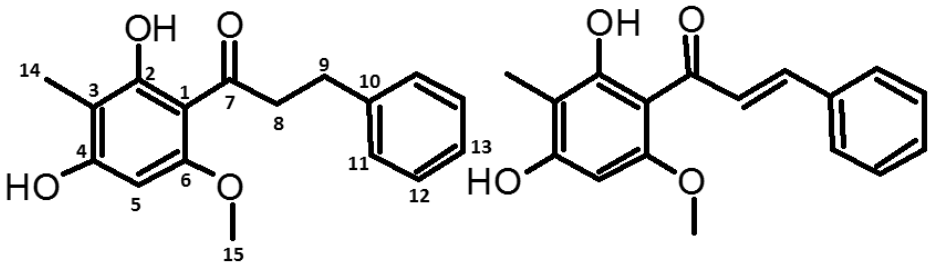

Figure 26. Structures of myrigalone H (**41**) and stercurensin (**42**).

It was possible to observe a fluorescent compound in fraction 17 of the TLC at 365 nm; the fraction showed a high chlorophyll content as well as many other interferences. Thus, it was submitted to Sephadex in MeOH, yielding 27 new fractions. The fraction containing the fluorescent compound was analyzed by HPLC-MS. The HRMS in positive mode displayed a $[M+H]^+$ ion of 280.0972 Da corresponding to the molecular formula $C_{17}H_{13}NO_3$ and the spectroscopic data ^1H NMR (500 MHz, $CDCl_3$) δ 9.28 – 9.22 (m, 1H), 8.39 (s, 1H), 7.82 (d, J = 8.4 Hz, 2H), 7.63 (s, 1H), 7.61 – 7.55 (m, 2H), 4.13 (s, 3H), 4.08 (s, 3H) showed the same pattern and chemical shifts than cepharanone B (**37**) (Desai et al., 1988). The presence of this compound is remarkable because there are no previous reports for the species. Thus, as stated in Chapter 1, this could indicate aristolactams as an essential component in *Piper´*s metabolome.

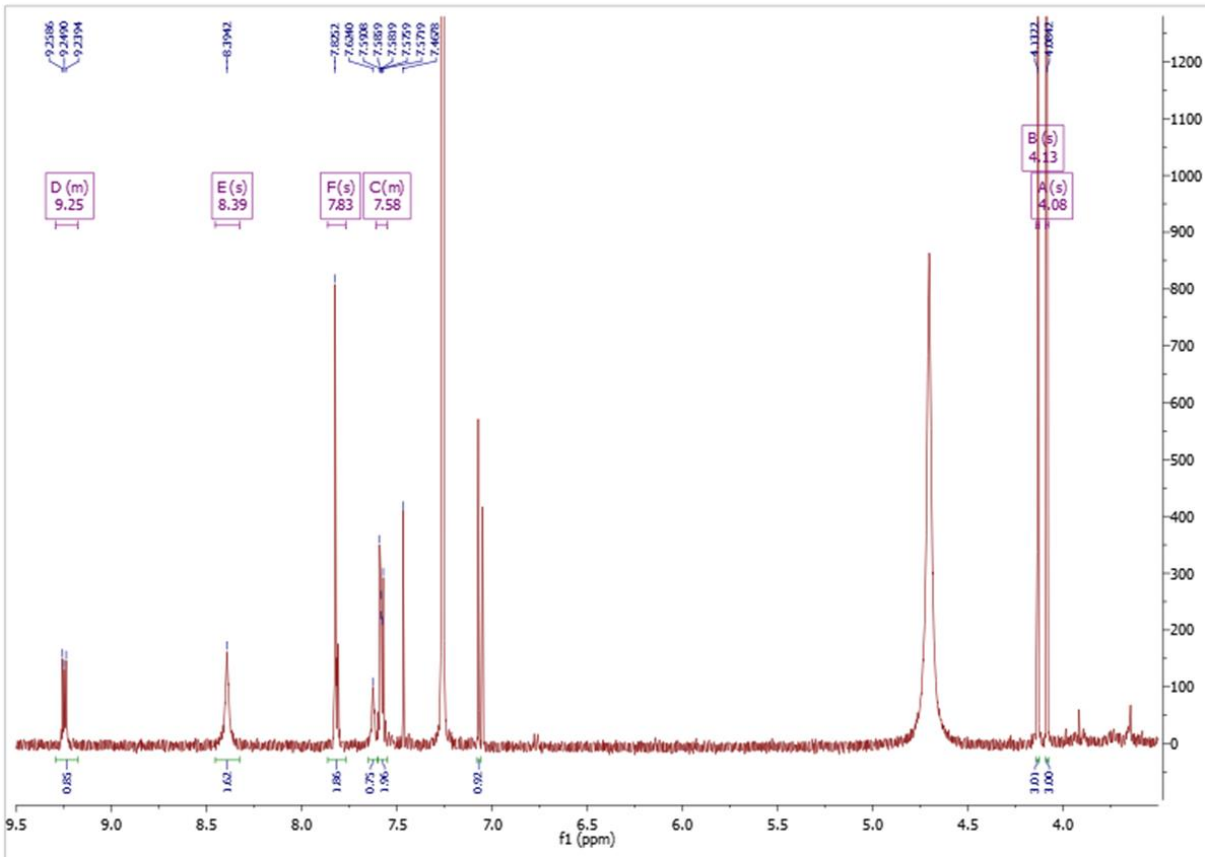

Figure 27. ^{1}H NMR spectrum of cepharanone B (**37**).

Several minor peaks between 11 and 30 min (*Figure 28*) were also analyzed by HPLC-MS^{2} (*Table 8*). Most of those compounds were grouped into three different categories: vitexin derivates, stercurensin and cardamomin isomers. Annotations led to consider the species as a source of chalcone-type compounds with structural similarities to **41** and **42**, most of these C-methylated chalcone derivates like triangularin, aurentiacin, alpinetin and several myrigalones from Pteridaceae, Myrtaceae, Pinaceae and Fabaceae (Adityachaudhury et al., 1976; Amor et al., 2005; Domínguez et al., 1980; Hansel et al., 1963; Kuo et al., 2004; Mustafa et al., 2005; Star et al., 1978; Wollenweber et al., 1985).

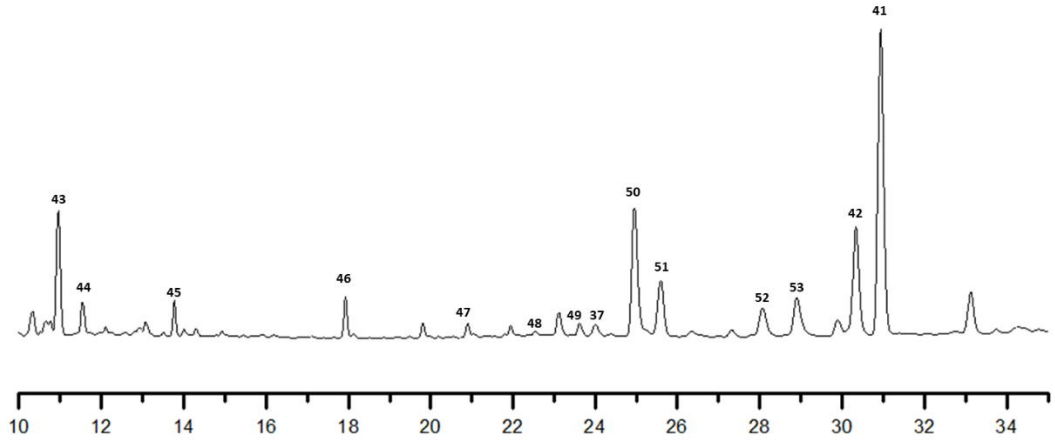

Figure 28. HPLC chromatogram of the annotated compounds from leaves of *P. lindbergii. C.DC.*

Initial fractions F1 to F4, which coeluted with the solvent´s front, were analyzed by GCMS. The major compounds were: α-copaene (**54**), caryophyllene (**55**), octadecane (**56**), α-amorphene (**57**), aromadendrene (**58**), α-muurolene (**59**), γ-muurolene (**60**), β-bisabolene (**61**), δ-cadinene, calamenene (**62**), caryophyllene oxide (**63**) and γ-cadinene (**64**).

Finally, as fraction 6 displayed a high complexity, the amount of 323.0 mg was submitted to a new chromatographic step using a 25g SNAP Cartridge KP-Sil (Biotage) with a Hex-$CHCl_3$ system yielding 38 fractions. At least two major components were observed in the TLC, as the ^1H NMR spectra remained complex, similar to a carotenoid derivate (Bench et al., 2011), while ESI accomplished no ionization. From fraction 6-8, approximately 1.0 mg of red crystals were obtained, ^1H, HSQC and HMBC NMR analysis suggested a carotenoid-like structure similar to lutein (Otaka et al., 2016).

Table 8. Annotations for secondary metabolites from leaves of *P. lindbergii. C.DC*.

No	rt (min)	$[M+H]^+$ (Da)	$[M-H]^-$ (Da)	Fragmentary Ions (m/z)	Formula	ID	Error (ppm)	Ref
43	11.0	595.1704	593.1485	595.1847, 433.1167, 313.0757	$C_{27}H_{30}O_{15}$	vitexin glucososide	-4.5	(Baldoqui et al., 2009)
44	11.8	545.1899	543.1711	527.1782, 509.1682, 425.1422, 407.1344, 329.1018, 305.1009	$C_{32}H_{36}N_2O_6$	Nigramide isomer	< 10	(Wei et al., 2005)
45	13.9	579.1740	577.1552	579.1722, 433.1148, 313.0699, 415.1044	$C_{27}H_{30}O_{14}$	vitexin rhamnoside	-1.9	
46	18.0	285.1178	283.0984	285.1134, 267.1008	$C_{17}H_{16}O_4$	stercurensin isomer	2.8	(Hansel et al., 1963; Terreaux et al., 1998)
47	20.9	271.1018	269.0857	271.0924, 167.0332,	$C_{16}H_{14}O_4$	cardamomin isomer	3.0	(Harborne and Mabry, 1982; Kimura et al., 1968)
48	22.5	285.1182	283.0980	285.1113, 181.0487,131.0491	$C_{17}H_{16}O_4$	stercurensin isomer	1.4	(Hansel et al., 1963; Terreaux et al., 1998)
49	23.5	285.1178	283.0982	285.1101, 181.0500	$C_{17}H_{16}O_4$	stercurensin isomer	2.1	(Hansel et al., 1963; Terreaux et al., 1998)
50	25.0	285.1343	283.1152	299.1279, 195.0645	$C_{14}H_{20}O_6$	1-(2,4,5-trimethoyphenyl)-2-acetoxy-1-hyroxypropane	< 10	(Koul et al., 1993)
51	25.8	271.1019	269.0828	271.0952, 167.0349	$C_{16}H_{14}O_4$	7-hydroxy-5-methoxyflavone	3.3	(Harborne and Mabry, 1982; Kimura et al., 1968)
52	28.0	273.1152	271.0978	273.1228, 255.0985, 223.0722, 177.0539, 153.0571, 115.0544, 105.0678	$C_{16}H_{16}O_4$	cardamomin isomer	0.7	(Harborne and Mabry, 1982; Kimura et al., 1968)
53	29.0	285.1270	283.0970	285.1068, 267.0986, 235.0738, 207.0773, 179.0809	$C_{17}H_{16}O_4$	stercurensin isomer	-2.1	(Hansel et al., 1963; Terreaux et al., 1998)

Electrospray Ionization was more efficient in the negative mode.

2.3.2. P. chimonantifolium

Several tests were conducted to establish the best system for extracting the secondary metabolites analyzed by ^{1}H NMR and HPLC-DAD using piper's seedlings methodology. First, leaves were extracted using solvents of increasing polarities: hexane, chloroform, and MeOH, with the latter proving as the most efficient. Then, a liquid-liquid partition was also tested; 50 mg of dried leaves were poured into 1.5 mL a mixture of H_2O-MeOH-$CHCl_3$ (1-1-2) and shaken in a vortex for 5 minutes in the presence of several stainless steel beads (Kim et al., 2010), the aqueous and organic fractions were separated and analyzed. No significant differences were observed between the methanolic extraction and the organic fraction from the partition; thus, methanolic extraction was chosen as the work methodology.

Once the extraction methodology was established, leaves, roots and stem of *P. chimonanthifolium* were analyzed by HPLC-DAD. The chromatograms (*Figure 29*) displayed notorious differences between the profiles and portrayed the leaves as the organs with the highest amount of metabolites.

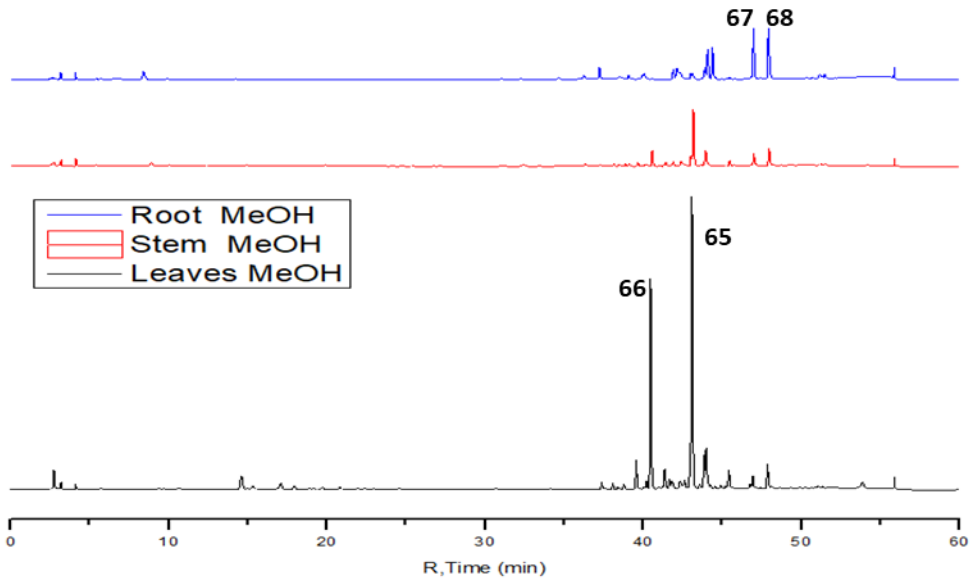

Figure 29. HPLC-DAD chromatogram of leaves, stem, and roots of *P. chimonantifolium* (270 nm).

HPLC-MS analysis was conducted for roots and leaves; stems were discarded because its similarity with leaves. Leaves showed two major peaks in 40.5 min and 43.1 minutes, with a $[M+H]^+$ of 289.0725 Da and 303.1347 Da, respectively. The calculated formulas for both compounds were $C_{16}H_{16}O_5$ and $C_{17}H_{18}O_5$. The ^1H NMR spectrum of the organic fraction (*Figure 30*) was compared with the methanolic extract (see supplementary data), with the first showing fewer interferences and better resolution for several peaks. It was possible to observe a clear pattern similar to compounds 41 and 42. The ^1H NMR spectrum (500 MHz, $CDCl_3$) δ 14.04 (s, 1H), 7.16 – 7.09 (m, 4H), 6.82 – 6.74 (m, 4H), 6.10 (d, J = 2.4 Hz, 1H), 5.98 – 5.93 (m, 2H), 3.86 (s, 4H), 3.84 (s, 3H), 3.30 (dd, J = 8.5, 7.0 Hz, 3H), 2.98 – 2.92 (m, 3H), at first sight, looked as a single compound with irregular integration values. This feature supported the idea of a mixture of two compounds with high structural similarity, the molecular formulas from the major compounds also differ in 14 Da, suggesting an extra methyl group in one of them.

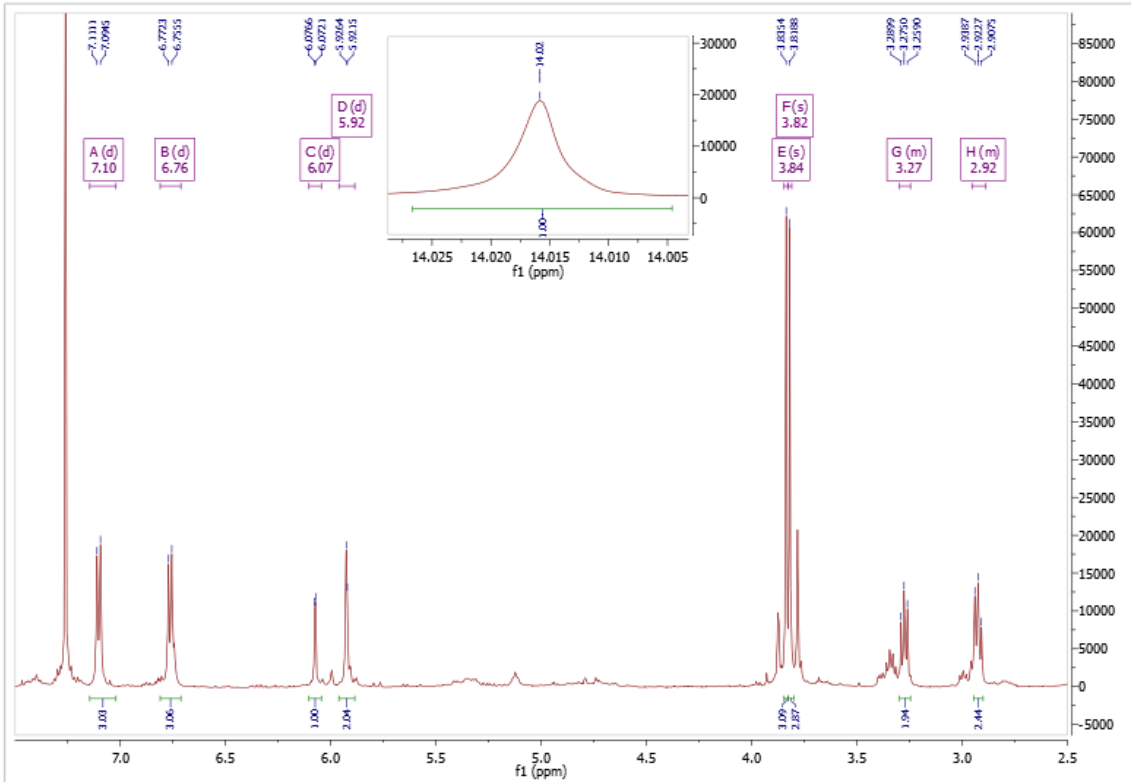

Figure 30. ^1H NMR spectrum for the organic fraction of leaves (partition).

The major compounds were identified as dihydroflavokawain C (**65**) and asebogenin (**66**) in a proportion of 2:1, respectively. These compounds were reported for propolis (Christov et al., 2012), *Pityrogramma chrysophyla* (Nilson, 1961)*, Pityrogramma calomelanos* (Hitz et al., 1982)*, Populus balsamifera* (Lavoie et al., 2013), *Piper gaudichaudianum* (Rapado et al., 2014) and *Piper methysticum* (Xuan et al., 2008).

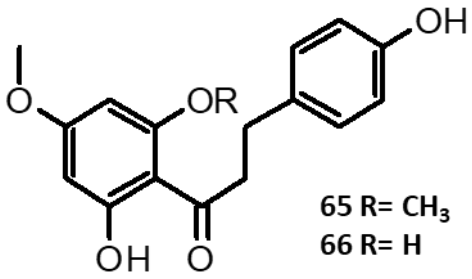

Figure 31. Structures of dihydroflavokawain C (**65**) and asebogenin (**66**).

Roots were also analyzed by HPLC-MS, and the peaks in 44.3 and 47 min were identified as piperaduncin A (**67**) and B (**68**), respectively, reported for *Piper aduncum* (Orjala et al., 1994).

2.4. Conclusions

Both species possessed similar chemistry, with chalcones, dihydrochalcones and derivates as the most common metabolites. Myrigalone H and stercurensin were reported for the first time in the family, and the presence of many isomeric compounds analog to cardamonin and stercurensin in *P. lindbergii* C.DC. suggested the presence of a wide diversity of chalcone-type compounds in this species. *P. chimonanthifolium* was mainly composed of dihydroflavokawain C and asebogenin.

Dihydrochalcones were some of the most expressed metabolites, their role in the ecological relationship of the species is still not well known but turns into a future target for studies.

Once again, cepharanone B was found as a conspicuous metabolite in *Piper* and suggested the importance of an unknown role of aristolactams in the ecology of *Piper* species.

Chapter 3. Ontogeny of *Piper* species

3.1. Introduction

3.1.1. Plant ontogeny

Plants are dynamic and complex entities that are the product of the variable environment in which they live. Individuals must adapt to a mosaic of changing conditions like seasons, moisture, light intensity, and temperature, some of them changing as fast as hours or minutes. It is advantageous for organisms to be able to sense these differences and changes and respond to them. Most plants are large enough that their bodies live in different micro-environments; roots are submitted to more stable conditions than aerial parts, as the trunk and lower branches are amid both scenarios. In the case of leaves, they must be coordinated to avoid malfunctions during the development; for example, the petiole must know when there is enough xylem and phloem tissue to permit adequate transport of water and nutrients to the blade. Otherwise, it would end in water stress or the inability to export vital compounds like sugars to the rest of the plant. On the other hand, the production of excessive conductive material will lead to the waste of energy and material. Phytohormones play a vital role in the plant´s response to stimuli as well as the genetic material that would be expressed during the development (Mauseth, 1998).

Seeds are an exceptional adaptation for the embryo's survival, allowing opportunities for dispersal and protecting it from the attack of fungi or bacteria, not only because of the hard coating but the presence of substances like phenolics, lectins, toxic glycosides or enzymatic inhibitors that discourages predation by rodents, insects, and herbivores. The seed contains most of the necessary elements for germination and early seedling growth (like a source of energy and minerals), most dependent on temperature and water availability to complete the early stage of development. This early embryogenesis results in the differentiation of the embryo´s body, cotyledons, root-shoot axis, root, shoot apices, etc. This process is mediated by phytohormones, especially auxin-, cytokinin- and gibberellin-like substances (Srivastava, 2002).

3.1.2. Plant Defense

Another important factor that involves a quick response from the plant is herbivory; the impact suffered by herbivores on a plant´s fitness is the result of the interaction with other plants, the herbivore and its natural enemies like predators or parasitoids. Thus, the resistance mechanisms become vital to the plant's survival. These defense traits vary and change with the plant ontogeny and could also be influenced by demographic priorities o resource allocation constraints. It is theorized that, in the beginning, plants had a limited pool of resources for specific purposes, and it is the primary role of the plant´s ontogeny to decide how to invest them during the early development. Plants have two major processes associated with their development. First: the increase in the size of the plant produces resource acquiring organs that allow the diversification of defense strategies. Additionally, as long as the plant advances in its development, functional priorities as growth rate and metabolic activity decrease in favor of other functional priorities of growth, resistance, storage or reproduction (Boege and Marquis, 2005).

There are three mechanisms of herbivory resistance: Escape, Defense and Tolerance.

The escape helps the plant to reduce the likelihood of being found by the herbivores. There are different ways to accomplish this: the higher dispersion of seeds, growing out of the reach of the consumer or early leafing in seedlings when herbivores are seasonal.

There are two types of defenses: direct and indirect. The direct defense involves all those strategies that reduce the herbivore damage by decreasing the plant quality as food, and it could be accomplished by the anatomic or chemical way. The production of defensive secondary metabolites is the most relevant trait that would be addressed in this chapter, while other processes like the generation of defensive structures like spines and thorns are out of this work's scope. These processes demand certain energetic independence because of the need for the production of biomass, a rise of shoot/root ratio and allocation of new resources. This feature

is essential when the reproductive stage is reached. If the species reproduce only once, this is prioritized over the defense and decreases in the vegetative parts. For species with multiple reproductive events, defense maintenance plays a vital role and cannot be left behind (*Figure 32*).

The indirect defense involves tritrophic interactions with the herbivore's natural enemy, sometimes a predator or parasitoid, via the production of volatile compounds. The plant can also modify its structure to provide housing and feeding to several ant species, which protects the plant against any herbivore (Boege and Marquis, 2005).

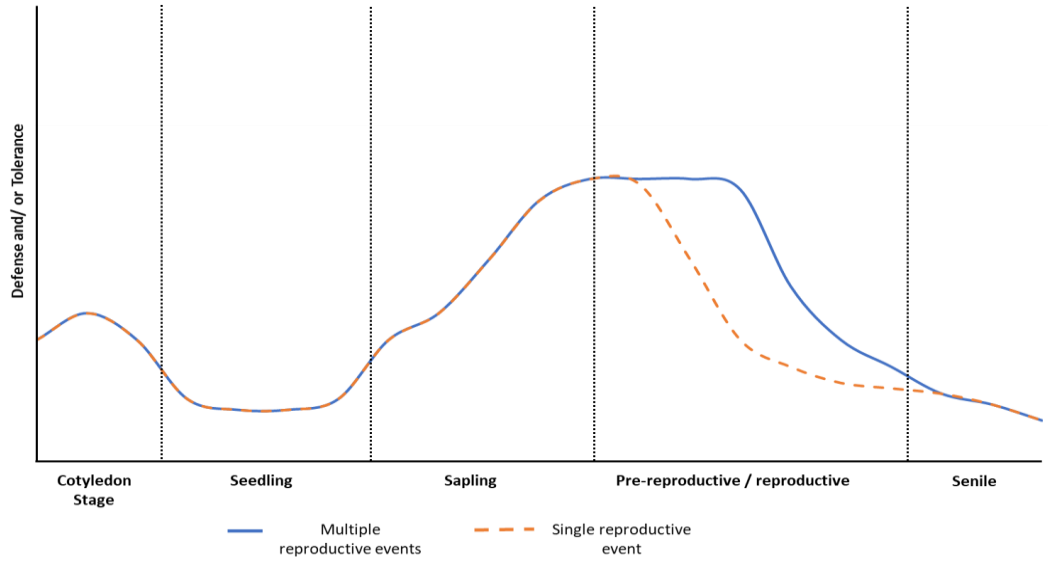

Figure 32. The pattern of change in defenses and tolerance during plant ontogeny (Boege and Marquis, 2005).

The environmental conditions are also crucial for the expression of plant defense; it is theorized that plants from nutrient-poor soils produce a higher amount of defensive secondary metabolites because of the constraints in resources and the loss of a leaf means a high cost for the plant. Another factor of great importance is the diversity of the plant populations in a determined area, clusters of individuals from the same species or family which possess a related chemistry defense trend to be less resistant to herbivory, also favoring the escape (Janzen,

1974). Thus, defense comprises complex mechanisms that respond to a series of biotic and abiotic factors, as well as adaptative, macroevolutive and phylogenetic causes (Agrawal, 2007).

Plant defense is a matter of major importance; the understanding of the response of plants to herbivores and pathogens will have a direct effect on the development of alternatives to chemical pesticides, which are detrimental to most ecosystems (Zaynab et al., 2018).

Consequently, the study and understanding of the plant ontogeny become an area of great interest, not only because of the possible applications of biologically active secondary metabolites but the ecological role of plants within the community, the harnessing of its resources and the unveiling of the complex mechanisms involved during the process. Different approaches to the study of vegetal secondary metabolism are currently applied. Metabolomics is a promising area that provides reliable information about the changes in the metabolome of an individual, displaying a quicker response to slight changes in the conditions of its development than other ‘‘omics’’. Modern analytical platforms allow a deep study of biological systems, with two main approaches, first the hyphenated chromatographic techniques LCMS and GCMS, which provide high resolution, sensitivity and the possibility of integration with databases (Ma and Qi, 2021). The other one is NMR, which provides a holistic view of the metabolites, providing structural information directly and the possibility of high throughput analysis with simple sample preparation (Kim et al., 2011). NMR also allows global to fine descriptions of sample composition for characterization diagnosis, with ^{1}H NMR still being a predominant tool to understand major families of compounds in extracts. *In vivo* and *In vitro* approaches can also be used, as well as several elements isotopes and two-dimensional experiments (Deborde et al., 2017).

3.2. Objectives

3.2.1. Main Goal

To evaluate the changes in the secondary metabolism of seven species of *Piper* during its development.

3.2.2. Specific Goals

To conduct a metabolic fingerprinting by HPLC-DAD and ^{1}H NMR of methanolic extracts from *Piper´*s 3-6-month-old-month-old seedlings and adults.

To identify or annotate the main compounds of each species at the different development stages by HPLC-HRMS.

To establish possible differences in the metabolic profile between seedlings and adults by multivariate analysis from chromatographic and spectroscopic data.

3.3. Results and Analysis

3.3.1. HPLC and NMR profiling

First, HPLC samples from the adults were prepared using 50 mg of dry and ground leaves by triplicate. Then, 50 μL of each sample were pooled into a vial and named the working mix. The HPLC profiling was based on the method for *P. auritum*, but the high complexity of the working mix demanded a more extended gradient. It is essential to clarify the differences in seedling cultivation overtime at this level. Initially, the first three species (*P. umbellatum, P. glabratum* and *P. diospyrifolium)* were planted as was stated in the methodology section and then, Then, germinated individuals were transferred into new pots (in a maximum of five plants per pot), placed into the growing chambers, watered weekly, and periodical growth checking. When possible, samples were separated by organ (leaves, stem, and roots), ground with liquid

nitrogen, and stored under −20 °C. HPLC and NMR samples from these species were prepared from individuals, a unique plant was used in each case.

For *P. caldense, P. regnellii, P. crassinervium* (IQ and Colombia) and *P. chimonantifolium,* more seeds were planted per pot, and no transplantation after germination was conducted. Samples for HPLC and NMR from these species were prepared from the pooled individuals of each pot. Additionally, another set of *P. glabratum* seeds was planted using these conditions.

For adult *P. umbellatum, P. glabratum* and *P. diospyrifolium,* the chromatograms displayed low complexity profiles (Figure *33*), with most of the major peaks at the chromatogram's end suggesting a low polar nature for these compounds. The other region between 18 - 30 min showed several minor peaks of higher polarity.

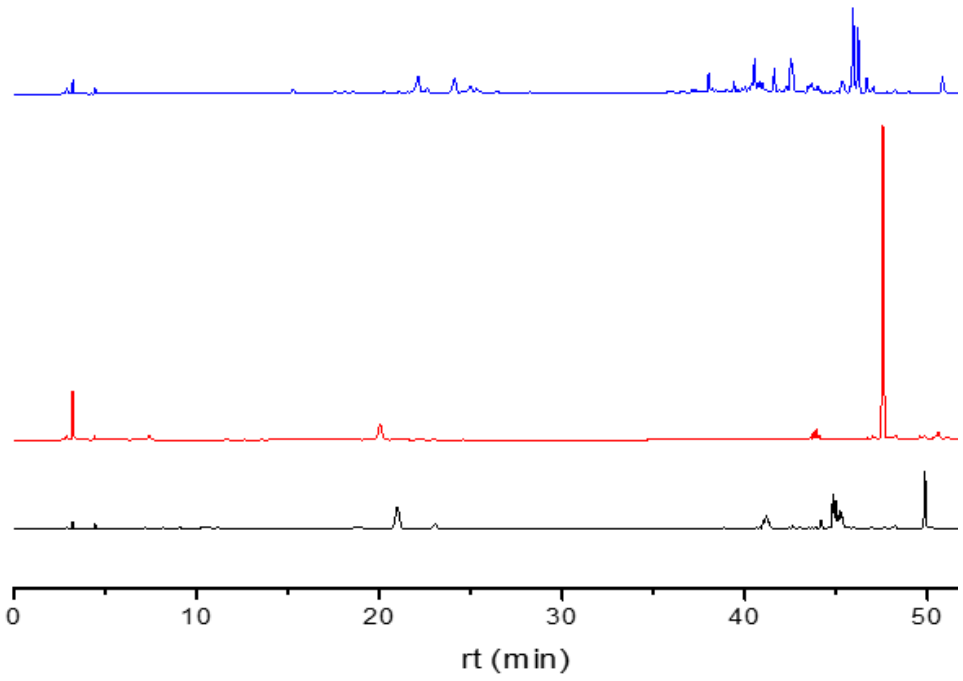

Figure 33. HPLC-DAD (270 nm) chromatograms of adult *P.umbellatum* (black), *P. glabratum* (red) and *P. diospyrifolium* (blue).

In the case of seedlings, significant differences showed up between individuals of the same pot. For P. *umbellatum* (Figure *34*), these differences were evident between individuals, with the

major peak around 44 min being absent in individual 1 (U1) while remaining unaltered in the others.

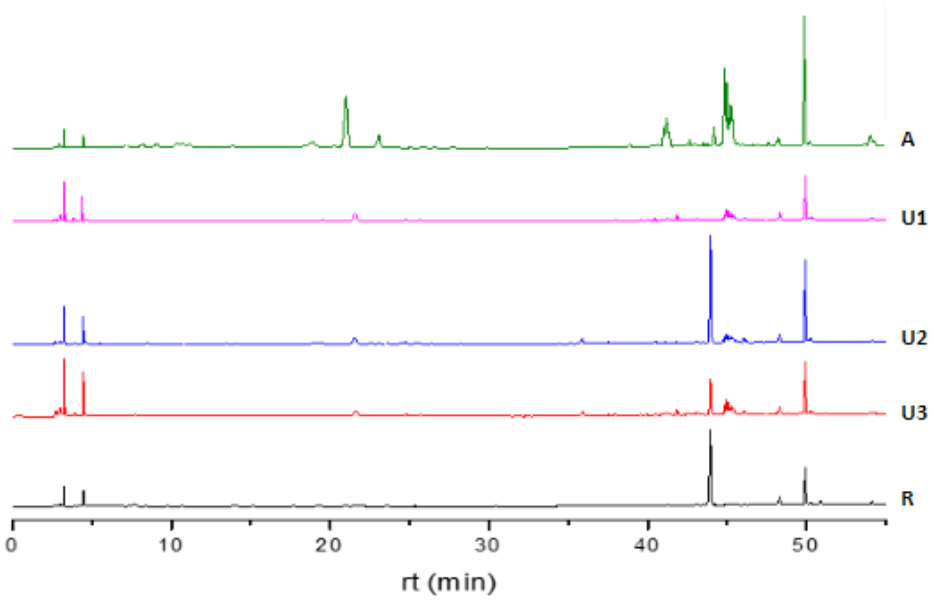

Figure 34. HPLC-DAD (270 nm) chromatograms of *P. umbellatum* adult (A), seedlings (U1-3) and roots (R).

The differences between the chromatograms of the pooled species were minimal (only one of the triplicates is shown). On the other hand, the changes during the development were evident, with most seedlings displaying a preference for more polar compounds while adults showed a shift to the production of less polar metabolites (Figure 35).

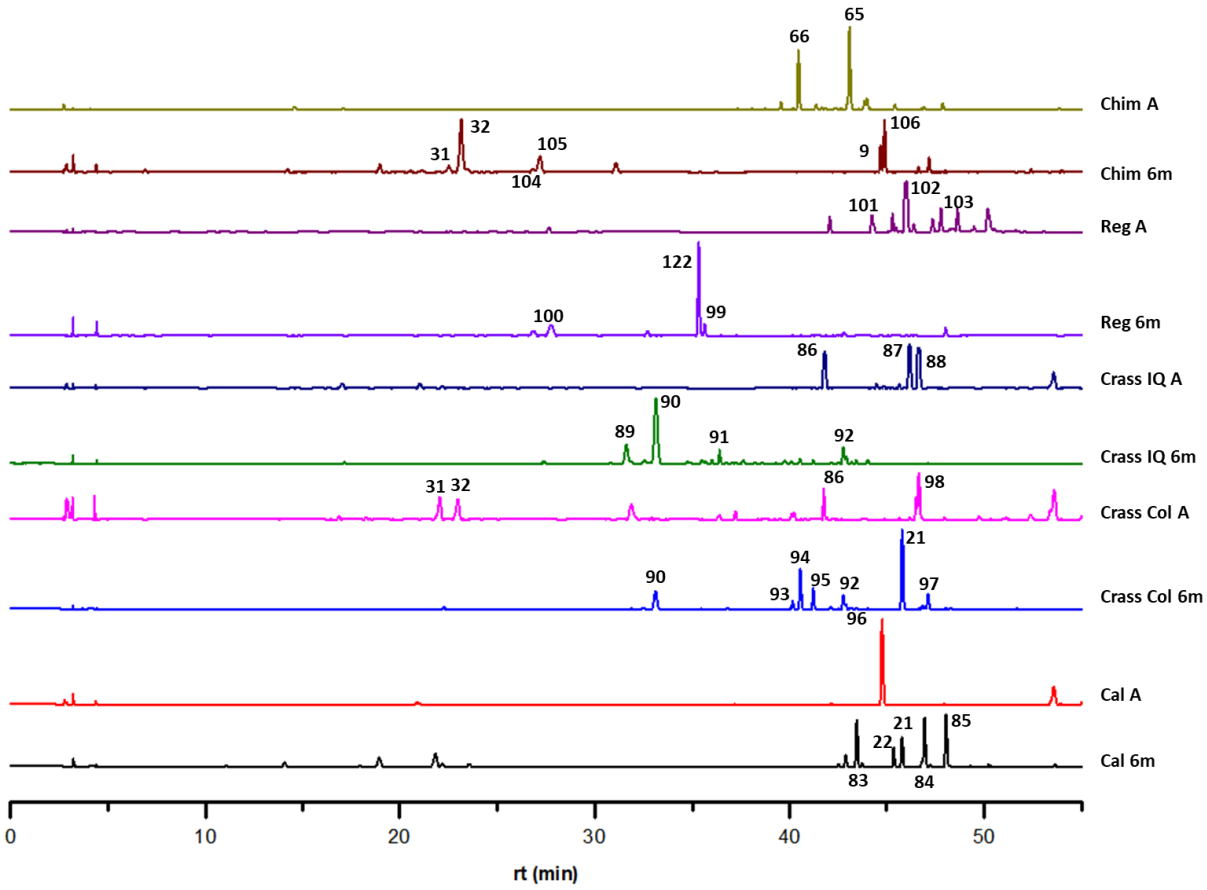

Figure 35. HPLC-DAD (270 nm) chromatograms of pooled species (adults and seedlings).

The ^{1}H NMR profiling was more challenging, although it used the same samples as HPLC after drying under nitrogen flow and redissolved in MeOD. These species represented the general overview of ^{1}H NMR spectra of methanolic extracts (*Figure 36*), with a bulky region of overlapped signals between 3.0 - 4.25 ppm, an intense peak around 1.25 ppm and low-intensity signals above 4.5 ppm.

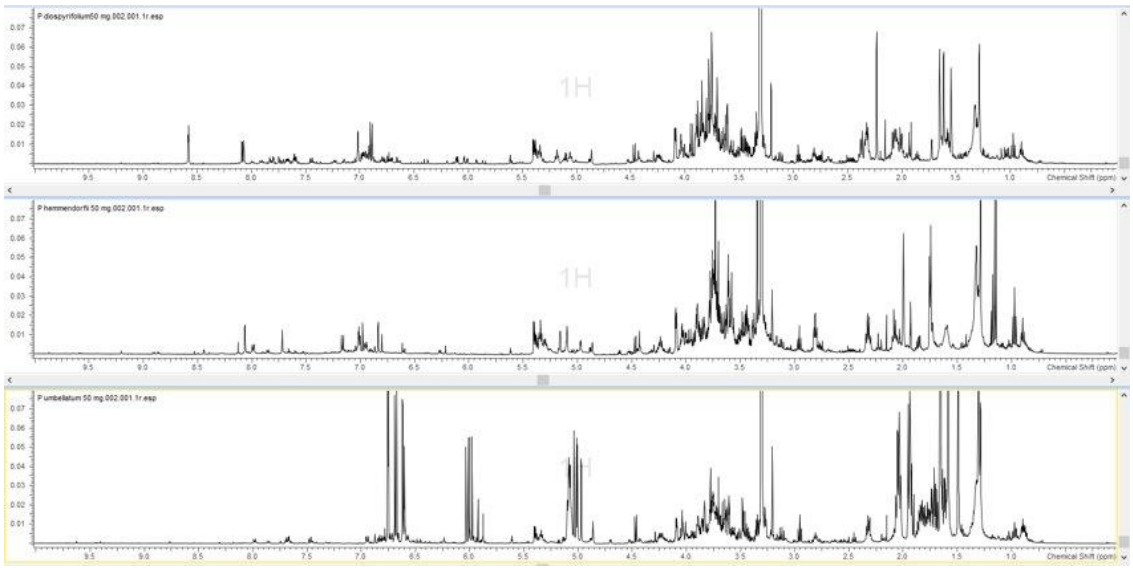

Figure 36. ^{1}H NMR spectra (MeOD) of adult *P. umbellatum* (bottom), *P. glabratum* (middle) and *P. diospyrifolium* (up).

This is due to the high complexity of the matrix and the non-selective nature of the extraction process, where primary and secondary metabolites are extracted, with the first representing the bulk of the extract. Signals from polar compounds like carbohydrates (Ward et al., 2003), organic acids and amino acids (Deborde et al., 2017) agglomerate between 2.0 and 4.25 ppm, eclipsing the peaks from minor metabolites in this range. Only a few cases like adult *P. umbellatum* could differentiate the signals from the major component over the background.

According to these observations, apparently, the HPLC-DAD analysis provided a more suitable methodology for the analysis of differences between samples (species or age) because of its higher sensitivity to secondary metabolites, the lesser influence of interferents from the extraction process and the possibility of individual identification of metabolites when hyphenated with MS.

3.3.2. Statistical differences among species/age

The ^{1}H NMR and HPLC-DAD approaches were used to evaluate the differences in the profiles of seedlings and adults. Due to the complexity of the resulting data, PCA was used as the main

analytic method. Three sets of samples were chosen for further comparison: Individuals of *P. umbellatum, P. glabratum* and *P. diospyrifolium*; Pooled individuals of *P. caldense, P. regnelli, P. chimonantifolium* and *P. crassinervium* (Colombia and IQ/USP) from the same pot; and finally, the two culture methodologies applied to *P. glabratum*. As was stated before, both approaches turned out to be very different, with HPLC-DAD displaying a better clustering and resolution than NMR.

The crude data was aligned (Nielsen et al., 1998), normalized and autoscaled (Goodacre et al., 2007) previously to its analysis in JMP®15.2.1 (SAS). The PCA for all methodologies was summarized in *Figure 37* with a Hotelling of 95%.

For individuals, the HPLC-DAD (Figure 37-A) displayed a fuzzy clustering of two sets of species (*P. diospyrifolium* and *P. glabratum / P. umbellatum*) alongside the axis of PC1, with no differentiation by age, roots of *P. umbellatum* as an outsider (not explained by the model) and PC1 and PC2 explaining the 82.8% of the variance.

NMR data (Figure 37-B) showed only a slight clustering for the adults of all species in the limit of the confidence ellipse. Most of the data were placed around a diagonal line between PC1 and PC2. This suggested some boundaries resulting from the data treatment like the fine binning (0.004 δ) or the normalization.

For the pooled samples, with HPLC (Figure 37-C), there was possible to observe a better grade of clustering, in most cases, especially for adults. Most seedlings and adults showed clear clusters as well as good separation between them. *P. caldense* (seedlings) was the only species with an irregular behavior, with samples spread over the PCA and even as an outlier. This was very peculiar because it resembles the behavior of the individuals, indicating some differentiation

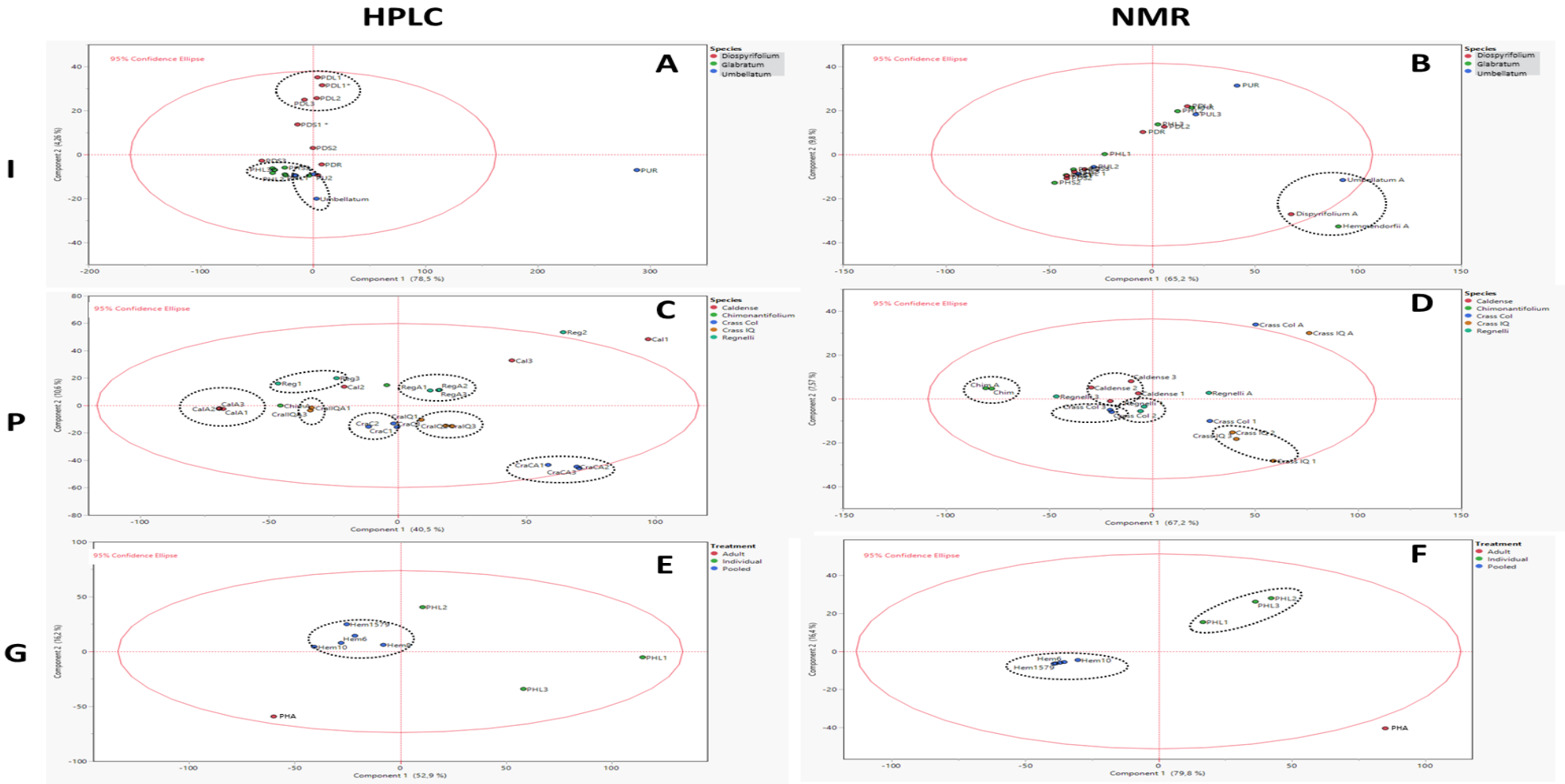

Figure 37. PCA summary for NMR and HPLC approaches of individuals (I), pooled (P) and *P. glabratum* (G) samples. (L: leaves, R: roots and S: stem)

between the pots in the growing chamber, like the existence of different microenvironments that lead to the expression of different metabolites. NMR (Figure *37*-D) showed similar results but with a more significant difference between seedlings and adults.

The most remarkable results were for *P. glabratum. O*nce individuals and pooled samples were compared (both sets of seeds (peppercorns) had the same origin), HPLC-DAD (Figure *37*-E) and NMR (Figure *37*-F) results showed the best clustering among pooled seedlings as well as the best separation with the adult and individuals, with the latter displaying high dispersion all over the quadrants, this feature was more notorious in HPLC than NMR.

3.3.3. Annotated Metabolites (HPLC-ESI-MS)

The HPLC-HRMS analyses displayed different levels of complexity for the species. In most cases, the changes between stages of development were notorious, and the multivariate analysis showed good clustering between samples of the same age and species. For individuals, the annotations were conducted using the most common chemotype.

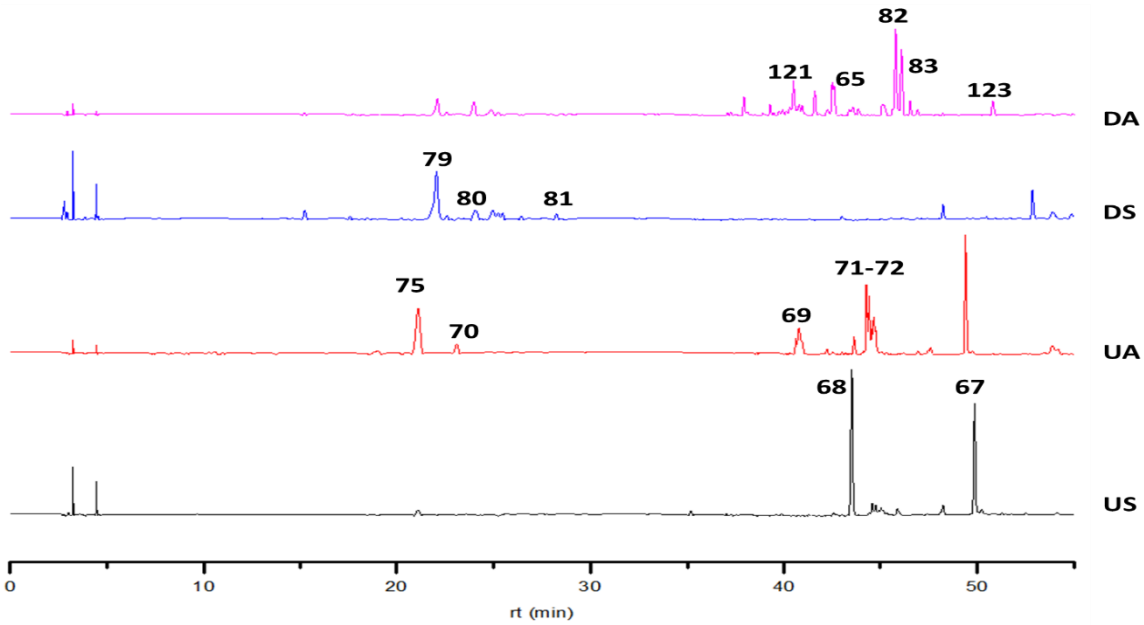

Figure 38. HPLC-DAD chromatograms of *P. umbellatum* (U) and *P. diospyrifolium* (D) adult (A) and seedlings (S).

P. umbellatum (Figure 39) kept the production of **67** 4-nerolidylcathecol (Baldoqui et al., 2009; Kijjoa et al., 1980) constant during all its development while **68** elemicin (Martins et al., 2000) decreased over time, while lignan **69** piperphilippinin VI (Chen et al., 2007) and a series of unknown compounds (**71-72**) became significant. As reported for *P. auritum* in Chapter 1, the production of polar compounds like C-glycosylflavonoids (**70** and **75**) was a constant feature, while the production of lignan **69** was exclusive to the adult.

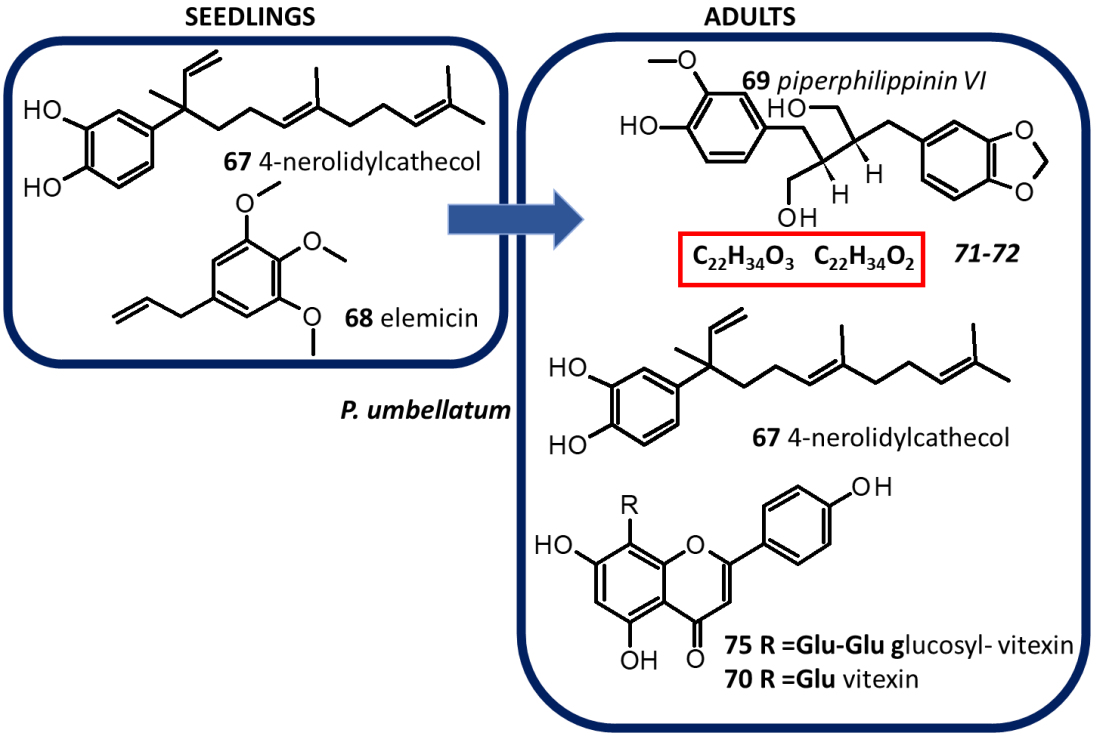

Figure 39. Annotated metabolites from adult and seedlings of *P. umbellatum*.

The changes for *P. diospyrifolium* (Figure 39) were more evident, with the adult´s chemical profile becoming much more complex. In this case, the profile of the early stages could be included in the adult´s one. The seedling showed C-glycosylflavonoids exclusively (vitexin derivate isomers **79**-**80** and the apigenin derivate **81**). The adult stage also included dihydrochalcones asebogenin **65** (Hitz et al., 1982; Orjala et al., 1994), 2',4'-dihydroxy-6'-methoxy-3,4-methylenedioxydihydrochalcone **82** and 2',6'-Dihydroxy-4'-methoxy-3,4-methylenedioxydihydrochalcone **83** (Phrutivorapongkul et al., 2003), chalcone flavokawain **121**

(Dieter Strack, 1994; Hansel et al., 1963) and lignan piperphilippinin I **123** (Chen et al., 2007). Despite the presence of lignans in adults, no phenylpropanoids were identified in any development stages, and this suggested the production of the phenylpropanoids monomers and their instant conversion into lignans.

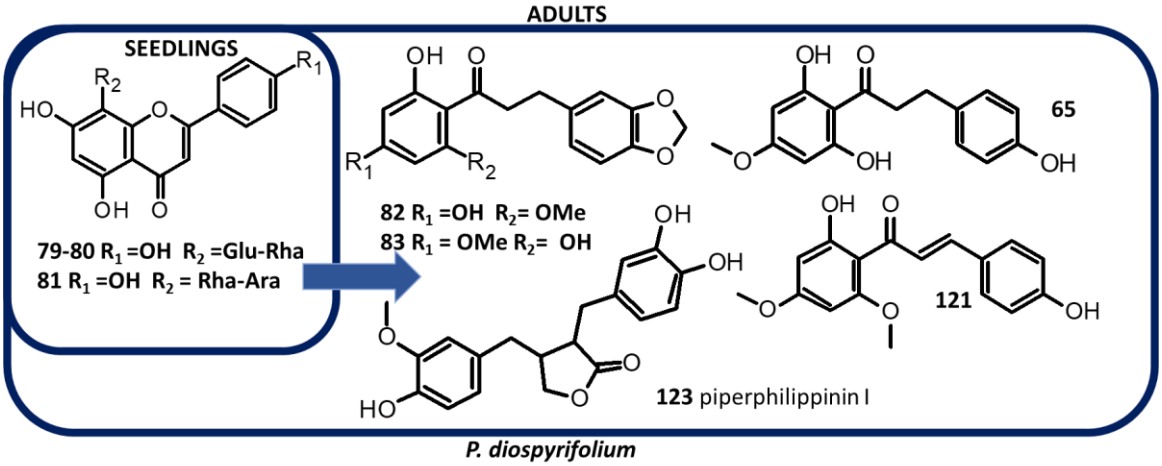

Figure 40. Annotated metabolites from adult and seedlings of *P. diospyrifolium.*

P. caldense (Figure 41) was one of the most impressive species, although seedlings showed a richer profile with the presence of the flavone **84** 7-methyl-luteolin (Ahmad et al., 2000; Lemeszenski, 2013), and amides **21** pellitorine,**22** 2,4-undecadienoic acid isobutylamide and **83** pipgulzarine (Siddiqui et al., 2003), the adult displayed a single significant compound which could not be characterized through HPLC-HRMS despite the total absence of ionization in both polarities. During the planting process, it was observed that a sticky and oily substance covered seeds. Even a previous washing with EtOH was required previous to the established protocol. This washed substance also was analyzed by HPLC-HRMS and ^{1}H NMR, with a $[M+H]^{+}$ ion of 457.2418 Da and a molecular formula $C_{27}H_{36}O_6$ was concluded that it was composed mainly of caldensinic acid **85** (Freitas et al., 2009). The isolation and identification of the major metabolite from adult leaves will be required for a future perspective.

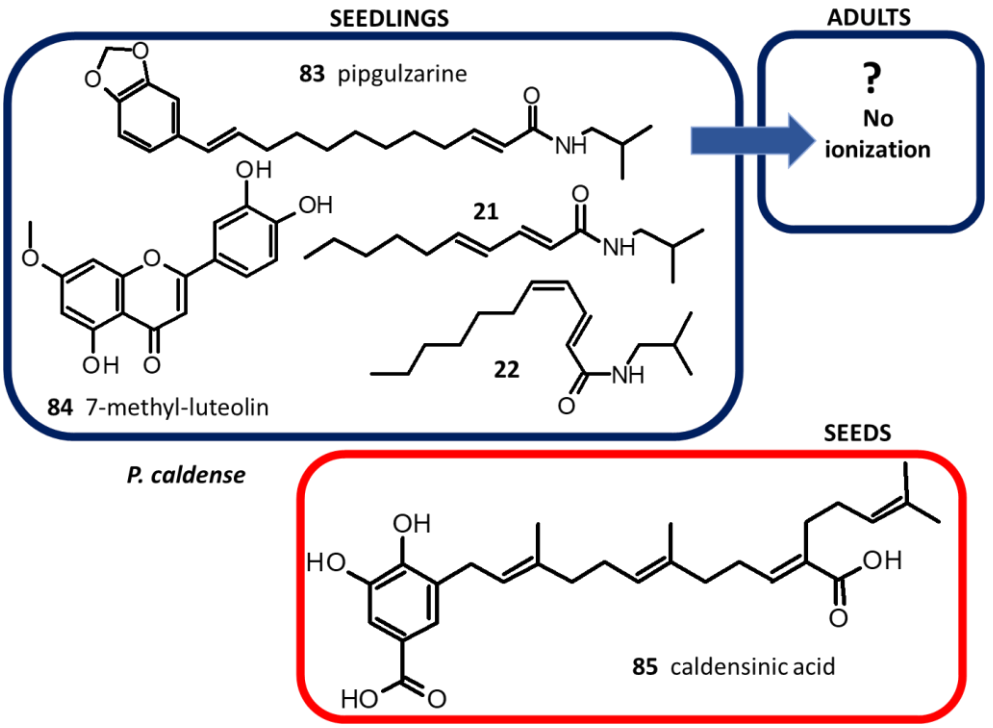

Figure 41. Annotated metabolites from adult and seedlings of *P. caldense*.

P. crassivervium was divided into two sets, with the first one collected from the IQ-USP garden (*Figure 42*), while the other was native from Colombia (*Figure 43*). This was due to the possibility of studying these two identified individuals from different locations, intending to compare the differences between their chemical profiles. The individuals from both locations displayed slight differences in the type of metabolites produced but with a very different profile.

For *P. crassinervium* IQ could be observed the production of dominant C-glycosylflavonoids 4',7-dimethyl-2''-O-β-D-glucopyranosyl-8-C-β-D-Glucopyranosyl-4',5,7-trihydroxyflavone **89** (Thao et al., 2016), 4',7-dimethyl-2''-O-α-L-rhamnopyranosyl-8-C-β-D-Glucopyranosyl-4',5,7-trihydroxyflavone **90** (Mota et al., 2011) and an acetylembinin isomer **91** (Pryakhina et al., 1984; Whaley et al., 2017), as well as the minor amide coumaperine **92** (Nakatani et al., 1980). The adult displayed the C-glycosylflavonoid margaritene **31** exclusively, the flavanone sakuranetine **86** (Danelutte et al., 2003), the prenylated quinone 1,4-dihydroxy-2-(3',7'-dimethyl-1'-oxo-octa-2'-*E*-6'-dienyl)benzene **87**, and the prenylated carboxylic acid 4-hydroxy-(3',7'-dimethyl-1'-oxo-octa-2'-*E*-6'-dienyl)benzoic acid **88** (Lago et al., 2004).

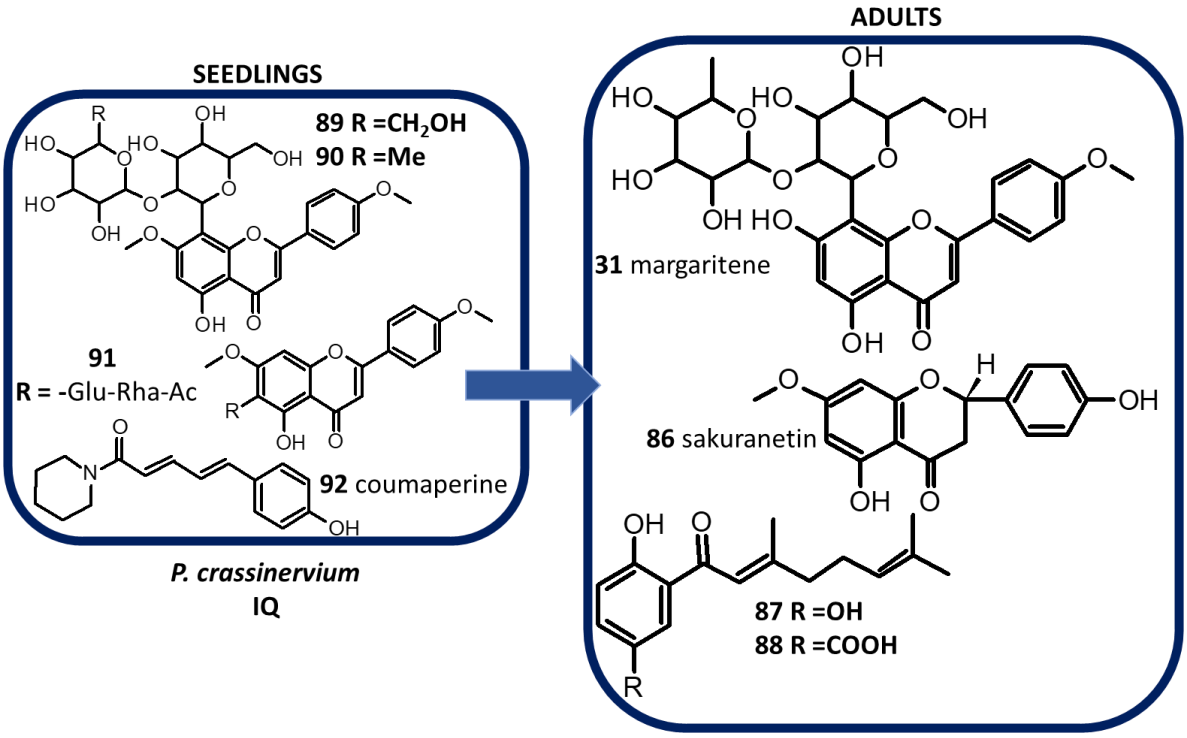

Figure 42.Annotated metabolites from adult and seedlings of *P. crassinervium* (IQ-USP)

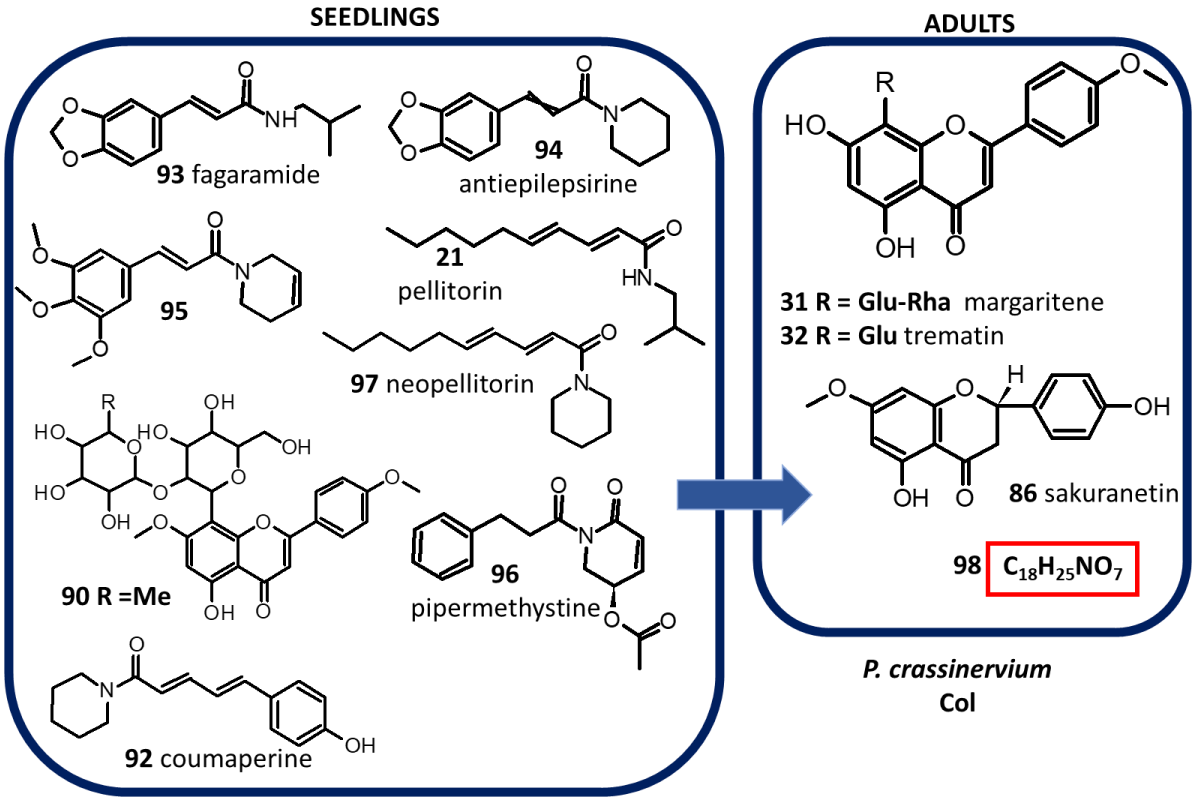

Figure 43.Annotated metabolites from adult and seedlings of *P. crassinervium* (Colombia).

For *P. crassivervium* Col, the situation was quite different. Amides faragamide **93**, antiepilepsirine **94**, coumaperine **92**, pipermethystine **96**, pellitorine **21** and neopellitorine **97** were the dominant metabolites in seedlings. Additionally, a peak with a $[M+H]^+$ ion of 304.1615 Da and formula $C_{17}H_{21}NO_4$ was observed; the main fragment observed in MS/MS was 221 Da and suggested a methylsinapic acid moiety of an amide with the loss of a neutral dihydropiperidine. Structure **95** was proposed as an analog to a deoxopiplartine. Isolation and NMR studies are required to demonstrate the existence of this compound. The adult displayed a more complex profile, where only margaritene **31**, trematin **32** and sakuranetin **86** could be identified.

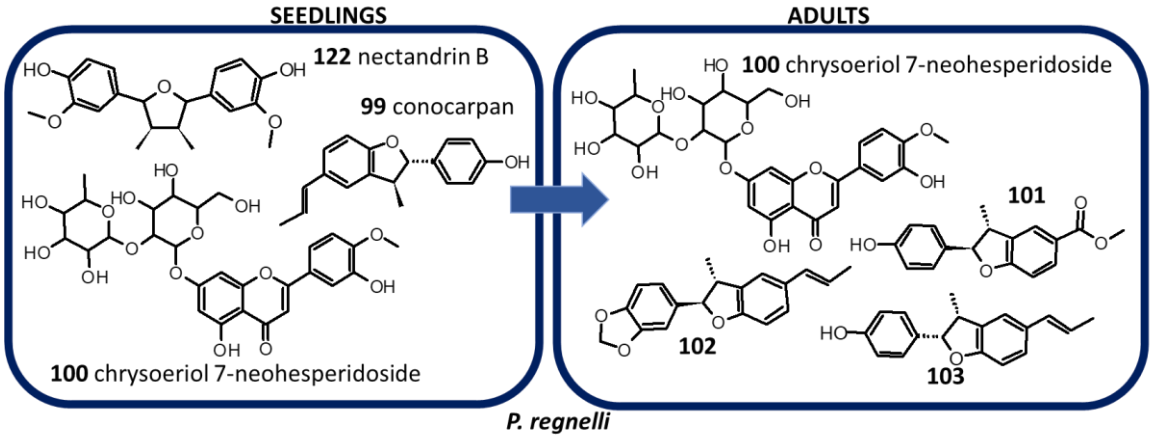

Figure 44. Annotated metabolites from adult and seedlings of *P. regnelli*.

P. regnelli displayed notorious differences between phenological stages. The glycosylflavonoid chrysoeriol-7-neohesperidoside **100** (Cimanga et al., 1995), lignan nectandrin B **122** (Herath and Priyadarshani, 1996; Le Quesne et al., 1980), and neolignan conocarpan **99** (Benevides et al., 1999; Saleem et al., 2010) were dominant for seedlings. In the adult, the chemical profile shifted to the production of less polar compounds where neolignans methyl-(7*R*,8*R*)-4-hydroxy-8',9'-dinor-4',7-epoxy8,3'-neolignan-7'-ate **101**, (7R,8R)-3,4-methylenedioxy-4',7-epoxy-8,3'-neolignan-7'[*E*]-ene **102** and (7*S*,8*R*)-4-hydroxy-4',7-epoxy-8,3'-neolignan7'[*E*]-ene **103** were identified (Benevides et al., 1999).

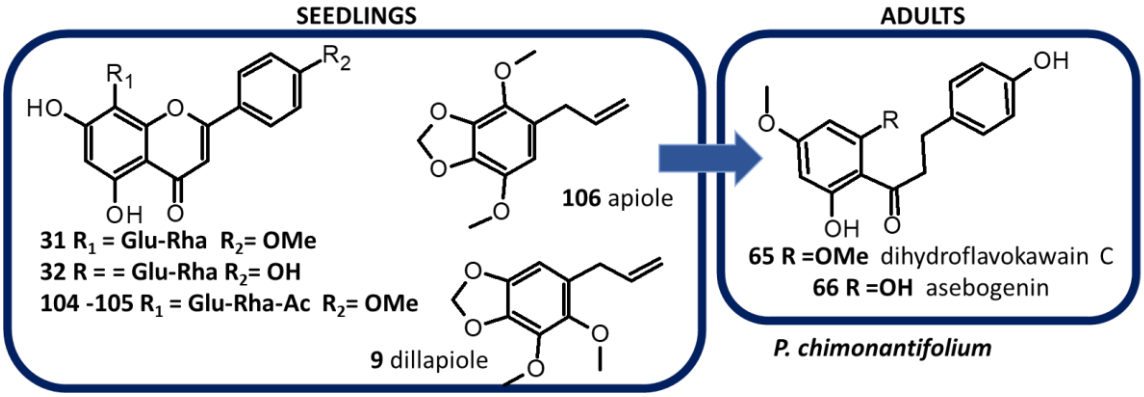

Figure 45. Annotated metabolites from adult and seedlings of *P. chimonantifolium*.

P. chimonantifolium was discussed in Chapter 2, and it was concluded that its profile was dominated by two major compounds, dihydrochalcones dihydroflavokawain C **65** and asebogenin **66**, which were identified by ^{1}H NMR and HPLC-HRMS. For the seedlings, C-glycosylflavonoids margaritene **31**, vitexin rhamnoside **32**, 4'''-*O*-acetyl-acacetin-8-*C*-[α-L-rhamnopyranosyl-(1⟶2)-β-D-glucopyranoside] isomers **104** and **105** (Thao et al., 2016) as well as phenylpropanoids apiole **106** and dillapiole **9** (Benevides et al., 1999; Harborne, 1997; Parmar et al., 1997).

Finally, in the case of *P. glabratum* (*Figure 46*), the two scenarios showed differences between profiles. For seedlings, a set of four C-glycosylflavonoids were identified. Initially, they were taken as the same two compounds, which displayed a slight shift in their retention times, caused by an unknown variation during the analysis. However, after alignment and LCMS analysis, it was established that they corresponded to four different compounds.

These C-glycosylflavonoids were identified as vitexin glucoside **75**, two isomers of vitexin apiofuranoside **76-77** and an analog of 4'-methyl-2''-O-β-D-apiofuranosyl-8-C-β-D-glucopyranosyl-4',5,7-trihydroxyflavone **78** (Thao et al., 2016).

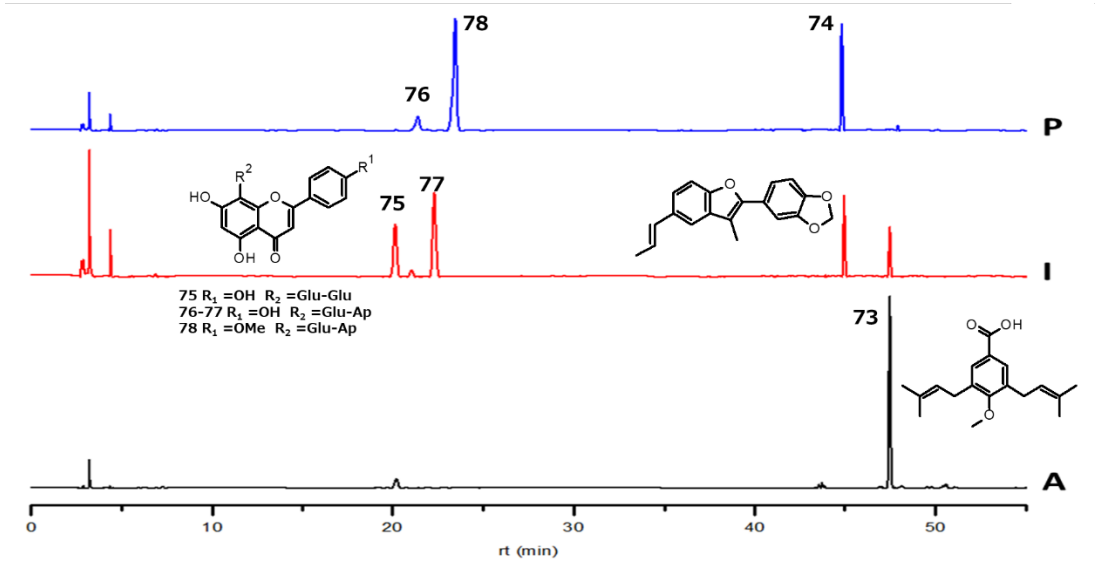

Figure 46. HPLC-DAD chromatogram of adult (A), pooled (P) and individual (I) seedlings of *P. glabratum*.

It was remarkable the difference in the expression of C-glycosylflavonoids between individual and pooled samples. The individuals produced mainly **75** and **77**, while the pooled plants expressed **78** as the major compound, with some traces of **76**. Additionally, were observed neolignan eupomatenoid 3 **74** (Saleem et al., 2010) and prenylated benzoic acid 3,5-bis(3-methyl-2-butenyl)-4-methoxybenzoic acid **73** (Parmar et al., 1998), with the latter being the dominant compound in the adult stage.

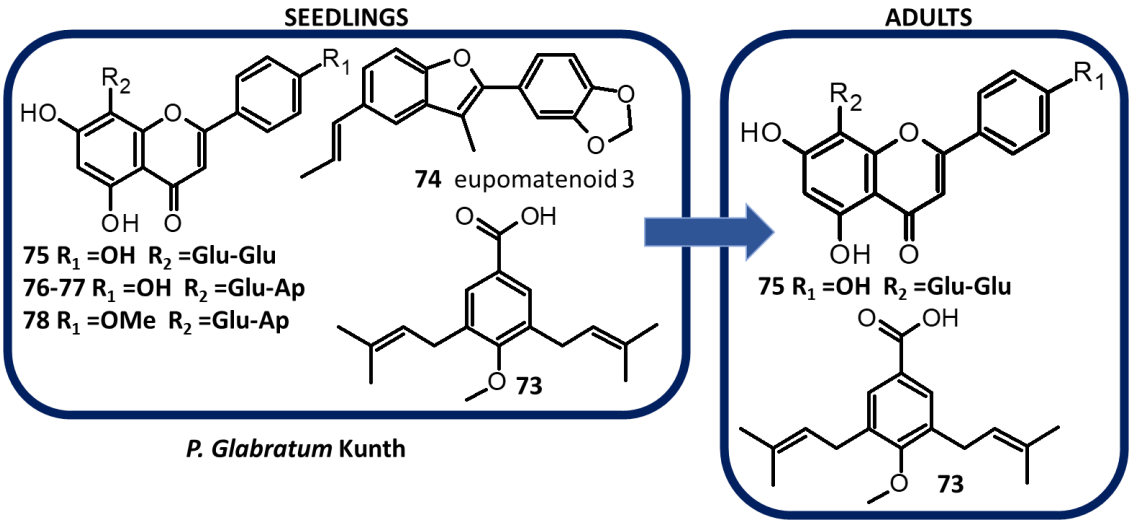

Figure 47. Annotated metabolites from adult and seedlings (individuals and pooled) of *P. glabratum* Kunth.

The individual also displayed a mixture of eupomatenoid 3 **74** and prenylated benzoic acid **73,** with the latter absent as a probable response to the lower density during the development; this factor was the main difference between both methodologies.

It is still not clear if the emergence of a specific metabolite occurred at the expense of another, as the expression of **73** depends on the reduction of C-glycosylflavonoids **75-78** or neolignan **74**. In principle, this should not happen because all these metabolites result from different biosynthetic pathways. This fact must respond to a redirection process of resources from the young plant, from its original metabolome to an expanded chemical space as a response to the aging process and environmental response.

3.4. Conclusions

In summary, the changes during the ontogeny of the studied species of *Piper* were demonstrated by its profiling using HPLC-DAD, ^{1}H NMR, HRMS and multivariate analysis. For this purpose, HPLC-DAD showed to be a more helpful approach than ^{1}H NMR, especially when combined with HRMS, due to the lower interference of primary metabolites, reproducibility and the resolution of the complex matrix into its components. Multivariate analysis was a suitable tool for the study, highlighting the differences between species and stages of development. The differentiation between organs was also accomplished for cases where this variable was used, demonstrating that composition changes significantly according to age, anatomy and environment.

Slight variations in the cultivation process produced remarkable changes in the metabolic profile of adults and seedlings, and this fact was way more evident when compared *P. crassinervium* from IQ-USP and Colombia. The production of amides in seedlings was more diverse and copious for the individuals from IQ-USP, while the adults displayed the additional production of prenylated quinones and benzoic acids.

Different compounds like phenylpropanoids, C-glycosylflavonoids, phenols, lignoids, amides, dihydrochalcones and prenylated benzoic acids were annotated, with flavonoid derivates being the most common and constant metabolites in the early stages and showing a high diversification during the development. No clear trends for the metabolite differentiation were found for this study, as was displayed in a different report (Gaia et al., 2021). Several annotations suggested the existence of novel compounds; isolation and spectroscopic analyses are required for this purpose.

Chapter 4. Diversity and quantification of aristolactams in roots of *Piper* species

4.1. Introduction

4.1.1. Natural occurrence, bioactivity and biosynthesis.

Aristolactams are compounds derived from aristolochic acids (*Figure 48*), a modified aporphine containing a nitro group from an oxidative reaction leading to a ring cleavage and the loss of a carbon atom (Dewick, 2009). AA and AL have been widely studied in Aristolochiaceae, and Annonaceae families, becoming a significant fraction of its metabolome. Several *Aristolochia* species are used in Traditional Chinese Medicine (TCM) preparations. Nevertheless, it has been demonstrated that AA was the main cause of several renal diseases like the Balkan endemic nephropathy (Vanherweghem et al., 1993) as well as mutagenic and carcinogenic effects (Kumar et al., 2003) while AL, naturally occurring and synthetic analogs, reported varied activities as antitumoral (Choi et al., 2009; Ji et al., 2020), neuroprotective (Kim et al., 2004) and cytotoxicity against LI210 leukemia cell line (Couture et al., 2002).

For *Piper* species; aristolactam AII, cepharanone B, 4-hydroxy-3-methoxy-*N*-methylpiperolactam, piperolactams A-E, piperolactam S (Parmar et al., 1997), aristolactam BIII, cepharanone A, goniothalactam, goniopedaline C, *N*-methylpiperolactam A and 2,3,4-trimethoxy-*N*-methyl-aristolactam (Chen et al., 2004; Danelutte et al., 2005; De Oliveira Chaves et al., 2006; Rachel Mata et al., 2004; Peña and Díaz, 1995; Ruangrungsi et al., 1992; Singh et al., 1996; Tsai et al., 2005) have been reported.

Aristolactams were some of the most remarkable compounds identified in Chapters 1 and 2, mainly because of their characteristic fluorescence. These compounds can be detected in almost the entire plant but were especially notorious in roots. Thus, the presence of these fluorescent compounds in an underground environment, lacking natural light, suggests another kind of activity or ecological role, which so far it is not been described

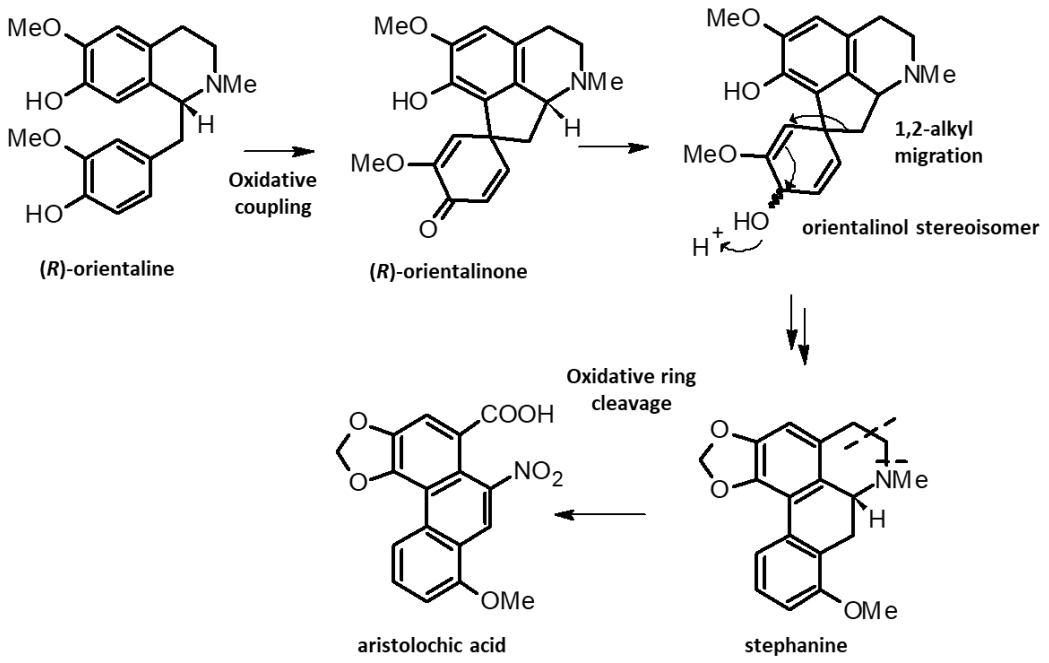

Figure 48. Biosynthetic pathway of aristolochic acid (Dewick, 2009).

4.1.2. Photoluminescence.

Fluorescence and phosphorescence are two phenomena of photoluminescence caused by the absorbance of photons and subsequent emission of light. Despite this similarity, they possess several fundamental differences, turning fluorescence especially useful for quantitative purposes. Both phenomena could be understood through the molecular orbitals theory; considering an electronic pair at its ground state that absorbs a photon will generate two possibilities for an excited state; the first one where an electron is promoted to the next energetic level, maintaining its spin paired to the remaining one is called a singlet (S). The other option involves the spin inversion of the promoted electron; this state is called a triplet (T). Properties of a molecule differ significantly from one state to the other, with S-T transitions being less probable than S-S. The average lifetime of T lies in the range of 10^{-4} s to several seconds, while it is about 10^{-8} s for S; the probability for a radiation-induced promotion from the ground state to T is lower than S, with an energy difference of several orders of magnitude. Figure 49 displays the dynamics of all processes, with the heavy lines representing the ground

state S_0, two singlet excited states S_1 and S_2 and a triplet excited state T_1. Additional lines represent the numerous vibrational states associated with each electronic level; generally, those vibrational states decay into the main forms after several deactivation processes; this also can lead to internal conversions between two overlapped vibrational states of the same multiplicity, going down to the lowest level, ending with the emission of a photon of a higher wavelength.

Florescence is related to an instantaneous emission of light, a product of the decay of an electron from an excited S state to the ground state; despite absorbance occurring in a range of frequencies, the emitted photon wavelength is constant. Phosphorescence is caused by an intersystem crossing process between two states of different multiplicity S and T. No direct promotion to the excited T level from the ground state is accomplished; this kind of excitation involves a multiplicity change, thus, is considered forbidden.

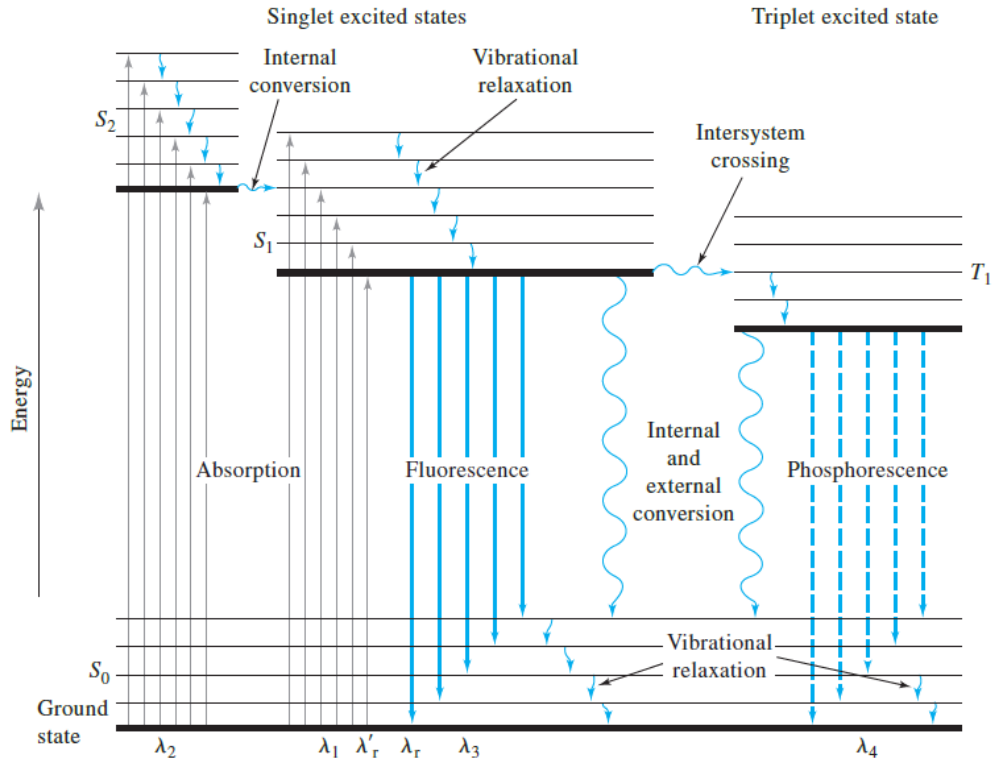

Figure 49. Jablonski diagram for fluorescence and phosphorescence (Skoog et al., 2018).

Several structural features enhance the probability of fluorescence: aromatic rings, highly conjugated double bonds or carbonyl groups (with low energy π-π* transitions), fused rings and heterocycles. Structural rigidity is also a key feature; this enhances the fluorescence by restricting the internal conversion rate. External factors such as pH, solvent viscosity and concentration are also important (Skoog et al., 2018).

Due to all these conditions, not all molecules display this phenomenon; it turns helpful in detecting or quantifying a determined analyte. Fluorescence also proves to be highly sensitive, with detection levels as low as 10^{-12} M . The dependence of a specific range of wavelengths for absorption and an exclusive one for emission turns this technique highly selective due to the low probability of interferences (regardless of quenching), especially when is coupled to a chromatographic system (Settle, 1997).

HPLC-FLD has displayed a remarkable efficiency for the separation and quantification of fluorescent species, allowing the detection of complex mixtures in a short time, with high selectivity, precision, and accuracy. The FLD (Figure 50) consists of a source, usually, a Xenon lamp, which excites any fluorescent species due to its wide emission window between 100 and 1100 nm, and a photodetector used to measure the photons emitted by the sample; this is situated orthogonally to the Xe lamp to avoid parasite light.

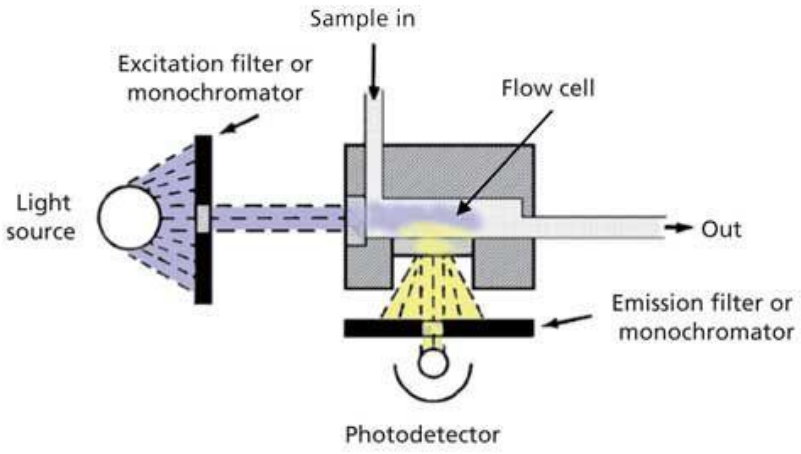

Figure 50. FLD detector scheme. (https://www.chromatographyonline.com/view/how-does-it-work-part-v-fluorescence-detectors).

A previous analysis of the aristolactam content in several species of Aristolochiaceae and herbal preparations (Yuan et al., 2008) was considered as a base for this study, with a new chromatographic methodology and method validation strictly designed for this purpose. Due to the use of a single standard, it was hypothesized that the response factor for all aristolactams was the same as for cepharanone B.

4.2. Objectives

4.2.1. Main Goal

To identify and quantify the total content of aristolactams in the roots of sixteen *Piper* species.

4.2.2. Specific Goals

To develop and optimize a selective chromatographic methodology for the quantification of aristolactams.

To validate the analytic method by establishing its linearity, accuracy, precision, LOD and LOQ.

To quantify the total amount of aristolactams in roots of *Piper* species relative to an isolated standard of cepharanone B.

To elucidate the chemical structures of the isolated novel compounds.

4.3. Results and Analysis

4.3.1. Preparation of samples and isolation of standards

A total of twenty-one samples (six-teen species) of *Piper* (Table 9) were extracted using ethyl acetate and dried under reduced pressure; finally, 30 mg/mL samples for HPLC were prepared. The TLC (Figure 51) displayed several fluorescent spots, with the characteristic blue brightness of aristolactams.

Table 9. *Piper* species for HPLC-DAD-FLD analysis.

Sample code	TLC Code	Species	Source
986	1	*P. aleyrianum*	PA, Carajás.
970	2	*P.reticulatum*	PA, Carajás (Serra Sul)
1023	3	*P.cernuum*	SP, Parque Ecológico do Perequê
999	4	*P. lucaenum var grandifolium*	PA, Parauapebas.
1554	5	*P. martiana*	MG, Santuário do Caraça.
P. aduncum	6	*P. aduncum*	SP, São Paulo.
975	7	*P. aleyreanum*	PA, Carajás (Serra Sul)
1622	8	*P. corcovadensis*	SP, Bertioga.
1260	9	*P. aequali*	Colombia, Cundinamarca, Fusagasugá.
1654	10	*P. cubatoanum*	MG, Bueno Brandão.
P. auritum	11	*P. auritum*	SP, São Paulo.
1060	12	*P. cubatoanum*	MG, Pedra Selada (Visconde de Mauá)
1705	13	*P. dilatatum*	PA, Carajás (Serra Sul)
1465	14	*P. aleyreanum*	AM, Manaus.
985	15	*P. hispidum*	PA, Carajás (Serra Sul)
1006	16	*P. cubatoanum*	SP, Serra da Cantarera.
1711	17	*P. anonifolium*	PA, Floresta Nacional do Tapajós.
1442	18	*P. reticulatum*	PA, Belterra.
983	19	*P. hostmanniuanum*	PA, Carajás (Serra Sul)
1133	20	*P. solmsianum*	RS, Dom Pedro de Alcântara
984	21	*P. krukoffii*	PA, Carajás (Serra Sul)

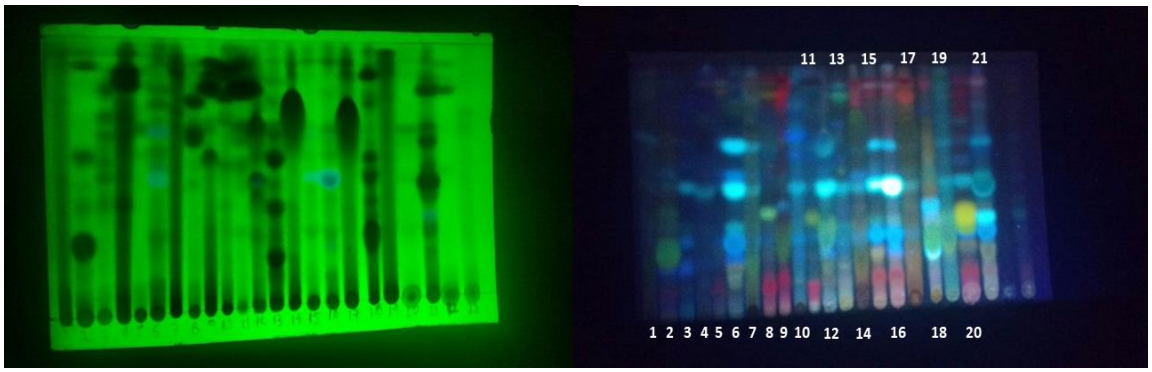

Figure 51. TLC of root extracts (Hex/EtOAc 6-4) at 254 nm (left) and 365 nm (right).

The standard of cepharanone B was isolated from roots of *P. lindbergii*; leaves, fruits and root extracts were prepared by Vivian Cornelio Megna, Ph.D. postdoctoral researcher (CNPq

158851/2015-3), in a previous study of this species. First, 3.56 g of methanolic extract were extracted again using DCM-water to remove the polar compounds. The organic fraction (2.37 g) was dried and concentrated under reduced pressure, then was submitted to a VLC fractioning with 160 g of silica flash and gradient of Hex-EtOAc, yielding 23 fractions (Figure 52).

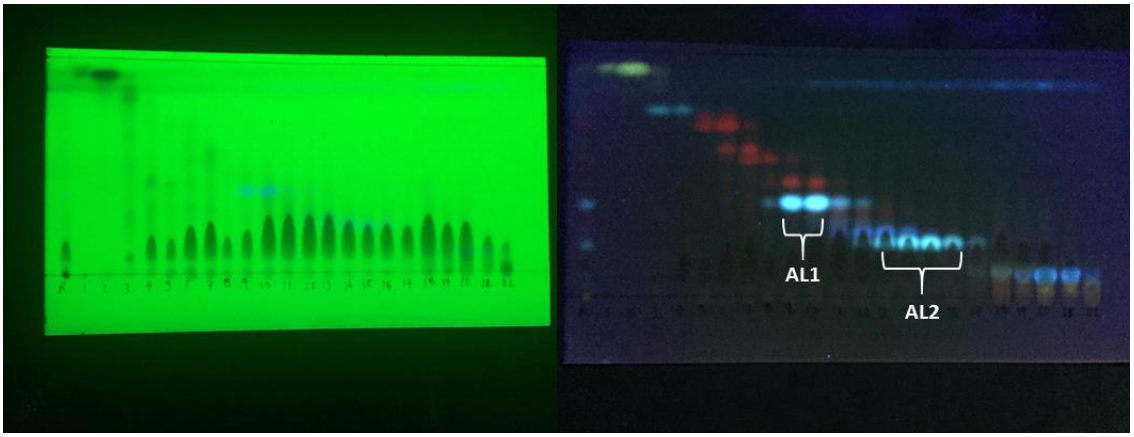

Figure 52. TLC of VLC from *P. lindbergii* roots (Hex/EtOAc 7-3) at 254 nm (left) and 365 nm (right).

Despite the good fractioning of the fluorescent compounds, the principal component was present in most fractions, with plenty of crystalline solids in each one. Fractions 9-10 (AL1) and 13-16 (AL2) were pooled, yielding 87.0 mg and 76.8 mg, respectively. The new fractions were submitted to a further purification step using a Sephadex® LH-20 in methanol; several light-absorbing and fluorescent bands (365 nm) were observed during the process. Thus, larger fractions were collected based on this fact. AL1 and AL2 yielded nine new fractions (four bands, front, ending and in-between) collected in the same way; four compounds were annotated (Figure 53).

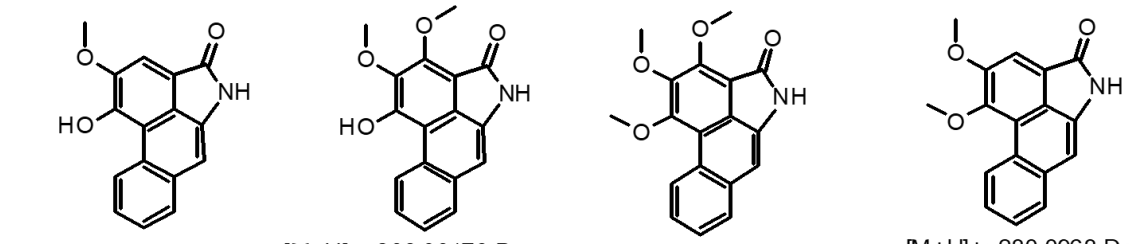

107 **108** **109** **37**

Figure 53. Aristolactams from roots of *P. lindbergii*: **107** piperolactam A, **108** piperolactam B, **109** piperolactam C and **37** cepharanone B.

Finally, fractions AL1-6 (3.6 mg) and AL2-7 (2.0 mg) were selected for further purification with column chromatography using regular silica (1.0 g) and a Hex-EtOAc gradient; the latter resolved the two fluorescent compounds present in the pooled fraction. After LCMS and ^{1}H NMR analyses, structures **37**, **108** and **109** were confirmed as is shown next:

AL1-6 with an rt of 20.05 minutes and a $[M+H]^+$ of 310.1074 (calculated for $C_{18}H_{16}NO_4$) and ^{1}H NMR spectra (500 MHz, $CDCl_3$) δ 9.24 – 9.18 (m, 1H), 7.90 (s, 1H), 7.86 – 7.81 (m, 1H), 7.59 – 7.53 (m, 2H), 7.19 (s, 1H), 4.53 (s, 3H), 4.20 (s, 3H), 4.01 (s, 3H), corresponding to piperolactam C **109**, reported for *P. longum* (Priestap, 1985), *P. argyrophylum*, *P. boehimerfolium* and *P. wightii* (Parmar et al., 1997).

AL2-7 with an rt of 18.12 minutes and a $[M+H]^+$ of 280.0968 (calculated for $C_{17}H_{14}NO_3$) and ^{1}H NMR spectra (500 MHz, $CDCl_3$) δ 9.29 – 9.20 (m, 1H), 7.90 – 7.76 (m, 3H), 7.63 – 7.55 (m, 2H), 7.08 (s, 1H), 4.13 (s, 3H), 4.09 (s, 3H), corresponding to cepharanone B **37**, reported for *P. argyrophylum, P. attenuatum , P. boehimerfolium, P. chiadoense, P. longum and P. wightii* (Parmar et al., 1997).

AL2-9 (0.9 mg) was obtained with a rt of 15.7 minutes and a $[M+H]^+$ of 296.0917(calculated for $C_{17}H_{14}NO_4$). ^{1}H NMR 500 MHz, $CDCl_3$) δ 9.20 (d, J = 7.8 Hz, 2H), 7.85 (d, J = 9.0 Hz, 2H), 7.74 (s, 2H), 7.71 (dd, J = 5.7, 3.3 Hz, 2H), 7.56 – 7.50 (m, 3H), 7.41 (s, 2H), 7.20 (s, 2H), 4.54 (s, 6H), 4.07 (s, 6H) corresponding to piperolactam B **108**, reported for *P. argyrophylum, P. boehimerfolium,*

P. longum and P. acutisleginum (Parmar et al., 1997), the fraction was obtained as a mixture with cepharanone B. Due to its low amount, further purification was not considered.

Fraction 21 was not further purified despite its fluorescence, suggesting the presence of an aristolactam. HPLC-MS analysis of this fraction showed a significant peak in 14.46 min, and a $[M+H]^+$ of 266.0812 (calculated for $C_{16}H_{12}NO_3$); the previous report suggested the presence of piperolactam A **107**, present in *P. longum, P. attenuatum P. boehmerifolium*, and *P. hamiltonii* (Desai et al., 1988). Its MS^2 showed peaks in 251.0712 Da (methyl loss), 223.0739 Da (CO and methyl loss) from the amide breakdown, 195.0775 Da (two CO and methyl loss) and 167.0815 Da (three CO and methyl loss). This fragmentation pattern supports the idea of the annotation, as CO losses are expected for this kind of compound (Demarque et al., 2016), and the peak in 167 Da has been previously observed (Priestap, 1985), the fragmentation mechanism (*Figure 54*) is explained below.

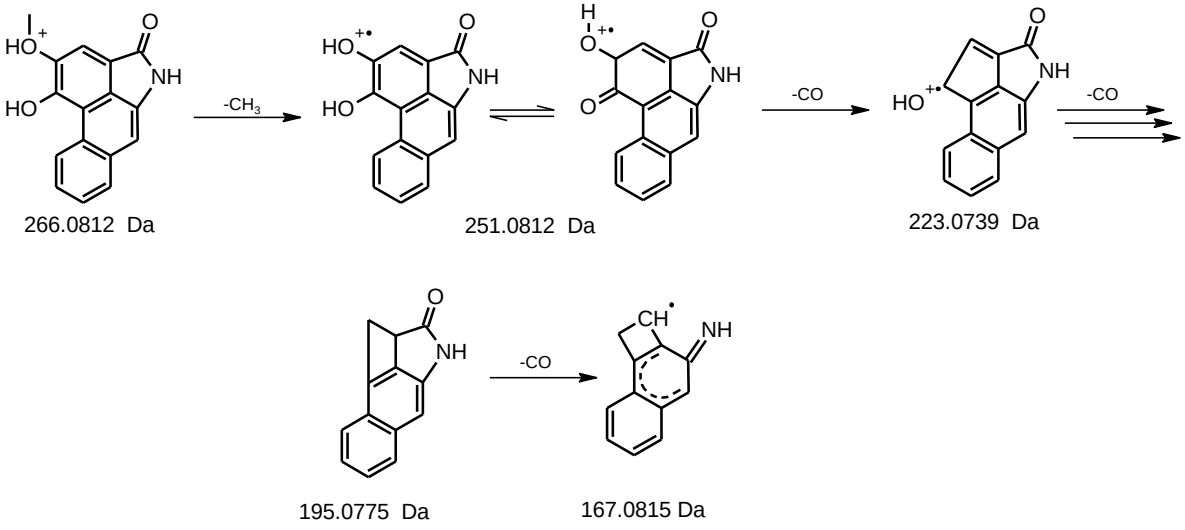

Figure 54. Proposed fragmentation mechanism for piperolactam A **107** (Priestap, 1985).

According to the amount of isolated compounds, purity, and quality of the ^1H NMR spectra, cepharanone B was chosen as the standard for quantification.

4.3.2. Method Validation and Quantification

The HPLC method of *P. lindbergii* was initially considered for this analysis because of previous studies of *P. lindbergii* (due to an identification setback, both species were considered the same at the beginning of this study). However, 65 min were deemed excessive for this new analysis; thus, a new HPLC-DAD method using the actual samples was developed. Aliquots of 100 µL from all samples were pooled; this new sample was named the working mix.

4.3.2.1 Selectivity

The analysis was conducted using the HPLC-FLD equipment from the Laboratório de Biologia Celular de Plantas (Lab. Biocel Depto. de Botânica - Instituto de Biociências, USP) thanks to the collaboration of the Prof. Eny I. S. Floh. Different tests were conducted, sample injection volumes, calibration curves and additional samples were established. The response for both detectors was not comparable, as the sensitivity was enhanced, and interferent compounds which were predominant in the DAD chromatogram were invisible for the FLD (Figure 55). Previous fluorimetry tests were conducted in an RF-6000 spectrofluorophotometer (Shimadzu) in the Central Analítica (IQ-USP) to establish the optimal excitation and emission wavelengths. In addition to another quantification of aristolactams by HPLC-FLD (Yuan et al., 2008), these values were verified as 270 nm and 390 nm, respectively.

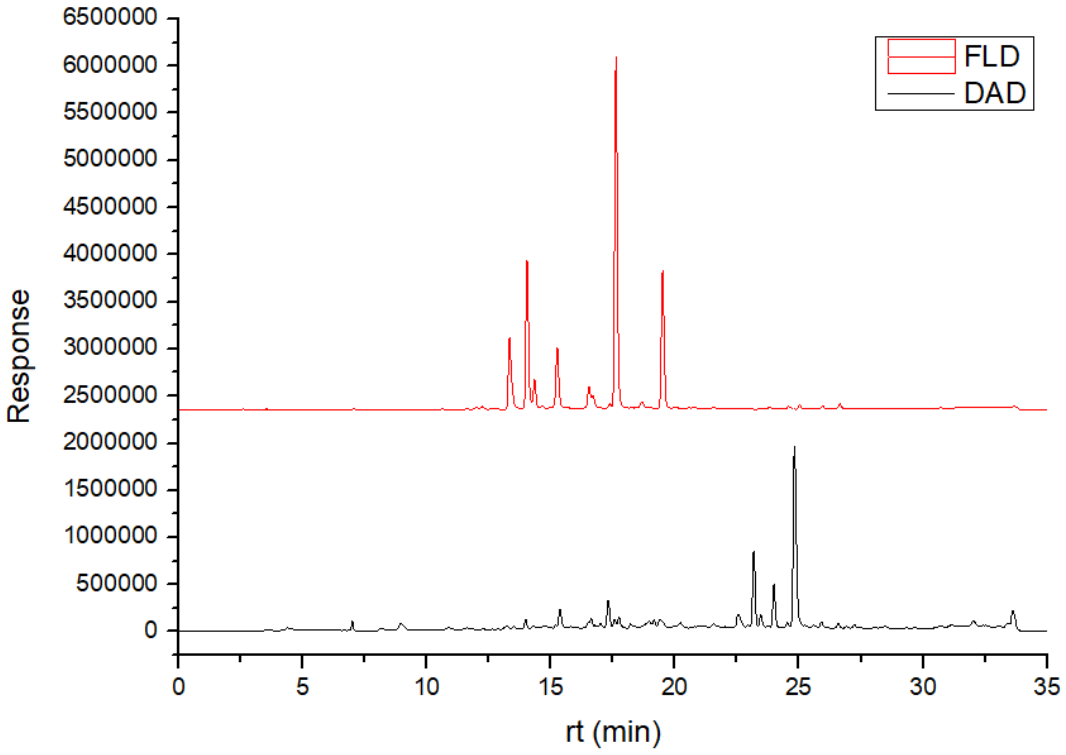

Figure 55. Detector's response comparison for the working mix. FLD (up) and DAD (bottom).

4.3.2.2. Linearity.

Linearity was evaluated by plotting the concentration in ppm versus the detector's response; seven concentration values were chosen for every curve, 5µL of the standard were injected by triplicate, and the mean value of the areas was calculated; the results are shown in Figure 56. The high concentration curve (C1) was conducted between 1.0 and 100.0 ppm, while the low concentration curve (C2) was conducted between 1.0 $x10^{-3}$ and 1.0 ppm. Pearson's coefficient of linearity for both cases was superior to 0.998, probing an optimal linear range as the slopes were around 4.5x 10^{5}, showing a high sensitivity.

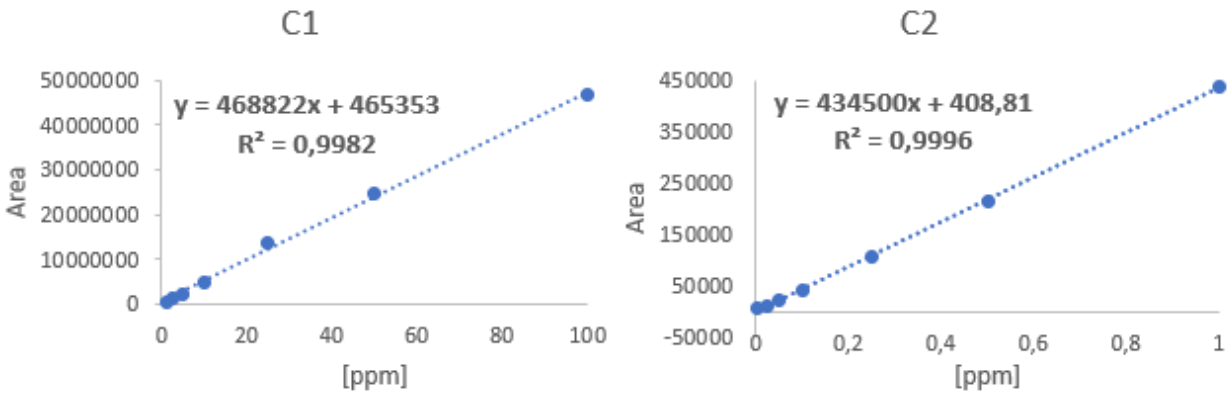

Figure 56. Calibration curves for cepharanone B standard. High concentration C1 (left) and low concentration C2 (right), line equations and Pearson's coefficient.

4.3.2.3. Precision and Accuracy

Precision was evaluated with a standard solution of cepharanone B of 50.0 ppm, and the measurements were carried out by injecting 5 µL of the standard, by triplicate, over three consecutive days (Table 10). The peak area's relative standard deviation, RSD (Taylor, 1983), was lower than 2.5%.

Table 10. Precision inter-day measurements for cepharanone B standard.

# Injection	Area	rt (min)
D1 1	23624637	18.12
D1 2	25022782	18.13
D1 3	24714898	18.11
D2 1	24506156	18.15
D2 2	24231093	18.15
D2 3	24526319	18.16
D3 1	25167742	18.20
D3 2	25635503	18.31
D3 3	25326819	18.50
Mean	24750661	18.20
SD	613614.5	0.126
%RSD	2.48	0.69

Accuracy was evaluated by spiking the known content of a standard into a sample with no significant aristolactam content (M9*, P. aequali*); the final concentration of cepharanone B was 25.2 ppm. The RSD and the recovery were calculated after several corrections in the area values (Table 11). A small amount of standard was retained in the column; thus, the initial blank (MeOH) area value was subtracted from the obtained result. 2 µL of the spiked sample were injected, and the concentration was calculated by correcting the dilution factor in C1. Recovery was 101.1%; this value was considered acceptable for the proposed method.

Table 11. Accuracy measurements with spiked sample M9(*P. aequali*), retention times and recovery.

#	A[a]	A_{cor}[b]	A_{dil}[c]	C_{calc}[d]	% Rec
1	4995709	4900276	12250690	25.14	99.8
2	4940780	4845347	12113368	24.85	98.6
3	5042336	4946903	12367258	25.39	100.7
4	5027926	4932493	12331233	25.31	100.4
5	4935321	4839888	12099720	24.82	98.5
6	4712350	4616917	11542293	23.63	93.8
Mean	4942403.67	4846970.67	12117427	25.48	101.1
SD	120929.31				
%RSD	2.45				

[a] Original area.
[b] Corrected area by subtracting the value from the blank.
[c] Corrected area by the dilution factor.
[d] Calculated concentration according to C1.

4.3.2.4. Limit of Detection and Limit of Quantification

LOD and LOQ for the calibration curves were calculated by linear regression (Rao, 2018) using Microsoft Excel® and estimating the standard deviation of the intercept of the response (SD_{int}) and the slope (ICH.GUIDELINE, 2005).

$$LOD = 3.3\ x\ \left(\frac{SD_{int}}{Slope}\right)$$

$$LOQ = 10\ x\ \left(\frac{SD_{int}}{Slope}\right)$$

Equation 1. Definitions for Limits of Detection and Quantification.

The estimated LOD and LOQ for C1 and C2 are shown in Table 12; for high concentration, this value is on the ppm level while low concentrations lie in ppb. This result demonstrates the technique's high sensitivity and utility for quantifying metabolites in very low concentrations.

Table 12. LOD and LOQ for C1 and C2.

	C1	C2	
SE_{int}	383934,2	1753,2	
SD_{int}^{*}	145113,5	662,7	
Slope	475614	435094	
LOD	1,01	0,0050	µg/mL
LOQ	3,05	0,0152	µg/mL

*$SD_{int} = SE_{int}/\sqrt{N}$, N=7.

4.3.2.5. Sample Analysis

Purified standards, enriched fraction 21 and samples were analyzed; according to the previous tests carried out with the working mix, it was concluded that sample M6 (*P. aduncum*) corresponded to the dominant chemotype (Figure 57). It was also established that most of the aristolactams present in the samples matched with the previously isolated standards

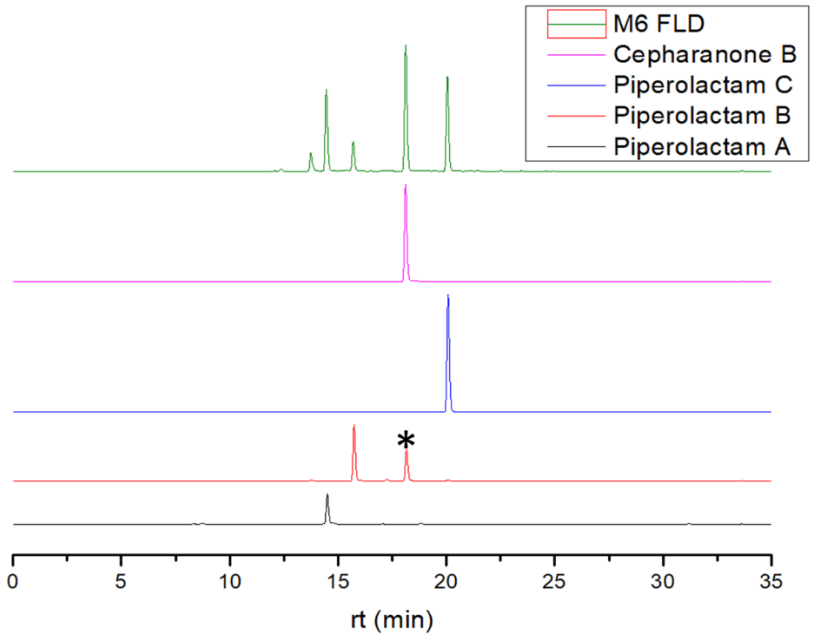

Figure 57. Comparison between purified aristolactams and dominant chemotype M6.
**cepharanone B remained as an impurity.*

Samples M1 to M21 were analyzed by injecting 2 µL by triplicate, and the obtained data were aligned using the algorithm COW (Correlation Optimized Warping) downloaded from http://www.models.kvl.dk/ in ®MatLab 2016a (Nielsen et al., 1998). The aligned data were normalized, auto-scaled (Goodacre et al., 2007), and plotted in OriginPro 8.5 (Figure 58 to Figure 60).

The compound corresponding to the peak in 13.74 min for M21 (*P. krukoffii*) did not match any previously isolated aristolactams; the HPLC-MS data showed a $[M+H]^+$ of 340.1190 Da (calculated for $C_{18}H_{13}NO_6$). The only compound belonging to this family that matches the formula was aristolactam DIII **110**, reported for *Aristolochia argentina* (Aristolochiaceae) and *Goniothalamus sesquipedalis* (Wall.) (*Annonaceae*) (Priestap, 1985; Talapatra et al., 1988). Additionally to the $[M+H]^+$ ion, a fragment ion at 221.0806 m/z was observed; the successive decarboxylation, amide cleavage and loss of methanol would explain this fact, similarly to the fragmentation of aristolactam I (Chan et al., 2006)

As can be seen, in most cases, peaks were located between 12 and 21 min, with most of the chromatograms displaying a particular grade of homogeneity in the number of compounds but with remarkable differences in their relative abundance. Cepharanone B and piperolactam C seemed to be the dominant compounds, and in some cases, were the only significant ones, like in M1 or M10.

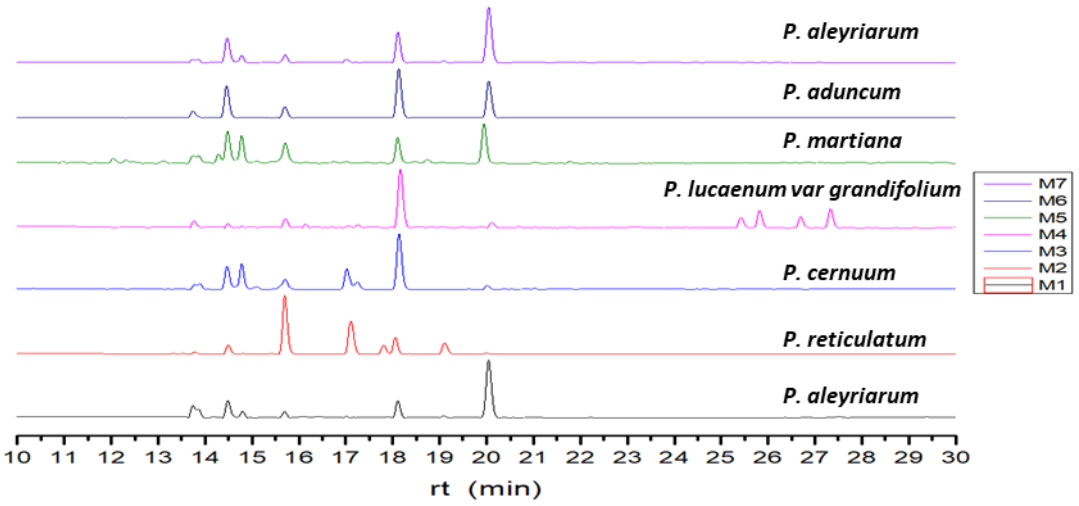

Figure 58. *HPLC-FLD chromatograms of samples M1-7.*

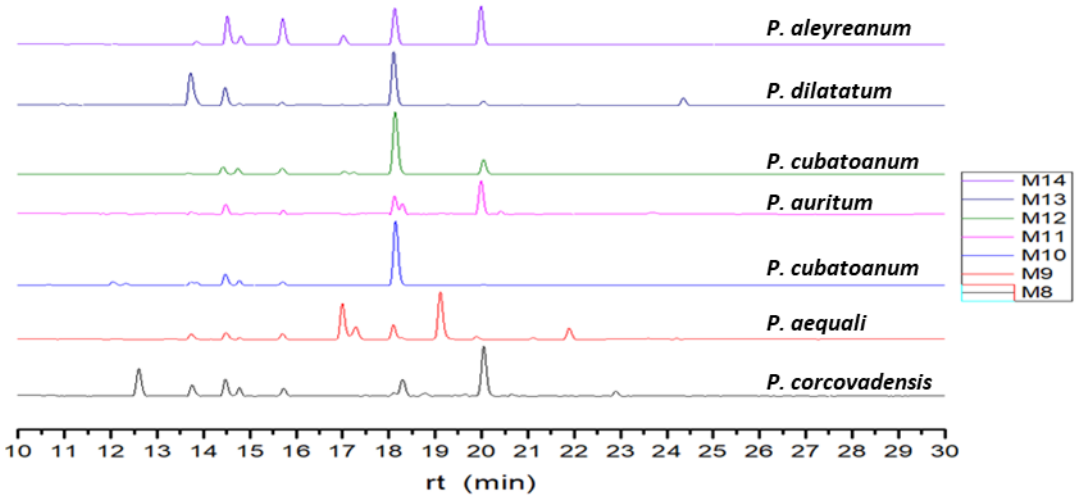

Figure 59. *HPLC-FLD chromatograms of samples M8-14*

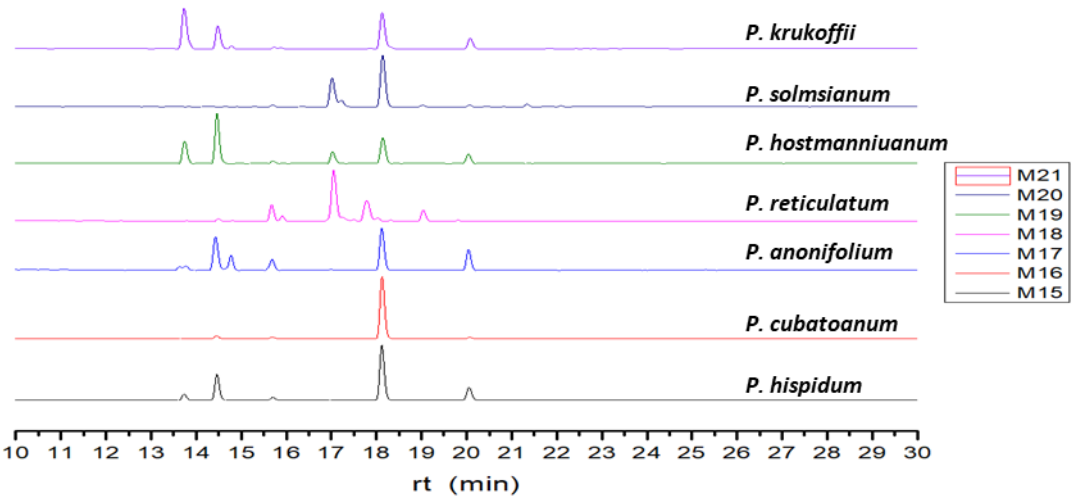

Figure 60. HPLC-FLD chromatograms of samples M15-21.

The aristolactams content was calculated in ppm (for the HPLC samples, Table 13) and mg of cepharanone B per g of dry extract (Table 14) using C1 and C2. M6, M7, M15, M16 and M21 displayed the highest amount.

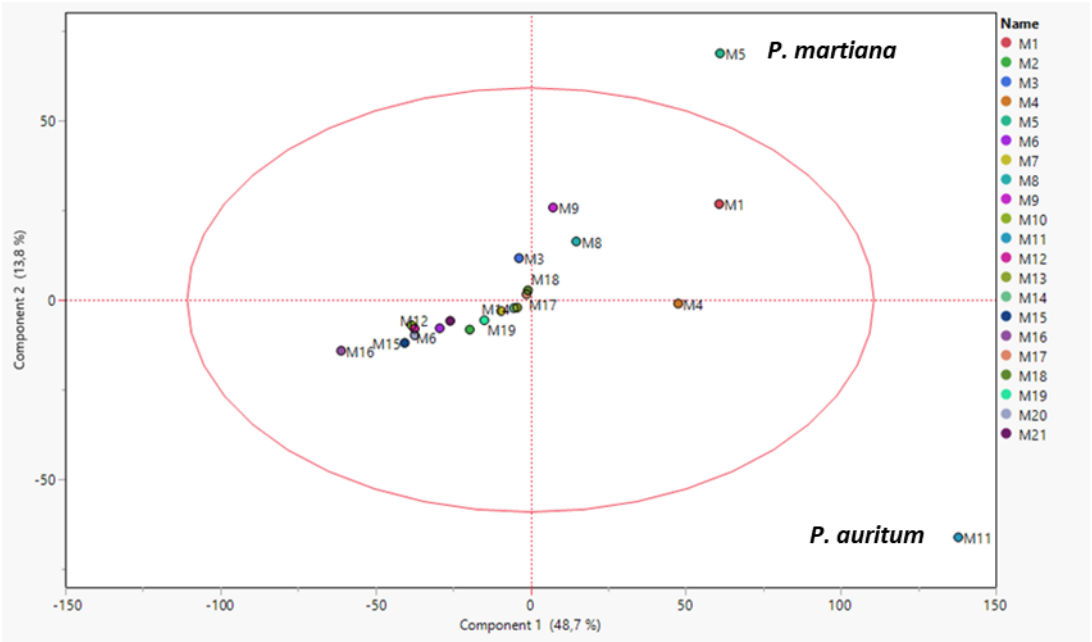

Figure 61. PCA for HPLC-FLD data of samples M1-21.

Multivariate analysis of the chromatographic data was conducted (Figure 61). The PCA did not show an apparent clustering between samples or the influence of the first two components

except for outliers M5 (*P. martiana*) and M11 (*P. auritum*), suggesting a notorious difference in the composition of such samples. As was described in Table 14, the samples M4, M5, M9-M11, M18, and M20, contained a negligible amount of aristolactams while M6, M7, M15, M16 and M21 contained the highest quantity. According to the mean, median, and standard deviation (global and by compound), cepharanone B had the highest content and variation (0.90, 0,39 and 1.23 mg of cepharanone B/dry extract, respectively) and was the most significant for all the analyzed species. Cepharanone B has displayed a notable role as a topoisomerase-poison despite not describing any additional biological activity.

Most samples showed some aristolactam content, with *P. aduncum, P. aleyreanum, P. hispidum, P. cubatoanum* and *P. krukoffi* displaying the highest amounts, with mean values between 0.75 and 1.97 mg of cepharanone B /g of dry extract. Cepharanone B had the highest content in all samples with a maximum of 4.98 μg/mg of dry extract for *P. cubataonum* and a mean value of 0.90 μg/mg of dry extract. Surprisingly, those values were superior, in almost an order of magnitude, to the reported values from Aristolochiaceae preparations (Yuan et al., 2008).

Table 13. Quantified aristolactams in ppm relative to cepharanone B in HPLC samples.

	M1	M2	M3	M4*	M5	M6	M7	M8	M9	M10	M11	M12	M13	M14	M15	M16	M17	M18	M19	M20	M21
aristolactam DIII	3.20	1.49	1.18	3.62	1.39	16.50	3.99	5.35	0.69	1.63	0.12	0.62	3.57	1.61	6.45	2.30	1.14	0.49	6.80	0.63	64.33
piperolactam A	4.95	4.19	5.10	1.88	5.06	63.87	24.10	6.22	0.75	4.93	0.60	1.91	1.76	8.06	25.55	7.53	8.15	0.56	16.08	0.00	35.26
piperolactam B	3.16	25.52	3.78	3.86	4.69	28.44	13.13	5.82	0.26	2.56	0.34	2.22	0.43	8.04	4.49	7.39	4.05	2.68	1.01	1.63	5.05
cepharanone B	6.18	7.11	15.72	19.37	4.79	95.75	34.49	4.69	1.17	29.24	0.90	15.83	5.93	10.98	56.68	149.29*	11.56	0.00	7.92	28.25	59.03
piperolactam C	15.45	1.06	0.94	3.12	6.81	91.07	78.44	22.56	0.26	0.75	1.90	4.10	0.49	14.53	18.84	4.02	10.42	0.00	3.23	1.54	21.49

*cepharanone B for M16 was out of the measured range, and quantification was carried out by extrapolation.

Values less than 3.0 ppm were calculated using C2.

Table 14.Quantified aristolactams in mg of cepharanone B/g of dry extract.

	M1	M2	M3	M4*	M5	M6	M7	M8	M9	M10	M11	M12	M13	M14	M15	M16	M17	M18	M19	M20	M21
aristolactam DIII	0.107	0.050	0.039	0.121	0.046	0.550	0.133	0.178	0.023	0.054	0.004	0.021	0.119	0.054	0.215	0.077	0.038	0.016	0.227	0.021	2.144
piperolactam A	0.165	0.140	0.170	0.063	0.169	2.129	0.803	0.207	0.025	0.164	0.020	0.064	0.059	0.269	0.852	0.251	0.272	0.019	0.536	0.000	1.175
piperolactam B	0.105	0.851	0.126	0.129	0.156	0.948	0.438	0.194	0.009	0.085	0.011	0.074	0.014	0.268	0.150	0.246	0.135	0.089	0.034	0.054	0.168
cepharanone B	0.206	0.237	0.524	0.646	0.160	3.192	1.150	0.156	0.039	0.975	0.030	0.528	0.198	0.366	1.889	4.976*	0.385	0.000	0.264	0.942	1.968
piperolactam C	0.515	0.035	0.031	0.104	0.227	3.036	2.615	0.752	0.009	0.025	0.063	0.137	0.016	0.484	0.628	0.134	0.347	0.000	0.108	0.051	0.716

Low High

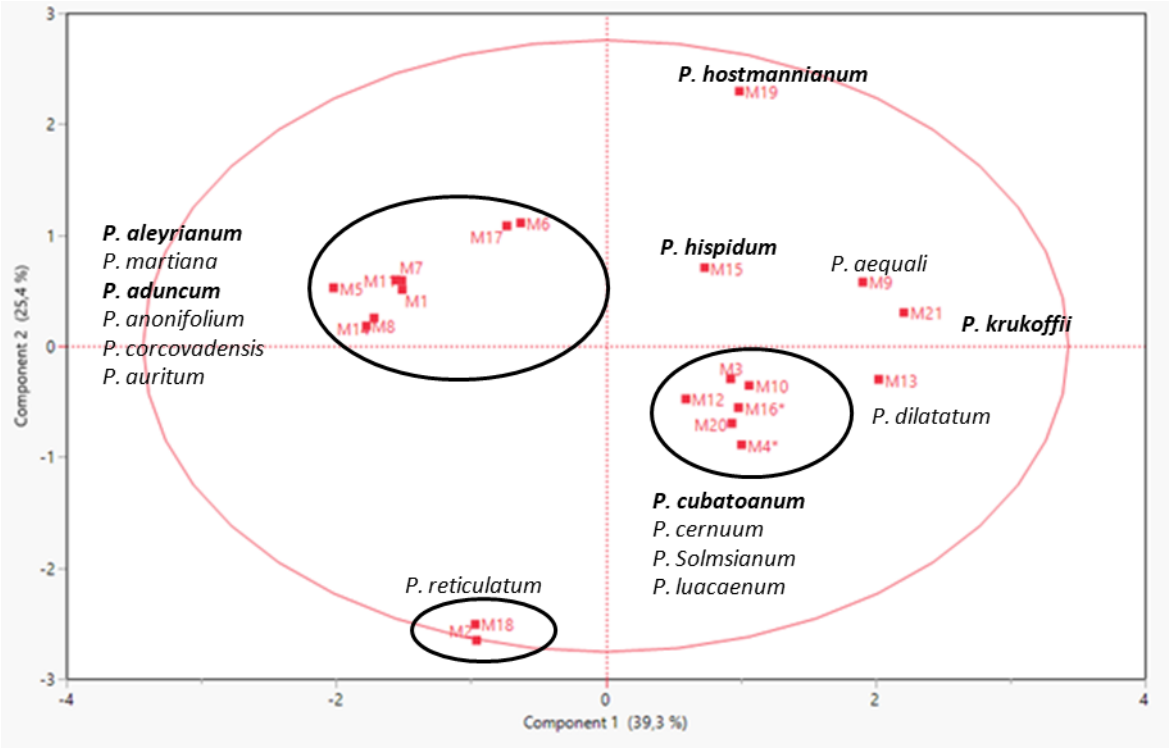

Figure 62. PCA for aristolactams content of samples M1-21.

The PCA with aristolactam-content as the target variable showed several main clusters with a clear relationship between species; on the other hand, the loading plot (Figure 63) described a positive correlation between cepharanone B and aristolactam DIII, while negative correlations were evident between piperolactam A and B as well as piperolactam C with cepharanone B and aristolactam DIII.

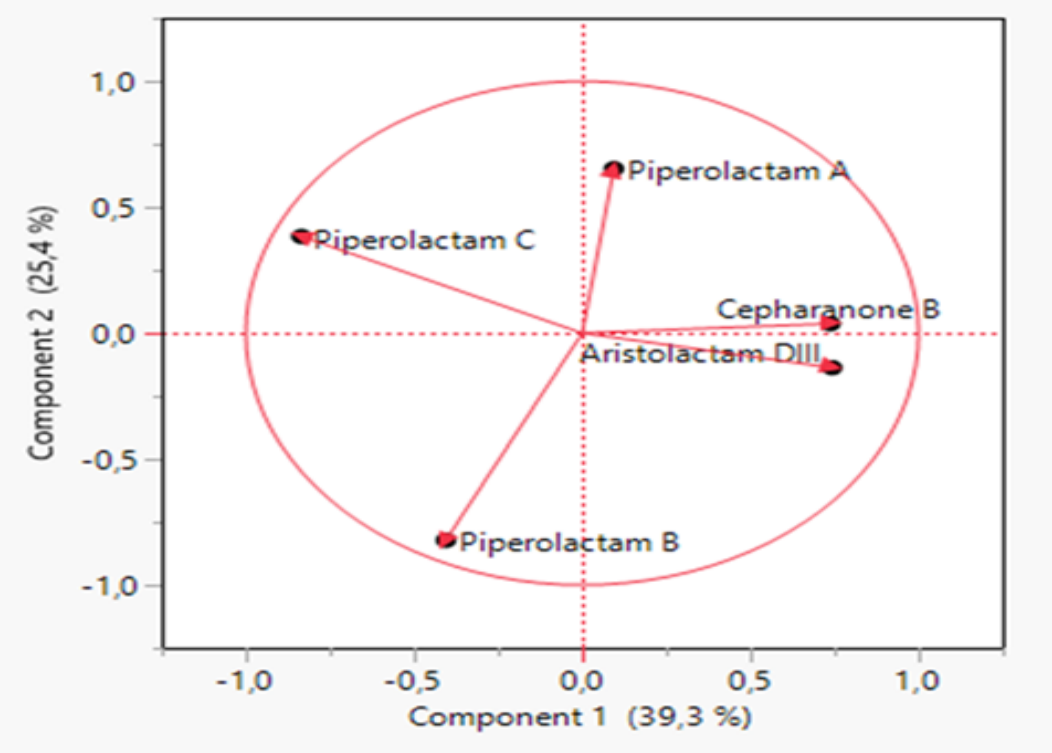

Figure 63. Loading Plot from aristolactam content as the target variable.

These relationships tended to be cooperative or mutually exclusive; while cepharanone B was the most influential factor and was always accompanied by aristolactam DIII, in some cases, this fact seems to decrease the expression of piperolactam C and vice versa. This trend was also observed for piperolactams B and C, while the first escalated and the latter lowered its relative concentration.

4.3.3. Novel compounds from roots of *P. lindbergii*

The methanolic extract from roots of *P. lindbergii* was chosen to isolate the standard because it contained piperolactams A-C and cepharanone B, as demonstrated in a previous study. During the purification process of these metabolites, which were minor compounds, many solids were obtained in most of the twenty-two fractions; as observed in Figure 52, there was a constant compound between fractions 3-22 with a strong UV absorption at 270 and 365 nm. The spots in the TLC showed a notorious tailing, with a low migration for the chosen eluent system. After the

analysis of fraction 5, which showed a considerable amount of well-defined crystals, using a Sephadex and a MeOH-DCM (1-1) eluent system, two main subfractions were obtained, the first corresponding to a phytosterol according to the coloration obtained after the use of acidic anisaldehyde as a visualization reagent and the profile of the ^{1}H and ^{13}C NMR spectra (El-Gamal et al., 2016). The other subfraction, containing white crystals, was analyzed by HPLC-DAD (Figure 64) and ^{1}H NMR (Figure 65).

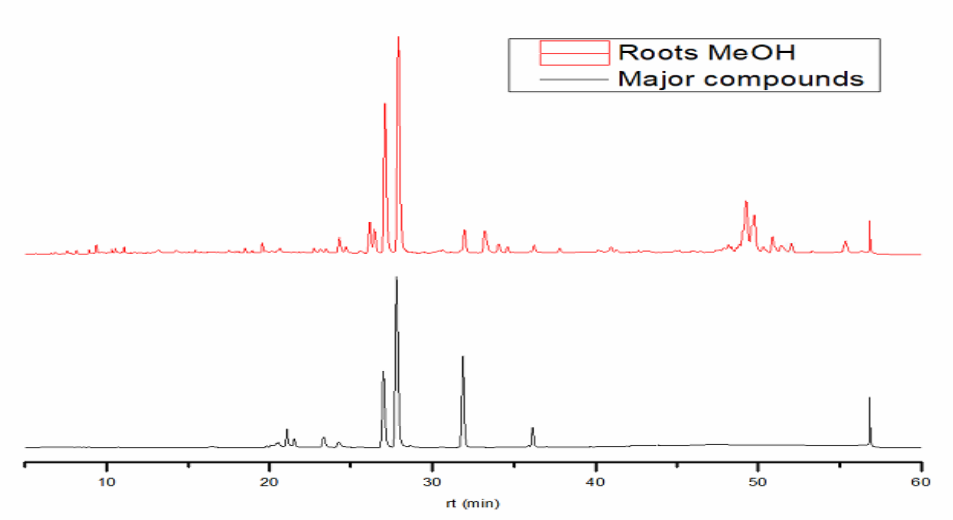

Figure 64. HPLC-DAD chromatogram of major compounds from roots of *P. lindbergii* at 270 nm. MeOH extract (up) and isolated crystals (bottom).

The chromatogram showed at least three major compounds with significant absorbance at the detecting wavelength, while the ^{1}H NMR spectrum (Figure 65) displayed a profile of signals corresponding to a mixture of two compounds in a proportion of 2.8 - 1 and similar features. At first sight, the broad signals over 13 δ are characteristic of "chelated" phenolic OH protons while the peaks around 10.2 δ suggested the presence of aldehyde or carboxylic acid groups; the peaks around 5.8 δ could be assigned to olefinic protons, and the signals under 2.5 δ suggested an aliphatic moiety with the pattern of an ethyl and methyl groups.

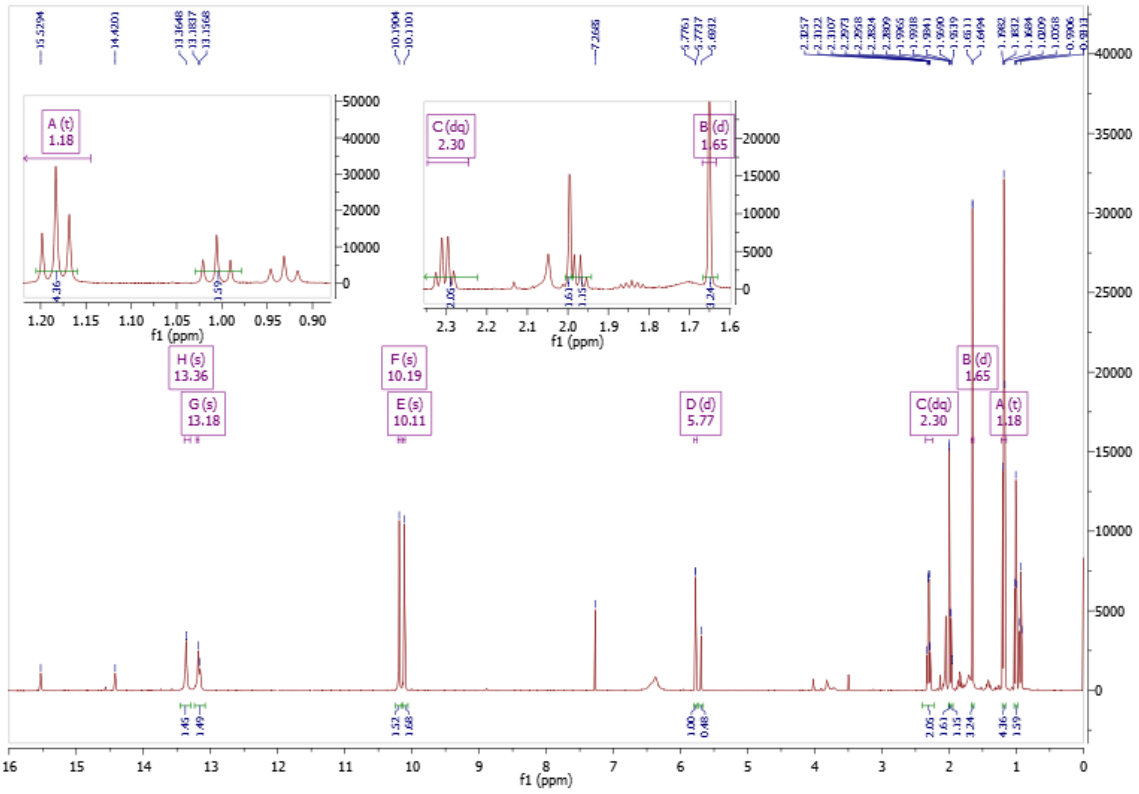

Figure 65. ^{1}H NMR spectrum of major compounds from roots of *P. lindbergii.*

The LC-MS^{2} analysis, using the new method of 35 min in negative mode, showed that the major peaks in 18.6 and 19.1 min possessed the same $[M-H]^-$ ion (249.0782 and 249.0783 Da, respectively), corresponding to a molecular formula of $C_{13}H_{14}O_5$. During the further purification process of cepharanone B, two collected fractions (A1S2 and A1S4) from the Sephadex contained the same mixture but in different proportions (6-1 and 1-2 respectively).

The enriched fractions were analyzed by ^{1}H NMR:

A1S2: ^{1}H NMR (500 MHz, $CDCl_3$) δ 13.37 (s, 1H), 13.20 (s, 1H), 10.20 (s, 1H), 10.11 (s, 1H), 6.27 (bs, 1H), 5.78 (m, 1H), 2.31 (qd, *J* = 7.5, 1.4 Hz, 2H), 1.65 (d, *J* = 1.3 Hz, 3H), 1.19 (t, *J* = 7.5 Hz, 3H).

A1S4: ^{1}H NMR (500 MHz, $CDCl_3$) δ 13.37 (s, 1H), 13.17 (s, 1H), 10.20 (s, 1H), 10.10 (s, 1H), 6.33 (bs, 1H), 5.70 (m, 1H), 2.00 (d, *J* = 1.4 Hz, 3H), 1.98 (q, *J* = 7.5, 2H), 1.01 (t, *J* = 7.6 Hz, 4H).

With this information, it was possible to propose two structures for the major compounds as the **111** 2,4,6-trihydroxy-5-[(1*E*)-2-methylbut-1-en-1-yl]benzene-1,3-dicarbaldehyde (A1S4), and **112** 2,4,6-trihydroxy-5-[(1*Z*)-2-methylbut-1-en-1-yl]benzene-1,3-dicarbaldehyde (A1S2) (Figure 66); these compounds were reported for the first time.

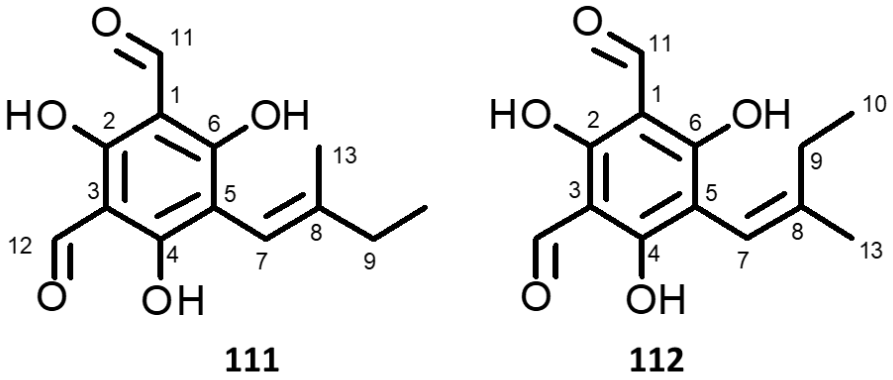

Figure 66. Novel compounds **111** and **112** from roots of *P. lindbergii.*

1D and 2D NMR data (Table 15) confirmed the presence of two chelates, two aldehydes, an olefinic proton, an olefinic methyl and ethyl groups (q coupled with t and *J* =7.5 Hz). Due to the triple substitution of the double bond, it was not trivial to establish the stereochemistry of each compound. It was also possible to observe a slight coupling between the isolated methyl and the methylene, *J* = 1.4 Hz, a typical value for a J^4 coupling of olefins.

The most remarkable differences between both spectra were the chemical shifts for ethyl and methyl groups; in *Z,* the methyl shifted to a higher field while the ethyl went to a lower one. With *E*, it was possible to observe the opposite effect. It is coherent to associate this behavior with the presence of the OH group in C-6, which seemed to be shielding its closest neighbor (C-9 in *Z* and C-13 for *E*) because of its proximity to the shape of a six-membered ring; this effect was extended to C-10.

Due to the lack of literature references for the compounds, the data was reprocessed using ACD/Spectrus Processor 2016.2.2, and ^{1}H, ^{13}C and 2D simulations were conducted in ACD/C+H

NMR Predictors and DB 2016.2.2 (ACD Labs), with the ^{13}C and simulations obtaining a match factor < 90%, confirming the proposed structures.

Table 15. Proton and carbon NMR assignments for **111** and **112** from roots of *P. lindbergii* in $CDCl_3$.

Position	111		112	
	^{1}H δ *J (Hz)*	^{13}C δ	^{1}H δ *J (Hz)*	^{13}C δ
1	-	104.48	-	104.51
2-OH	13.37 (s)	168.33	13.37(s)	168.41
3	-	103.40	-	103.76
4-OH	6.27 (bs)	162.17	6.33(bs)	162.38
5	-	104.60	-	104.67
6-OH	13.20 (s)	168.84	13.17(s)	168.87
7	5.78 (d, 1.2)	109.91	5.70 (s)	109.73
8	-	150.83	-	151.76
9	2.31 (dq, 7.4, 3.7)	32.31	1.98 (q, 7.6)	26.76
10	1.19 (t, 7.4)	12.84	1.01 (t, 7.6)	12.30
11-CHO	10.20 (s)	192.17	10.20(s)	191.17
12-CHO	10.10 (s)	192.30	10.10(s)	191.24
13-CH_3	1.65 (d, 0.8)	18.34	2.00 (d, 1.35)	22.45

Additional tests were conducted for leaves, and stem extracts, the HPLC-DAD chromatogram (Figure 67) displayed remarkable differences between the profiles, especially for roots and leaves, while the stem looked like a hybrid. For roots, there are two additional peaks in 18.0 and 18.2 min (**115** and **116** respectively), which were not identified during the purification of the aristolactams. The HPLC-MS^2 analysis showed that both peaks also shared the same $[M-H]^-$ ion (297.0974 and 297.0971 Da, respectively, corresponding to a molecular formula of $C_{14}H_{18}O_7$) and base peak (265.0680 and 265.0681 Da, respectively), which suggested the loss of methanol as the only significant fragmentation, additionally, a peak in 617.185 Da was observed and assigned to the $[2M+Na-2H]^-$ ion.

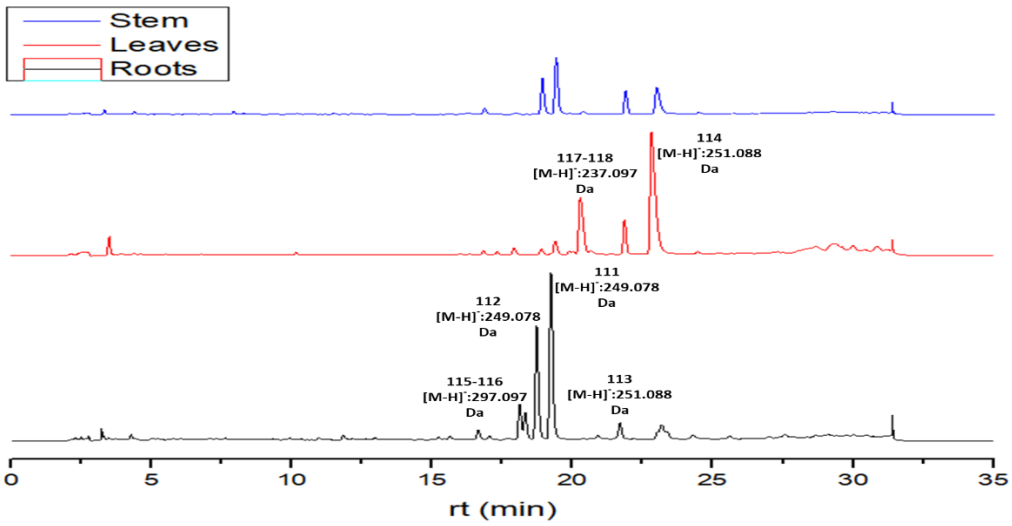

Figure 67. HPLC-DAD (270 nm) chromatogram and $[M-H]^-$ of each peak. of extracts from roots, leaves and stem of *P. lindbergii.*

Two more peaks (**113** and **114**) were observed in 21.6 and 22.6 min; despite the weak UV absorption, the ionization was comparable to the major compounds. These peaks were much more significant in leaves; the HPLC-MS^2 showed, like with the previous compounds, the same $[M-H]^-$ ion was observed (251.0877 and 251.0880 Da, respectively), suggesting the presence of another isomeric pair with formula $C_{13}H_{16}O_5$. ^1H, HSQC, HMBC and COSY analyses concluded that **114**; ^1H NMR (500 MHz, Acetone) δ 10.17 (s, 2H), 2.58 (dd, J = 13.9, 6.6 Hz, 1H), 2.47 (dd, J = 13.9, 8.3 Hz, 1H), 1.75 – 1.64 (m, 1H), 1.47 – 1.35 (m, 1H), 1.24 – 1.12 (m, 1H), 0.89 (t, J = 7.5 Hz, 3H), 0.86 (d, J = 6.7 Hz, 3H), corresponded to the 2,4,6-trihydroxy-5-(2-methylbutyl)benzene-1,3-dicarbaldehyde, a saturated analog of **111** and **112**.

Finally, another peak (**117**) in 20.0 min with a $[M-H]^-$ ion of 237.0969 Da, with formula $C_{12}H_{14}O_5$, was observed. ^1H, HSQC, HMBC and COSY analyses showed that compound **117**; ^1H NMR (500 MHz, Acetone) δ 10.17 (s, 2H), 2.50 (d, J = 7.5 Hz, 2H), 1.92 (non, J = 6.7 Hz, 1H), 0.91 (d, J = 6.7 Hz, 6H), corresponded to the 2,4,6-trihydroxy-5-(2-methylpropyl)benzene-1,3-dicarbaldehyde, which structure is very close to the other isolated metabolites.

All these compounds seemed to have a structural likeness to the **111** and **112**; it is fascinating that most came along as couples. This fact seemed to support the existence of a series of derivatives from both isomers. Some of these compounds are similar to several naturally occurring phloroglucinols with remarkable activities (McLean et al., 2004; Singh et al., 2010). Their purification and identification of **114**-**116** and **118** are still in progress.

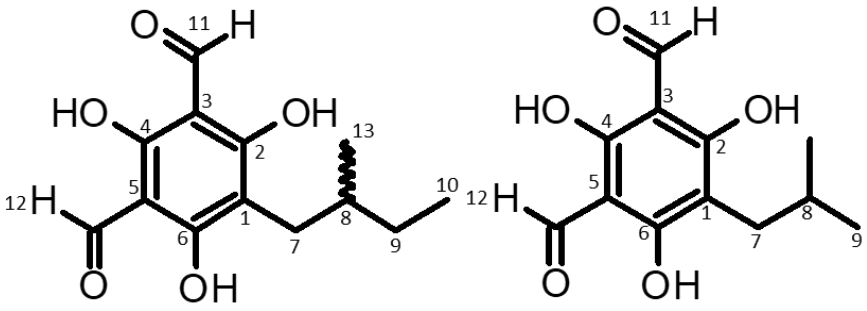

114 **117**

Figure 68. Structures of compounds **114** and **117** from leaves of *P. lindbergii.*

Table 16. *NMR assignments for **114** and **117** from leaves of P. lindbergii in $(CD_3)_2CO$.*

	114			**117**		
Position	^{1}H δ *J* (Hz)	^{13}C δ	HMBC	^{1}H δ *J* (Hz)	^{13}C δ	HMBC
1	-	107.40	-	-	107.34	-
2	-	168.46	-	-	169.02	-
3	-	105.20	-	-	105.64	-
4	-	168.46	-	-	169.02	-
5	-	105.20	-	-	105.64	-
6	-	168.46	-	-	169.02	-
7	2.59 (dd, 13.9, 6.6) 2.47 (dd, 13.9, 8.3)	28.78	C-8, C-9	2.50 (d,7.5)	30.30	C-9,C-8,C-1C-2,C-6
8	1.75 - 1.64 (m)	35.20	C-10,C-13, C-7,C-9, C-1	1.92 (non, 6.7)	28,79	C-9,C-7,C-1
9	1.47 - 1.35 (m) 1.24 - 1.12 (m)	30.06	C-10,C-13, C-7,C-8	0.91 (d,6.7)	22.43	C-8,C-7,C-1
10	0.89 (t, 7.5)	11.97	C-9,C-8	-	-	-
11	10.17 (s)	192.70	C-3,C-2,	10.17 (s)	192.89	C-3,C-2,

			C-4,C-1			C-4,C-1
12	10.17 (s)	192.80	C-5,C-6, C-4,C-1	10.17 (s)	192.89	C-5,C-6, C-4,C-1
13	0.86 (d, 6.7)	19.0	C-9,C-8, C-7	-	-	-

4.4. Conclusions

Five known aristolactams were identified in extracts of roots from twenty-one species of *Piper*; after the isolation of cepharanone B as standard, an HPLC-FLD method was developed and validated for the quantitation of major compounds. Piperolactams A-C, cepharanone B, and aristolactam DIII were identified and quantified, with *P. aduncum, P. aleyreanum, P. hispidum, P. cubataonum* and *P. krukoffi* displayed the highest content of these compounds. The method was highly selective and sensitive for this study and also demonstrated high ruggedness.

The multivariate analysis showed that most species maintained high homogeneity in their composition. At the same time, the expression of the aristolactams was positively correlated for cepharanone B and aristolactam DIII. However, negative relationships between piperolactam A and B, aristolactam DIII and cepharanone B with piperolactam C were observed. In other words, the expression of these compounds was mutually excluding, despite their structural similarity. Some species, such as *P. cubataonum,* can be considered as remarkable sources of aristolactams.

During the isolation process of the standards from roots of *P. lindbergii*, two novel prenylated 2,4-diformylphloroglucinols (**111**-**112**) were identified by HPLC-MS and NMR. Additionally, two more compounds (**114** and **117**) were identified from leaves in the same way; both roots and leaves also yielded six additional annotations (**113**, **115** - **116**, **118** – **120**), which spectrometric data suggested as analogs of the novel **111-112** prenylated 2,4-diformylphloroglucinols.

General Conclusions

In general terms, *Piper's* species described in this work showed a diverse landscape of secondary metabolites, with most of the non-volatiles described for the first time, even for the genus. The ontogenic changes in most cases were notorious, and the critical influence of the developing conditions was observed.

P. auritum displayed high diversity of secondary metabolites; these could be grouped into four main sets of compounds: C-glycosylflavonoids, phenylbutenolides, amides and phenylpropanoids, with C-glycosyl flavonoids being the most conspicuous type in most of the organs but the root, which displayed a high content of amides, with pellitorine being the most abundant. The ontogenic changes in the composition of leaves showed a reduction in the amount of C-glycosyl flavonoids, while the production of pellitorine increased and displayed a profile that corresponds to a hybrid between young leaves and roots

P. lindbergii C.DC. and *P. chimonantifolium* are two species not well chemically investigated, with most of their studies focused on their ecological relations. For these species, a broad set of chalcone-type compounds was identified, projecting them as promising sources of chalcone-type metabolites

Seven species of *Piper (P. umbellatum, P. glabratum, P. diospyrifolium, P. caldense, P. regnellii, P. crassinervium* (IQ and Colombia) and *P. chimonantifolium* were profiled by HPLC-DAD and ^{1}H NMR. Adults and seedlings were compared by multivariate analysis, with the best results obtained for HPLC methodology. Most species described notorious changes in their composition during the ontogeny, with several C-glycosyl flavonoids being conserved during the development process. For *P. glabratum*, two different culture methodologies were compared,

and the results showed the critical influence of the culture and developing conditions in the expressed metabolites.

Finally, after the constant finding of aristolactams in the studied species, especially in roots, an HPLC-FLD method was developed and validated for their quantification in root extracts of six-teen species of *Piper*. Piperolactams A-C, cepharanone B, and aristolactam DIII were identified and quantified, with *P. aduncum, P. aleyreanum, P. hispidum, P. cubataonum* and *P. krukoffi* displayed the highest content of these compounds. The method was highly selective and sensitive for this study and also demonstrated high ruggedness.

During the isolation process of the standards from roots of *P. lindbergii*, two novel prenylated 2,4-diformylphloroglucinols (**111**-**112**) were identified by HPLC-MS and NMR. Two analogs (**114** and **117**) were identified from leaves; both leaves and roots yielded six additional annotations (**113**, **115** - **116**, **118** – **120**), which spectrometric data suggested as analogs of the novel **111-112** prenylated 2,4-diformylphloroglucinols.

Perspectives

As future considerations for the proper completion of this study, the isolation of key metabolites from roots of *P. auritum* and leaves of *P. chimonantifolium* and *P. lindbergii*, adult and seedlings from *P. umbellatum, P. glabratum, P. diospyrifolium, P. caldense, P. regnellii, P. crassinervium* (IQ and Colombia) and *P. chimonantifolium* are necessary for a total identification of the main metabolites by spectroscopic and spectrometric techniques.

To better match the annotations by MS^2, the use of different databases as GNPS is necessary.

The quantification of aristolactams could be extended to a higher number of species and the different organs of the studied ones. This expansion could lead to a better understanding of the distribution of these metabolites and their role.

Materials and Methods

Solvents and Reagents

Samples for HPLC-DAD and HPLC-MS were prepared in HPLC grade methanol (J.T. Baker). Acetonitrile and formic acid were HPLC grade, purchased from Sigma-Aldrich. Ultrapure water (18.2 MΩ) was produced by a Milli-Q system (Millipore). The organic solvents used for extractions, columns and fractioning were distilled and provided by the IQ distillation facility.

Plant Material

Adult leaves of *P. auritum* were collected from an identified individual growth in the garden of the Institute of Chemistry, São Paulo, SP, Brazil. Seedlings were obtained from cultivation made in La Selva Biological Station (Costa Rica) under the supervision of Dr. Lee Dyer (University of Nevada Reno).

Seedlings of the species analyzed in Chapter 3 were cultivated in the Laboratory of Natural Product Chemistry, Institute of Chemistry, University of São Paulo, São Paulo, SP, Brazil. The seeds were obtained from peppercorns collected from mature plants and were surface sterilized by soaking in a solution of 20% v/v bleach (1% w/v NaOCl) for approximately 30 minutes, followed by immersion for 30 seconds in 70% v/v EtOH. Seeds were then rinsed three times with distilled water, and all floating seeds were discarded. The remaining seeds were submerged in 10mL sterile water and were spread aseptically using a 1 mL wide-bore pipette on 300 g of compacted sterile topsoil Tropstrato HA Hortaliças (Vida Verde Indústria e Comércio de Insumos Orgânicos Ltd, Mogi Mirim, São Paulo, Brazil) contained in 14 cm diameter clear plastic pots with a height of 9 cm sterilized for approximately 24 h in a solution of 20% v/v bleach (1% w/v NaOCl). Afterward, the seeds were covered aseptically with the top layer of soil, such that they were approximately 0.5 cm below the surface, after which the pots were watered with 100 ml ddH_20 and sealed with clear lids. Planted seeds were then placed in a variable environment growth chamber (Panasonic MLR-351M, Kadoma, Osaka, Japan) under fluorescent lighting (intensity) at

27°C, 70% humidity, and a day/night cycle of 14/10 hours until germination took place. Adult leaves were collected from previously identified adults in the Institute of Chemistry's garden.

Piper lindbergii C.DC. (adults and seeds) was sampled at Reserva Biológica da Serra do Japi from an identified individual (https://serradojapi.jundiai.sp.gov.br/rebio/) (23°13'58.3"S 46°55'30.5"W).

Samples of leaves, roots, and stems from *P. chimonanthifolium* (Kato-2564) were collected in Serra do Japi, State of São Paulo (SP).

Samples of leaves, roots, and stems from *P. lindbergii* (K-2314) were collected in Morretes, State of Paraná (PR), the vouchers were deposited at the Herbário do Instituto de Biociências da Universidade de São Paulo, and were identified by Prof. Dra. Elsie F. Guimarães.

All sampling was authorized by MJK SISBIO (15780-1; 37818-2), CNPq (010203/2011-7), COTEC (SMA 260108 – 010.320/2013).

Column Chromatography and Purification

Flash column chromatography was carried out using flash silica gel (Sigma-Aldrich, 200-400 Mesh), a column with a sintered glass disk, a Büchner flask, and a vacuum pump. Regular column chromatography was carried out using common silica Sigma-Aldrich (70-230 Mesh). RPCC was carried out using Bondapack® C18 (Waters®, 125 Å 15-20 μm). The gel filtration was carried out using a Sephadex® LH-20 in methanol.

HPLC-DAD and HPLC-ESI-HRMS Analysis

All samples were prepared in HPLC grade methanol, filtered using an HPLC PTFE filter (0.45 μm and 13 mm, Allcrom), and transferred into a 1.5 mL labeled vial. For the samples from dry material (leaves, roots, fruits and stem), 50 mg were weighted in a 2.0 mL Eppendorf tube, then 1.5 mL of HPLC grade MeOH were added, and finally, ten clean stainless steel beads were added

into the tube. Samples were shaken for five minutes in a vortex (Kasvi K40-1020), centrifuged at 10000 rpm for ten minutes, and filtered 1.0 mL of the supernatant.

Analyses were conducted in a Shimadzu Prominence L.C. equipped with two LC-20AD pumps, DGU-20A Degasser, SIL-20A autosampler, CTO-20A column oven, and an SPD- M20A Diode array detector, using a Luna C 18 100A (Phenomenex) column (250 mm x 4.60 mm x 5 μm) with (A) 0.1 % formic acid solution in ultrapure water (18.2 MΩ) produced by a Milli-Q system (Millipore) and (B) acetonitrile in gradient at 40 °C. Obtained data was managed with L.C. Solutions V.1.25. This system was hyphenated to a Bruker microTOF-Q II with the flu reduced to 0.20 mL/ min approximately using a flux splitter. In scan mode, the mass range was fixed from 100 to 1000 m/z. For the source, the End Plate Offset was set at 500 V, the capillary at 4500 V, the nebulizer gas in 4 Bar, the drying gas in 8 L/min at 200 °C. The quadrupole energy was 6 eV, while the collision energy was 12 eV. The column, phases, and gradients were the same used in HPLC-DAD. The monitoring wavelength was 270 and 365 nm. Obtained data was managed with the software DataAnalysis 4.3.

For *P. auritum*, starting from 10 % of B and keeping it constant until 2 min, then increasing it to 30% in 6 min, maintaining for two minutes and rising again up to 60% in 25 min, increasing again up to 100% in 34.5 min holding for two minutes. Then, turn back to initial conditions decreasing B to 10% in 40 min and keeping it until 45 min. The flow rate was 0.7 mL/min, the injection volume of 10 μL, and detection at 254, 270, and 365 nm.

For C-glycosylflavonoids, starting from 10% of B and keeping it constant for 2 min, then increasing it to 25% in 28 min and increasing it again up to 100% in 30min maintaining stable for 3 min. Then, turn back to initial conditions decreasing B to 10% in 35 min and keeping it until 40 min. The flow rate was 1.0 mL/ min, injection volume of 10 μL, and detection at 270 nm. HPLC-MS analyses of fractions were carried out with a collision energy of 40 eV instead of the standard 12 eV.

For the analysis of *P. lindbergii*, the method started at 10% B and kept it constant for 2 min, then increased to 60% in 20 min, stable for 5 min, and then increased it again to 100% in 45 min, keeping it constant until 53 min and returning to initial conditions by decreasing to 10% in 60 min and holding for 5 min. The flow rate was 1.0 mL/ min, injection volume of 10 μL, and detection at 270 nm.

For the analysis of *P. chimonanthifolium* and *Piper* species from chapter 3, the method started at 15% of B for 5 min, then increased to 30% in 30 min and then to 100% in 47 min maintaining constant until 52 min and returning to the initial conditions by decreasing B to 15% in 56 min and keeping it steady until 60 min. The flow rate was 0.9 mL/ min, the injection volume of 10 μL, and detection at 254, 270, and 365 nm.

For the analysis of aristolactams, the method started at 30% B and kept it constant for 1 min, then increasing it to 90% in 25 min and then increasing it again until 100% in 26 min. Holding until 28 min and then returning to initial conditions by decreasing B to 30% at 30 min and keeping it constant until 35 min. The flow rate was 1.0 mL/ min, injection volume of 2 μL, and detection at 270 nm.

For the analysis of the novel aldehydes, an isocratic method in 65% B with a flow of 0.8 mL/ min was used, keeping the other parameters constant.

Semipreparative HPLC

Samples were analyzed in a Shimadzu L.C. equipped with two LC-10AD pumps, DGU-2A degasser, and SPD-M10A diode array detector, using a Luna C 18 100A (Phenomenex) column (250 mm x 10.0 mm x 5 μm) with a 0.1 % formic acid solution in water (A) and acetonitrile (B) in the same gradient of analytical conditions.

For C-glycosylflavonoids, the same method was used, with a flow rate of 4.72 mL/ min, injection volume of 200 μL (50 mg/mL), and detection was at 270 nm. A total of 15 injections were carried out.

For the analysis of the novel aldehydes from *P. lindbergii*, the method started at 50% B and kept it constant for 1 min, then increasing it to 65% in 20 min and kept it constant for 1 min, then increasing it again until 100% in 25 min. Holding until 27 min and then returning to initial conditions by decreasing B to 50% at 30 min and keeping it constant until 32 min. The flow rate was 3.78 mL/ min with an injection volume of 500 μL (10 mg/mL) and detection at 270 and 365 nm.

HPLC-FLD

Samples were analyzed in a Shimadzu L.C. equipped with two LC-10AD pumps, DGU-2A Degasser, SIL-10AF autoinjector, CTO-10AC column oven, an SPD- 10A Diode array detector, and an RF-20A fluorescence detector (Xe lamp, 200- 650 nm), using a Luna C 18 100A (Phenomenex) column (250 mm x 4.60 mm x 5 μm) with 0.1 % formic acid solution in ultrapure water (A) (18.2 MΩ) produced by a Milli-Q system (Millipore) and acetonitrile (B) in gradient. The flow rate was 1.0 mL/ min, injection volume of 5 μL and 2 μL for standard and samples, respectively, detection at 270 nm for the PDA detector, λ_{ex} and λ_{em} of 270 nm and 490 nm, respectively, with medium sensitivity and gain factor of x1. Obtained data was managed with L.C. Solutions V.1.25. Quantification was carried out using two calibration curves (high and low concentrations) of cepharanone B; this standard was isolated from a methanolic extract of roots from *P. lindbergii.*

NMR

The NMR spectra were recorded on Bruker AIII (Central Analítica, IQ/USP) operating at 500 MHz to ^{1}H in $CDCl_3$ with TMS as an internal standard, equipped with a 5 mm TXI probe for ^{1}H, ^{13}C of reverse detection and field gradient. Twenty milligrams of obtained fractions or compounds

were dissolved in 700 µL of $CDCl_3$ (0.03% v/v TMS, Sigma-Aldrich) or MeOD and filtered with degreased cotton; the whole fraction or compound was used for sample preparation if needed. Data were analyzed using ACD/Spectrus Processor 2016.2.2 (ACD/ Labs) and MestReNova 14.2.0.

GCMS

Samples were analyzed in a Shimadzu GC-2010 Plus chromatograph, coupled to a QP2010 Ultra mass analyzer and AOC-5000 Plus autosampler, using an HP-5 MS column (30 m x 0.250 mm x 0.25µm. Agilent) with He as the carrier gas with a flow of 1.55 mL/min, a split ratio of 20, and liner temperature of 260°C. The temperature gradient starts at 60 °C for 2 minutes, increasing at a rate of 10 °C/min until 280 °C and holding for 2 minutes. The source and interface temperatures were 260 °C with a solvent cut time of 3 min, a mass range between 50 and 800 m/z, and a scan speed of 20000. Samples were dissolved in HPLC grade dichloromethane or hexane, and the injection volume was 1 µL.

Multivariate Analysis

Multivariate analysis was carried out using JMP®15.2.1 (SAS). Data alignment was conducted using the algorithm COW (Correlation Optimized Warping) downloaded from http://www.models.kvl.dk/ in ®MatLab 2016a (Nielsen et al., 1998).

References

Achenbach, H., Witzke, J., 1979. Synthese des piperolids. *Tetrahedron Lett.* 1579–1580.

Adityachaudhury, N., Das, A.K., Choudhury, A., Daskanungo, P.L., 1976. Aurentiacin, a new chalcone from *Didymocarpus aurentiaca. Phytochemistry* 15, 229–230.

Agrawal, A.A., 2007. Macroevolution of plant defense strategies. *Trends Ecol. Evol.* 22, 103–109.

Ahmad, V.U., Ali, Z., Zahid, M., Alam, N., Saba, N., Khan, T., Qaisar, M., Nisar, M., 2000. Phytochemical study of *Salvia moorcroftiana. Fitoterapia* 71, 84–85.

Amor, E.C., Villaseñor, I.M., Ghayur, M.N., Gilani, A.H., Choudhary, M.I., 2005. Spasmolytic Flavonoids from *Syzygium samarangense* (Blume) Merr. & L.M. Perry. *Zeitschrift fur Naturforsch*. 60, 67–71.

Baldoqui, D.C., Bolzani, V., Furlan, M., Kato, M., Marques, M., 2009. Flavonas, lignanas e terpeno de *Piper umbellata* (Piperaceae). *Quim. Nova* 32, 1107–1109.

Bench, B.J., Foulke-Abel, J., Watanabe, C.M.H., 2011. Milk, revealed “silent” chemistry: New mode of cycloretinal synthesis. *Mol. Biosyst*. 7, 162–168.

Benevides, P.J.C., Sartorelli, P., Kato, M.J., 1999. Phenylpropanoids and neolignans from *Piper regnellii. Phytochemistry* 52, 339–343.

Bergo, C.L., 2010. Identificação e potencialidades de uso de *Piper sp* no município de Morretes no Paraná. Universidade Federal do Paraná.

Bhardwaj, A., Kumar Tewary, D., Kumar, R., Kumar, V., Kumar Sinha, A., Shanker, A., 2010. Larvicidal and Structure-Activity Studies of Natural Phenylpropanoids and Their Semisynthetic Derivatives against the Tobacco Armyworm *Spodoptera litura* (Fab.) (Lepidoptera: Noctuidae). *Chem. Biodivers*. 7, 168–177.

Boege, K., Marquis, R.J., 2005. Facing herbivory as you grow up: The ontogeny of resistance in plants. *Trends Ecol. Evol.* 20, 441–448.

Calderari, M.T., 2002. Estudo Dos Oleos Essenciais De Piperaceae Do Vale Do Itajaí Em Santá Catarina. Universidade Federal de Santa Catarina.

Castañeda, M., Muñoz, A., Martínez, J., Stanshenko, E., 2007. Estudio de la composición química y la actividad biológica de los aceites esenciales de diez plantas aromáticas colombianas. *Sci. Tech.* 13, 165–166.

Chan, W., Cui, L., Xu, G., Cai, Z., 2006. Study of the phase I and phase II metabolism of nephrotoxin aristolochic acid by liquid chromatography/tandem mass spectrometry. *Rapid Commun. Mass Spectrom*. 20, 1755–1760.

Chase, M.W., Christenhusz, M.J.M., Fay, M.F., Byng, J.W., Judd, W.S., Soltis, D.E., Mabberley, D.J., Sennikov, A.N., Soltis, P.S., Stevens, P.F., Briggs, B., Brockington, S., Chautems, A., Clark, J.C., Conran, J., Haston, E., Möller, M., Moore, M., Olmstead, R., Perret, M., Skog, L., Smith, J., Tank, D., Vorontsova, M., Weber, A., 2016. An update of the Angiosperm Phylogeny Group classification for the orders and families of flowering plants: APG IV. *Bot. J. Linn. Soc*. 181, 1–20.

Chen, Y.C., Chen, J.J., Chang, Y.L., Teng, C.M., Lin, W.Y., Wu, C.C., Chen, I.S., 2004. A new aristolactam alkaloid and anti-platelet aggregation constituents from *Piper taiwanense. Planta Med.* 70, 174–177.

Chen, Y.C., Liao, C.H., Chen, I.S., 2007. Lignans, an amide and anti-platelet activities from *Piper philippinum. Phytochemistry* 68, 2101–2111.

Choi, Y.L., Kim, J.K., Choi, S.U., Min, Y.K., Bae, M.A., Kim, B.T., Heo, J.N., 2009. Synthesis of aristolactam analogues and evaluation of their antitumor activity. *Bioorganic Med. Chem. Lett.* 19, 3036–3040.

Christov, R., Trusheva, B., Popova, M., Bankova, V., Bertrand, M., 2012. Natural Product Research : Formerly Natural Product Letters Chemical composition of propolis from Canada, its antiradical activity and plant origin. *Nat. Prod. Res.* 20, 531–536.

Cimanga, K., De Bruyne, T., Lasure, A., Li, Q., Pieters, L., Claeys, M., Berghe, D. Vanden, Kambu, K., Tona, L., Vlietinck, A., 1995. Flavonoid O-Glycosides from the leaves of *Morinda morindoides. Phytochemistry* 38, 1301–1303.

Costa, M., Di Stasi, L., Kirizawa, M., Mendaçolli, S., Gomes, C., Trolin, G., 1989. Screening Analgesic Part Ii * Plants Used for Purposes in the State of Sao Paulo. *J. Ethno* 27, 25–33.

Couture, A., Deniau, E., Grandclaudon, P., Rybalko-Rosen, H., Léonce, S., Pfeiffer, B., Renard, P., 2002. Synthesis and biological evaluation of aristolactams. *Bioorganic Med. Chem. Lett*. 12, 3557–3559.

Danelutte, A.P., Costantin, M.B., Delgado, G.E., Braz-Filho, R., Kato, M.J., 2005. Divergence of secondary metabolism in cell suspension cultures and differentiated plants of *Piper cernuum* and *P. crassinervium. J. Braz. Chem. Soc*. 16, 1425–1430.

Danelutte, A.P., Lago, J.H.G., Young, M.C.M., Kato, M.J., 2003. Antifungal flavanones and prenylated hydroquinones from *Piper crassinervium* Kunth. *Phytochemistry* 64, 555–559.

De Almeida, R.R.P., Souto, R.N.P., Bastos, C.N., Da Silva, M.H.L., Maia, J.G.S., 2009. Chemical variation in *Piper aduncum* and biological properties of its dillapiole-rich essential oil. *Chem. Biodivers.* 6, 1427–1434.

De Oliveira Chaves, M., De Oliveira Santos, B., De Oliveira, A., 2003. 1-cinnamoylpyrrolidide from *Piper marginatum. Biochem. Syst. Ecol.* 31, 1213–1214.

De Oliveira Chaves, M.C., De Oliveira, A.H., De Oliveira Santos, B.V., 2006. Aristolactams from *Piper marginatum* Jacq (Piperaceae). *Biochem. Syst. Ecol.* 34, 75–77.

Deborde, C., Moing, A., Roch, L., Jacob, D., Rolin, D., Giraudeau, P., 2017. Plant metabolism as studied by NMR spectroscopy. *Prog. Nucl. Magn. Reson. Spectrosc*. 102–103, 61–97.

Demarque, D.P., Crotti, A.E.M., Vessecchi, R., Lopes, J.L.C., Lopes, N.P., 2016. Fragmentation reactions using electrospray ionization mass spectrometry: An important tool for the structural elucidation and characterization of synthetic and natural products. *Nat. Prod. Rep.* 33, 432–455.

Dembitsky, V.M., 2007. Bioactive cyclobutane-containing alkaloids. *J. Nat. Med.* 62, 1–33.

Desai, S.J., Prabhu, B.R., Mulchandani, N.B., 1988. Aristolactams and 4,5-dioxoaporphines from *Piper longum. Phytochemistry* 27, 1511–1515.

Dewick, P.., 2009. Medicinal Natural Products. A biosynthetic approach., John Wiley and Sons.

Dieter Strack, V.W., 1994. The Flavonoids: Advances in Research Since 1986. Springer US.

Domínguez, X.A., Franco, R., Zamudio, A., Barraidas, D.M., Watson, W.H., Zabel, V., Merijanian, A., 1980. Flavonoids from Dalea scandens var. *Paucifolia* and *Dalea thyrsiflora. Phytochemistry* 19, 1262–1263.

Dyer, L.A., Palmer, A.D.N. (Eds.), 2004. Piper A Model Genus For Studies Of Phytochemistry,Ecology and Evolution., First Edit. ed. Kluwer Academic/ Plenum Publishers, New York.

El-Gamal, A.A., Al-Massarani, S.M., Shaala, L.A., Alahdald, A.M., Al-Said, M.S., Ashour, A.E., Kumar, A., Abdel-Kader, M.S., Abdel-Mageed, W.M., Youssef, D.T.A., 2016. Cytotoxic compounds from the Saudi red sea sponge *Xestospongia testudinaria. Mar. Drugs* 14.

Fernandes, A.M.A.P., Prado, A.L., Barata, L.E.S., Paulo, M.Q., Azevedo, N.R., Ferri, P.H., 1997. A method to separate lignoids from *Virola* leaves. *Phytochem. Anal*. 8, 18–21.

Freitas, G.C., Kitamura, R.O.S., Lago, J.H.G., Young, M.C.M., Guimarães, E.F., Kato, M.J., 2009.

Caldensinic acid, a prenylated benzoic acid from *Piper caldense. Phytochem*. Lett. 2, 119–122.

Gafner, S., Wolfender, J., Mavi, S., Hostettmann, K., 1996. Antifungal and Antibacterial Chalcones from *Myrica serrata* Stefan. *Planta Med.* 62, 67–69.

Gaia, A.M., Yamaguchi, L.F., Guerrero-Perilla, C., Kato, M.J., 2021. Ontogenetic Changes in the Chemical Profiles of *Piper* Species. *Plants* 10(6); 1085.

Garcia Rios, A., Leyva, M.A., Martínez, J.R., Stashenko, E.E., 2007. Determinación de la composición química y actividad antioxidante in vitro del aceite esencial de *Piper auritum* kunth (piperaceae) difundida en la costa colombiana. *Sci. Tech.* 1, 439–442.

Gbewonyo, W.S.K., Candy, D.J., Anderson, M., 1993. Structure-activity relationships of insecticidal amides from *Piper guineense* root. *Pestic. Sci.* 37, 57–66.

Goodacre, R., Broadhurst, D., Smilde, A.K., Kristal, B.S., Baker, J.D., Beger, R., Bessant, C., Connor, S., Capuani, G., Craig, A., Ebbels, T., Kell, D.B., Manetti, C., Newton, J., Paternostro, G., Somorjai, R., Sjöström, M., Trygg, J., Wulfert, F., 2007. Proposed minimum reporting standards for data analysis in metabolomics. *Metabolomics* 3, 231–241.

Hansel, R., Ranft, G., Bahr, P., 1963. Zwei Chalkonpigmente aus *Piper Methysticum* Forst. *Zeitschrift für Naturforsch. B* 18, 370–373.

Harborne, J., Mabry, T.J., 1982. The Flavonoids Advances in Research, Biochemical Society Transactions. Springer.

Harborne, J.B., 1997. Plant Secondary Metabolism, Second Edi. Ed, Plant Ecology. Blackwell Science.

Hartmann, T., 1996. Diversity and variability of plant secondary metabolism: A mechanistic view. *Entomol. Exp. Appl.* 80, 177–188.

Herath, H.M.T.B., Priyadarshani, A.M.A., 1996. Two lignans and an aryl alkanone from *Myristica dactyloides. Phytochemistry* 42, 1439–1442.

Hitz, C., Mann, K., Wollenweber, E., 1982. New Flavonoids from the farina of *Pityrogramma* Species. *Zeitschrift für Naturforsch. C* 37, 337–339.

ICH.GUIDELINE, 2005. Validation of Analytical Procedures: Text and Methodology. Q2(R1). [WWW Document]. Textb. Pharm. Med. URL http://www.ich.org/products/guidelines/quality/%0Aarticle/quality-guidelines.html.

Isnard, S., Prosperi, J., Wanke, S., Wagner, S.T., Samain, M.-S., Trueba, S., Frenzke, L., Neinhuis, C., Rowe, N.P., 2012. Growth Form Evolution in Piperales and Its Relevance for Understanding Angiosperm Diversification: An Integrative Approach Combining Plant Architecture, Anatomy, and Biomechanics. *Int. J. Plant Sci.* 173, 610–639.

Janzen, D.H., 1974. Tropical Blackwater Rivers, Animals, and Mast Fruiting by the Dipterocarpaceae. *Biotropica* 6, 69.

Jaramillo, M.A., Manos, P.S., 2001. Phylogeny and Patterns of Floral Diversity in the Genus *Piper* (Piperaceae). *Am. J. Bot.* 88, 706–716.

Jayasinghe, U.L.B., Ratnayake, R.M.S., Medawala, M.M.W.S., Fujimoto, Y., 2007. Dihydrochalcones with radical scavenging properties from the leaves of *Syzygium jambos*. *Nat. Prod. Res.* 21, 551–554.

Ji, H.-J., Li, J.-Y., Wu, S.-F., Wu, W.-Y., Yao, C.-L., Yao, S., Zhang, J.-Q., Guo, D.-A., 2020. Two New Aristolochic Acid Analogues from the Roots of *Aristolochia contorta* with Significant Cytotoxic Activity. *Molecules* 26, 44.

Joly, L.G., 1981. Feeding and trapping fish with *Piper auritum. Econ. Bot*. 35, 383–390.

Kijjoa, A., Giesbrecht, A.M., Akisue, M.K., Gottlieb, O.R., Gottlieb, H.E., 1980. 4-Nerolidylcatechol

from *Potomorphe umbellatal. Planta Med*. 39, 85–87.

Kim, H.K., Choi, Y.H., Verpoorte, R., 2011. NMR-based plant metabolomics: Where do we stand, where do we go? *Trends Biotechnol.* 29, 267–275.

Kim, H.K., Choi, Y.H., Verpoorte, R., 2010. NMR-based metabolomic analysis of plants. *Nature* 5, 536–549.

Kim, S.R., Sung, S.H., Kang, S.Y., Koo, K.A., Kim, S.H., Ma, C.J., Lee, H.S., Park, M.J., Kim, Y.C., 2004. Aristolactam BII of *Saururus chinensis* attenuates glutamate-induced neurotoxicity in rat cortical cultures probably by inhibiting nitric oxide production. *Planta Med.* 70, 391–396.

Kimura, Y., Takahashi, S., Yoshida, I., 1968. Studies on the constituents of *Alpinia*. XII. On the constituents of the seeds of *Alpinia katsumadai* hayata. I. The structure of cardamomin. *Yakugaku Zasshi* 88, 239–41.

Koul, S.K., Taneja, S.C., Malhotra, S., Dhar, K.L., 1993. Phenylpropanoids and (-)-ledol from two *Piper* species. *Phytochemistry* 32, 478–480.

Kumar, V., Poonam, Prasad, A.K., Parmar, V.S., 2003. Naturally occurring aristolactams, aristolochic acids and dioxoaporphines and their biological activities. *Nat. Prod. Rep*. 20, 565–583.

Kuo, Y.C., Yang, L.M., Lin, L.C., 2004. Isolation and immunomodulatory effect of flavonoids from *Syzygium samarangense. Planta Med*. 70, 1237–1239.

Kyung, R.M., Kim, K.S., Jai, S.R., Seung, H.L., Jeong, A.K., Jong, K.S., Kim, Y., 2004. Piperlonguminine from *Piper longum* with inhibitory effects on alpha-melanocyte-stimulating hormone-induced melanogenesis in melanoma B16 cells. *Planta Med.* 70, 1115–1118.

Lago, J., Souza-Ramos, C., Campos, D., Bolzani, V., Furlan, M., Guimarães, E., Kato, M., 2004.

Benzoic Acid Derivatives from Piper Species and Their Fungitoxic Activity against *Cladosporium cladosporioides* and *C . sphaerospermum. J. Nat. Prod.* 1783–1788.

Lago, J.H.G., Ito, A.T., Fernandes, C.M., Young, M.C.M., Kato, M.J., 2012. Secondary metabolites isolated from *Piper chimonantifolium* and their antifungal activity. *Nat. Prod. Res.* 26, 770–773.

Lago, J.H.G., Tanizaki, T.M., Young, M.C.M., Guimarães, E.F., Kato, M.J., 2005. Antifungal piperolides from *Piper malacophyllum* (Prels) C. DC. *J. Braz. Chem. Soc.* 16, 153–156.

Lavoie, S., Legault, J., Simard, F., Chiasson, É., Pichette, A., 2013. New antibacterial dihydrochalcone derivatives from buds of *Populus balsamifera*. *Tetrahedron Lett.* 54, 1631–1633.

Le Quesne, P.W., Larrahondo, J.F., Raffauf, R.F., 1980. Antitumor Plants. X. Constituents of *Nectandra rigida. J. Nat. Prod*. 43, 353–359.

Lehninger, A.L., Nelson, D.L., Cox, M.M., 2004. Lehninger Principles of Biochemistry, 4th ed. W. H. Freeman.

Lemeszenski, G.C. de F., 2013. Protoflavonoides e meroterpenos de espécies de *Piper*. Universidade de São Paulo.

Likhitwitayawuid, K., Ruangrungsi, N., Lange, G.., Decicco, C.., 1987. Elucidation and Synthesis of New Components Isolated from *P. sarmentosum. Tetrahedron* 43, 3689–3694.

Lima, L.M., 2015. Safrole and the versatility of a natural biophore. *Rev. Virtual Quim.* 7, 495–538.

Lin, C.F., Hwang, T.L., Chien, C.C., Tu, H.Y., Lay, H.L., 2013. A new hydroxychavicol dimer from the roots of *Piper betle. Molecules* 18, 2563–2570.

Loder, J.W., Moorhouse, A., Russell, G.. B., 1969. Tumour inhibitory plants. Amides of *Piper novae- hollandiae* (Piperaceae). *Aust. J. Chem* 22, 1531–1538.

Ma, A., Qi, X., 2021. Mining plant metabolomes: Methods, applications, and perspectives. *Plant Commun.* 2, 100238.

Malhotra, S., Koul, S.K., Taneja, S.C., Pushpangadan, P., Dhar, K.L., 1990. A neolignan from *Piper sumatranum. Phytochemistry* 29, 2733–2734.

Marentes-Culma, R., Orduz-Díaz, L., Coy-Barrera, E., 2019. Targeted Metabolite Profiling-Based Identification of Antifungal 5-n-alkylresorcinols Occurring in Different Cereals against *Fusarium oxysporum. Molecules* 24, 770.

Martin Luckner, 2013. Secondary Metabolism in Microorganisms, Plants and Animals., 2nd ed. Springer Science & Business Media.

Martins, R.C.C., Latorre, L.R., Sartorelli, P., Kato, M.J., 2000. Phenylpropanoids and tetrahydrofuran lignans from *Piper solmsianum. Phytochemistry* 55, 843–846.

Mata, Rachel, Morales, I., Pérez, O., Rivero-Cruz, I., Acevedo, L., Enriquez-Mendoza, I., Bye, R., Franzblau, S., Timmermann, B., 2004. Antimycobacterial compounds from *Piper sanctum. J. Nat. Prod.* 67, 1961–1968.

Mata, R, Morales, I., Pérez, O., Rivero-Cruz, I., Acevedo, L., Timmermann, B., 2004. Antimycobacterial Compounds from *Piper sanctum. J. Nat. Prod.* 67, 8–12.

Mauseth, J., 1998. BOTANY : An Introduction to Plant Biology., Jones and Bartlett Publishers.

Mazid, M., Khan, T.A., Mohammad, F., 2011. Role of secondary metabolites in defense mechanisms of plants. *Biol. Med.* 3, 232–249.

McBurnett, B.G., Chavira, A.A., López, A.C., Mosso, J., Collins, S.M., 2006. Analysis of *Piper auritum* : A Traditional Hispanic Herb, in: *Hispanic Foods.* pp. 67–76.

McLean, S., Brandon, S., Davies, N.W., Foley, W.J., Muller, H.K., 2004. Jensenone: Biological reactivity of a marsupial antifeedant from *Eucalyptus. J. Chem. Ecol*. 30, 19–36.

Michinori, A., Hideji, I., Mitiiti, F., 1974. Four new fluorescent Components isolated from The callus tissue of *Stephania cepharanta. Tetrahedron Lett.* 3609–3612.

Miyakado, M., Nakayama, I., Yoshioka, H., Nakatani., N., 1979. The Piperaceae Amides I: Structure of Pipercide , A New Insecticidal Amide from *Piper nigrum* L. *Agric. Biol .Chem.* 43, 1609–1611.

Monteiro, D., Guimarães, E.F., 2009. Flora do Parque Nacional do Itatiaia – Brasil: Manekia e Piper (Piperaceae). Rodriguésia 60, 999–1024.

Monzote, L., García, M., Montalvo, A.M., Scull, R., Miranda, M., 2010. Chemistry, cytotoxicity and antileishmanial activity of the essential oil from *Piper auritum*. Mem. Inst. Oswaldo Cruz 105, 168–173.

Mota, J.D.S., Leite, A.C., Kato, M.J., Young, M.C.M., Bolzani, V.D.S., Furlan, M., 2011. Isoswertisin flavones and other constituents from *Peperomia obtusifolia. Nat. Prod. Res.* 25, 1–7.

Mustafa, K., Perry, N.B., Weavers, R.T., 2005. Lipophilic C-methylflavonoids with no B-ring oxygenation in *Metrosideros* species (Myrtaceae). *Biochem. Syst. Ecol.* 33, 1049–1059.

Nair, M.G., Mansingh, A.P., Burke, B.A., 1986. Insecticidal Properties of Some Metabolites of Jamaican Piper spp., and the Amides Synthesized from 5,6-Z and *E*-Butenolides of *Piper fadyenii. Agric. Biol. Chem.* 50, 3053–3058.

Nakatani, N., Inatani, R., Fuwa, H., 1980. Structures and syntheses of two phenolic amides from *Piper nigrum l. Agric. Biol. Chem*. 44, 2831–2836.

Navickiene, D., Alecio, A.C., Kato, M.J., Bolzani, V., Young, M.C., Cavalheiro, A.J., Furlan, M., 2000. Antifungal amides from *Piper hispidum* and *Piper tuberculatum. Phytochemistry* 55, 621–626.

Nielsen, N.P.V., Carstensen, J.M., Smedsgaard, J., 1998. Aligning of single and multiple

wavelength chromatographic profiles for chemometric data analysis using correlation optimized warping. *J. Chromatogr. A* 805, 17–35.

Nilson, M., 1961. Dihydrochalcones from the Fronds of *Pityrogramma chrysophyla* var. marginata, Domin. *Acta Chem. Scand.* 15, 154–158.

Orjala, J., Mian, P., Rali, T., Sticher, O., 1998. Gibbilimbols A - D, Cytotoxic and Antibacterial Alkenylphenols from *Piper gibbilimbum*. J. Nat. Prod. 3864, 939–941.

Orjala, J., Wright, A.D., Behrends, H., Folkers, G., Sticher, O., Rüegger, H., Rali, T., 1994. Cytotoxic and antibacterial dihydrochalcones from *Piper aduncum*. *J. Nat. Prod.* 57, 18–26.

Otaka, J., Seo, S., Nishimura, M., 2016. Lutein, a natural carotenoid, induces α-1,3-glucan accumulation on the cell wall surface of fungal plant pathogens. *Molecules* 21, 1–5.

Parmar, V., Jain, S., Bisht, K., Jain, R., Taneja, P., Jha, A., Tyagi, O., Prasad, A., Wengel, J., Olsen, C., Boll, P., 1997. Phytochemistry of the genus *Piper. Phytochemistry* 46, 597–673.

Parmar, V.S., Jain, S.C., Gupta, S., Talwar, S., Rajwanshi, V.K., Kumar, R., Azim, A., Malhotra, S., Kumar, N., Jain, R., Sharma, N.K., Tyagi, O.D., Lawrie, S.J., Errington, W., Howarth, O.W., Olsen, C.E., Singh, S.K., Wengel, J., 1998. Polyphenols and alkaloids from *Piper* species. *Phytochemistry* 49, 1069–1078.

Pelter, A., Al-bayatia, R., Rudolf, H., Dinter, H., Burke, B., 1981. The structure and synthesis of a fadyenolide, a new butenolide from *Piper fadyenii. Tetrahedron Lett.* 22, 1545–1548.

Peña, L.A., Díaz, A.M., 1995. Aristolactama y esteroles del tallo de *Piper chiadoense*. *Rev. Colomb. Química* 24, 17–23.

Pereira Filho, A.A., Pessoa, G.C.D., Yamaguchi, L.F., Stanton, M.A., Serravite, A.M., Pereira, R.H.M., Neves, W.S., Kato, M.J., 2021. Larvicidal Activity of Essential Oils From *Piper* Species Against Strains of *Aedes aegypti* (Diptera: Culicidae) Resistant to Pyrethroids. *Front. Plant*

Sci. 12, 1–13.

Phrutivorapongkul, A., Lipipun, V., Ruangrungsi, N., Kirtikara, K., Nishikawa, K., Maruyama, S., Watanabe, T., Ishikawa, T., 2003. Studies on the chemical constituents of stem bark of *Millettia leucantha*: Isolation of new chalcones with cytotoxic, anti-herpes simplex virus and anti-inflammatory activities. *Chem. Pharm. Bull*. 51, 187–190.

Priestap, H.A., 1985. Two carboxy- and two hydroxymethyl-substituted aristololactams from *Aristolochia argentina. Phytochemistry* 24, 3035–3039.

Pring, B., 1982. Isolation and Identification of Amides from *Piper callosum*. Synthesis of Pipercallosine and Pipercallosidine*. J. Chem. Soc. Perkin trans*. I 135, 1493–1498.

Pryakhina, N.I., Sheichenko, V.I., Blinova, K.F., 1984. Acylated C-glycosides of *Iris lactea. Chem. Nat. Compd*. 20, 554–559.

Rao, T.N., 2018. Validation of Analytical Methods, in: Calibration and Validation of Analytical Methods - A Sampling of Current Approaches. InTech, pp. 600A-608A.

Rapado, L.N., FreitasB, G.C., Polpo, A., Rojas-Cardozo, M., Rincón, J. V., Scotti, M.T., Kato, M.J., Nakano, E., Yamaguchi, L.F., 2014. A benzoic acid derivative and flavokawains from *Piper* species as schistosomiasis vector controls. *Molecules* 19, 5205–5218.

Rauter, A.P., Lopes, R.G., Martins, A., 2007. C-Glycosylflavonoids: Identification, Bioactivity and Synthesis. *Nat. Prod. Commun*. 2, 1175–1196.

Ravindran, P.N., 2000. Medicinal and Aromatic Plants. Vol 12 Other Economically Important Species of Piper. Hardwood Academic Publishers.

Riani, L.R., Macedo, A.L., Chedier, L.M., Pimenta, D.S., 2017. Chemical analysis of essential oil and hydrolates of leaves, inflorescences and stems of *Piper chimonanthifolium* Kunth. Rev. Virtual Quim. 9, 1560–1569.

Richards, L.A., Dyer, L.A., Smilanich, A.M., Dodson, C.D., 2010. Synergistic Effects of Amides from Two Piper Species on Generalist and Specialist Herbivores. *J. Chem. Ecol.* 36, 1105–1113.

Richards, L.A., Dyer, L.A., Smilanich, A.M., Dodson, C.D., 2003. Synergistic effects of three *Piper* amides on generalist and specialist herbivores. *J. Chem. Ecol*. 29, 2499–2514.

Ruangrungsi, N., Sompop, P., Lange, G.L., Otgan, M.G., 1992. An N-Methyl and an Oxygenated Derivative From *Piper Ribeszozdes *. Phytochemistry* 31, 2397–2400.

Saleem, M., Nazir, M., Ali, M.S., Hussain, H., Lee, Y.S., Riaz, N., Jabbar, A., 2010. Antimicrobial natural products: an update on future antibiotic drug candidates. *Nat. Prod. Rep*. 27, 238–254.

Salehi, B., Zakaria, Z.A., Gyawali, R., Ibrahim, S.A., Rajkovic, J., Shinwari, Z.K., Khan, T., Sharifi-Rad, J., Ozleyen, A., Turkdonmez, E., Valussi, M., Tumer, T.B., Fidalgo, L.M., Martorell, M., Setzer, W.N., 2019. Piper species: A comprehensive review on their phytochemistry, biological activities and applications, Molecules.24 (7), 1364.

Salleh, W.M.N.H.W., 2021. A systematic review of botany, phytochemicals and pharmacological properties of “Hoja santa” (*Piper auritum* Kunth). *Zeitschrift fur Naturforsch. - Sect. C J. Biosci*. 76, 93–102.

Santos, V., Da Cunha, E., Chaves, M., Gray, A., 1998. Phenylalkanoids from *Piper marginatum. Phytochemistry* 45, 270–273.

Seigler, D.S., 1998. Plant Secondary Metabolism, 1st Editio. ed. Springer Science + Business Media, New York.

Settle, F.A., 1997. Handbook of Instrumental Techniques for Analytical Chemistry. Pretice Hall.

Siddiqui, B.S., Gulzar, T., Begum, S., Rasheed, M., Sattar, F.A., Afshan, F., 2003. Two new insecticidal amides and a new alcoholic amide from *Piper nigrum* LINN. *Helv. Chim. Acta*

86, 2760–2767.

Singh, I.P., Sidana, J., Bharate, S.B., Foley, W.J., 2010. Phloroglucinol compounds of natural origin: Synthetic aspects. *Nat. Prod. Rep*. 27, 393–416.

Singh, S.K., Prasad, A.K., Olsen, C.E., Jha, A., Jain, S.C., Parmar, V.S., Wengel, J., 1996. Neolignans and alkaloids from *Piper argyrophylum. Phytochemistry* 43, 1355–1360.

Skoog, D.A., Holler, J.F., Crouch, S.R., 2018. Atomic Absorption and Atomic Fluorescence Spectrometry, Seventh Ed. ed, Principles of Instrumental Analysis. Cengage Learning.

Solecka, D., 1997. Role of phenylpropanoid compounds in plant responses to different stress factors. *Acta Physiol. Plant.* 19, 257–268.

Srivastava, L.M., 2002. Seed Development and Maturation. Plant Growth Dev. 431–446.

Star, A.E., Mabry, T.J., Smith, D.M., 1978. Triangularin, a new chalcone from *Pityrogramma triangularis. Phytochemistry* 17, 586–587.

Stohr, J.R., Xiao, P.G., Bauer, R., 1999. Isobutylamides and a new methylbutylamide from *Piper sarmentosum. Planta Med.* 65, 175–177.

Talapatra, S.K., Basu, D., Chattopadhyay, P., Talapatra, B., 1988. Aristololactams of *Goniothalamus sesquipedalis* wall. Revised structures of the 2-oxygenated aristololactams. *Phytochemistry* 27, 903–906.

Talhi, O., Silva, A.M.S., 2012. Advances in C -glycosylflavonoid Research. Curr. Org. Chem. 16, 859–896.

Terreaux, C., Gupta, M.P., Hostettmann, K., 1998. Antifungal benzoic acid derivatives from *Piper dilatatum. Phytochemistry* 49, 461–464.

Thao, N.P., Luyen, B.T.T., Widowati, W., Fauziah, N., Maesaroh, M., Herlina, T., Manzoor, Z., Ali, I., Koh, Y.S., Kim, Y.H., 2016. Anti-inflammatory flavonoid C-glycosides from *Piper aduncum*

leaves. *Planta Med*. 82, 1475–1481.

Tsai, I.L., Lee, F.P., Wu, C.C., Duh, C.Y., Ishikawa, T., Chen, J.J., Chen, Y.C., Seki, H., Chen, I.S., 2005. New cytotoxic cyclobutanoid amides, a new furanoid lignan and anti-platelet aggregation constituents from *Piper arborescens. Planta Med.* 71, 535–542.

Tuntiwachwuttikul, P., Hansa, P., Pootaeng-on, Y., Taylor, C., 2006. Chemical Constituents of the Roots of *Piper Sarmentosum*. Chem Pharm Bull. 54(2), 149–151.

Usia, T., Watabe, T., Kadota, S., Tezuka, Y., 2005. Potent CYP3A4 inhibitory constituents of *Piper cubeba. J. Nat. Prod*. 68, 64–68.

Vanherweghem, J.L., Depierreux, M., Tielemans, C., Abramowicz, D., Dratwa, M., Jadoul, M., Richard, C., Vandervelde, D., Verbeelen, D., Vanhaelen-Fastre, R., Vanhaelen, M., 1993. Rapidly progressive interstitial renal fibrosis in young women: Association with slimming regimen including Chinese herbs. *Lancet* 341, 387–391.

Vasques, R., Debonsi, H., Kato, M., Young, M., Bolzani, V., Méda, C., Furlan, M., 2002. Antifungal amides from Piper arboreum and *Piper tuberculatum. Phytochemistry* 59, 521–527.

Velozo, L.S.M., Ferreira, M.J.P., Santos, M.I.S., Moreira, D.L., Guimarães, E.F., Emerenciano, V.P., Kaplan, M.A.C., 2009. C-glycosyl flavones from *Peperomia blanda. Fitoterapia* 80, 119–122.

Wanke, S., Jaramillo, M.A., Borsch, T., Samain, M.S., Quandt, D., Neinhuis, C., 2007. Evolution of Piperales-matK gene and trnK intron sequence data reveal lineage-specific resolution contrast. *Mol. Phylogenet. Evol.* 42, 477–497.

Ward, J.L., Harris, C., Lewis, J., Beale, M.H., 2003. Assessment of ^{1}H NMR spectroscopy and multivariate analysis as a technique for metabolite fingerprinting of *Arabidopsis thaliana. Phytochemistry* 62, 949–957.

Wei, K., Li, W., Koike, K., Chen, Y., Nikaido, T., 2005. Nigramides A-S, dimeric amide alkaloids

from the roots of *Piper nigrum. J. Org. Chem*. 70, 1164–1176.

Whaley, A.K., Ebrahim, W., El-Neketi, M., Ancheeva, E.U., Özkaya, F.C., Pryakhina, N.I., Sipkina, N.U., Luzhanin, V.G., Liu, Z., Proksch, P., 2017. New acetylated flavone C-glycosides from *Iris lactea. Tetrahedron Lett.* 58, 2171–2173.

Whitton, P.A., Lau, A., Salisbury, A., Whitehouse, J., Evans, C.S., 2003. Kavalactones and the kava-kava controversy. *Phytochemistry* 64, 673–679.

Wollenweber, E., Kohorst, G., Mann, K., Bell, J.M., 1985. Leaf Gland Flavonoids in *Comptonia peregrina* and *Myrica pensylvanica* (Myricaceae). *J. Plant Physiol.* 117, 423–430.

Xuan, T.D., Masakazu, F., Chang, A.W., Elzaawely, A.A., Khanh, T.D., Tawata, S., 2008. Efficacy of extracting solvents to chemical components of kava (*Piper methysticum*) roots. *J Nat Med* 62, 188–194.

Yuan, J., Liu, Q., Zhu, W., Ding, L., Tang, F., Yao, S., 2008. Simultaneous analysis of six aristolochic acids and five aristolactams in herbal plants and their preparations by high-performance liquid chromatography-diode array detection-fluorescence detection. J. *Chromatogr. A* 1182, 85–92.

Zaki, M.A., Nanayakkara, N.P.D., Hetta, M.H., Jacob, M.R., Khan, S.I., Mohammed, R., Ibrahim, M.A., Samoylenko, V., Coleman, C., Fronczek, F.R., Ferreira, D., Muhammad, I., 2016. Bioactive Formylated Flavonoids from *Eugenia rigida*: Isolation, Synthesis, and X-ray Crystallography. *J. Nat. Prod.* 79, 2341–2349.

Zaynab, M., Fatima, M., Abbas, S., Sharif, Y., Umair, M., Zafar, M.H., Bahadar, K., 2018. Role of secondary metabolites in plant defense against pathogens. *Microb. Pathog*. 124, 198–202.

Curriculum Vitae.

Name: Andrés Camilo Guerrero-Perilla.

Birthplace: Bogotá, Colombia.

Birth Date: January 16, 1989.

Education

Colegio Champagnat – Bogotá (Highschool)

Bogotá- Colombia.

2003-2005.

Bachelor's Degree in Chemistry.

Universidad Nacional de Colombia. Bogotá, Colombia.

2006 -2013.

Project: Study of reactivity of 4-aminopyrazoles and cyclic ketones in the synthesis of spiro-4-thiazolidinone derivatives with antimicrobial potential.

Supervisor: Fabián Orozco López.

Ph.D. Fellow, Institute of Chemistry.

Universidade de São Paulo, Brazil.

2016 – 2021.

Project: Secondary metabolites and ontogeny of *Piper* species.

Funded by Fundação de Amparo à Pesquisa do Estado de São Paulo (FAPESP 2016/00778-0).

Supervisor: Massuo J. Kato.

COMPLEMENTARY EDUCATION

Introduction to the Concepts and Practice of Metrology.

Instituto de Química, Universidade de São Paulo, São Paulo, Brazil.

April 2019.

HPLC -Teoria Básica e Prática.

Instituto de Química, Universidade de São Paulo, São Paulo, Brazil.

February - March 2018.

NMR 300 MHz, INOVA (Varian) & NMR 500 MHz, Bruker AIII 500 MHz.

Central Analítica, Instituto de Química, Universidade de São Paulo, São Paulo, Brazil.

March-May 2017.

Thermo Scientific Trace 1310 – ISQ Single Quadrupole Gas Chromatograph Mass

Spectrometer course.

Innovatek LTDA, Cajicá, Colombia. July 2015.

LCMS-8030/8040/8050 course.

Shimadzu Scientific Instruments, Inc., Columbia, MD, USA. June 2015.

LCMS-2020 Single Quadrupole Liquid Chromatograph Mass Spectrometer course.

Purificación y Análisis de Fluidos PAF LTDA. Cajicá, Colombia. January 2014.

EMPLOYMENT

Direct Ph.D. Scholarship holder, FAPESP 2016/00778-0 (1/4/2016 - 31/3/2021)

Conferences and Meetings

Chemodiversity of aristolactams in *Piper* species by HPLC-FLD - Poster.

8th BCNP Brazilian Conference on Natural Products. (Universidade Federal de Goiás – UFG (virtual event), Brazil. November 9-12, 2021.

Secondary metabolites and ontogeny of *Piper* species – Talk.

Course: Tópicos em Fitoquímica II. Departamento de Botânica, Instituto de Biociencias, USP. São Paulo, Brazil. September 2019.

Chemical diversity during ontogeny of *Piper auritum* (Kunth) - Poster.

7th BCNP Brazilian Conference on Natural Products. Instituto Militar de Engenharia (IME), Río de Janeiro, Brazil. November 10-13, 2019.

Phytochemical diversity of *Piper auritum* (Kunth)-Poster.

57th Annual meeting of the Phytochemical Society of North America. Universidad Autónoma de San Luis Potosí, San Luis Potosí, México. August 4-8, 2018.

Secondary metabolism during ontogeny of *Piper* species - Poster.

6th BCNP Brazilian Conference on Natural Products. Universidade Federal de Espiritu Santo, Vitória, Brazil. November 5-8, 2017.

Publications.

Gaia, A.M.; Yamaguchi,L.F.; Guerrero-Perilla, C.; Kato, M.J. **Ontogenetic Changes in the Chemical Profiles of *Piper* Species**. *Plants* 2021,10, 1085.

Singh. R, Tiwari. P, Sharma. B, Guerrero-Perilla. C, Coy-Barrera. E**; Chapter 23 - Analysis of polyacetylenes.** *Recent Advances in Natural Products Analysis*, 707–722, 2020.

Meza. A., Rojas. P., Cely-Veloza. W, Guerrero-Perilla. C, Coy-Barrera. E; **Variation of isoflavone content and DPPH• scavenging capacity of phytohormone-treated seedlings after in vitro germination of cape broom (*Genista monspessulana).*** *South African J Bot.* 2019;130:64–74.

Guerrero-Perilla. C, Bernal. F.A, Coy-Barrera E**; Insights into the interaction and binding mode of a set of antifungal azoles as inhibitors of potential fungal enzyme-based targets.** *Mol Divers*. 2018;22(4):929–42.

Altamar-Varón. P, Pérez-Maldonado. D, Rodríguez-Caicedo. D, Guerrero-Perilla. C, Coy-Barrera. E; **Chemical Composition of the Low-Polar Fraction of the *Copitarsia uncilata* Burgos & Leiva (Lepidoptera: Noctuidae) Eversible Pheromone Gland.** *Neotrop Entomol*. 2016;45(6):734–9.

Bernal F.A, Orduz-Diaz. L.L, Guerrero-Perilla. C, Coy-Barrera. E.D; **Diazo Coupling Reaction of Catechins and Alkylresorcinols with Diazotized Sulfanilic Acid for Quantitative Purposes in Edible Sources: Method Development and Validation.** *Food Anal Methods.* 2016; 9;411-418.

Appendix

Cap 1.

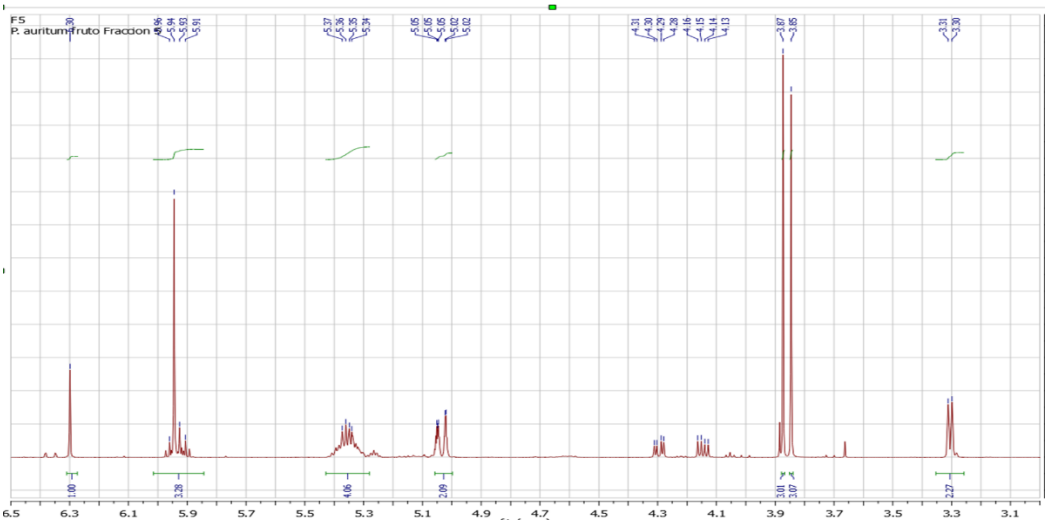

Figure 69. ^{1}H NMR spectrum of dillapiole.

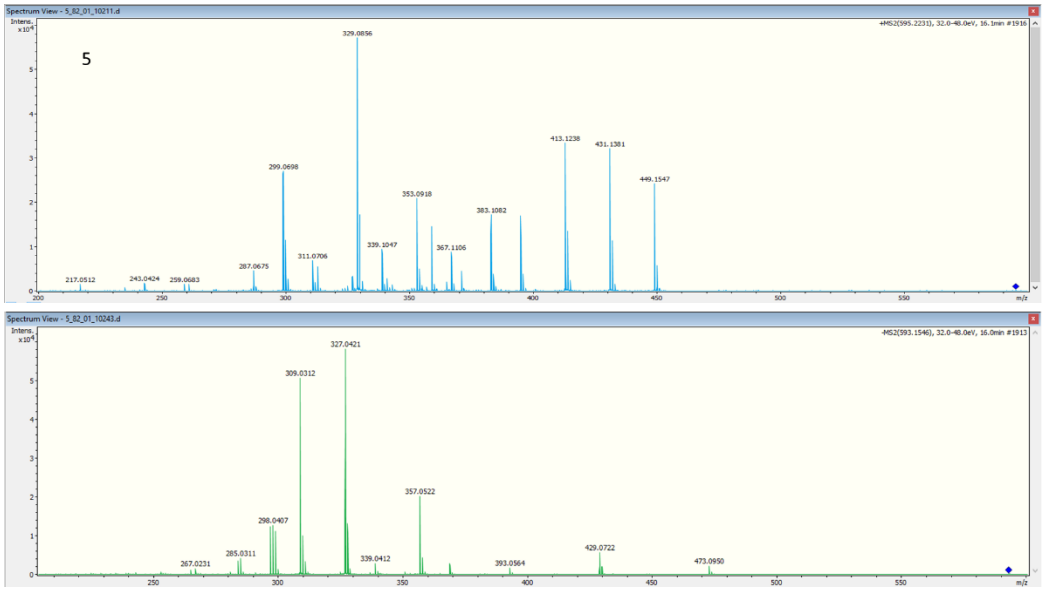

Figure 70. Semiprep fraction 5 from fruits of *P. auritum*. Positive and negative modes.

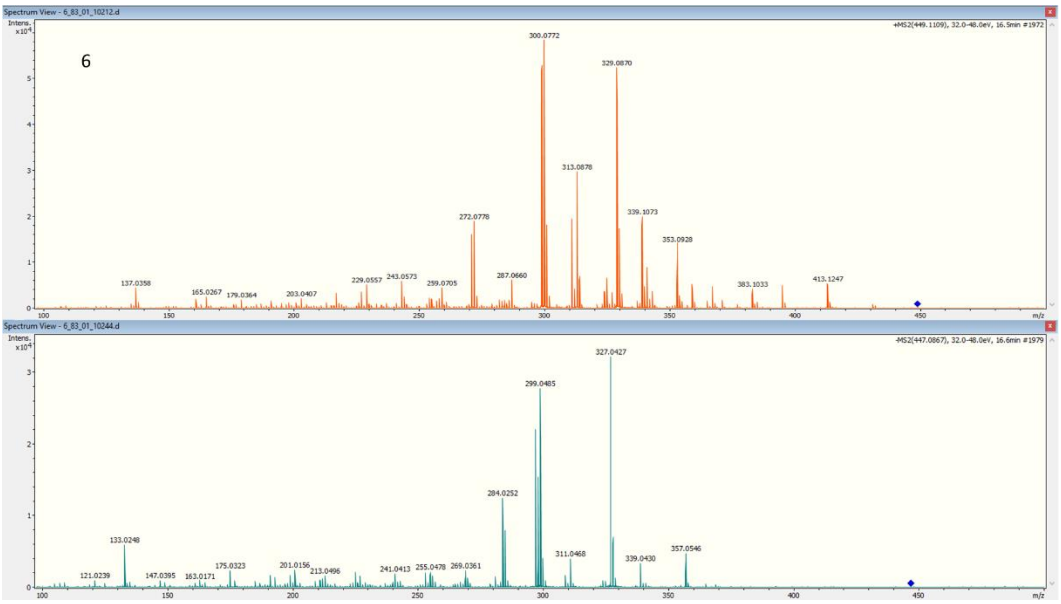

Figure 71. Semiprep fraction 6 from fruits of *P. auritum*. Positive and negative modes.

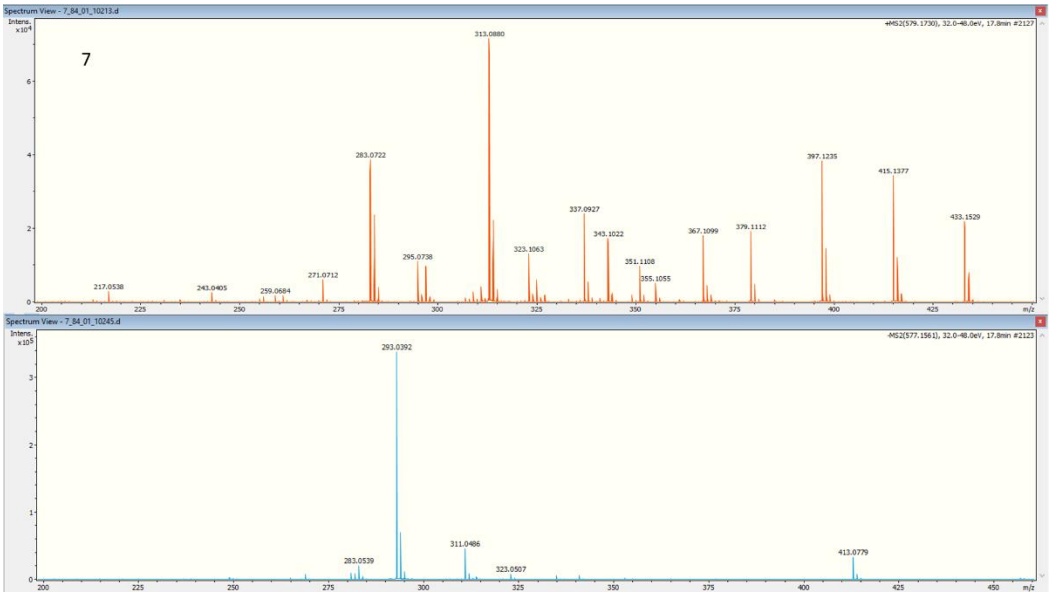

Figure 72. Semiprep fraction 7 from fruits of *P. auritum*. Positive and negative modes.

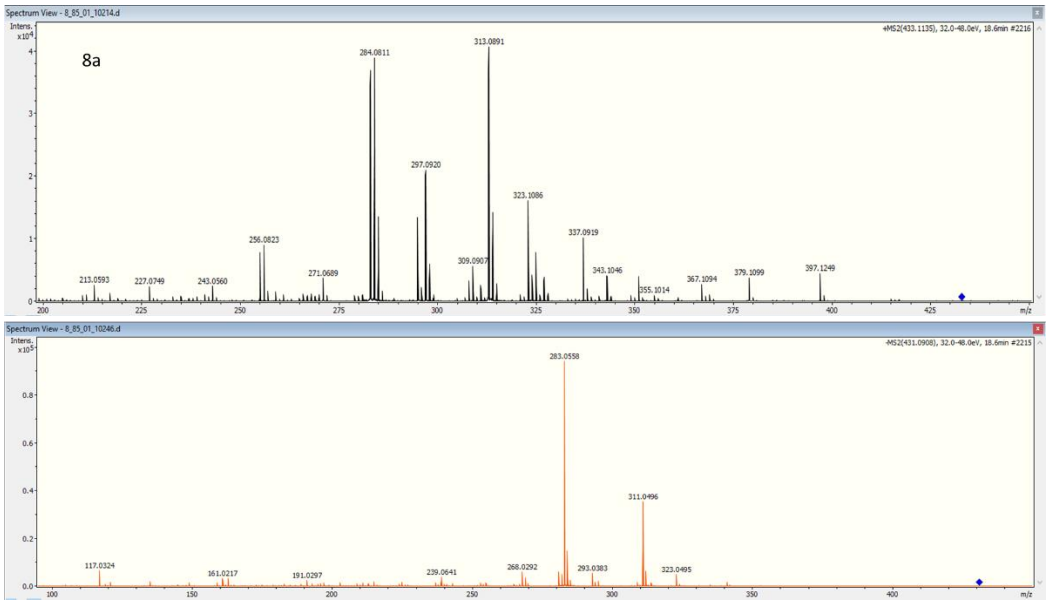

Figure 73. Semiprep fraction 8a from fruits of *P. auritum*. Positive and negative modes.

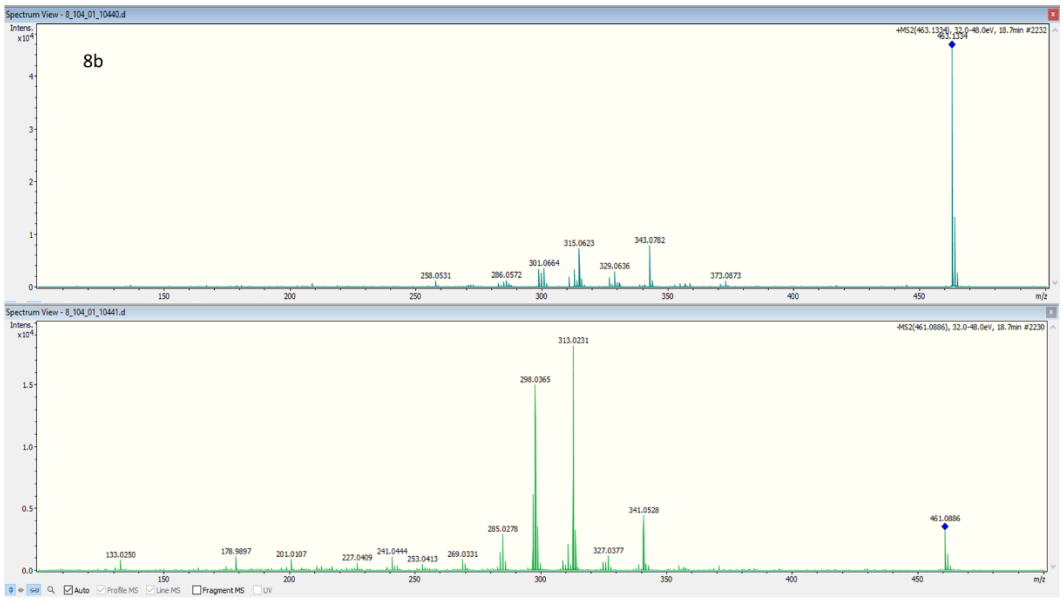

Figure 74. Semiprep fraction 8b from fruits of *P. auritum*. Positive and negative modes.

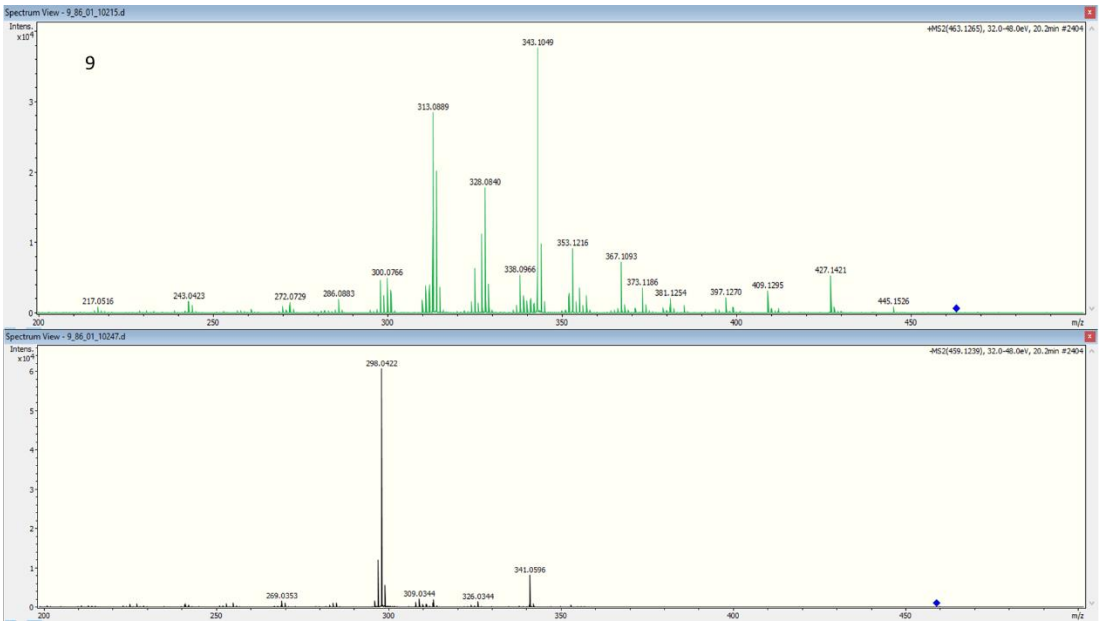

Figure 75. Semiprep fraction 9 from fruits of *P. auritum*. Positive and negative modes.

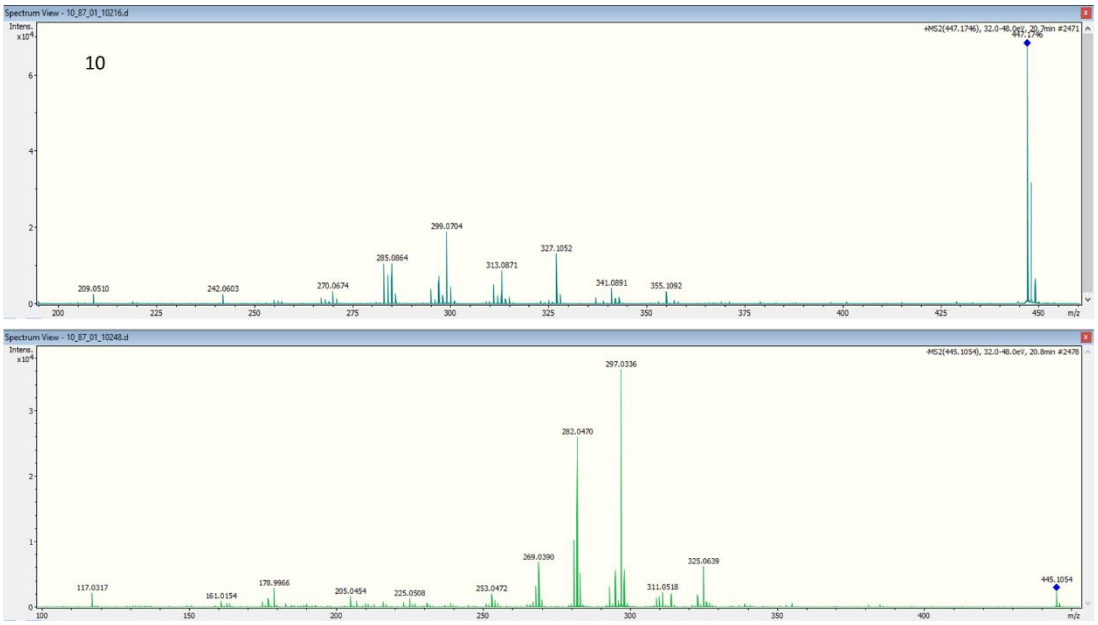

Figure 76. Semiprep fraction 10 from fruits of *P. auritum*. Positive and negative modes.

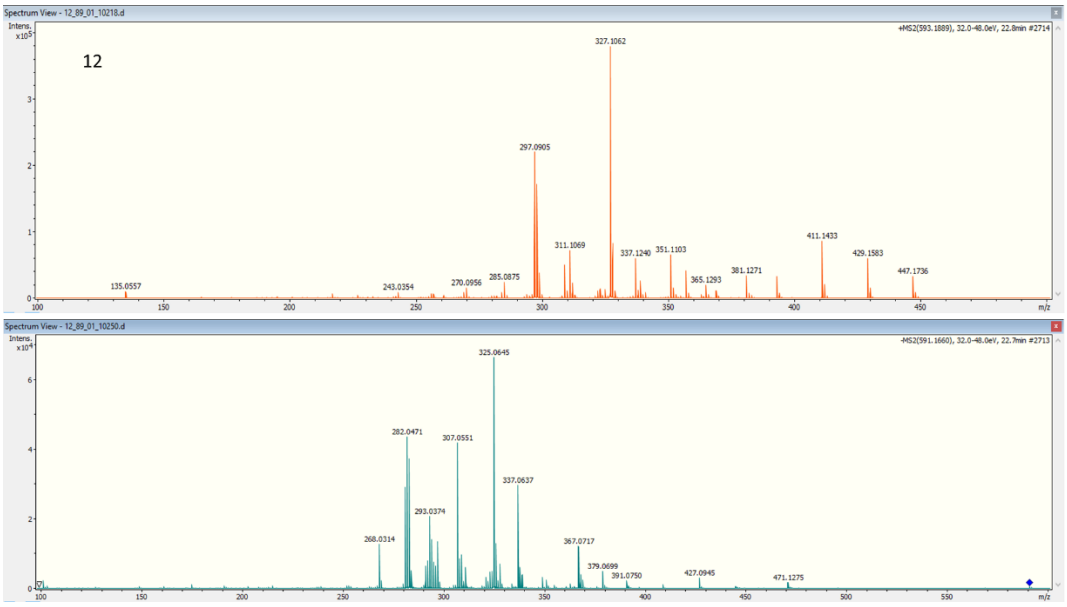

Figure 77. Semiprep fraction 12 from fruits of *P. auritum*. Positive and negative modes.

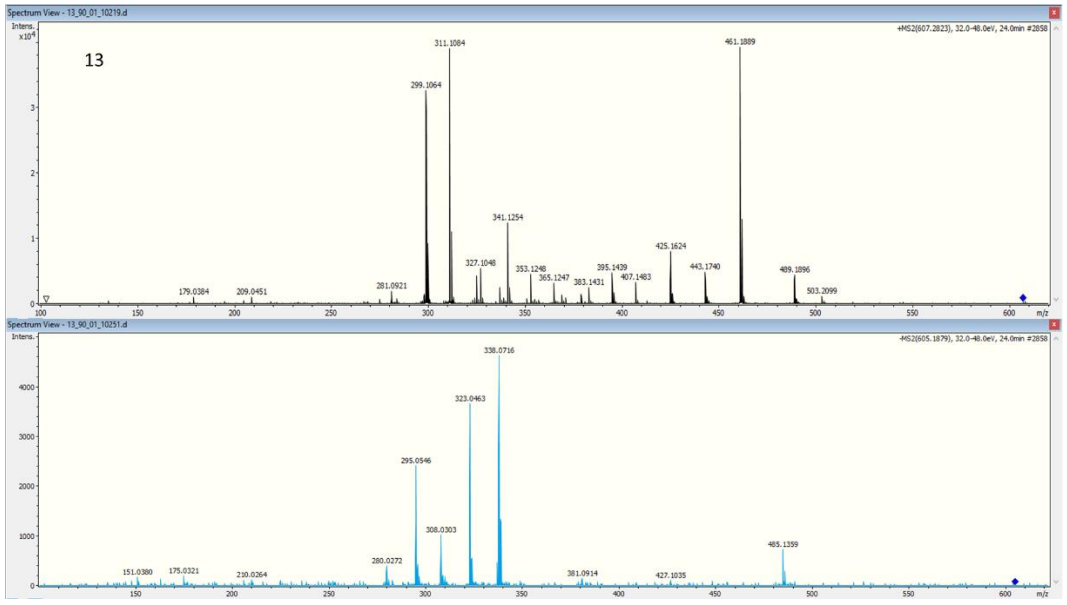

Figure 78. Semiprep fraction 13 from fruits of *P. auritum*. Positive and negative modes.

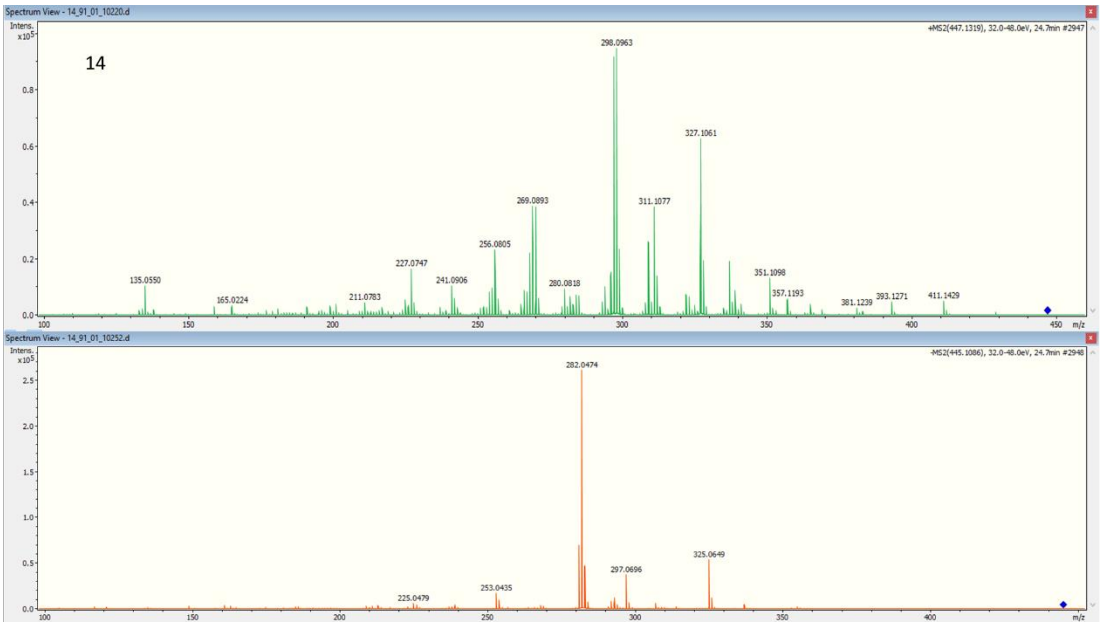

Figure 79. Semiprep fraction 14 from fruits of *P. auritum*. Positive and negative modes.

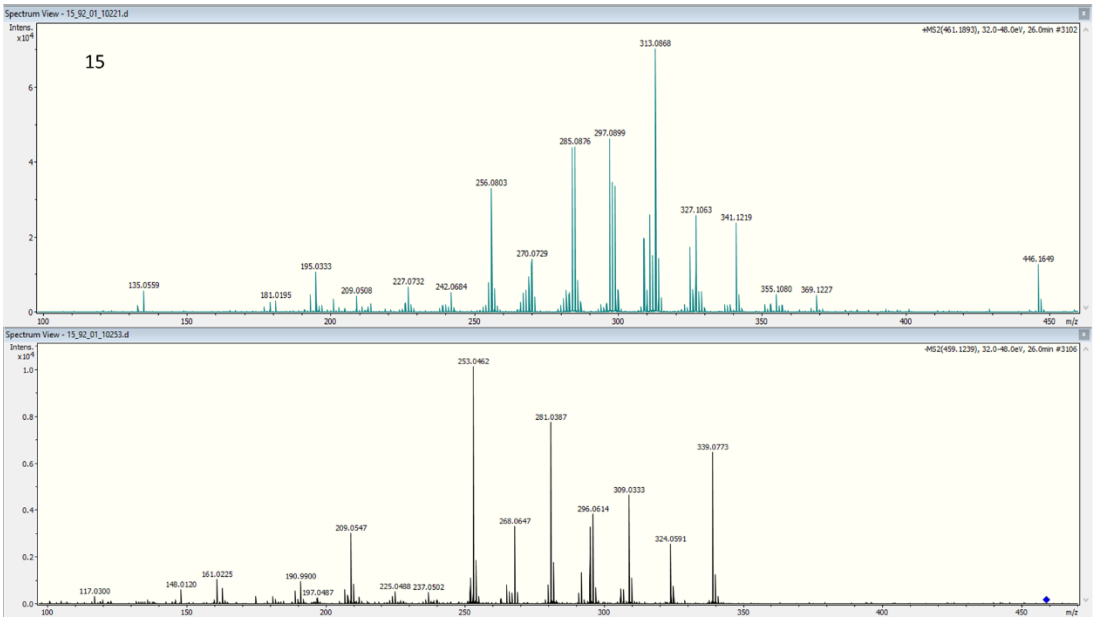

Figure 80. Semiprep fraction 15 from fruits of *P. auritum*. Positive and negative modes.

Column chromatography of Leaves

The DCM fraction obtained from *P. auritum* leaves (5.0 g) was redissolved and dried in flash silica gel (Sigma-Aldrich, 200-400 Mesh), a column (30 cm x 5 cm) was filled with 200 g of the same silica gel approximately, the dry sample was placed in the top and spread carefully (while the column was rotated) until a thin layer was obtained, then this layer is covered by filter paper and cotton. The sample was eluted with a hexane-ethyl acetate mixture (9-1) in three washes using 200 mL of the mixture. The mixture proportion was varied, increasing the amount of EtOAc by 10% till it reached 90% EtOAc and 10% Hex. Next, washes with pure EtOAc, EtOAc- MeOH (98-2), EtOAc- MeOH (95-5), and pure MeOH (two washes) were carried out. The 36 fractions were dried under reduced pressure and weighed; the same TLC system used to resolve the raw extract (Hex- EtOAc 6-4) was used to compare the fractions. It was possible to group all the fractions into six new groups:

Table 17. Subfractions from leaves of *P. auritum.*

Group	A	B	C	D	E	F	G
Fractions	**4**	**5-7**	**13-16**	**18-21**	**22-24**	**25-27**	**31-32**
Amount (mg)	**2,8**	**86,3**	**1368**	**257**	**248**	**128**	**54,1**

Subsequent analyses were conducted with fractions C and D due they were the fractions with higher amounts.

Fraction C

A 40 cm x 2,5 cm column was filled with 50 g of silica gel (Sigma-Aldrich, 70 – 230 Mesh) by the slurry method, applying the redissolved sample in the top and covering it with a layer of silica gel (1 cm approx.). The sample was eluted with a mixture of DCM-MeOH (99-1), and 40 new fractions were collected; these fractions were again grouped into five new subgroups (C1, C2. C3. C4, and C5). The major compounds were found in C2 (820 mg), and a remarkable compound (fluorescent at 340 nm) was found in C5.

For C2, new column chromatography was made using a 30 x 1,5 cm column, 15 g of silica gel, and a mixture of DCM-Hex (80-20). Twenty-three fractions were obtained and checked by TLC. Two different well-resolved spots were observed; fraction 1 contained the first spot (C2A, 300 mg) while the second was found among fractions 9-18 (C2B, 88 mg). C2A was obtained as a shapeless beige solid, while C2B was a white, needle-type crystal.

C5 was submitted to another purification using the same column as C2, using 16 g of silica and a mixture of DCM-MeOH (98-2) for the elution.

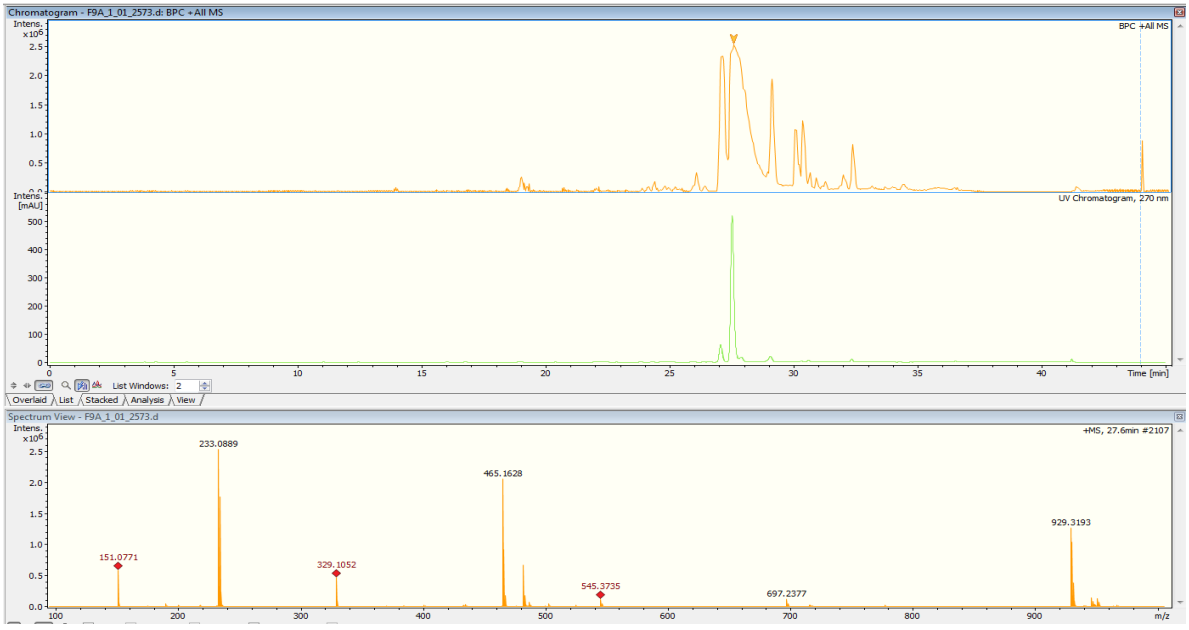

Figure 81. HPLC chromatogram (270 nm) and BPC (+) of compound **36**.

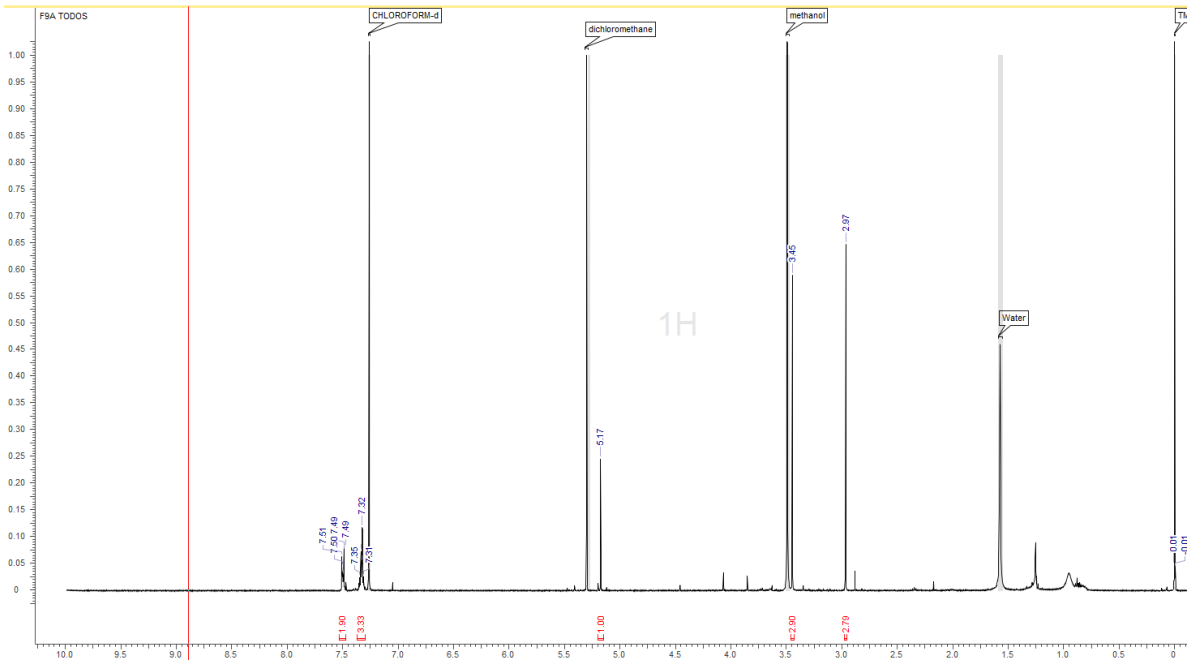

Figure 82. Detailed 500 MHz ^{1}H NMR spectrum of **36**.

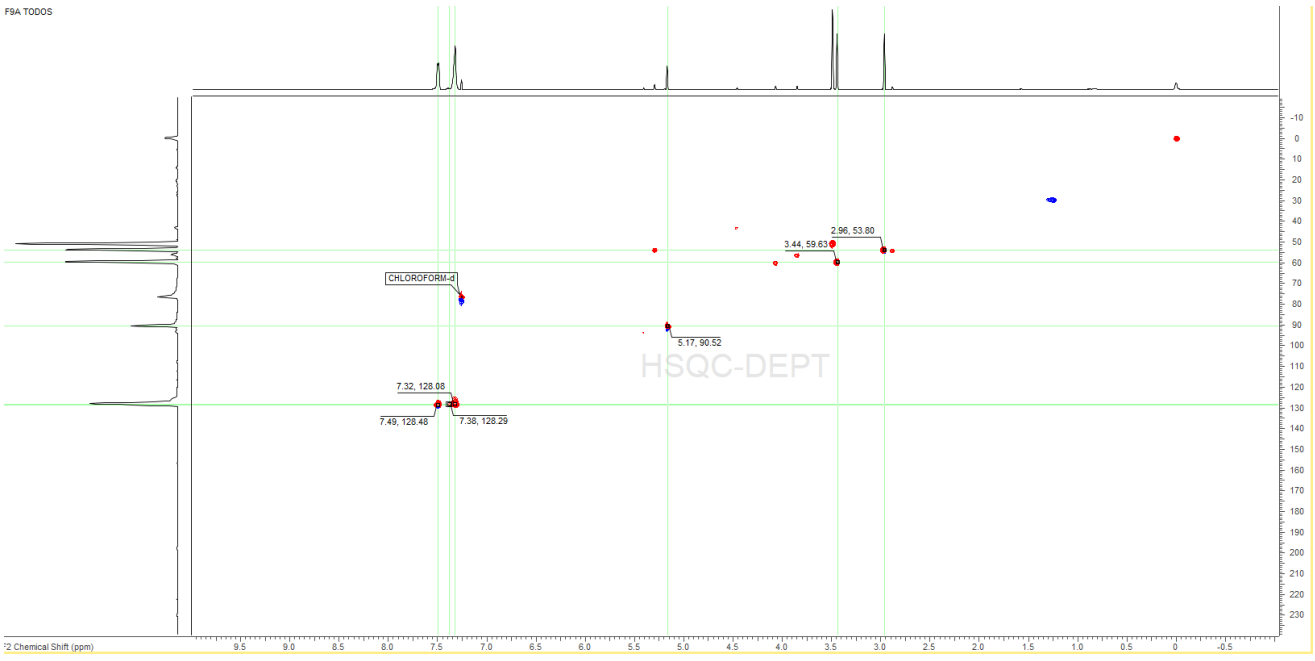

Figure 83. HSQC spectrum of **36**.

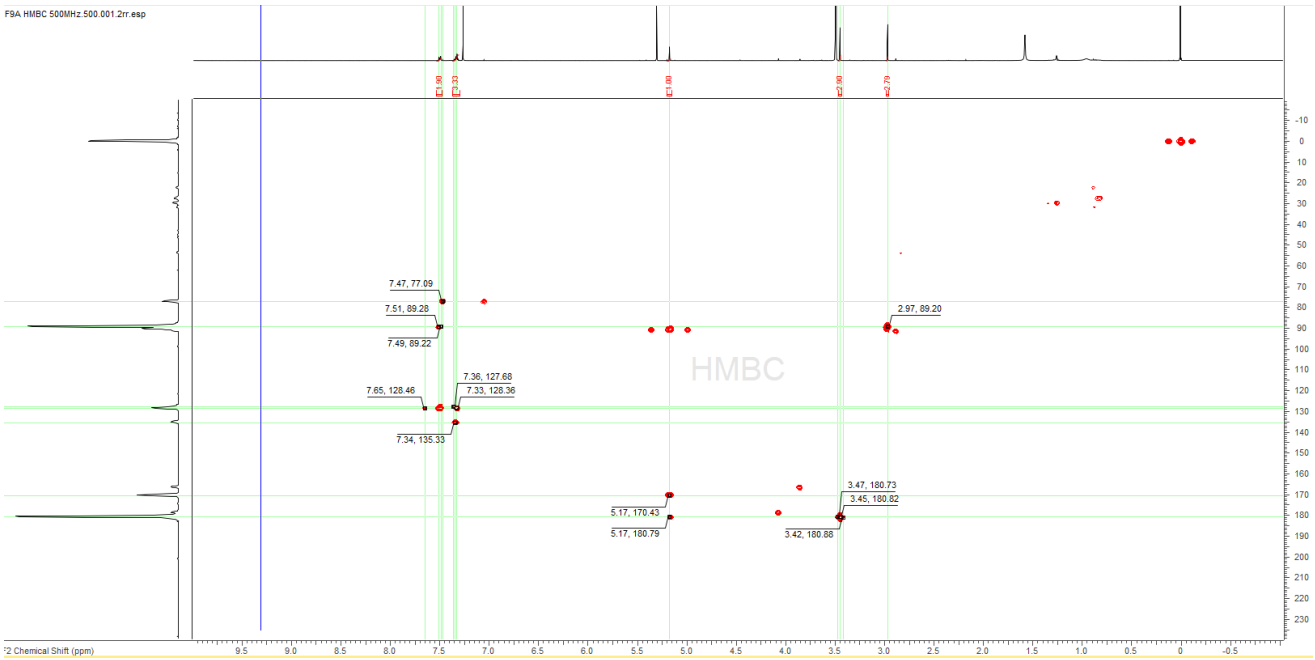

Figure 84. HSQC spectrum of **36**.

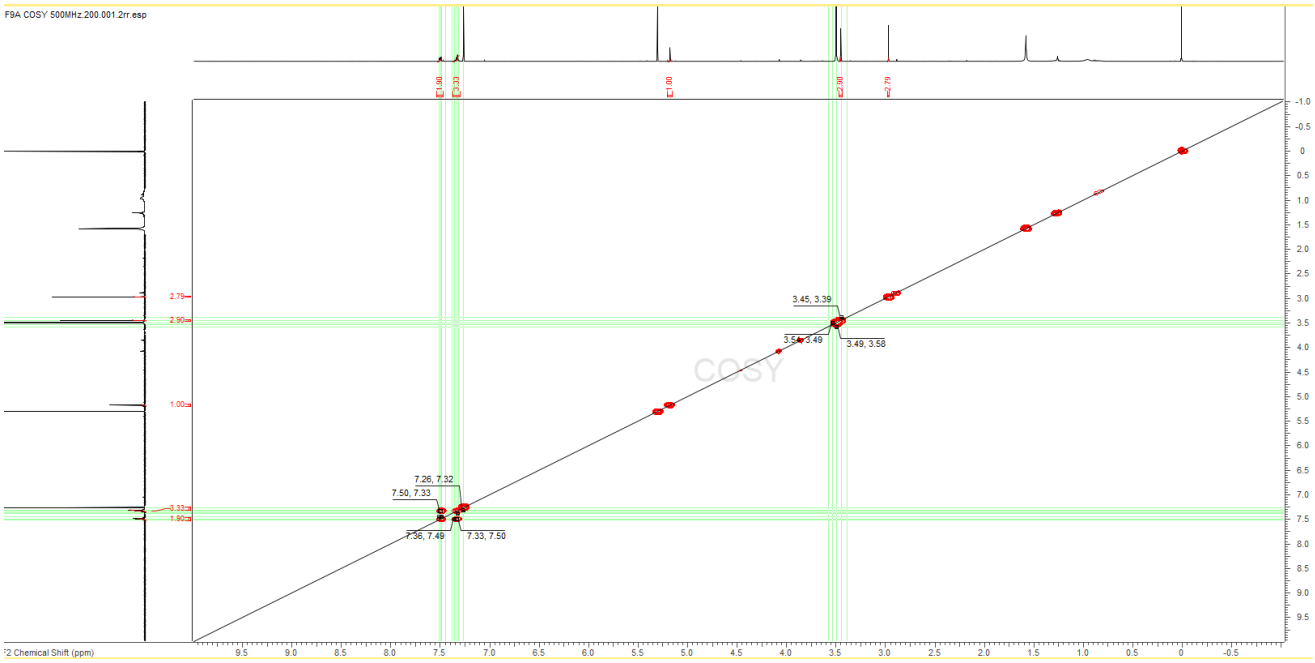

Figure 85. COSY spectrum of **36**.

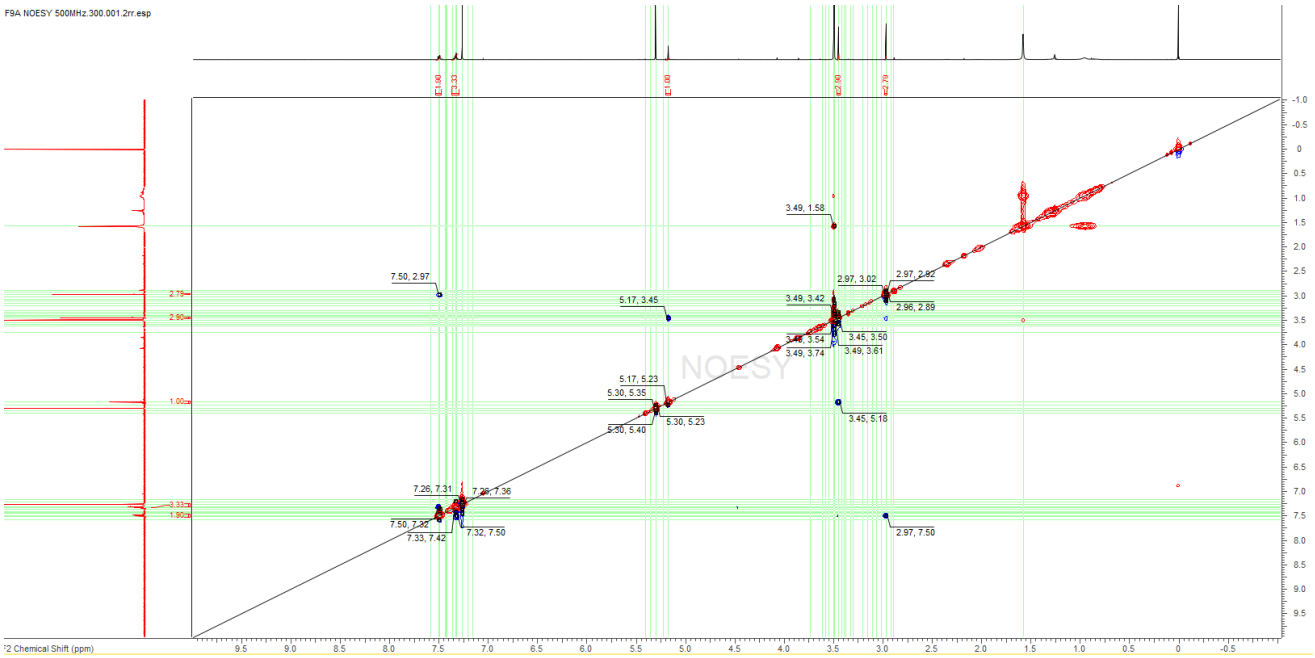

Figure 86. NOESY spectrum of **36**.

Fraction D

The 257 mg of the fraction were redissolved and dried in silica; the purification was carried out in a 40 cm x 2,5cm column filled with 50 g of silica gel and a mixture of DCM-MeOH (99-1). Thirty fractions were obtained, three relevant compounds were isolated, mixing the fractions into three different groups, D1 (7.0 mg, Fr 6-11), D2 (11 mg, Fr 12-15), and D3 (73 mg, Fr 16-24).

D3 was submitted to a new purification using a 30 cm x 1,5 cm column, filled with 15 g of silica, and DCM as mobile phase. Thirty-seven fractions were obtained (including a final wash with MeOH), 8,0 mg of the fluorescent compound (D3A) was isolated from fractions 17, 21, 22, and 24.

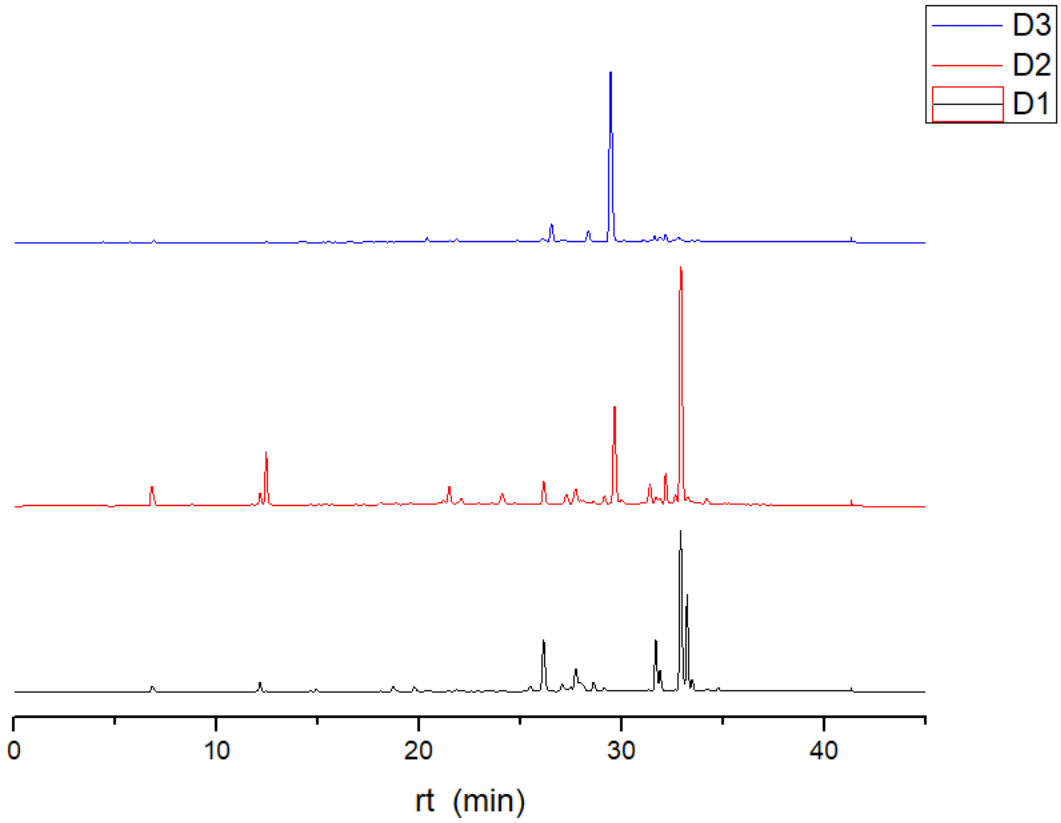

Figure 87. HPLC-DAD chromatogram (270 nm) from subfractions D1-D3.

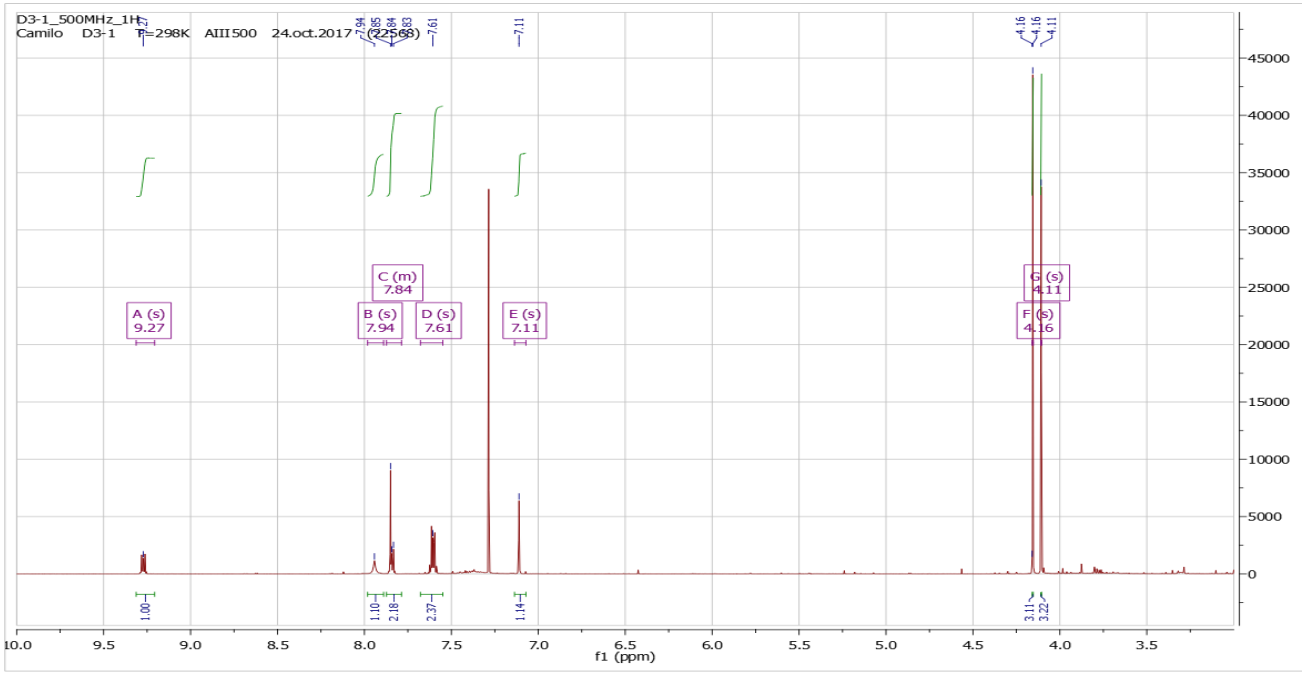

Figure 88. Detailed ^{1}H-NMR spectrum (500MHz) of cepharanone B.

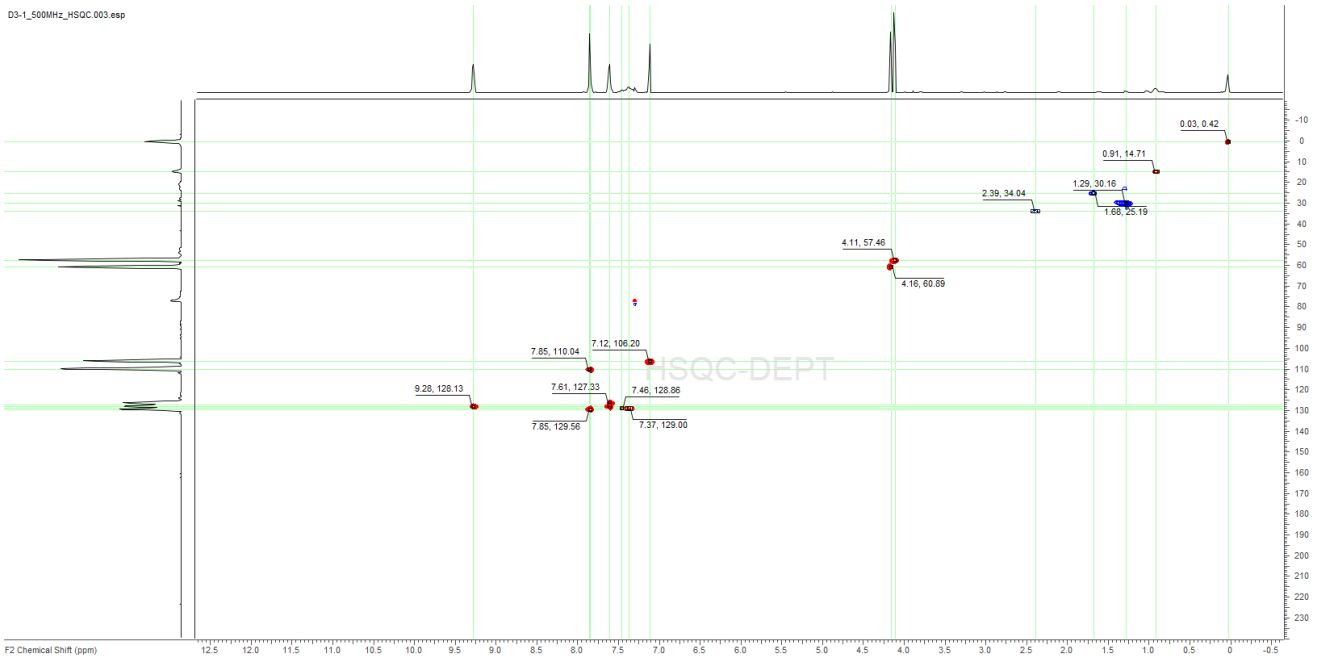

Figure 89. HSQC-DEPT spectrum (500MHz) of cepharanone B.

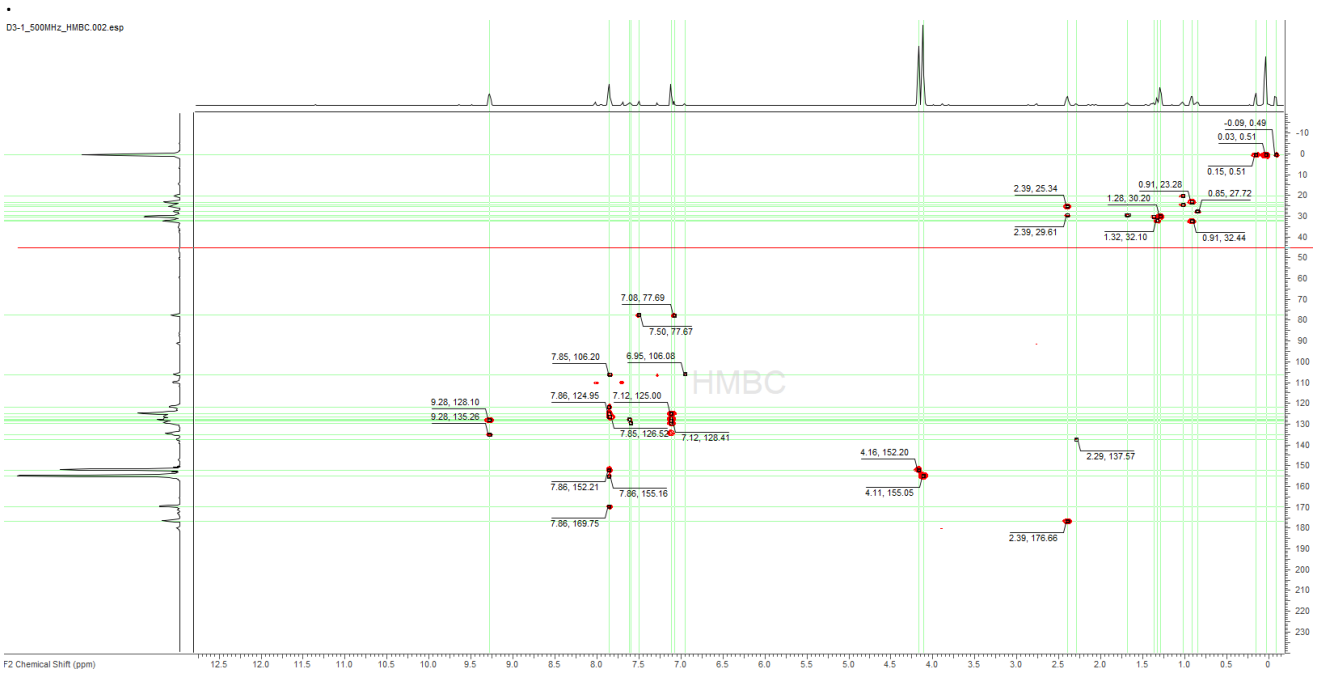

Figure 90. HMBC spectrum (500MHz) of cepharanone B.

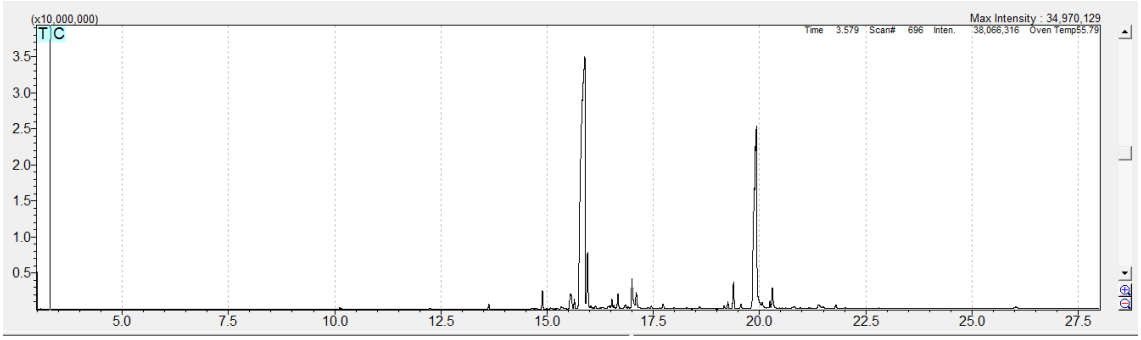

Figure 91. GC-MS chromatogram of fraction A from leaves of *P. auritum*.

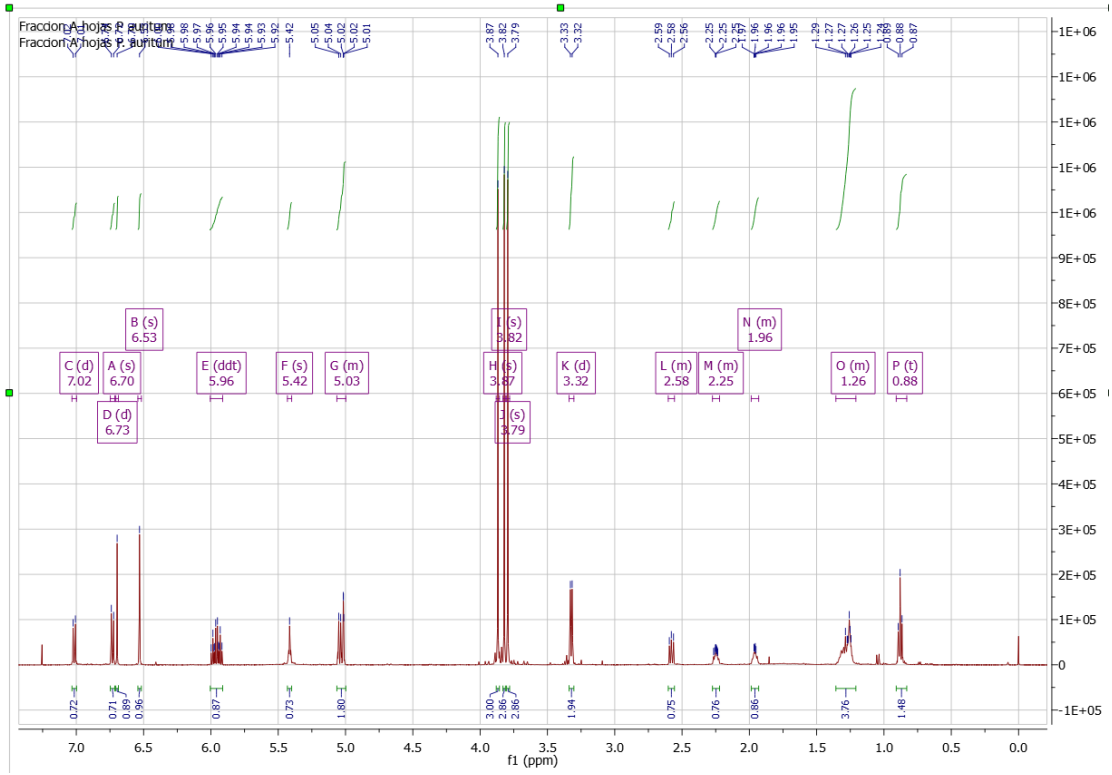

Figure 92. ^{1}H-NMR spectrum (500MHz) of fraction A from leaves of *P. auritum*.

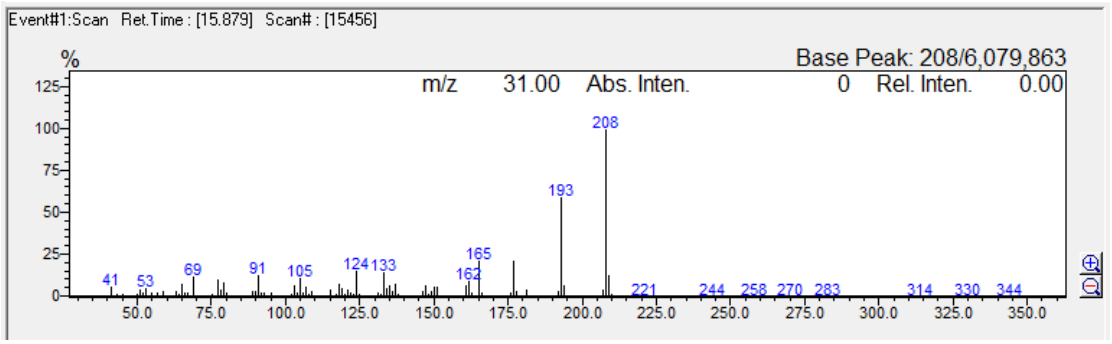

Figure 93. MS EI spectrum of isoasarone.

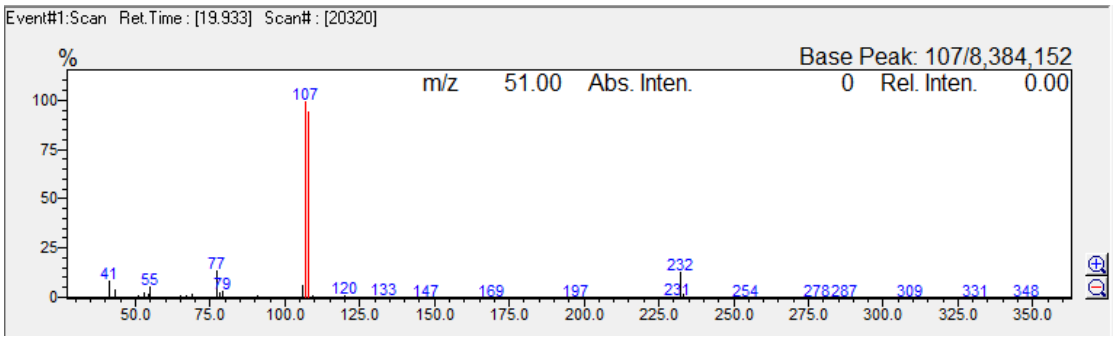

Figure 94. MS EI spectrum of gibbilimbol B.

Cap 2.

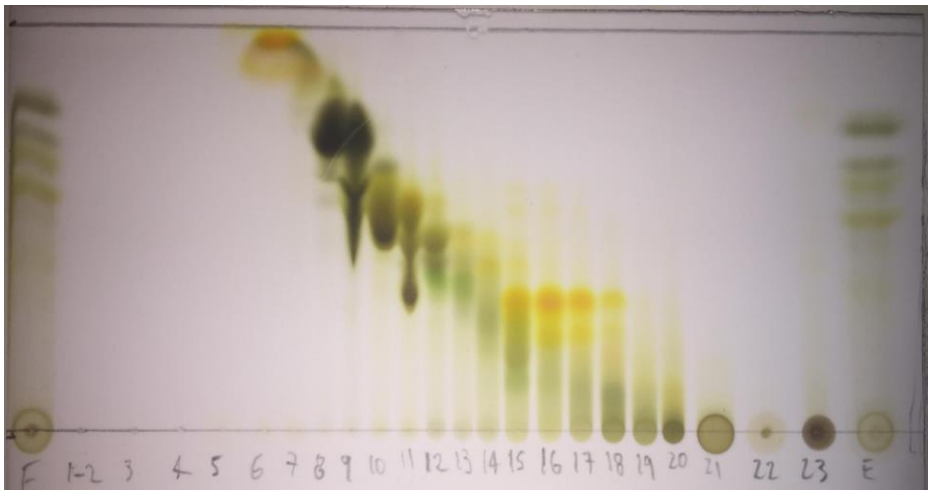

Figure 95. TLC leaves from *P. lindbergii* (Hex-EtOAc 6-4) Visible.

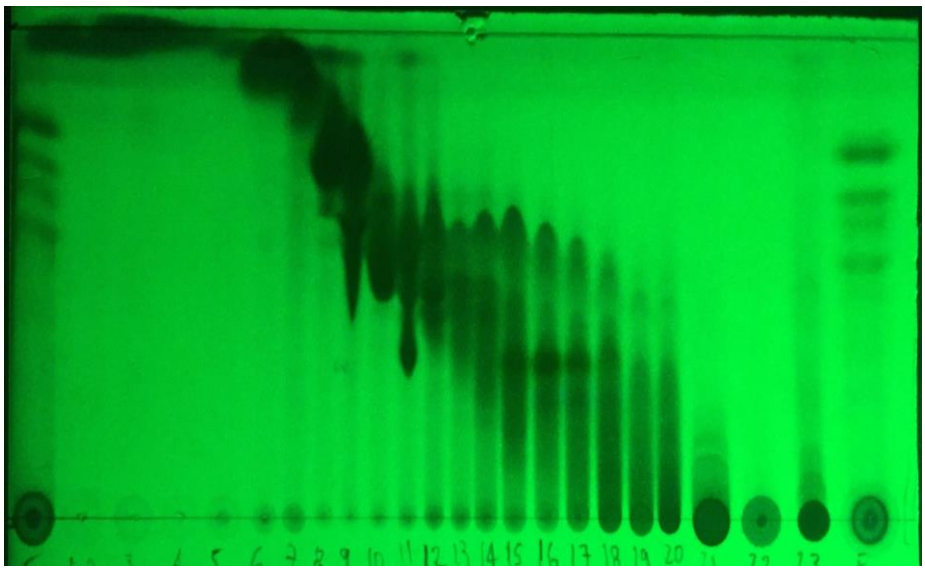

Figure 96. TLC leaves from *P. lindbergii* (Hex-EtOAc 6-4) 254 nm.

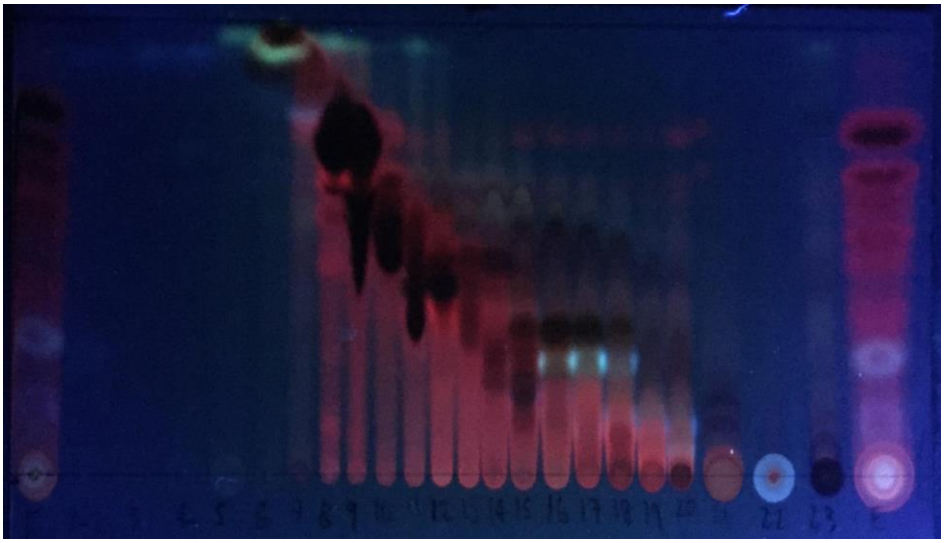

Figure 97. TLC of leaves from *P. lindbergii* (Hex-EtOAc 6-4) 365 nm.

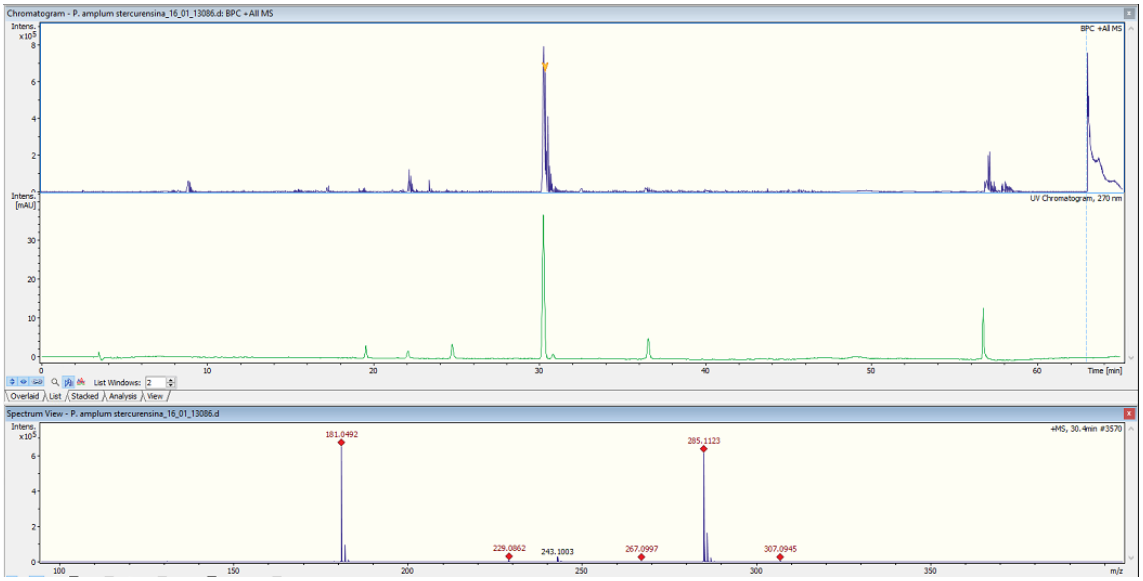

Figure 98. HPLC chromatogram, BPC and MS of stercurensin.

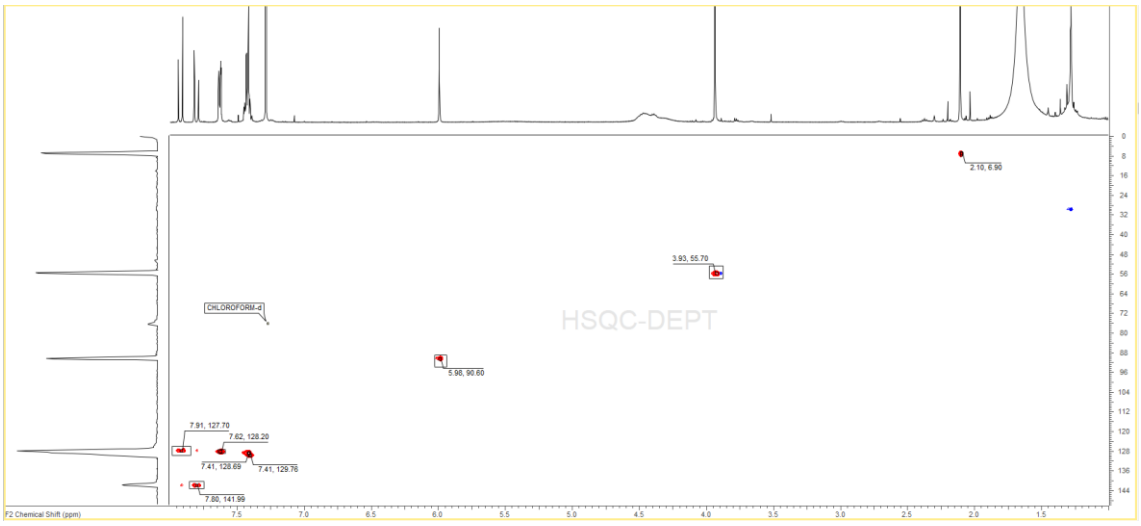

Figure 99. HSQC-DEPT of stercurensin.

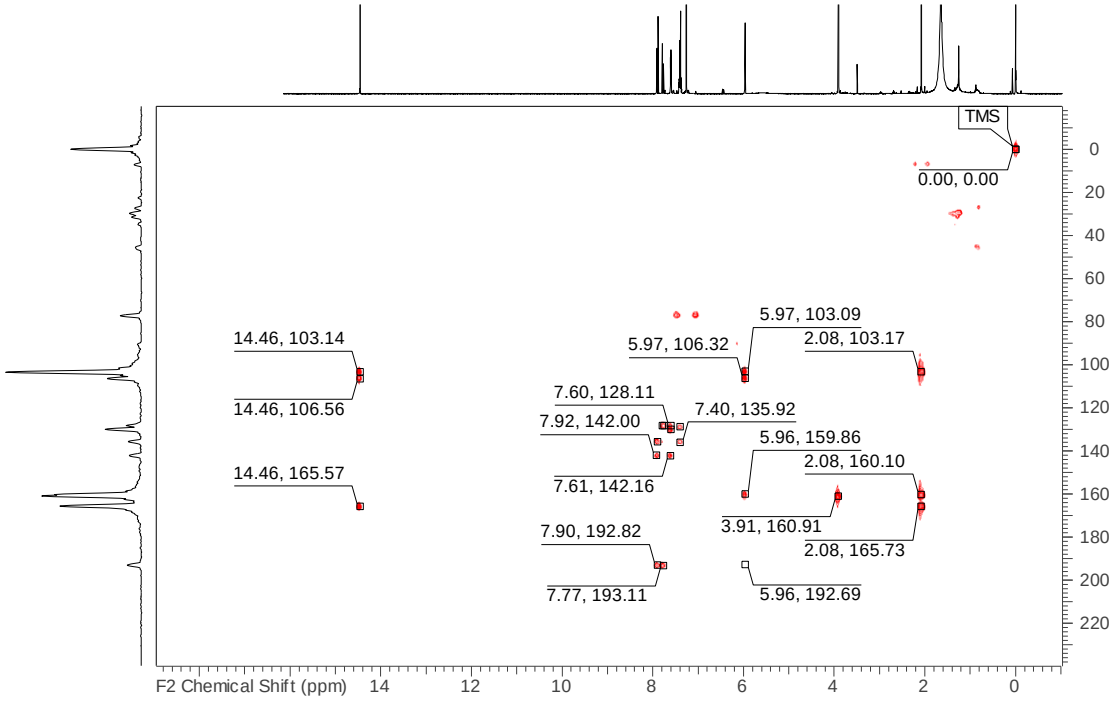

Figure 100. HMBC of stercurensin.

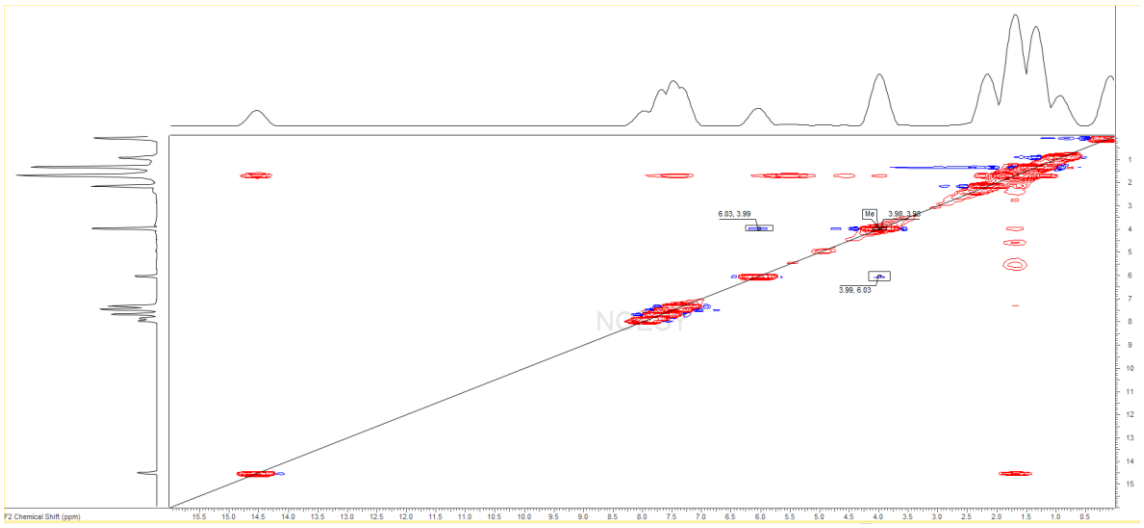

Figure 101. NOESY of stercurensin.

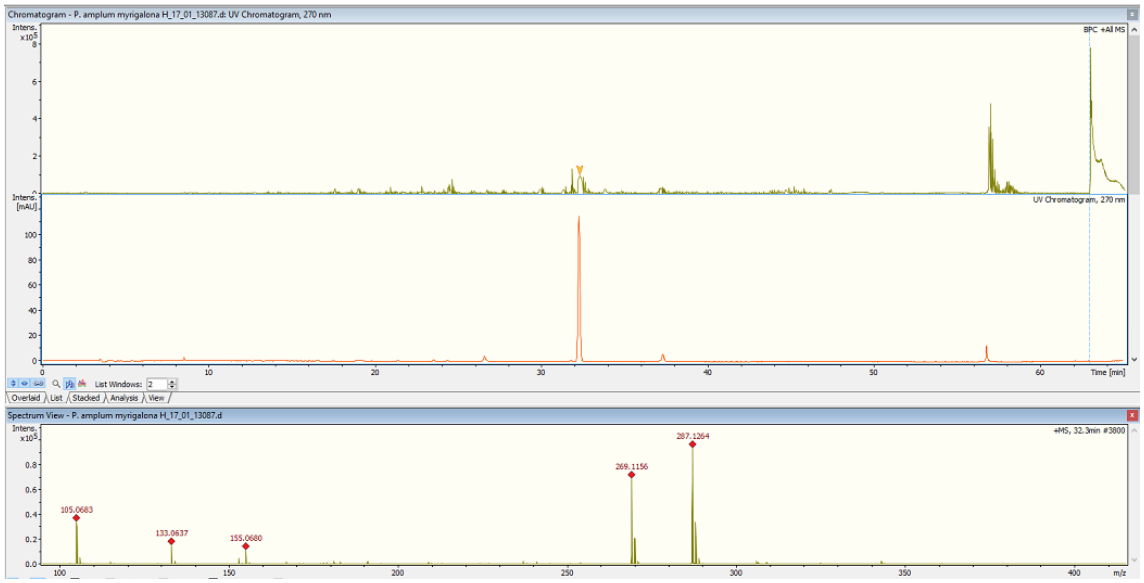

Figure 102. HPLC chromatogram, BPC and MS of myrigalone H.

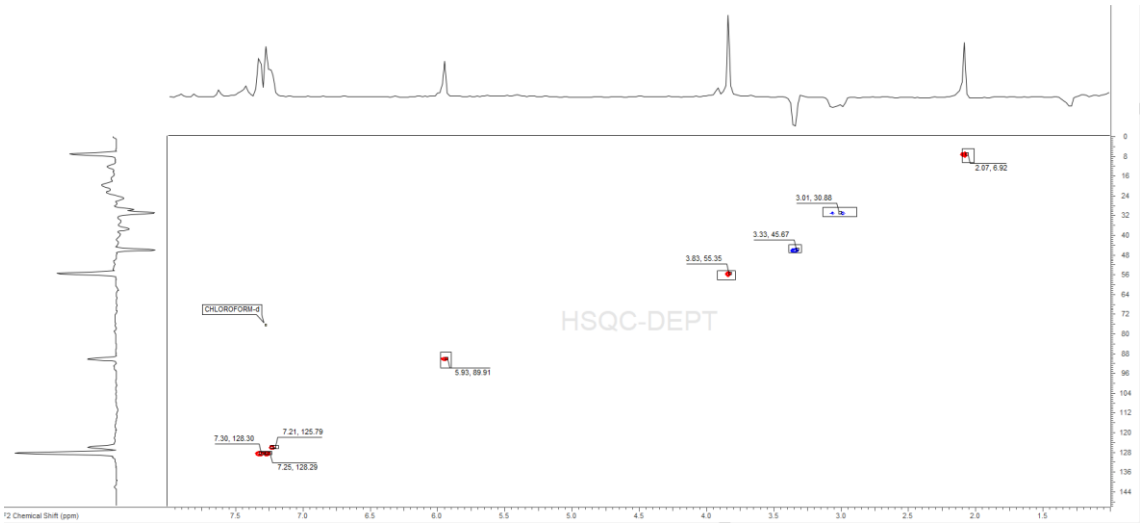

Figure 103. HSQC-DEPT of myrigalone H.

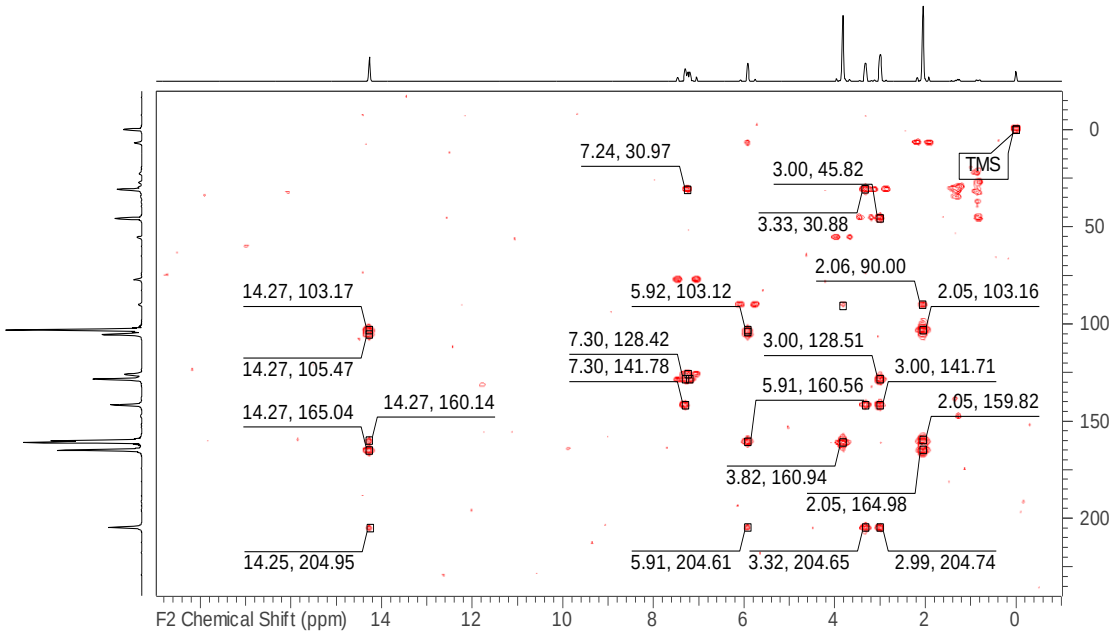

Figure 104. HMBC of myrigalone H.

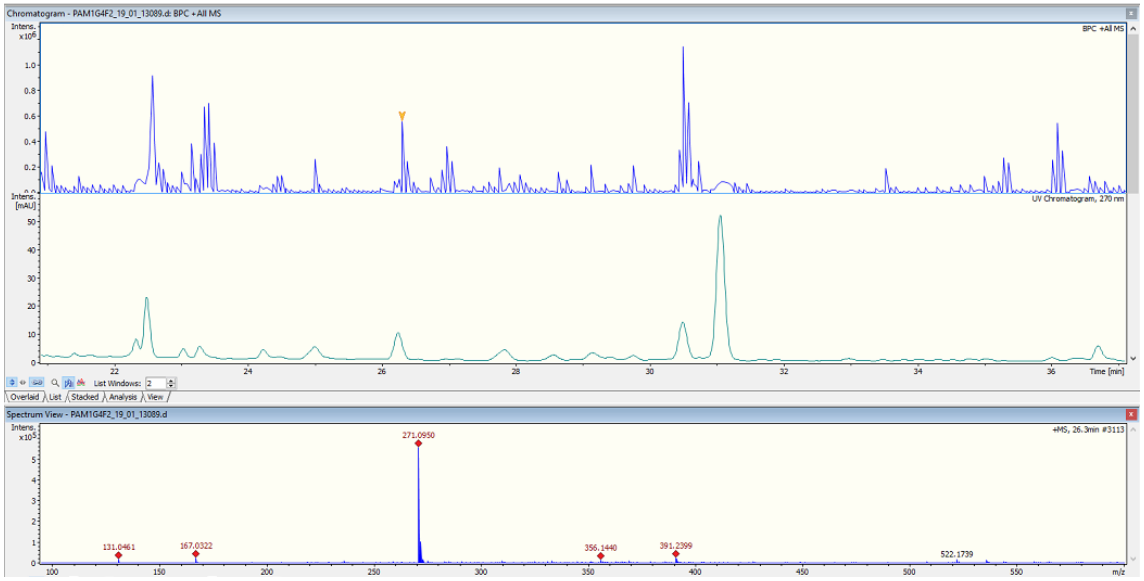

Figure 105. HPLC, BPC and MS of cardamomin.

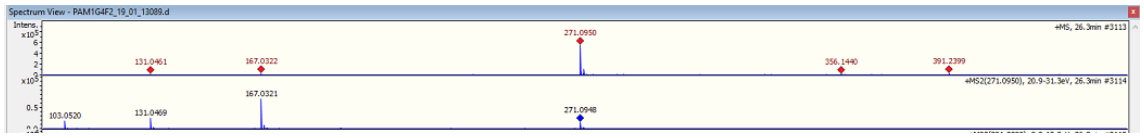

Figure 106. MS^2 spectra of cardamomin.

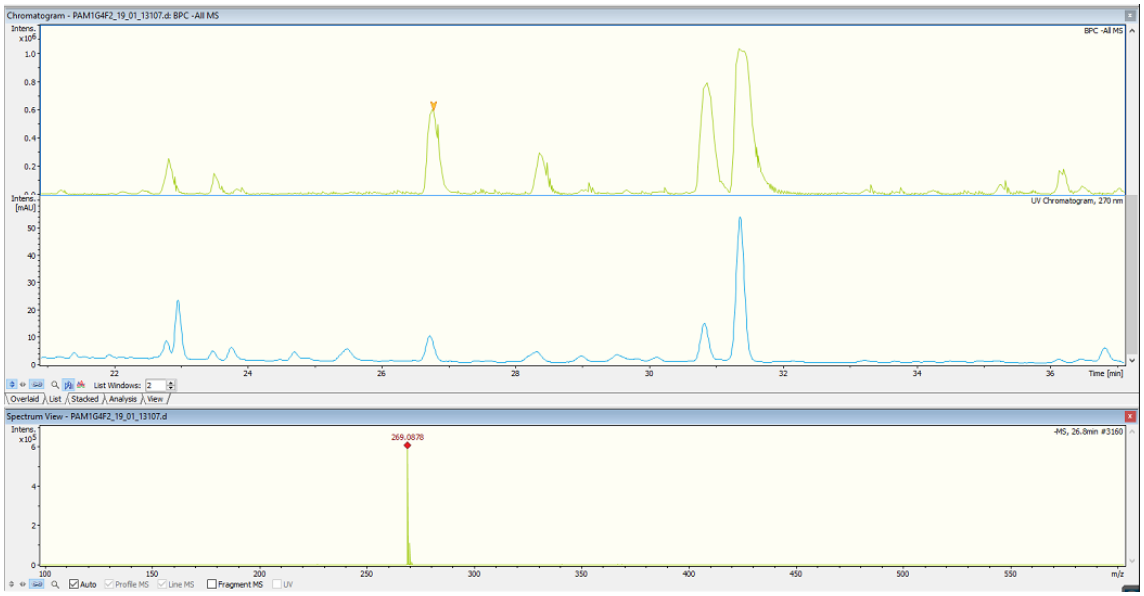

Figure 107. HPLC, BPC and MS of cardamomin.

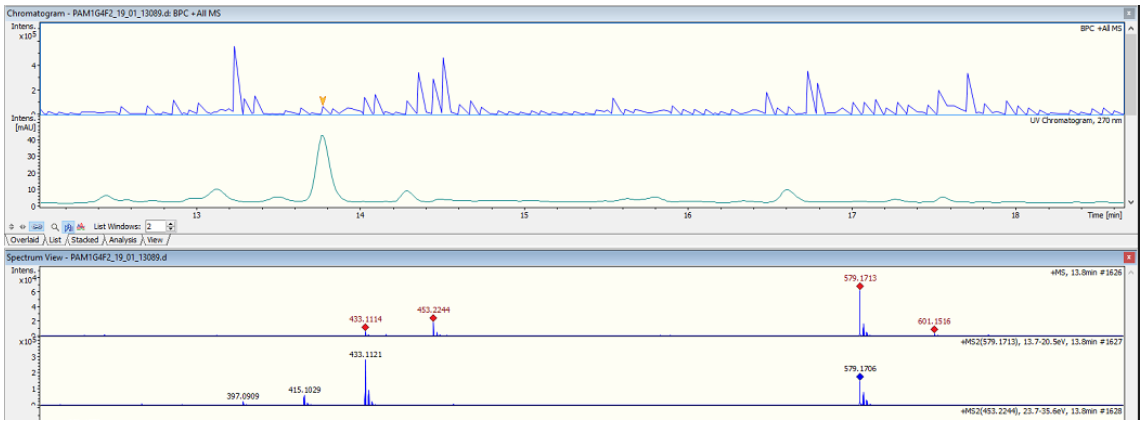

Figure 108. LCMS^2 of vitexin rhamnoside (positive).

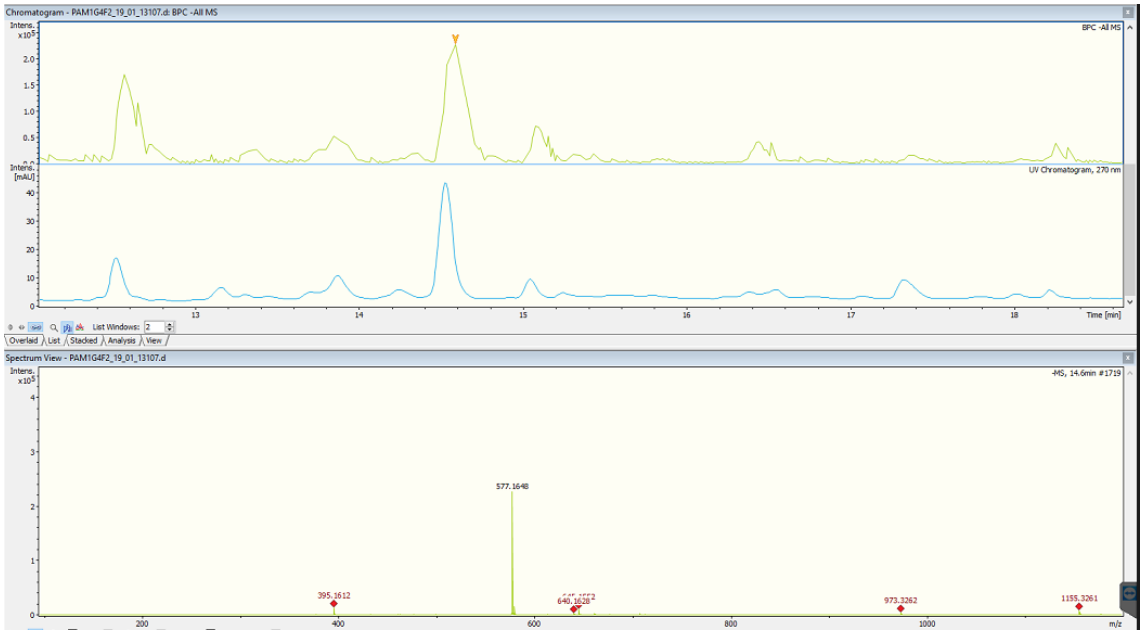

Figure 109. LCMS^2 of vitexin rhamnoside (negative).

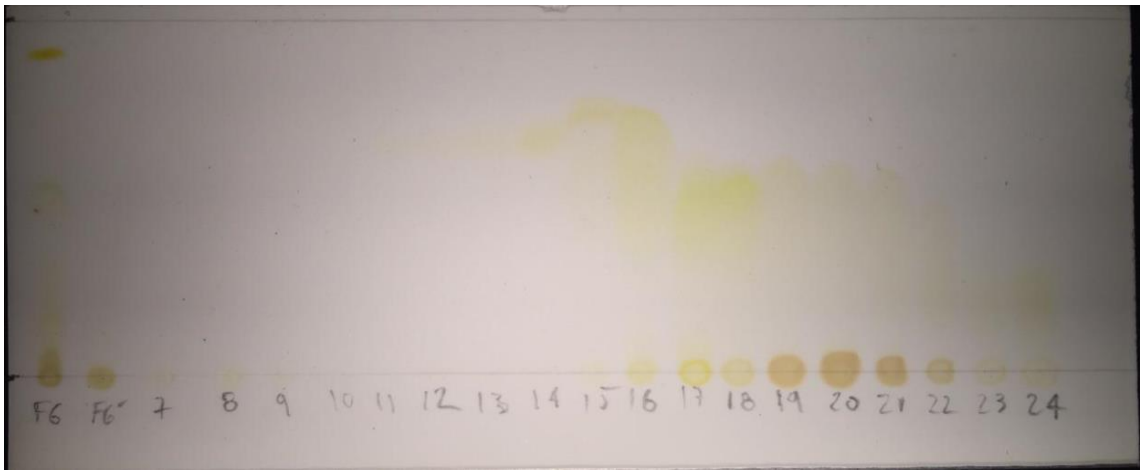

Figure 110. TLC from F6 of CC from *P. lindbergii* (Hex- $CHCl_3$ 75-25) visible.

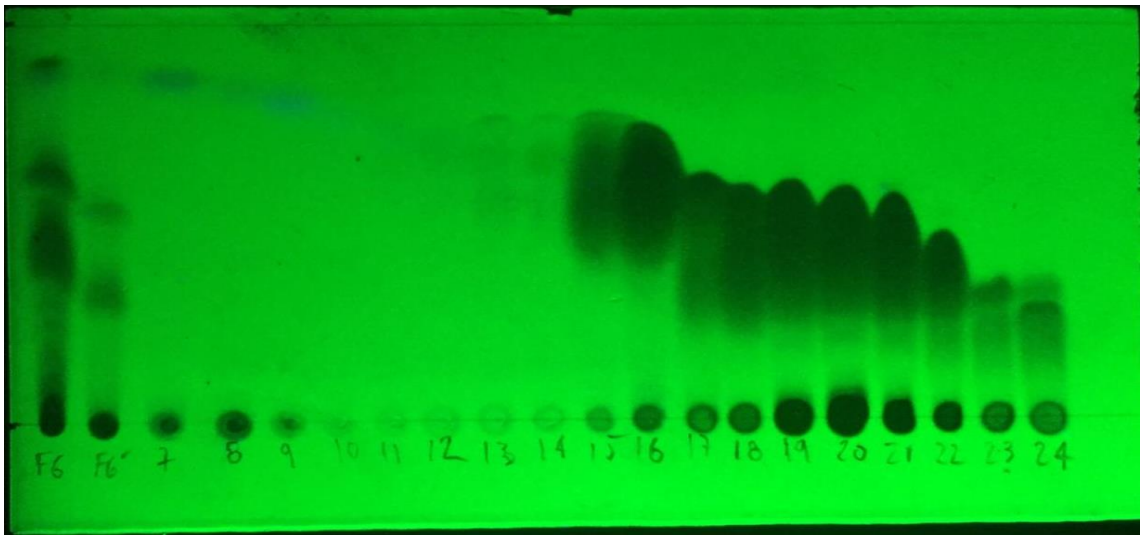

Figure 111. TLC from F6 of CC from *P. lindbergii* (Hex- $CHCl_3$ 75-25) 254 nm.

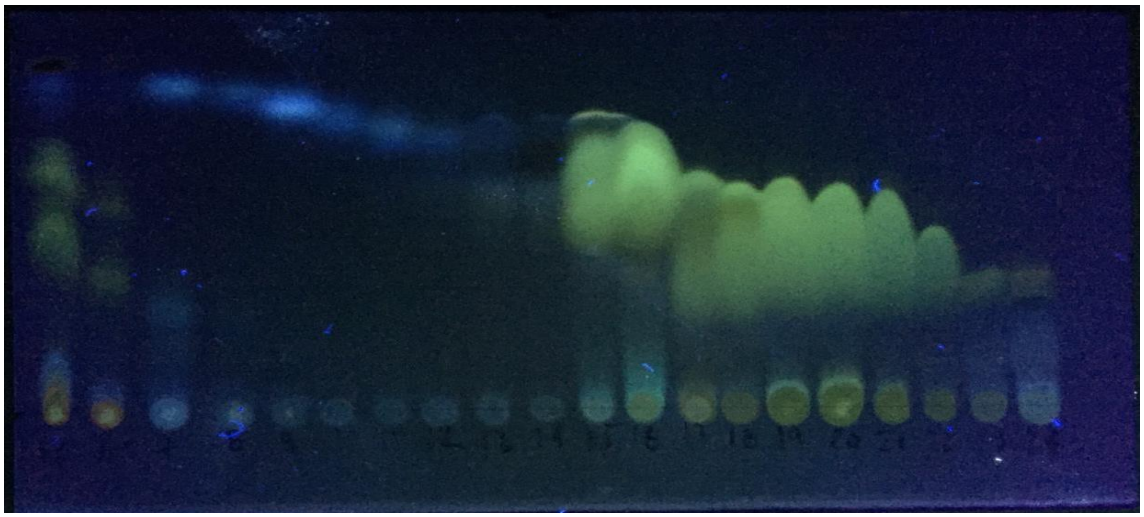

Figure 112. TLC from F6 of CC from *P. lindbergii* (Hex- $CHCl_3$ 75-25) 365 nm.

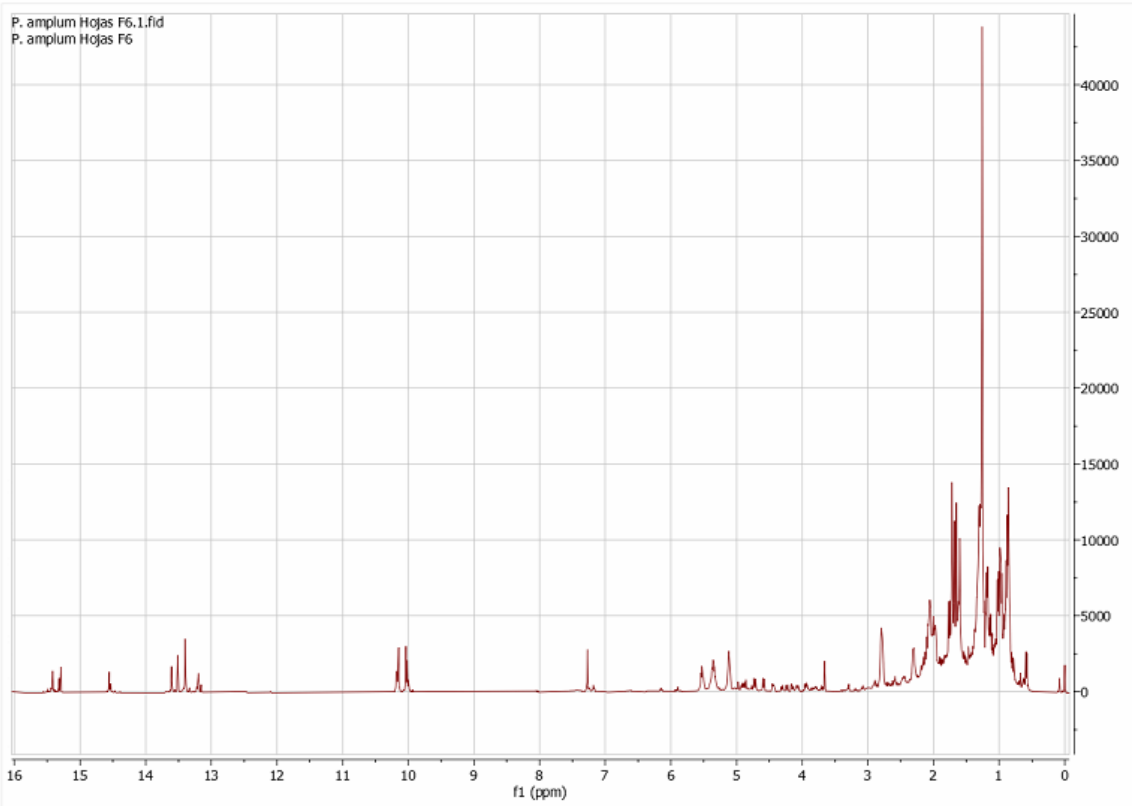

Figure 113. ^{1}H NMR of F6 from *P. lindbergii*.

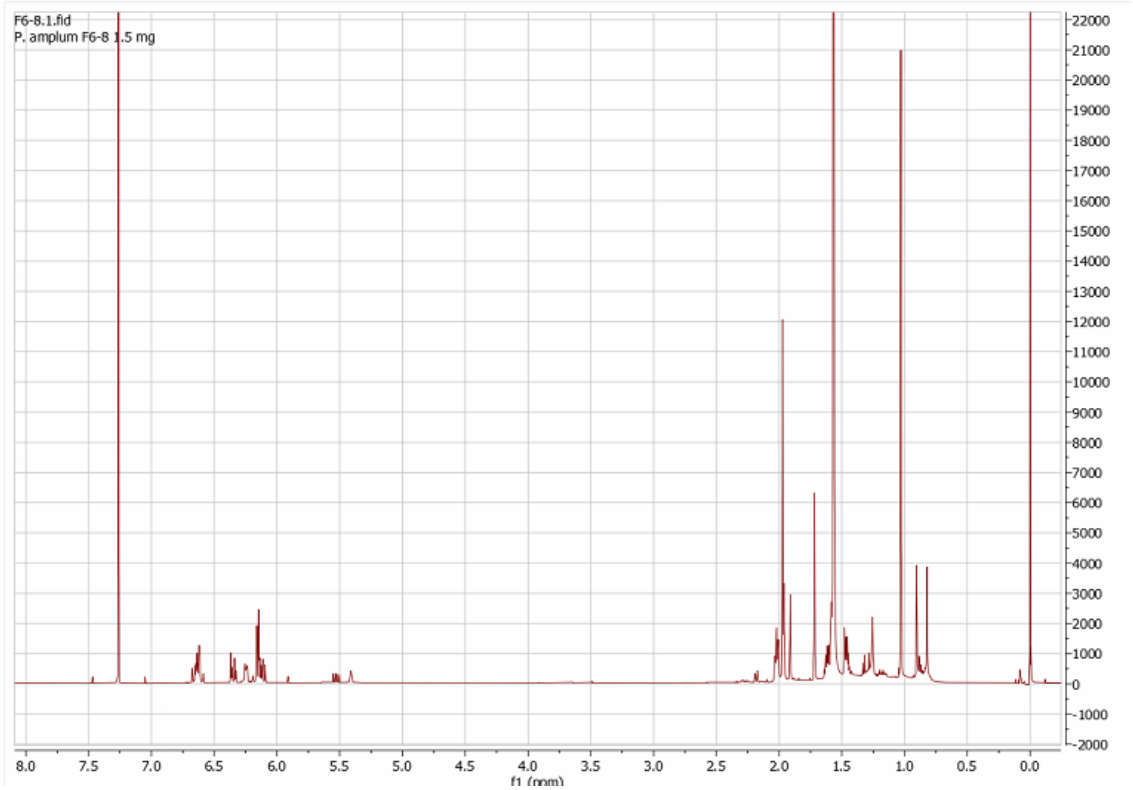

Figure 114. ^{1}H NMR of F8 from *P. lindbergii*.

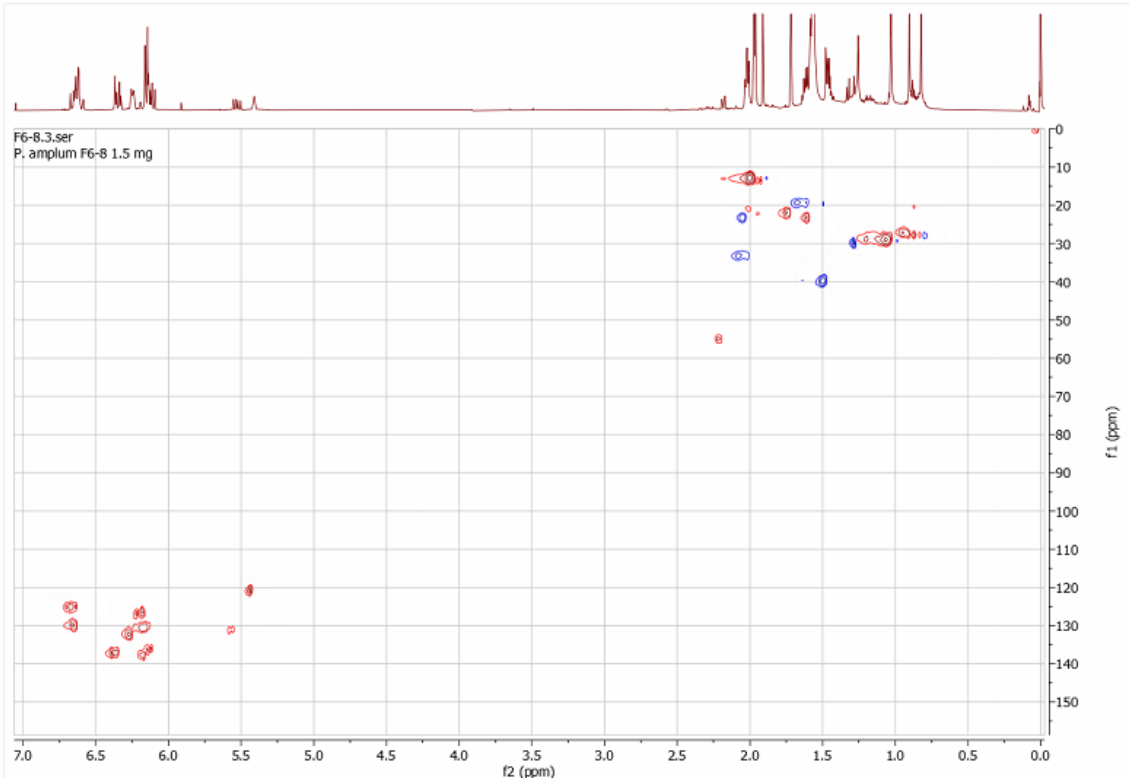

Figure 115. HSQC of F6 CC F8 from *P. lindbergii*.

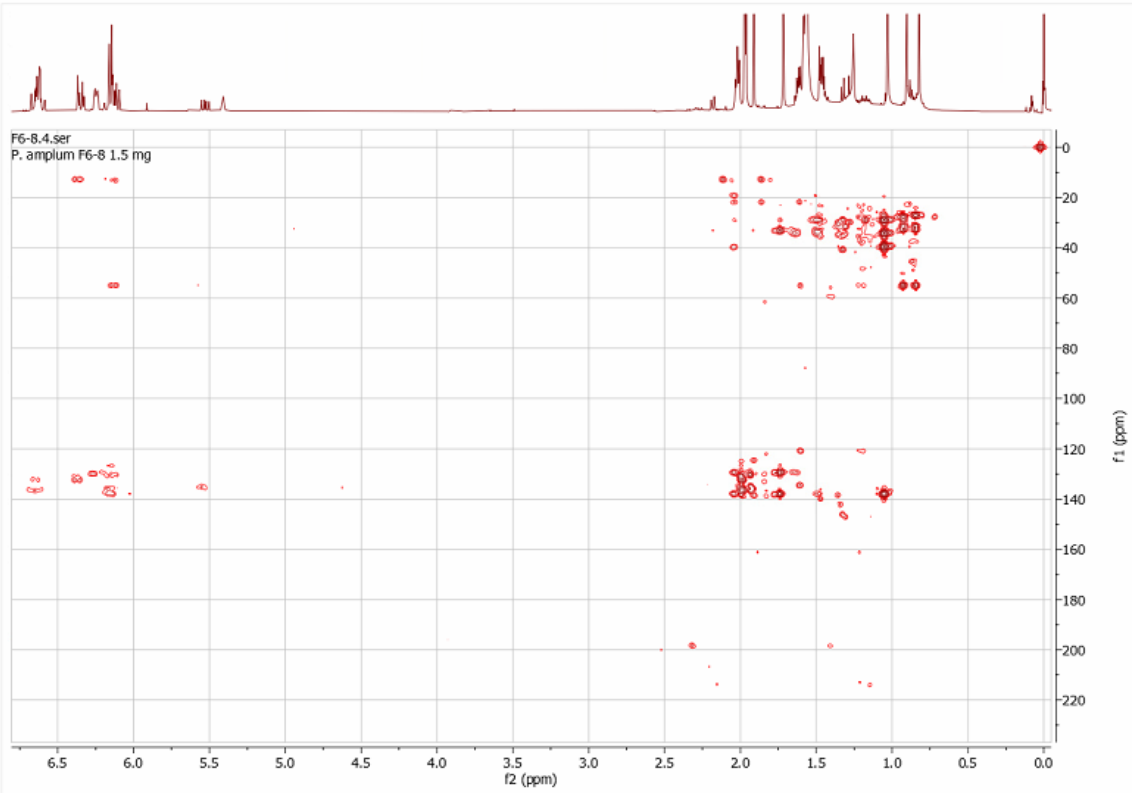

Figure 116. HMBC of F6 CC F8 from *P. lindbergii*.

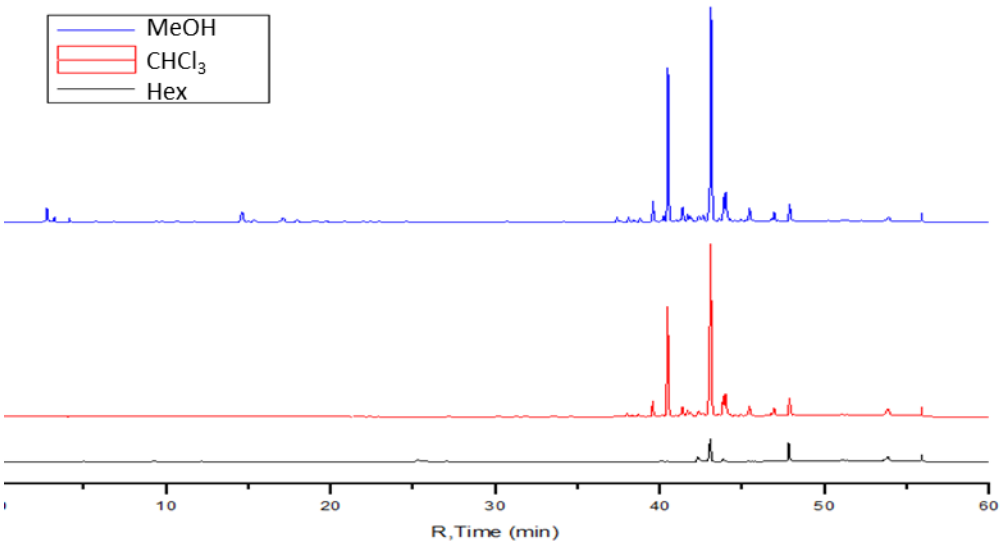

Figure 117. HPLC (270 nm) of the extraction test from *P. chimonantifolium*.

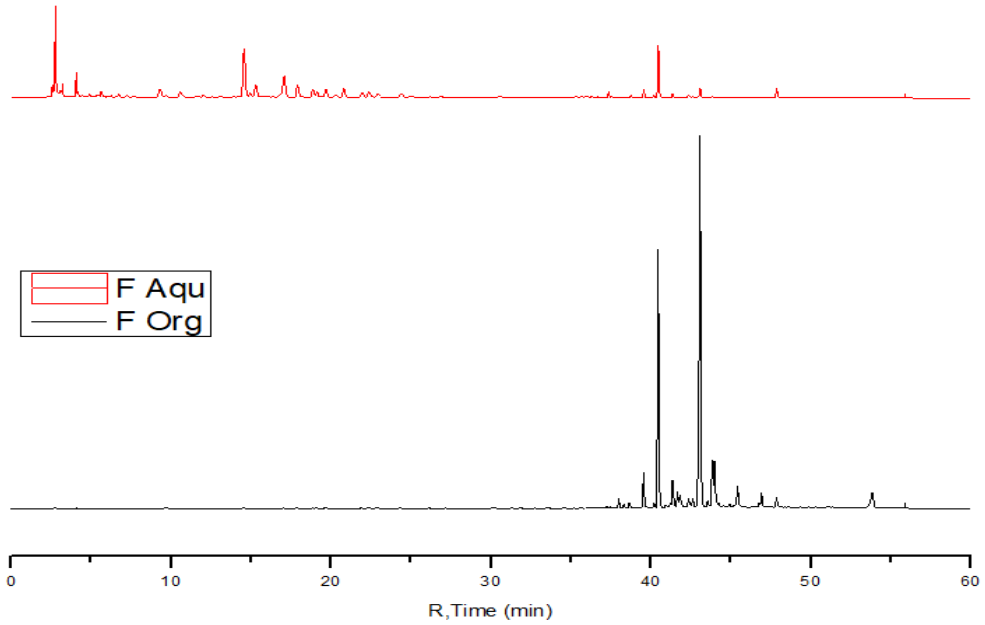

Figure 118. HPLC (270 nm) of the solvent partition *from P. chimonantifolium*.

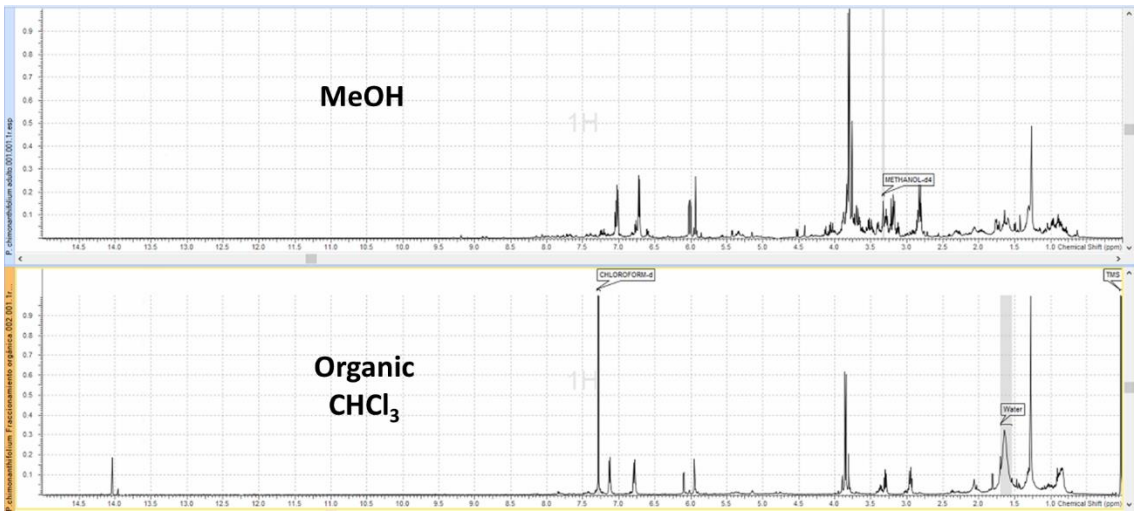

Figure 119. ^{1}H NMR spectrum of the solvent partition and MeOH extract from *P. chimonantifolium*.

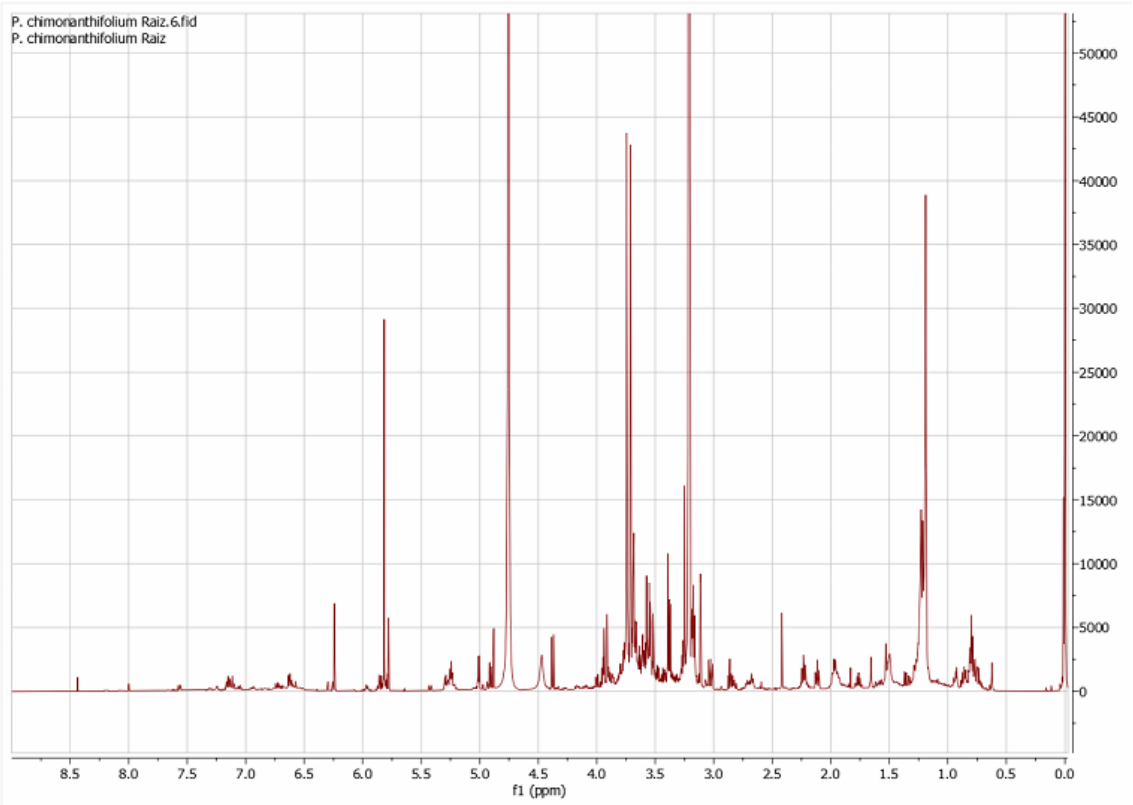

Figure 120. ^{1}H NMR spectrum from roots of *P. chimonantifolium* in MeOD.

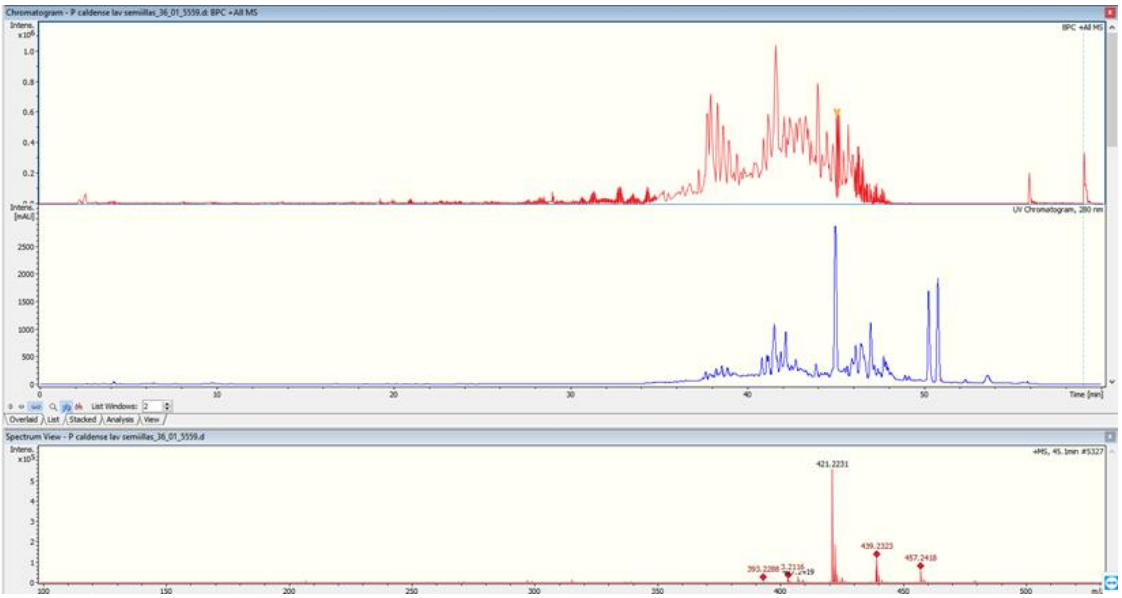

Figure 121. LCMS of caldensinic acid **85** from seeds of *P. caldense*.

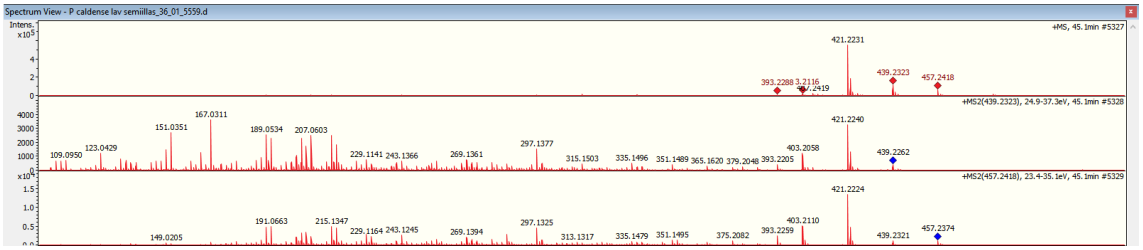

Figure 122. MS^2 spectra of caldensinic acid **85** from seeds of *P. caldense*.

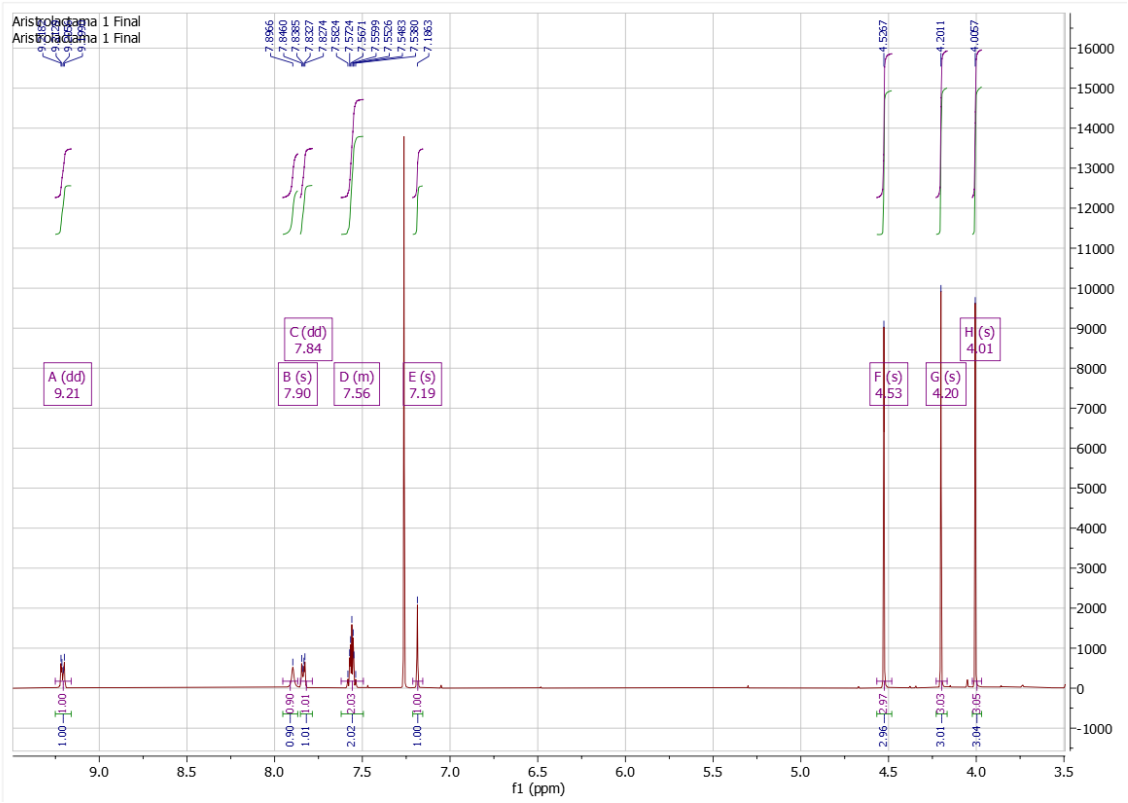

Figure 123. ^{1}H NMR spectrum of piperolactam C.

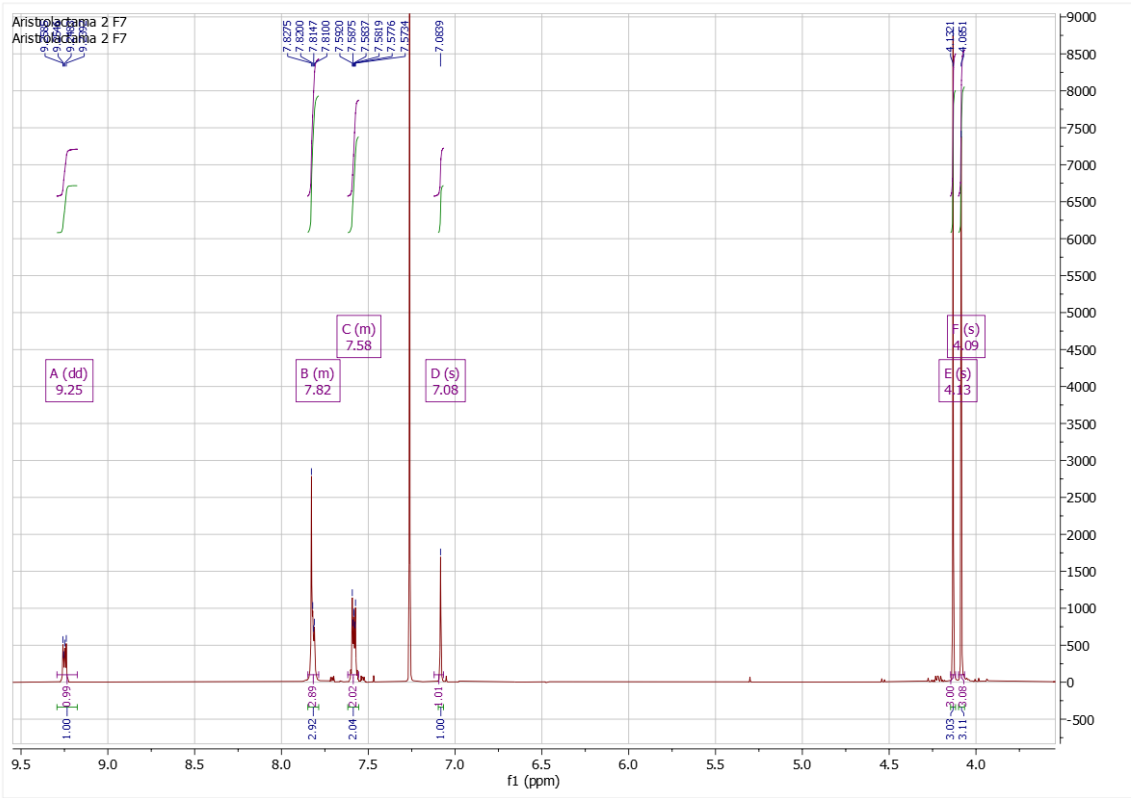

Figure 124. ^{1}H NMR spectrum of cepharanone B.

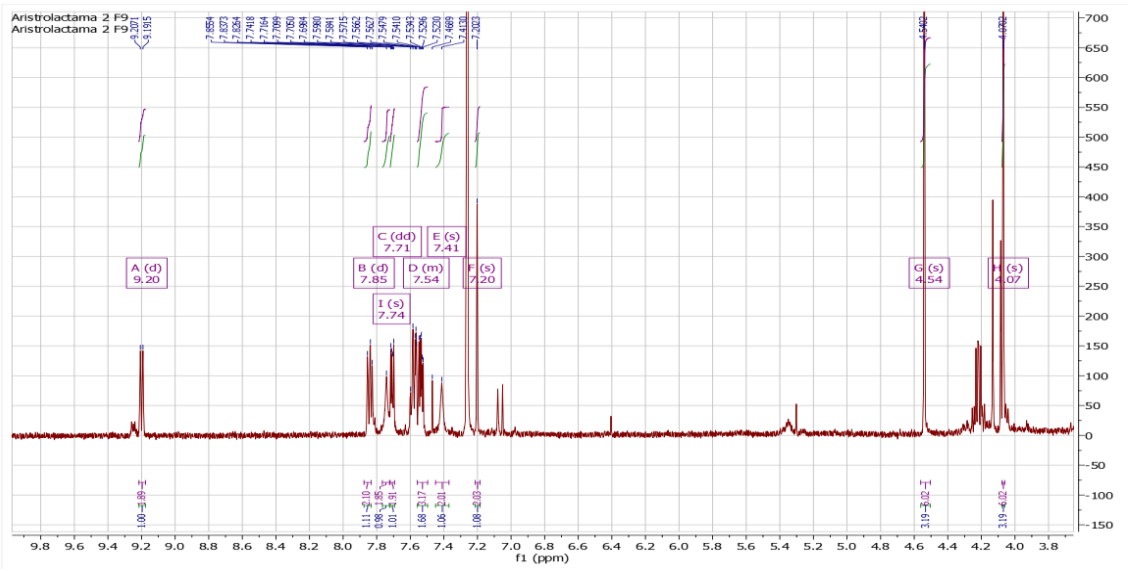

Figure 125. ^{1}H NMR spectrum of piperolactam B.

Table 18. Linearity. Area Vs concentration (By triplicate) for C1.

[ppm]	A1	A2	A3	Mean	SD	%RSD
1	484556	470883	458497	471312	13035	2,77
2,5	1353201	1368404	1367448	1363018	8515	0,62
5	2409355	2451027	2450658	2437013	23954	0,98
10	4858277	4914408	4860855	4877847	31689	0,65
25	13505301	13487655	13603313	13532090	62309	0,46
50	24148593	24548660	24930639	24542631	391058	1,59
100	46802191	46681962	46767531	46750561	61885	0,13

.

Table 19. Linearity. Area Vs concentration (By triplicate) for C2

[ppm]	A1	A2	A3	Mean	SD	%RSD
0,001	7778	6693	6369	6947	738,0	10,62
0,025	10366	10542	10609	10506	125,5	1,19
0,05	21258	21150	22503	21637	751,9	3,48
0,1	42628	43101	43012	42914	251,4	0,59
0,25	104589	106228	105495	105437	821,0	0,78
0,5	213655	214175	217161	214997	1892,0	0,88
1	437444	436820	437549	437271	394,1	0,09

Table 20. Linear regression for LOD and LOQ for C1.

Estatística de regressão	
R múltiplo	0.99911589
R-Quadrado	0.998232561
R-quadrado ajustado	0.997879073
Erro padrão	784552.8141
Observações	7

ANOVA

	gl	*SQ*	*MQ*	*F*	*F de significação*
Regressão	1	1.73821E+15	1.73821E+15	2823.951989	4.46184E-08
Resíduo	5	3.07762E+12	6.15523E+11		
Total	6	1.74129E+15			

C1

	Coefi	*Erro padrão*	*Stat t*	*valor-P*	*95% inferior*	*95% superior*	*Inferior 95,0%*	*Superior 95,0%*
Interseção	465353.2963	383934.1565	1.212065372	0.27963286	-521580.8725	1452287.47	-521580.873	1452287.47
Variável X 1	468821.6964	8822.243645	53.14086929	4.46184E-08	446143.3972	491499.996	446143.397	491499.996

SE int	383934.1565
SD int	145113.4711
LOD	1.02 ppm
LOQ	3.10 ppm

Table 21. Linear regression for LOD and LOQ for C2.

Estatística de regressão	
R múltiplo	0.999785128
R-Quadrado	0.999570302
R-quadrado ajustado	0.999484363
Erro padrão	3593.80319
Observações	7

ANOVA					
	gl	*SQ*	*MQ*	*F*	*F de significação*
Regressão	1	1.5022E+11	1.5022E+11	11631.09146	1.29973E-09
Resíduo	5	64577106.86	12915421.37		
Total	6	1.50285E+11			

	Coeficientes	*Erro padrão*	*Stat t*	*valor-P*	*95% inferior*	*95% superior*	*Inferior 95,0%*	*Superior 95,0%*
Interseção	408.8082731	1753.237954	0.233173296	0.82487 1914	-4098.033365	4915.64991	-4098.03337	4915.64991
Variável X 1	434499.8315	4028.834032	107.847538	1.29973 E-09	424143.3839	444856.279	424143.384	444856.279

SE int	1753.237954
SD int	662.6616594
LOD	5.03 ppb
LOQ	15.25 ppb

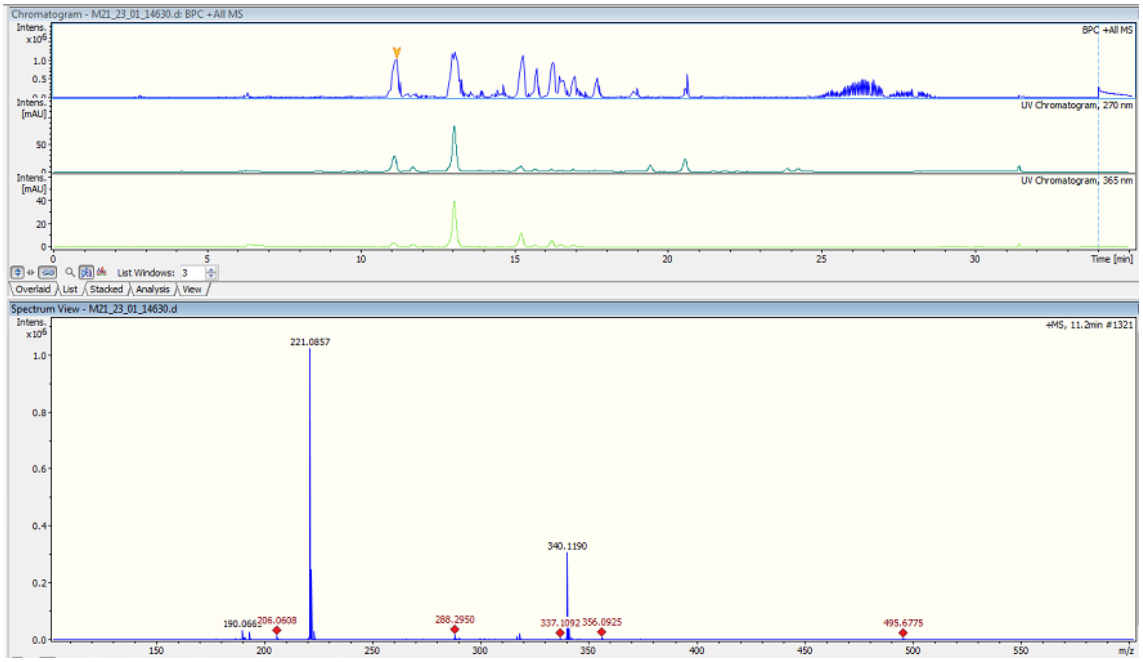

Figure 126. BPC and MS spectra of aristolactam DIII from M21.

Table 22. Eigenvalues for the PCA (chromatographic data).

Number	Eigenvalue	Percent	Cum Percent	Singular Value
1	2046.1	48.705	48.705	202.29
2	581.6	13.844	62.549	107.85
3	447.8	10.659	73.208	94.63
4	185.8	4.4218	77.630	60.95
5	177.0	4.2145	81.845	59.51
6	141.3	3.3624	85.207	53.15
7	132.2	3.1470	88.354	51.42
8	110.2	2.6236	90.978	46.95
9	80.7	1.9203	92.898	40.17
10	56.4	1.3425	94.240	33.59
11	51.3	1.2219	95.462	32.04
12	46.5	1.1078	96.570	30.51
13	42.1	1.0021	97.572	29.02
14	30.1	0.7156	98.288	24.52
15	21.7	0.5169	98.805	20.84
16	20.5	0.4876	99.292	20.24
17	15.2	0.3619	99.654	17.44
18	8.0	0.1909	99.845	12.67
19	5.1	0.1224	99.967	10.14

Table 23. Eigenvalues for the PCA (quantitative data).

Number	Eigenvalue	Percent	Cum Percent
1	1.9656	39.311	39.311
2	1.2685	25.371	64.682
3	1.0998	21.997	86.678
4	0.6661	13.322	100.000

Table 24. Statistical data from the quantification of aristolactams (by compound).

	Mean	Median	SD
aristolactam DIII	0.202	0.054	0.461
piperolactam A	0.360	0.169	0.513
piperolactam B	0.204	0.129	0.252
cepharanne B	0.897	0.385	1.228
piperolactam C	0.478	0.134	0.821

Table 25. Statistical data from the quantification of aristolactams (global).

Mean	0.43
Median	0.16
SD	1.54

Global

In mg of cepharanone B/g of dry extract

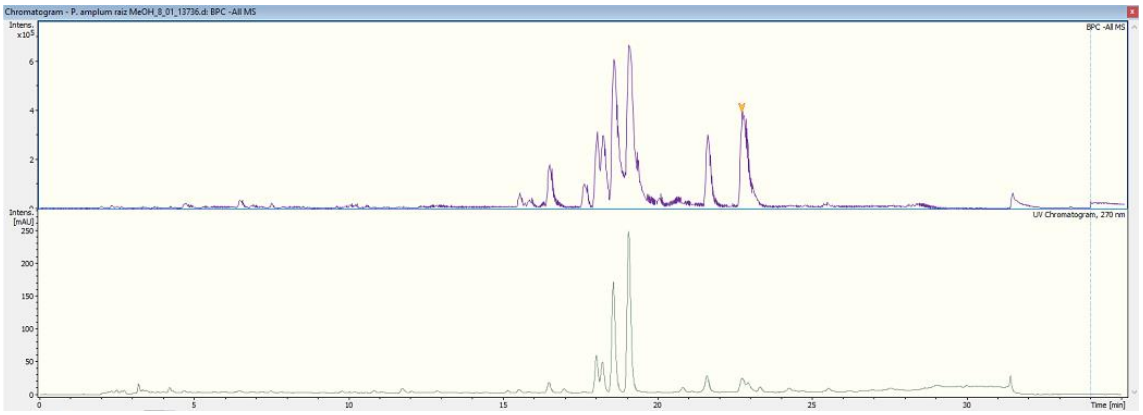

Figure 127. HPLC-UV chromatogram (270 nm) and BPC from roots of *P. lindbergii.*

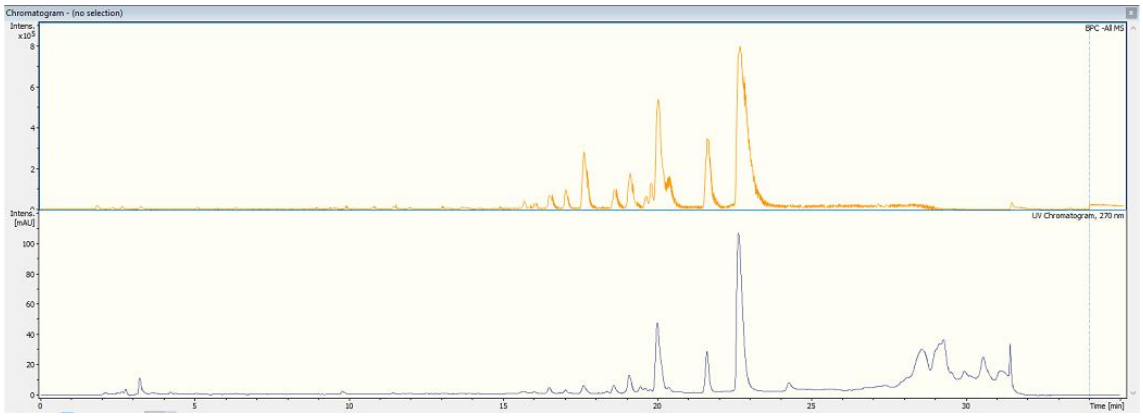

Figure 128. HPLC-UV chromatogram (270 nm) and BPC from leaves of *P. lindbergii*.